Evaluation of Coated Silk Fibroin Scaffolds with Modified Decellularized Pulp for Bone Tissue Engineering

Supaporn Sangkert

A Thesis Submitted in Fulfillment of the Requirements for the Degree of

Master of Science in Biomedical Engineering

Prince of Songkla University

2015

Thesis Title	Evaluation of Coated Silk Fibroin Scaffolds with Modified Decellularized Pulp for Bone Tissue Engineering
Author	Miss Supaporn Sangkert
Major Program	Biomedical Engineering

Major Advisor :

……
(Asst.Prof.Dr.Jirut Meesane)

Co-advisor :

……
(Assoc.Prof.Dr. Suttatip Kamonmattayakul)

……
(Assoc.Prof.Dr.Chai Wen Lin)

Examining Committee :

……Chairperson
(Assoc.Prof.Dr.Kanokwan Panyayong)

……
(Asst.Prof.Dr.Jirut Meesane)

……
(Assoc.Prof.Dr. Suttatip Kamonmattayakul)

……
(Assoc.Prof.Dr. Thongchai Nuntanaranont)

The Graduate School, Prince of Songkla University, has approved this thesis as fulfillment of the requirements for the Master of Science Degree in Biomedical Engineering

……
(Assoc.Prof.Dr.Teerapol Srichana)
Dean of Graduate School

This is to certify that the work here submitted is the result of the candidate's own investigations. Due acknowledgement has been made of any assistance received.

……..Signature
(Asst.Prof.Dr.Jirut Meesane)
Major Advisor

……..Signature
(Miss Supaporn Sangkert)
Candidate

I hereby certify that this work has not been accepted in substance for any degree, and is not being currently submitted in candidature for any degree.

……..Signature
(Miss Supaporn Sangkert)
Candidate

ชื่อวิทยานิพนธ์ การประเมินโครงร่างโปรตีนไหมไฟโบรอินที่เคลือบด้วยเนื้อเยื่อในฟันที่ย่อยเอาเซลล์ออกและผ่านการดัดแปลงสำหรับวิศวกรรมเนื้อเยื่อกระดูก
ผู้เขียน นางสาวสุภาพร แสงเกิด
สาขาวิชา วิศวกรรมชีวการแพทย์
ปีการศึกษา 2557

บทคัดย่อ

โครงร่างสามมิติไหมไฟโบรอินมักถูกนำมาใช้ทางด้านวิศวกรรมเนื้อเยื่อกระดูกเป็นเวลาหลายทศวรรษ เพื่อเพิ่มประสิทธิภาพของโครงร่างสามมิติไหมไฟโบรอินเป็นปัญหาที่ท้าท้ายสำหรับการพัฒนาของวิศวกรรมเนื้อเยื่อกระดูก ในงานวิจัยนี้โครงร่างสามมิติไหมไฟโบรอินถูกเตรียมด้วยวิธีการทำแห้งแบบแช่เยือกแข็งก่อนที่จะเคลือบด้วยเนื้อเยื่อในฟันที่ผ่านดัดแปลง การทดลองได้ออกแบบออกเป็น 10 กลุ่ม ได้แก่ กลุ่มที่ 1 โครงร่างสามมิติไหมไฟโบรอิน กลุ่มที่ 2 โครงร่างสามมิติไหมไฟโบรอินเคลือบคอลลาเจน กลุ่มที่ 3 โครงร่างสามมิติไหมไฟโบรอินเคลือบไฟโบรเนคติน กลุ่มที่ 4 โครงร่างสามมิติไหมไฟโบรอินเคลือบเนื้อเยื่อในฟัน กลุ่มที่ 5 โครงร่างสามมิติไหมไฟโบรอินเคลือบคอลลาเจนผสมไฟโบรเนคติน กลุ่มที่ 6 โครงร่างสามมิติไหมไฟโบรอินเคลือบคอลลาเจนผสมเนื้อเยื่อในฟัน กลุ่มที่ 7 โครงร่างสามมิติไหมไฟโบรอินเคลือบไฟโบรเนคตินผสมเนื้อเยื่อในฟัน กลุ่มที่ 8 โครงร่างสามมิติไหมไฟโบรอินเคลือบคอลลาเจนผสมไฟโบรเนคตินและเนื้อเยื่อในฟัน กลุ่มที่ 9 โครงร่างสามมิติไคโตซาน กลุ่มที่ 10 โครงร่างสามมิติไคโตซานเคลือบคอลลาเจน ผลการศึกษาพบว่าโครงร่างสามมิติไฟโบรอินเป็นอีกหนึ่งทางเลือกที่ดีสำหรับวิศวกรรมเนื้อเยื่อกระดูก จากนั้นเพิ่มประสิทธิภาพการทำงานของโครงร่างสามมิติไหมไฟโบรอินโดยการเคลือบด้วยเนื้อเยื่อในฟันที่ถูกดัดแปลงด้วยคอลลาเจนและไฟโบรเนคติน การดัดแปลงเนื้อเยื่อในฟันได้เตรียมขึ้นในรูปของสารละลายสำหรับเคลือบที่ประกอบด้วย เนื้อเยื่อในฟัน คอลลาเจนและไฟโบรเนคติน ก่อนที่จะใช้เคลือบโครงร่างสามมิติไฟโบรอิน ลักษณะการรวมตัวของโครงสร้างเนื้อเยื่อในฟันจะถูกสังเกตก่อนเคลือบลงบนโครงร่างสามมิติไหมไฟโบรอิน ลักษณะโครงสร้าง คุณสมบัติและหน้าที่การทำงานของโครงร่างสามมิติไหมไฟโบรอินจะถูกสังเกตและวิเคราะห์ผล โดยผลการทดลองแสดงให้เห็นว่าการดัดแปลงเนื้อเยื่อในฟันสามารถจัดเรียงตัว เป็นโครงสร้างเส้นใยที่เชื่อมต่อกันคล้ายกับโครงสร้างของสารเคลือบเซลล์ โครงสร้างดังกล่าวสามารถยึดเกาะในโครงร่างสามมิติไหมไฟโบรอินได้ แสดงให้เห็นว่าการเคลือบโครงร่างสามมิติไหมไฟโบรอินด้วยเนื้อเยื่อในฟันที่ผ่านการดัดแปลงสามารถกระตุ้นการเกาะ การเพิ่มจำนวน การสังเคราะห์แคลเซียมของเซลล์สร้างกระดูก นอกจากนี้

โครงสร้างสามมิติไหมไฟโบรอินมีคุณสมบัติทางกายภาพและเชิงกลที่เหมาะสมในการให้ความมั่นคง และสุดท้ายนี้ผลการทดลองแสดงให้เห็นว่าโครงร่างโปรตีนไหมไฟโบรอินที่เคลือบด้วยเนื้อเยื่อในฟันที่ผ่านการดัดแปลงมีประสิทธิภาพที่สูง และสามารถนำมาใช้ในวิศวกรรมเนื้อเยื่อกระดูกได้

Thesis Title	Evaluation of Coated Silk Fibroin Scaffolds with Modified Decellularized Pulp for Bone Tissue Engineering
Author	Miss Supaporn Sangkert
Major Program	Biomedical Engineering
Academic Year	2014

Abstract

A silk fibroin scaffold has been often used for bone tissue engineering for several decades. To enhance performance of a silk fibroin scaffold is challenge issue for development of bone tissue engineering. In this research, silk fibroin scaffolds were prepared by freeze drying before coating with modified decelluarized pulp. The experimental groups were designed in 10 groups. Group 1 was silk fibroin scaffold. Group 2 was silk fibroin scaffold coated with collagen. Group 3 was silk fibroin scaffold coated with fibronectin. Group 4 was silk fibroin scaffold coated with decellularized pulp. Group 5 was silk fibroin scaffold coated with collagen combined with fibronectin. Group 6 was silk fibroin scaffold coated with collagen combined decellularized pulp. Group 7 was silk fibroin scaffold coated with fibronectin combined decellularized pulp. Group 8 was silk fiboin scaffold coated with combination of collagen/fibronectin/decellularized pulp. Group 9 was chitosan scaffold and the last group was chitosan coated with collagen. The result showed that a silk fibroin scaffold was the good alterative for bone tissue engineering. Then, silk fibroin scaffolds were enhanced performance by coating with decellularized pulp that was modified by collagen and fibronectin. The modified decellularized pulp was prepared into coating solution include decellularized pulp,

collagen, and fibronectin before coating in silk fibroin scaffolds. The structural formation of modified decellularized pulp was observed and characterized before coating on silk fibroin scaffolds. The morphology, properties and functionalities of coated silk scaffolds was observed and analyzed. As the results, it showed that modified decellularized pulp organized themselves into fibrillar network structure as reconstructed extracellular matrix (ECM). Such reconstructed ECM adhered in silk fibroin scaffolds. The results demonstrated that coated silk fibroin scaffolds by modified decellularized pulp could induce cell adhesion, proliferation, and calcium synthesis. Furthermore, coated silk fibroin scaffold had suitable physical and mechanical properties for maintaining the stability. Eventually, the results indicated that coated silk fibroin scaffolds with modified decellularized pulp had high performance and promised to use in bone tissue engineering.

Contents

List of Tables

List of Figures

List of Figures (Continued)

List of Figures (Continued)

List of Figures (Continued)

List of Figures (Continued)

List of Figures (Continued)

List of Figures (Continued)

List of Abbreviations and Symbols

SF	=	Silk fibroin
ECM	=	Extracellular matrix
M	=	Molar
h	=	Hour
V	=	Volume
mm	=	Millimeter
cm	=	Centimeter
mg	=	Miligram
ml	=	Milliter
SEM	=	Scanning electron microscope
FT-IR	=	Fourier transform infrared
XRD	=	X-ray diffraction
AFM	=	Atomic Force Microscopy
FDA	=	Fluorescein diacetate
ANOVA	=	One-way analysis of variance
min	=	Minute
µm	=	Micrometer
et al	=	And others
H&E	=	Hematoxylin and eosin
OD	=	Optical density

CHAPTER 1

Introduction

Now a day many people around the world have the problem about the bone loss from the various diseases such as trauma, infections, neoplasms, congenital defects, periodontal diseases and age-related degeneration that affect quality of life. (1,2). Bone tissue engineering is the process of regeneration of functional tissue. 1Interestingly, bone tissue engineering can be used to treat bone tissue defect from disease (3).

Principally, tissue engineering is an interdisciplinary field including three knowledges: engineering materials, technology of cell and biomaterials (4). Especially, biomaterials for tissue engineering scaffolds is important to induce bone tissue regeneration (5).

Silk fibroin (SF) is the protein that is produced from the silkworm, Bombyx mori. The main protein of silk includes amino acids: glycine (43%), alanine (30%) and serine (12%). Importantly, silk fibroin can arrange themselves into three forms; 1) random coil, 2) alpha helix and 3) crystalline β-sheet. Predominantly, silk fibroin shows its interesting properties with slow degradation, biocompatibility, low immunogenicity and toxicity and good mechanical property. Silk-based biomaterials as tissue engineering scaffolds were used in a part of skeletal tissue like bone, cartilage, connective tissue skin and ligament (5). Particularly, in bone tissue engineering, the silk fibroin scaffold is a suitable choice and has the stability during bone tissue regeneration (6). However, to enhance

performance the structure and functionalities of silk fibroin scaffolds need to be modified (7). Therefore, in this research, we considered the approach to improve performance of silk fibroin scaffolds.

Pulp is the tissue that locates in the teeth and has a many extracellular matrix (ECM) in its texture (8). Such extracellular matrix has the significant role to be a native scaffold for bone tissue regeneration (9). There are some reports demonstrated the performance of ECM from different sources for bone tissue regeneration (10). Notably, there are rarely reports about decellulized pulp tissue for bone tissue engineering. Hence, the use of decellularized pulp is the proposed choice to enhance the performance of bone tissue engineering scaffold in this research. In this research, decellarized pulp was prepared into solution before coating on silk fibroin scaffolds. Generally, structure and functionalities of decellularized tissue was often damaged during the isolation (11). Therefore, decellularized pulp needs to be modified to maintain structure and functionalities by adding collagen and fibronectin in decellularized pulp solution.

Collagen is a natural protein that is the main component in extracellular matrix (ECM) in tissue. Especially, in bone tissue, collagen act as the template for calcium phosphate deposition. Collagen can enhance hold stability and strength of the bone (12). Therefore, collagen is a popular material for tissue regeneration because collagen has biological functionality that cells can recognize. Such functionality can enhance cell adhesion lead to the induction of tissue regeneration (13). So, in this

research collagen was chosen to modify decellularized pulp before coating on silk fibroin scaffolds.

Fibronectin is the glycoprotein in extracellular matrix implicated about the cell migration and adhesion, important embryogenesis, wound healing, hemostasis and thrombosis (14). Cellular fibronectin is secrete from fibroblast and other cell types and organized into fibrils contributing to the insoluble extracellular matrix. The network of fibronectin fibril can interaction with cell surface receptor and can improve cell growth and differentiation (15). Therefore, besides using collagen to modified decellularized pulp, fibronectin was selected to modify decellularized pulp before coating on silk fibroin scaffold.

As the crucial problem of bone disease, attractiveness of decellularized pulp and unique functionalities of collagen and fibronectin, we develop a high performance silk fibroin scaffold by coating with decellularized pulp that was modified with collagen and fibronectin. Characterization of morphological structure and biological function is considered in this research. Eventually, the aim of this research is to enhance biofunctionality of a porous silk scaffold with modified decellulized pulp for bone tissue engineering for treatment of bone diseases.

Objective of this Study

1. To enhance performance of silk fibroin scaffolds for bone tissue engineering
2. To prepare and characterize coated silk fibroin scaffolds with modified decellularized pulp.
3. To compare morphology, properties and functionalities of silk fibroin scaffold with and without modified decellularized pulp.

Hypothesis:

Modification of silk fibroin scaffold with collagen, fibronectin and decellulized pulp tissue will provide a better cellular response and improve quality of scaffold in terms of cell adhesion, proliferation and ECM synthesis.

Expected Benefits:

We expect that a modified silk fibroin scaffold can promote cell proliferation and differentiation. Finally, a modified silk scaffold is promising for bone tissue engineering.

Overall study design

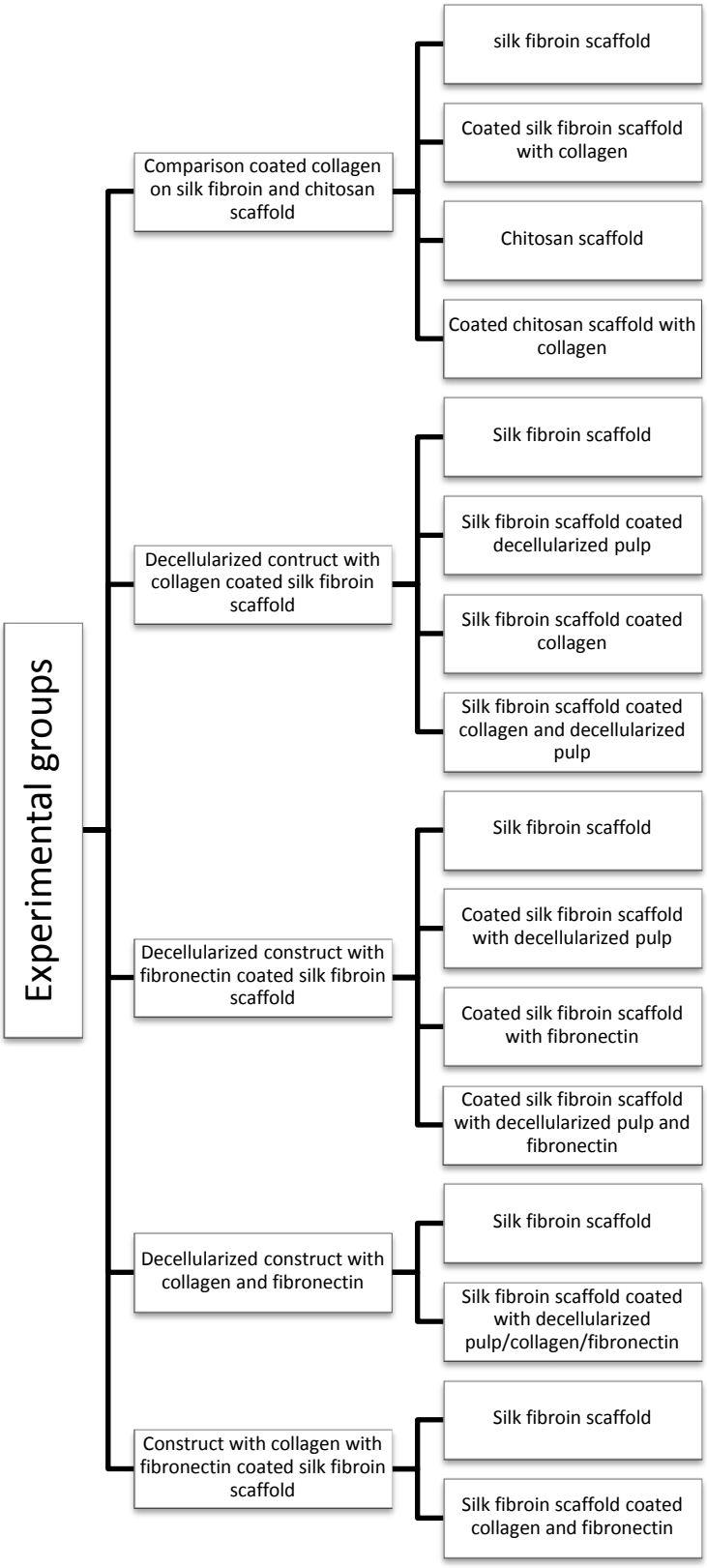

Reference

1. Wasim S. Khan, Faizal Rayan, Baljinder S. Dhinsa, David Marsh. An Osteoconductive, Osteoinductive, and Osteogenic Tissue-Engineered Product for Trauma and Orthopaedic Surgery:How Far AreWe?. Stem Cells International 2012; 2012: 1-7.
2. Ali Mobasheri, Gauthaman Kalamegam, Giuseppe Musumeci, Mark E. Batt. Chondrocyte and mesenchymal stem cell-based therapies for cartilage repair in osteoarthritis and related orthopaedic conditions. Maturitas 78; 2014: 188–198.
3. Giuseppe Maria de Peppoa, Ivan Marcos-Campos, David John Kahler, Dana Alsalman, Linshan Shang, Gordana Vunjak-Novakovic, Darja Marolt. Engineering bone tissue substitutes from human induced pluripotent stem cells. PNAS. 110; 2013: 8680–8685.
4. Hsin-I Chang, Yiwei Wang. Cell Responses to Surface and Architecture of Tissue Engineering Scaffolds. Regenerative Medicine and Tissue Engineering. 2011: 570-588.
5. Yongzhong Wang, Dominick J. Blasioli, Hyeon-Joo Kim, Hyun Suk Kim, David L. Kaplan. Cartilage tissue engineering with silk scaffolds and human articular chondrocytes. Biomaterials. 27; 2006: 4434–4442.
6. J. F. Mano, G. A. Silva, H. S. Azevedo, P. B. Malafaya, R. A. Sousa, S. S. Silva, L. F. Boesel, J. M. Oliveira, T. C. Santos, A. P. Marques, N. M. Neves, R. L. Reis. Natural origin biodegradable systems in tissue engineering and regenerative medicine: present status and some moving trends. J. R. Soc. Interface 4; 2007: 999–1030.
7. Charu Vepari, David L. Kaplan. Silk as a Biomaterial. Prog Polym Sci. 32; 2007: 991-1007.
8. Goldberg M, Smith J, Cells and Extracellular Matrices of Dentin and Pulp: A Biological Basis For Repair and Tissue Engineering. Crit Rev Oral Biol Med. 15(2004)13-27.
9. Cen L, Liu W, Cui L, Zhang W, Cao Y. Collagen Tissue Engineering: Development of Novel Biomaterials and Applications. Pediatric Research. 63; 2008: 492-496.

10. Shizuka Yamada, Kohei Yamamoto, Takeshi Ikeda, Kajiro Yanagiguchi, Yoshihiko Hayashi, Potency of Fish Collagen as a Scaffold for Regenerative Medicine. BioMed Research International. 2014: 1-9.
11. Peter M. Crapo, Thomas W. Gilbert, Stephen F. Badylak, D.V.M. An overview of tissue and whole organ decellularization processes. Biomaterials. 32; 2011: 3233–3243.
12. Takashi Matsuura, Kentaro Tokutomi, Michiko Sasaki, Michitsuna Katafuchi, Emiri Mizumachi, Hironobu Sato, Distinct Characteristics of Mandibular Bone Collagen Relative to Long Bone Collagen: Relevance to Clinical Dentistry. BioMed Research International. 2014; 2014: 1-9.
13. Shizuka Yamada, Kohei Yamamoto, Takeshi Ikeda, Kajiro Yanagiguchi, and Yoshihiko Hayashi. BioMed Research International. 2014; 2014: 852-8588.
14. Heinrich Sticht, Andrew R. Pickford, Jennifer R. Potts, Iain D. Campbell. Solution Structure of the Glycosylated Second Type 2 Module of Fibronectin. J. Mol. Biol. 276; 1998: 177-187.
15. Jielin Xu, Deane Mosher. Fibronectin and Other Adhesive Glycoproteins. Biology of Extracellular Matrix. 41; 2011: 41-75.

CHAPTER 2

Modified silk and chitosan scaffolds with collagen assembly for osteoporosis

Abstract

Currently, there are many patients who suffer from osteoporosis. Osteoporosis is a disease that leads to bone defect. Severe cases of bone defect from osteoporosis need an operation using a performance scaffold for bone tissue engineering. Therefore, to build a performance scaffold for bone defect from osteoporosis is the target of this research. Samples of silk fibroin and chitosan were fabricated into porous scaffolds before modification by coating with collagen self-assembly. The structure and morphology of the samples were characterized and observed by Fourier transform infrared (FTIR) spectroscopy, atomic force microscope (AFM) and scanning electron microscope (SEM). For biological functionality analysis, MC3T3-E1 osteoblasts were cultured on the samples. Afterward, biodegradation, cell proliferation, viability and mineralization were analyzed. The results demonstrated that collagen organized into a fibril structure covering the pores of the scaffold. The modified scaffolds showed low degradability, high cell proliferation, viability and mineralization. The results demonstrated that the modified scaffolds with a coating of mimicked collagen self-assembly had good performance and showed promise for bone tissue engineering in osteoporosis.

Materials and methods

Preparation of silk fibroin scaffolds

Degummed silk fibrin was extracted by boiling the cocoons for 30 min in 0.02 M Na_2CO_3 to remove sericin, the glue like protein that holds the fibers together. The degummed silk fibroin was dried in a hot oven (1). A 9.3 M lithium bromide solution was used to dissolve the silk fibroin. The solution was then subjected to dialysis to remove the lithium bromide (2). The silk fibroin solution was adjusted to 3% (w/v) and poured into 48 well plates for the forming of 3-dimensional silk fibroin after the freeze-dried method (1).

Preparation of type I collagen

The skin of the brown banded bamboo shark, *Chiloscylliumpunctatum*, was used for collagen extraction that followed the report of P. Kittiphattanabawon et al. 2010 (3). Briefly, the shark skin was cut into small sizes, combined with 0.1 M NaOH to remove the none collagen proteins. The skin continued to soak in 0.5 M acetic acid for 48 h. The collagen solution was filtered and then the final concentration of NaCl was adjusted to 2.6 M and 0.05 M of tris(hydroxymethyl)aminomethane at pH 7.5. The collagen solution was centrifuged using a refrigerated centrifuge machine. Then the collagen pellet was collected and dissolved in a minimum volume of 0.5 M acetic acid. The collagen solution was subjected to dialysis with 0.1 M acetic acid for 12 h and 48 h in distilled water. The freeze-dried method was used for removal of the water and kept at -20°C until use.

Preparation of chitosan scaffold

Sufficient chitosan powder (Marine Bio Resources Co., Ltd, Shrimp Chitosan) was dissolved in 0.1 M acetic acid for a 2% concentration and mixed continuously in a magnetic stirrer for 24 h. The chitosan solution was poured into 48 well plates and then kept at -20°C for overnight. The freeze-drying method was used to fabricate 3D chitosan scaffolds (4). After that they were cut into 10 mm diameter and 2 mm thick pieces.

Modification of silk fibroin and chitosan scaffolds

This study designed the scaffolds into 4 groups: 1) non-coated silk fibroin scaffolds without collagen, 2) coated silk fibroin scaffolds with collagen, 3) non-coated chitosan scaffolds with collagen and 4) coated chitosan scaffolds with collagen. 0.1 mg/ml collagen solution was used for coating (Table 1). To coat with the collagen solution, silk fibroin and chitosan scaffolds were immersed in a collagen solution for 4 h at 37°C. Afterwards, the immersed scaffolds were soaked in 1xPBS for 30 min to form self-assembly of collagen. These scaffolds were kept at -20°C for overnight before freeze-drying.

Table 1 Groups of scaffolds.

Group	Detail
A	Silk fibroin scaffold
B	Coated silk fibroin scaffold with collagen
C	Chitosan scaffold
D	Coated chitosan scaffold with collagen

Methods

Self-assembly of collagen type I

Collagen solution was mixed with PBS to observe self-assembly. The optical density (OD) at 313 nm was used to identify the form of the collagen fibrils (5). The OD of the mixed collagen solution was measured every 5 minutes for 30 minutes. The OD of each time point was plotted into a kinetic curve to explain the collagen self-assembly.

Atomic Force Microscopy Observing

A sample of the collagen solution at a concentration of 0.1 mg/ml was dropped and smeared onto a glass slide. After soaking in 1xPBS for 30 minutes, the glass slide was dried at room temperature. Then, the coated glass slide with collagen was observed for self-assembly formation of the collagen by atomic force microscopy (NanosurfeasyScan 2 AFM, Switzerland).

Fourier transform infrared (FTIR) spectroscopy

The chemical functional group of collagen was obtained using a FTIR spectrometer (EQUINOX 55, Bruker, Ettlingen, Germany). The internal reflection crystal (Pike Technologies, Madison, WI, USA), made of zinc selenide, had a 45° angle of incidence of the IR beam. The spectra were acquired at a resolution of 4 cm^{-1}. The spectral data analysis used the OPUS 3.0 data collection software program (Bruker, Ettlingen, Germany). To characteriz the chemical function groups of collagen self-assembly, the mixed collagen with PBS as in the previous experiment was freeze-dried before preparation into KBr discs and measured by FTIR.

Scanning Electron Microscopy (SEM) Observing

All groups of scaffolds were observed for morphology, surface and pore size by a scanning electron microscope (Quanta400, FEI, Czech Republic). The samples were pre-coated with gold using a gold sputter coater machine (SPI supplies, Division of STRUCTURE PROBE Inc., Westchester, PA USA).

Degradation

Lysozyme powder was mixed with PBS into solution at 4 mg/ml (pH = 7.4) before incubation at 37°C (6). The scaffolds were immersed in that solution. The scaffolds were then removed from the solution, rinsed and freeze-dried. The freeze-dried scaffolds were weighed at different time points: 1, 2, and 4 weeks. Afterward, the percentage of weight loss was calculated.

Cell culture

MC3T3-E1 osteoblast cells were seeded in each scaffold with 1×10^5 cells and maintained in an alpha-MEM medium (α-MEM, GibcoTM, Invitrogen, Carlsbad, CA) with the addition of 1% penicillin/streptomycin, 0.1% fungizone and 10% fetal bovine serum (FBS) at 37°C in a humidified 5% of CO_2 and 95% air incubator (7). The medium was changed every 3-4 days. An osteogenic medium (OS; 20 mM b-glycerophosphate, 50 μM ascorbic acid, and 100 nM dexamethasone; SigmaAldrich) was used for osteoblast differentiation of the MC3T3-E1 osteoblast cells (8).

Cell Proliferation

The measurement of cell proliferation was performed on days 3, 5 and 7 (9). Following the manufacturer's protocol, the scaffold was washed two times with 1xPBS and fresh media of 100 μl and 10 μl of 12 mM MTT (3-[4,5-dimethylthiazol-2-yl]-2,5-dimethyl tetrazolium bromide, and 5 mg/ml) were added into the cells/scaffolds, respectively. Afterward, the cells/scaffolds were incubated for 2 h at 37ºC. Then, 50 μl of dimethyl sulfoxide was added to each cells/scaffolds and incubated for 10 minutes. The solutions were moved to 96 well plates and measurements continued by monitoring the light absorbance at 540 nm.

Cell viability

On day 3, the MC3T3-E1 osteoblast cells in the scaffolds were stained with fluorescein diacetate (FDA). The FDA attached to the extracellular matrix and

cellular clusters. The FDA was dissolved with acetone at a concentration of 5 mg/ml. The medium was removed and replaced with 1 ml of fresh medium, then 5 µl of the FDA was added. The scaffolds were kept away from light for 5 minutes. The scaffolds were washed twice with 1xPBS and moved to a glass slide and the cell morphology was observed by a fluorescence microscope (10).

Alizarin red staining

The calcium deposition of the MC3T3-E1 osteoblast cells was inspected by alizarin red staining. On days 7, the scaffolds were washed with 1xPBS and the cells were fixed with 4% formaldehyde before the addition of 1 ml of alizarin red solution (2 g in 100 ml of distilled water to adjust the pH to 4.1-4.3) for 20 min at room temperature in the dark (11). The alizarin red was removed carefully from 48 well plates and the scaffolds were washed with distilled water until the red color disappeared. Afterward, that scaffolds were observed by light microscope.

Statistical analysis

All data were shown as mean ± standard deviation. The samples were measured and statistically compared by one-way ANOVA and Tukey's HDS test (SPSS 16.0 software package). $p < 0.05$ was accepted as statistically significant.

Results and discussion

Self assembly of collagen fibril

Before coating scaffolds, self-assembly of collagen was monitored by measuring the absorbance at a wavelength of 313 nm at each time point. Then, the absorbances were plotted into a kinetic curve (Fig. 1). The curve represented self-assembly of collagen fibrils (12). We monitored the collagen self-assembly in solution for 30 min that corresponded to the coating time of collagen on the scaffolds. The absorbance value increased with time (Fig. 1). During the time from 5 min to 30 min, the group absorbance was higher at each time point which meant collagen fibrils were forming in the solution. In this study, it showed that collagen type I solution 0.1 mg/ml (0.1 M acetic acid, pH 2.88) was mixed PBS with ratio 1:1 for neutralization. Under these conditions, collagen molecules organized and aggregated into the fibril structure (13). Notably, it indicated that the collagen organized into the fibril structure during the time of coating.

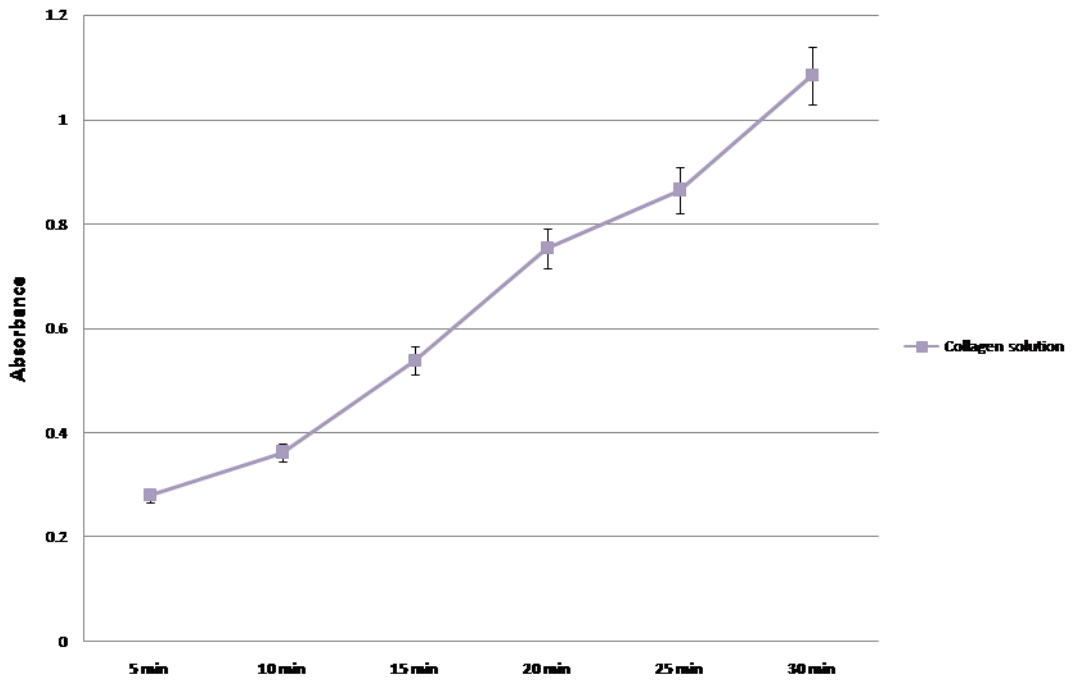

Figure. 1. Kinetic curve of self-assembly of collagen measured by absorbance at 313 nm vs. time (min).

Collagen self assembly by AFM observing

Neutralized collagen solution was dripped and dried on a glass slide to observe the structure formation by AFM of the collagen fibrils in the coating. The collagen fibrils organized themselves into small branches (Fig. 2). Interestingly, this indicated that the neutralized collagen solution had performed coating that could mimic the fibril structure as an extracellular matrix. Notably, the mimicked collagen fibril could induce cell adhesion and proliferation (14). Nevertheless, to confirm the fibril structure of collagen, the neutralized collagen solution was freeze-dried before characterization by FTIR in the next section.

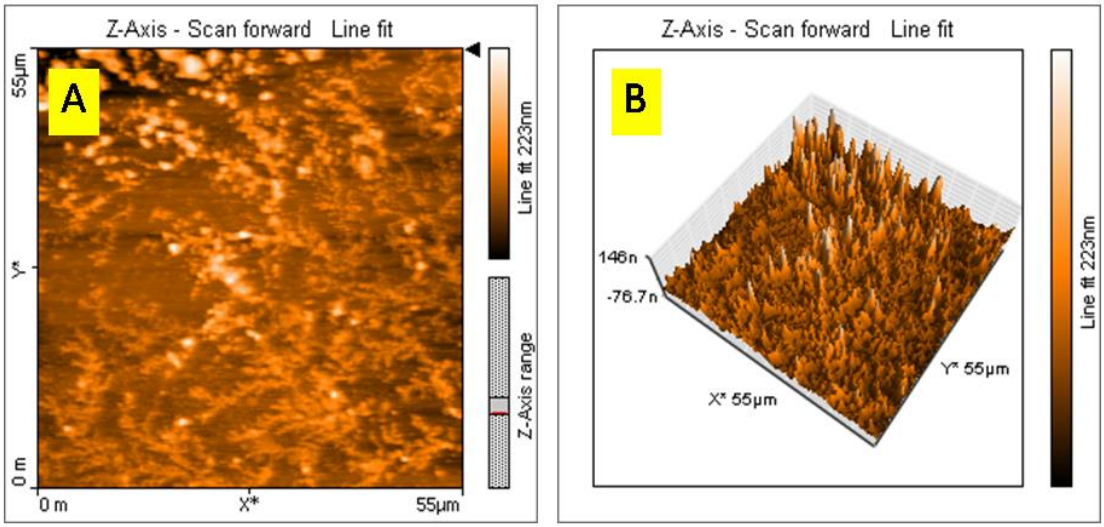

Figure. 2. Self-assembly of collagen into fibrils observed by AFM.

FTIR analysis

The freeze-dried neutralized collagen solution was characterized by FTIR to demonstrate the fibril structure of the collagen coating. Principally, the FTIR technique detected the vibration characteristics of the chemical functional groups of collagen. A specific wavenumber (cm^{-1}) range of IR radiation was absorbed by the chemical functional group (15). The amide A band of collagen was found at 3292 cm^{-1}, this was the general band associated with the N–H stretching vibration and indicated the existence of hydrogen bonds. When the NH group of peptides formed the hydrogen bond, the absorbance shifted to a lower wavenumber. The amide B was observed at 2921–2925cm^{-1}. The amide I of collagen was found at 1631 cm^{-1}. This band was due to C=O stretching vibration**.** Importantly, the FTIR results indicated that the collagen could organize into fibril structures (16). Therefore, these results confirmed the previous explanation that collagen could form into a fibril structure in the coating.

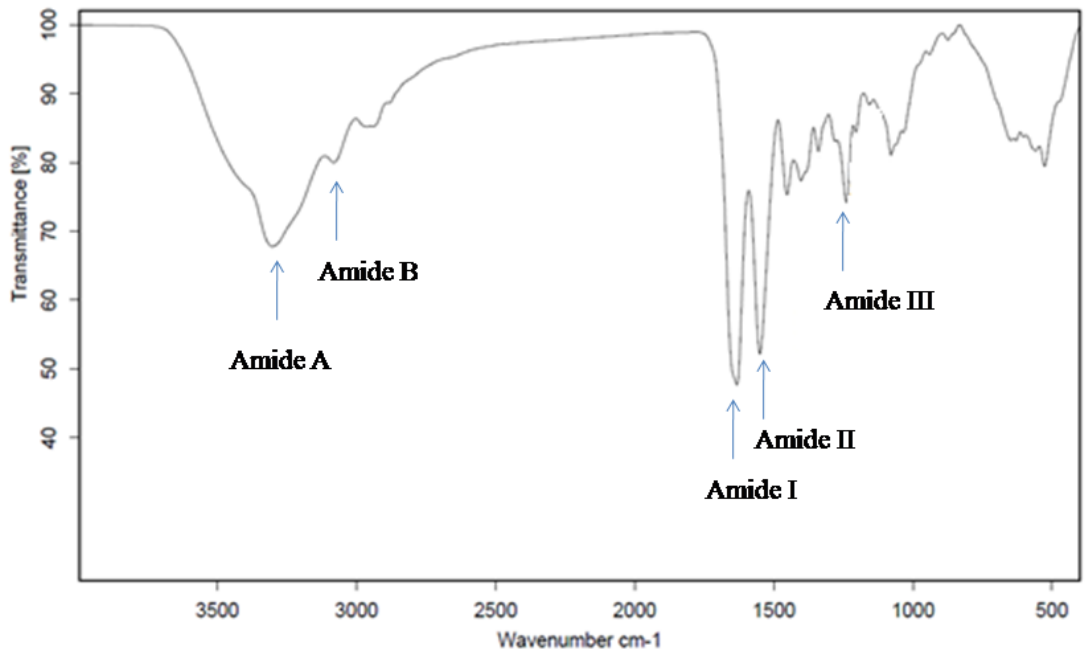

Figure. 3. Fourier transform infrared spectrum of collagen fibrils after freeze-drying.

Scanning electron microscopy analysis

After clarification that the collagen could arrange into a fibril structure, the coating solution was used for silk fibroin and chitosan scaffolds. For coating, silk fibroin and chitosan scaffolds were immersed in a collagen solution at pH 3 before soaking in PBS. Then, those scaffolds were freeze-dried before observation of the morphology by SEM. Interestingly, the morphology of the scaffolds showed that the coated scaffolds of silk fibroin and chitosan had deposited a fibril network structure of collagen inside the pores (Fig. 4). Therefore, the results from the SEM indicate that collagen could form a fibril network structure as a mimicked extracellular matrix that deposited inside the pores of the scaffolds. Importantly, the mimicked extracellular matrix might induce cell adhesion and proliferation as according to a previous report

(17). Besides the suitable structure for cell adhesion and proliferation, it is important to determine the biodegradation of scaffolds in tissue engineering. Biodegradation and cell experiments were undertaken to vindicate those issues,

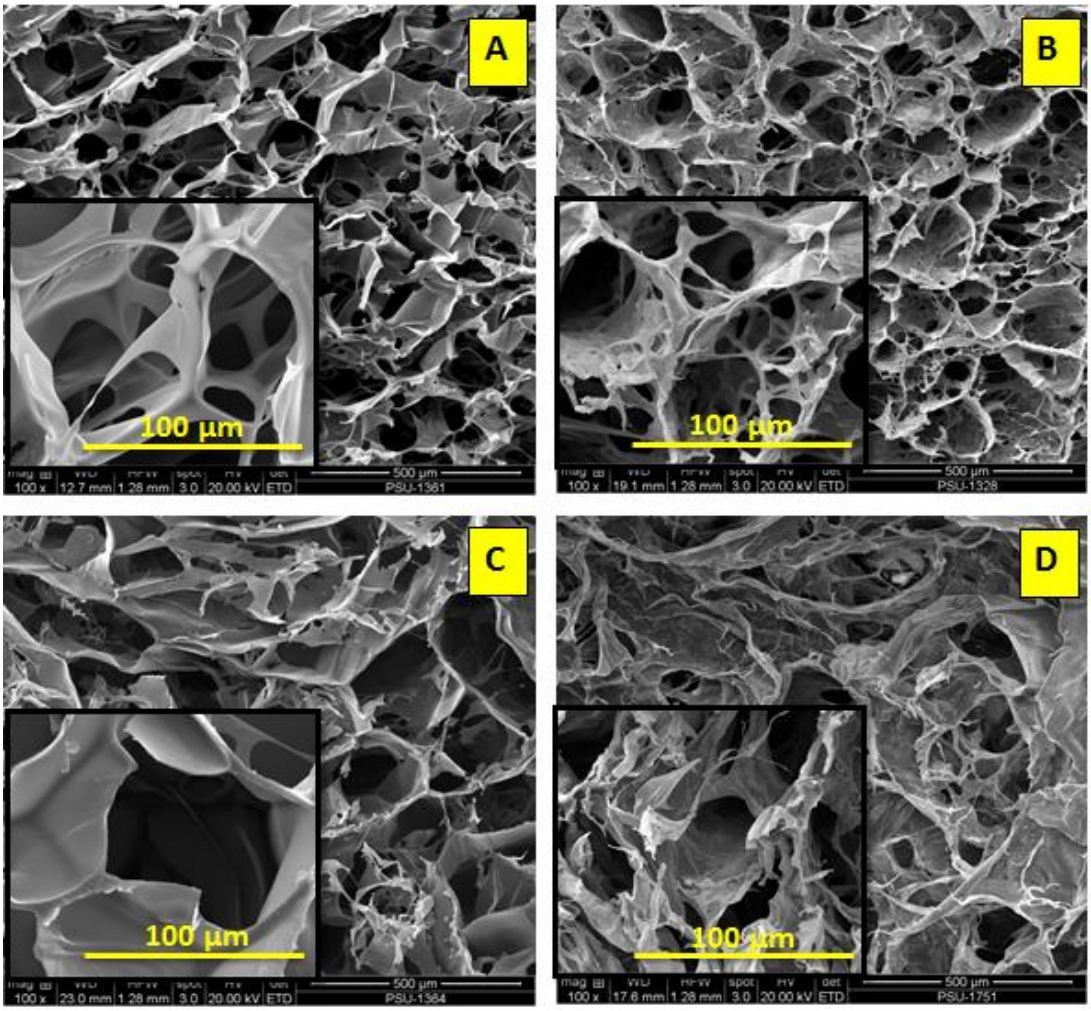

Figure. 4. Morphology and surface of scaffold in each group observed by scanning electron microscopy (SEM): A) silk fibroin scaffold, B) collagen coated silk fibroin scaffold, C) chitosan scaffold, D) collagen coated chitosan scaffold.

Analysis of scaffold degradation

The scaffolds in all groups showed a changed shape. The silk scaffold revealed the surface and margin areas that were digested with lysozyme (Fig. 5A). The surface area of the silk scaffold coated collagen group collapsed but maintained a good shape (Fig. 5B) when compared with the other groups. The chitosan scaffold was broken after digestion and the surface and margin areas were digested (Fig. 5C). The coated chitosan scaffold with collagen showed the most digestion in the marginal zone and the surface area collapsed after digestion (Fig. 5D). Both silk and chitosan scaffolds coated with collagen showed slow degradation compared to the non-coated scaffolds. The triple helix structure of collagen coated on the scaffold surface was the cause of difficult degradation. The silk fibroin scaffold coated with collagen showed the least amount of degradation. These results illustrated the same explanation as previously reported that the molecules of the enzyme had less opportunity to contact the scaffold (18). Furthermore, the literature was reported that the silk fibroin could extend biodegradability of the scaffolds (19).

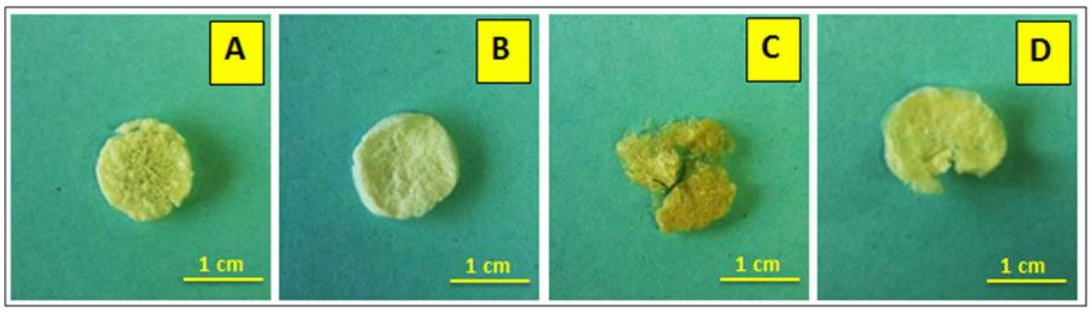

Figure. 5. Scaffolds after degradation with lysozyme at 4 weeks: A) silk fibroin scaffold, B) collagen coated silk fibroin scaffold, C) chitosan scaffold, D) collagen coated chitosan.

The silk fibroin scaffold with and without modification had more stability from biodegradtion than the modified and non-modified chitosan scaffold. Importantly, the results indicated that collagen could improve biodegradation of scaffolds. Interestingly, silk fibroin and chitosan scaffolds better tolerated the enzyme activity after coating (Fig. 6). The results of biodegradtion indicated that the coated scaffolds with mimicked collagen self-assembly had the performance for bone tissue engineering. However, to confirm the performance of those modified scaffolds experiments to determine cell proliferation, viability, and mineralization were undertaken.

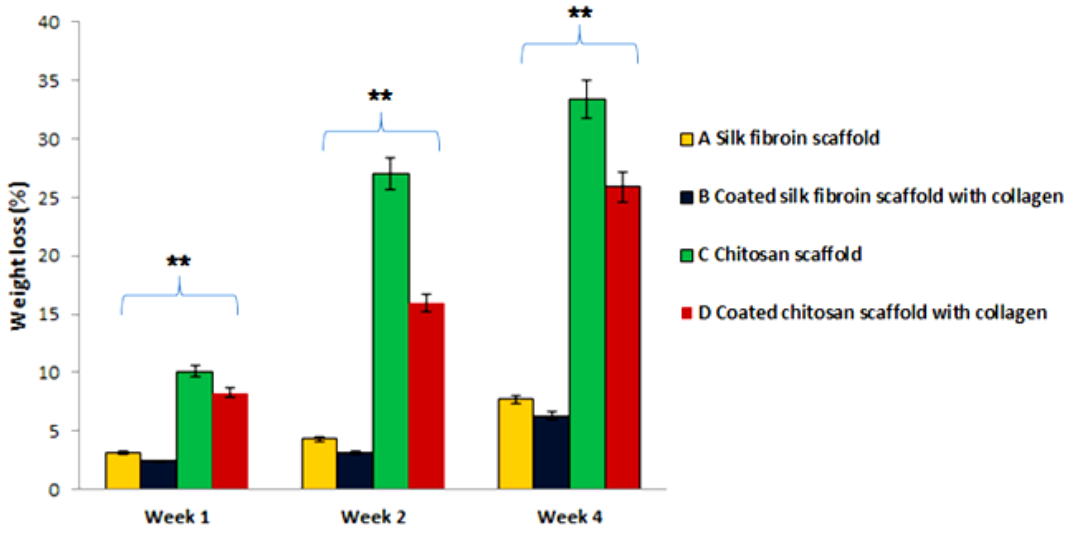

Figure. 6. Degradation of scaffold after digestion with lysozyme at weeks 1, 2 and 4. (**) ($p < 0.01$).

Cell proliferation

Figure 7 showed the MTT assay in cell proliferation on the scaffolds. The results showed that the OD values increased from day 3 to 5 and then decreased

on day 7 of the cell culture. On day 3, OD value of the silk fibroin scaffold was higher than the chitosan scaffold. The coated scaffold with mimicked collagen self-assembly had directly improved cell proliferation. The cell proliferation of the silk fibroin and chitosan scaffolds after coating with mimicked collagen self-assembly showed good performance for bone tissue engineering. Cell proliferation in all groups of the scaffold increased on day 5 which demonstrated that the cells adhered and proliferated in all groups. Notably, the collagen coated silk fibroin scaffold and the collagen coated chitosan scaffold showed the highest cell proliferations on day 7. The results indicated that collagen promoted cell proliferation and adhesion. The literature reported that collagen had the important role of inducing cell migration and differentiation (20).

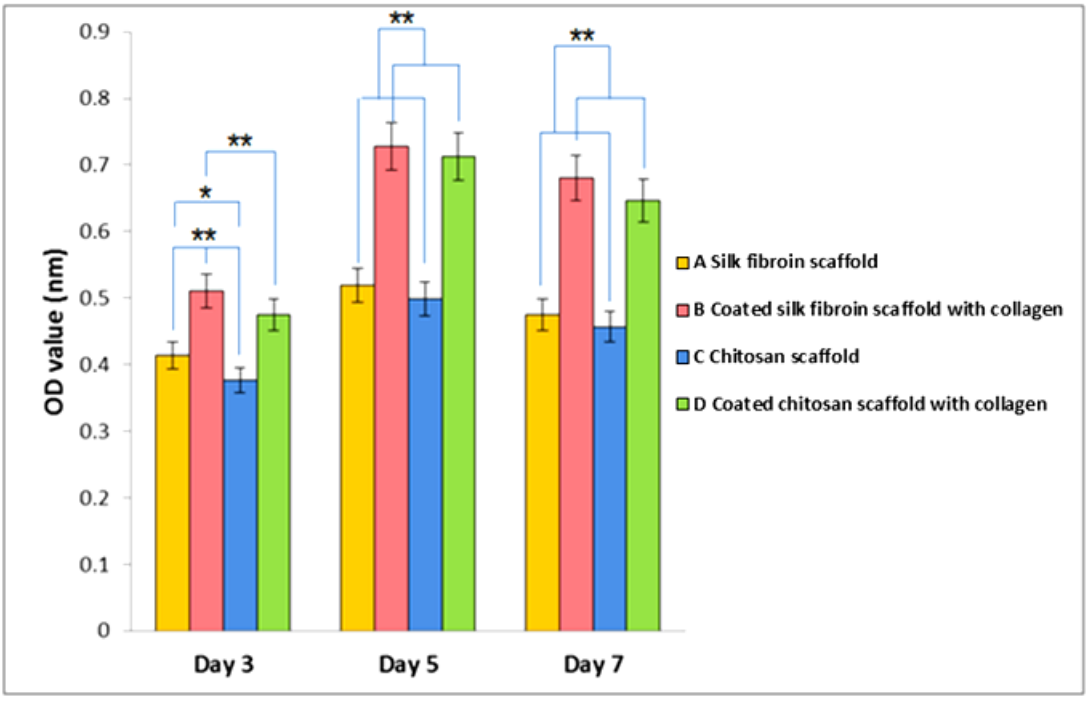

Figure. 7. MTT assay of MC3T3-E1 grown on various scaffolds at days 3, 5 and 7.

Fluorescein Diacetate (FDA) staining

The MC3T3-E1 cells adhered in all groups to the scaffolds. The bright green indicated the cell viability and morphology thoroughly on the surface. The coated scaffolds with mimicked collagen self-assembly showed a lot of cells compared to the non-coated scaffolds. The cells arranged and expanded themselves on the surface of the coated scaffolds. This demonstrated that the coated scaffolds with mimicked collagen self-assembly could enhance cell viability. However, to confirm the performance of scaffolds for bone tissue engineering, the presence calcium in the scaffold was analyzed and observed in the next section.

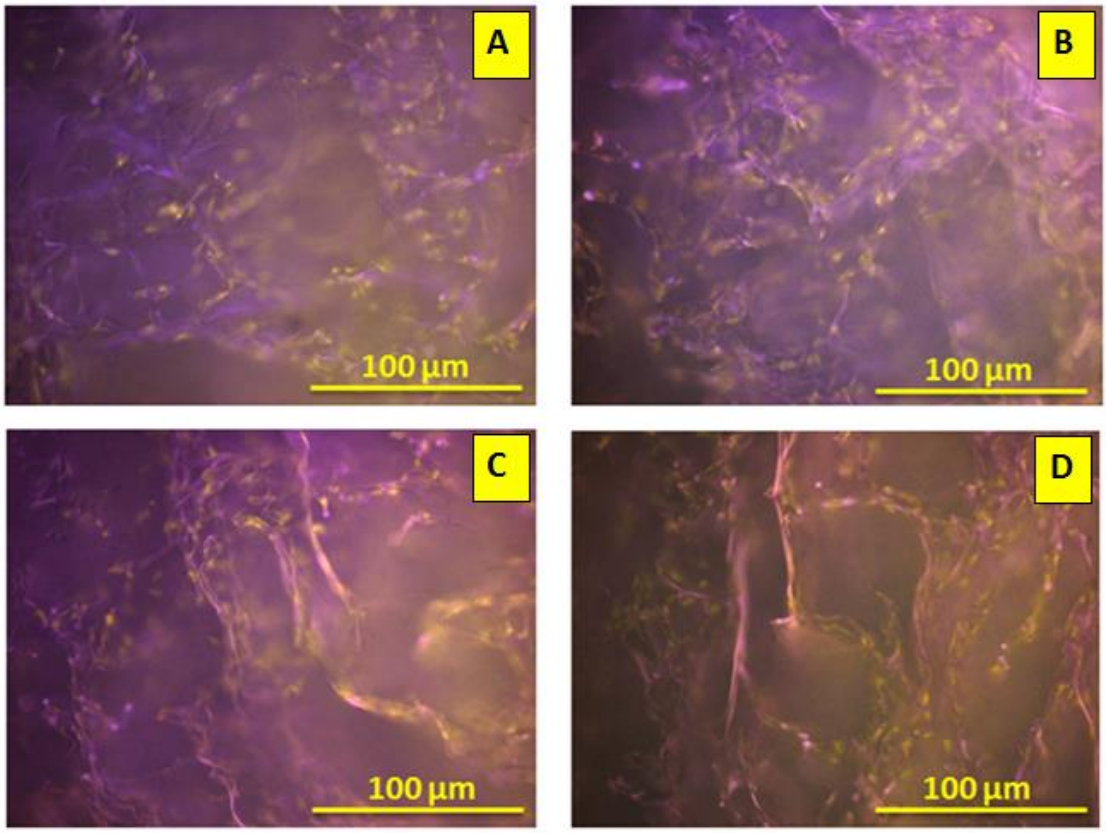

Figure. 8. Fluorescence image showed the viability (bright green) of MC3T3-E1 attached to the scaffolds in all groups: A) silk fibroin scaffold, B) collagen coated silk fibroin, C) chitosan scaffold, D) collagen coated chitosan.

Alizarin red staining

To confirm the presence of calcium that was secreted from the MC3T3-E1 cells, the scaffolds were stained with Alizarin red. Afterward, the stained scaffolds were observed by microscope. Calcium nodules were found in all groups of scaffolds (Fig. 9). The results showed that the MC3T3-E1 cells could grow in the scaffolds and secret calcuim onto the scaffolds. The staining with alizarin red indicated a high amount of calcium deposition. The coated scaffolds could induce calcium synthesis from the MC3T3-E1 cells. Notably, in the coated silk fibroin, the calcium deposition was more intensive than the coated chitosan scaffold. The results demonstrated that the coated scaffolds with mimicked collagen self-assembly had the performance for bone tissue engineering particularly in the coated silk fibroin scaffold.

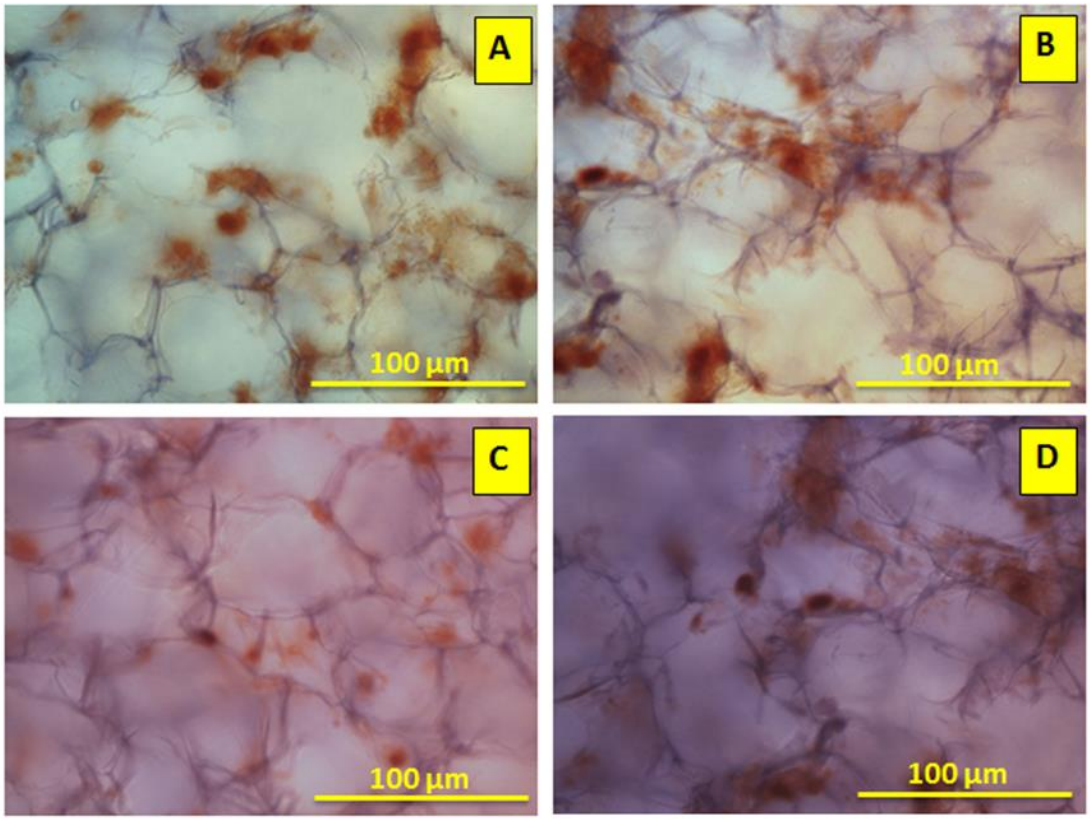

Figure. 9. Alizarin red staining of the scaffolds at day 7 of cell culture under OS media conditions. The red indicates calcium deposits on the scaffold: A) silk fibroin scaffold, B) collagen coated silk fibroin scaffold, C) chitosan scaffold, D) collagen coated chitosan scaffold.

Conclusion

The use the modified scaffolds by coatings with mimicked collagen self-assembly for tissue engineering was proposed in this research for osteoporosis treatment in the case of bone defect. The results of this research indicated that collagen organized into assembled fibril structures in the pores of the coated scaffolds. The fibril structures showed performance as an extracellular matrix that could induce biogical functionalities of coated scaffolds. Predominantly, the coated silk fibroin and chitosan scaffolds with collagen self-assembly had good biological functionalities: stability from biodegradation, good cell proliferation, viability and mineralization. Importantly, it can be

deduced that the modified scaffolds by coating with mimicked collagen self-assembly had the proformance for bone tissue engineering and showed promise for use in osteoporosis treatment.

Reference

1. Lisa D. Muiznieks.; Fred W. Keeley. Molecular assembly and mechanical properties of the extracellular matrix: A fibrous protein perspective. Biochimica et Biophysica Acta (BBA) - Molecular Basis of Disease. 1832; 2013: 866-875.
2. Shizuka Yamada.; Kohei Yamamoto.; Takeshi Ikeda.; Kajiro Yanagiguchi.; Yoshihiko Hayashi. Potency of Fish Collagen as a Scaffold for Regenerative Medicine. BioMed Research International. 2014; 2014: 1-8.
3. Blayne A. Roeder.; Klod Kokini.; Jennifer E. Sturgis.; J. Paul Robinson.; Sherry L. Voytik-Harbin. Tensile Mechanical Properties of Three-Dimensional Type I Collagen Extracellular Matrices With Varied Microstructure. Transactions of the ASME. 124; 2002: 214-222.
4. Timothy Douglas, Sascha Heinemann, Ute Hempel, Carolin Mietrach, Christiane Knieb, Susanne Bierbaum, Dieter Scharnweber, Hartmut Worch. Characterization of collagen II fibrils containing biglycan and their effect as a coating on osteoblast adhesion and proliferation. J Mater Sci: Mater Med. 4; 2008: 1653-1660.
5. Rucsanda C. Preda, Gary Leisk, Fiorenzo Omenetto, David L. Kaplan. Bioengineered Silk Proteins to Control Cell and Tissue Functions. Protein nanotechnology. 996; 2012: 19-41.
6. G. Chang, H.-J. Kim, D. Kaplan, G. Vunjak-Novakovic, R. A. Kandel. Porous silk scaffolds can be used for tissue engineering annulus fibrosus. Eur Spine J. 16; 2007: 1848-1857.
7. Phanat Kittiphattanabawon, Soottawat Benjakul, Wonnop Visessanguan, Hideki Kishimura, Fereidoon Shahidi. Isolation and Characterisation of collagen from the skin of brownbanded bamboo shark (Chiloscyllium punctatum). Food Chemistry. 119; 2010: 1519–1526.
8. Stephanie Tully-Dartez, B.S., Henry E. Cardenas, Ping-Fai Sidney Sit. Pore Characteristics of chitosan scaffolds studied by electrochemical impedance spectroscopy. Tissue engineering; Part C. 16; 2010: 339-343.
9. Barbara R. Williams, Robert A. Gelman, Donald C. Poppke, Karl A. Piez. Collagen Fibril Formation. The journal of biological chemistry. 253; 1978: 6578-6585.
10. Zhe Zhang, Huifei Cui. Biodegradability and Biocompatibility Study of Poly(Chitosan-g-lactic Acid) Scaffolds. Molecules. 17; 2012: 3243-3258.

11. Damla Cetin, A. Sera Kahraman, Menemse Gumusderelioglu. Novel Scaffolds Based on Poly(2-hydroxyethyl methacrylate) Superporous Hydrogels for Bone Tissue Engineering. Journal of Biomaterials Science. 22; 2011: 1157–1178.
12. E. Birmingham, G.L. Niebur, P.E. McHugh, G. Shaw, F.P. Barry, L.M. McNamara. Osteogenic differentiation of mesenchymal stem cells is regulated by osteocyte and osteoblast cells in a simplified bone niche. European Cells and Materials. 23; 2012: 13-27.
13. Fariba Mansourizadeh, Asadollah Asadi, Shahrbanoo Oryan, Ali Nematollahzadeh, Masoumeh Dodel, Mehdi Asghari-Vostakolaei. PLLA/HA Nano composite scaffolds for stem cell proliferation and differentiation in tissue engineering. Molecular Biology Research Communications. 2; 2013: 1-10.
14. Ting-Ting Li Katrin Ebert, Jurgen Vogel, Thomas Groth. Comparative studies on osteogenic potential of micro- and nanofibre scaffolds prepared by electrospinning of poly(ε-caprolactone). Progress in Biomaterials. 2; 2013: 1-13.
15. Stein GS, Lian JB. Molecular mechanisms mediating developmental and hormone-regulated expression of genes in osteoblasts: an integrated relationship of cell growth and differentiation. In: Noda M, editor. Cellular and molecular biology of bone. Tokyo: Academic Press. 1993: 47–95.
16. Barbara R. Williams, Robert A. Gelman, Donald C. Poppke, Karl A. Piez. Collagen Fibril Formation. The journal of biological chemistry. 253; 1978: 6578-6585.
17. Nima Saeidi, Edward A. Sander, Jeffrey W. Ruberti. Dynamic shear-influenced collagen self-assembly. Biomaterials. 30; 2009: 6581–6592.
18. Deok-Ho Kim, Paolo P. Provenzano, Chris L. Smith, Andre Levchenko. Matrix nanotopography as a regulator of cell function. JCB: Review. 197; 2012: 351-360.
19. Benedicto de Campos Vidal, Maria Luiza S. Mello. Collagen type I amide I band infrared spectroscopy. Micron. 42; 2011: 283–289.
20. Phanat Kittiphattanabawon, Soottawat Benjakul, Wonnop Visessanguan, Hideki Kishimura. Fereidoon Shahidi. Isolation and Characterisation of collagen from the skin of brownbanded bamboo shark (Chiloscyllium punctatum). Food Chemistry. 119; 2010: 1519–1526.

CHAPTER 3

Modified silk fibroin scaffolds with collagen/decellularized pulp for bone tissue engineering in cleft palate: morphological structures, and biofunctionalities

Abstract

Cleft palate is a crucial disease that generates a maxillofacial bone defect around the mouth area. To create performance scaffolds for bone tissue engineering in cleft palate is an issue that was proposed in this research. Because of its good biocompatibility, high stability, and non-toxicity, silk fibroin was selected as the scaffold of choice in this research. Silk fibroin scaffolds were prepared by freeze-drying before immerging in a solution of collagen, decellularized pulp, and collagen/decellularized pulp. Then, the immersed scaffolds were freeze-dried. Structural organization in solution was observed by Atomic Force Microscope (AFM). Molecular organization of those solutions and crystal structure of scaffolds were characterized by Fourier transform infrared (FT-IR) and X-ray diffraction (XRD), respectively. The weight increase of the modified scaffolds and pore size were determined. The morphology was observed by scanning electron microscope (SEM). Biofunctionalities were considered by seeding osteoblasts in silk fibroin scaffolds before analysis of the cell proliferation, viability, total protein assay, and histological analysis. The results demonstrated that dendrite structure of the fibrils occurred in those solutions. Molecular organization of the

components in solution arranged themselves into irregular structure. The fibrils were deposited in the pores of the modified silk fibroin scaffolds. The modified scaffolds showed amorphous structure. Following assessment of the biofunctionalities, the modified silk fibroin scaffolds could induce cell proliferation, viability, and total protein particularly in modified silk fibroin with collagen/decellularized pulp. Furthermore, the histological analysis indicated that the cells could adhere in modified silk fibroin scaffolds. Finally, it can be deduced that modified silk fibroin scaffolds with collagen/decellularized pulp had the performance for bone tissue engineering and a promise for cleft palate treatment.

Materials and methods

Preparation of silk fibroin scaffolds

Silk fibrin scaffolds were prepared by boiling the cocoons for 30 min in 0.02 M Na2CO3 and then rinsed with distilled water to extract the sericin. The silk was dried in a hot air oven at 60°C for 24 h. The silk was dissolved in a 9.3 M LiBr solution at 70°C for 3 h and then a silk solution was prepared yielding a 3% (w/v) solution (1). After dissolving the silk fibroin, it was centrifuged for 20 min at 9000 RPM at 4°C (2). The silk solution was purified by dialyzing against distilled water for 3 days (3). The silk fibroin solution was stored at 4°C until further use. Preparation of the 3D silk scaffold for experiment followed five steps. First, the silk fibroin solution was poured in 48 well plates. Second, the silk fibroin solution was freeze-dried to generate the porosity. Third,

the porous silk scaffolds were treated by immersion in 70% (v/v) methanol for 30 min. Fourth, porous silk scaffolds were freeze-dried again. Finally, all scaffolds were cut into a diameter of 10 mm and 2 mm in thickness.

Preparation of type I collagen

Type I collagen was extracted from the skin of brown banded bamboo shark (Chiloscyllium punctatum). The preparation of type I collagen followed the report of P. Kittiphattanabawon et al. 2010 (4). Briefly, shark skin (1.0 × 1.0 cm^2) was mixed with 0.1 M NaOH. Next, the deproteinized skin was soaked in 0.5 M acetic acid for 48 h. After filtering the mixture to get the collagen solution, NaCl was added to a final concentration of 2.6 M and 0.05 M Tris (hydroxymethyl) aminomethane at pH 7.5. To collect the collagen pellet using a refrigerated centrifuge, the pellet was dissolved in a minimum volume of 0.5 M acetic acid. For a more purified collagen solution, dialysis was performed with 0.1 M acetic acid for 12 h and 48 h with distilled water. The freeze-dried method was used to remove the water and it was kept at -20°C for later use.

Preparation of decellularized pulp

We collected teeth pulp from children who were 6 to 10 years old and segmented the teeth in half to harvest the pulp tissue. Collagenase and dispase were used to digest the pulp into solution for 1 h. The solution was separated from the debris pellet by using a centrifuge at 37°C. Then, the solution was washed with PBS

(phosphate-buffered saline) 2 times. Finally the solution was filtered to get the decellularized pulp and used the freeze drying machine for water sublimation (5).

Modification of silk fibroin scaffolds

For modification of silk fibroin scaffolds, we designed the silk fibroin scaffolds into 4 groups that were modified with a different coating solution as shown in Table 2. For coated silk scaffolds in the decellularized pulp group, the decellularized pulp powder was dissolved in 0.1% sodium hypochlorite to a concentration of 0.1 mg/ml. In the case of coated silk scaffolds with collagen, the collagen powder was dissolved in 0.1 M acetic acid to a concentration of 0.1 mg/ml (6). For coated silk scaffolds with collagen/decellularized pulp, the previous collagen and decellularized pulp were mixed together to obtain a 50:50 ratio. The collagen, decellularized pulp and collagen/decellularized pulp were used as the coating solutions to modify the scaffolds. To modify the scaffolds, the silk fibroin scaffolds were immersed into the coating solutions for 240 min. Then, the immersed scaffolds were soaked in 1X PBS for 30 min before they were freeze-dried (7).

Table 2 Groups of silk scaffolds coated with the coating solutions.

Group	Detail
A	Silk scaffold
B	Silk coated decellularized pulp
C	Silk coated collagen
D	Silk coated collagen and decellulize pulp

Pore size measurement

The ImageJ software (1.48v) was used to measure the pore size in each group. The pore distribution of the scaffolds was analyzed from SEM images. The pore size of the scaffolds in each group was a randomized area (n=25) to calculate the average pore size (8).

Weight increase of the modified scaffolds

The weight increase of the modified scaffolds was measured by the percentage deposition of components in the coating solution on the scaffolds. All groups of silk scaffold were weighed before and after coating (n=5). The difference in the weights after calculation showed the percentage of silk scaffold that increased from the components in the coating solution that attached onto the silk scaffold (9). Percentage deposition of components in the coating solution on the scaffold (w/w, %)

$$= (Wt - Wp) / Wt \times 100\%$$

Wt , weight of the coated scaffold, Wp , weight of scaffold.

Swelling testing

Silk scaffold in all groups were soaked in PBS at 37 ° C for 24 h. After removal of excess PBS by contact with a plastic surface. The swollen samples were weighed immediately, the swelling ratiowas calculated using the following equation (10):

$$\text{Swelling ratio} = (Ws - Wd)/Wd$$

Where the Ws and Wd are the weight of swollen scaffold and weight of dry scaffold, respectively.

Mechanical properties testing

Scaffold in wet phase was investigated about the mechanical properties by usingUniversal Testing Machine (Lloyd model LRX-Plus, Lloyd Instrument Ltd., London, UK). In this study scaffold all groups were cut with size diameter 10 mm, thickness 5 mm. The testing machine has been used with static load cell of 10 N at rate of 2 mm/min and stop at strain 40%.

Fourier transform infrared (FT-IR) characterization

Molecular organization of silk fibroin scaffolds, and silk fibroin scaffolds coated with decellularized pulp, collagen, and collagen/decellularized pulp were analyzed by FT-IR. The samples were analyzed as a KBr pellet in a FT-IR

spectrophotometer using the EQUINOX 55 (Bruker Optics, Germany) in the range of 4000-400 cm^{-1}.

X-ray diffraction (XRD) characterization

Crystal structure of silk fibroin scaffolds, and silk fibroin scaffolds coated with decellularized pulp, collagen, and collagen/decellularized pulp were analyzed by XRD (X'Pert MPD (PHILIPS, Netherlands). Samples were put in XRD instrument and measured diffraction patterns over a 2θ range of 5-90 θ with a step size of 0.05 θ and time per step of 1 s.

Scanning Electron Microscopy (SEM) Observations

A scanning electron microscope (Quanta400, FEI, Czech Republic) was used to observe the morphology and characterization of the SF scaffold that was coated with a special solution. The samples were pre-coated with gold using a gold sputter coater machine (SPI Supplies, Division of STRUCTURE PROBE Inc., Westchester, PA USA).

Atomic Force Microscopy Observations

The coating solution for each group was dropped into a glass slide, smeared and soaked in PBS for 30 min. When the slides were dried, the morphology and structure were observed by using atomic force microscopy (Nanosurf easyScan 2 AFM, Switzerland).

Cell culture experiments

The MG-63 cell line was cultured in alpha-MEM medium (α-MEM, Gibco™, Invitrogen, Carlsbad, CA) with the addition of 1% penicillin/streptomycin, 0.1% fungizone and 10% fetal bovine serum (FBS) at 37°C in a humidified 5% of CO_2 and 95% air incubator. The MG-63 was seeded with a 5 $\times 10^5$/silk scaffold and the medium was changed every 3-4 days (11). The osteogenic medium (10 mM b-glycerophosphate, 50 mg/ml ascorbic acid, and 100 nM dexamethasone; SigmaAldrich) was used for osteoblast differentiation of MG-63 (12).

Cell proliferation assay (PrestoBlue; Day 1, 3, 5, and 7)

To observe the cell proliferation, PrestoBlue assay was used based on resazurin reagent. When the live cells go through the reducing process in the cytoplasm they will react with the resazurin to form resorufin to produce a purple or red color. The measurement of cell proliferation was performed according to the manufacturer's instructions (PrestoBlue® Cell Viability Reagent, Invitrogen, USA) and measured at 1, 3, 5, and 7 days (13). Silk fibroin scaffolds from each group were washed twice with 1X PBS and then 1/10th volume of PrestoBlue reagent was added directly into the complete media and incubated for 1 hour at 37°C and the proliferation rate of the cells was measured by monitoring the wavelength absorbance at 600 nm emission. The untreated cell group was used for the negative control.

Cell viability (Fluorescence Microscope on Day 3)

Cell viability on silk fibroin scaffold in each group was evaluated by fluorescence microscope. The live cells on the SF scaffold were stained by fluorescein diacetate (FDA). The application of the FDA was to attach to the cells and embed them into the extracellular matrix and cellular clusters. FDA was dissolved in acetone at 5 mg/ml. Next the media was removed by replacement of fresh 1 ml medium and then 5 µl of the FDA was added to each well and kept in the dark at 37°C for 5 min. The silk fibroin scaffold was washed twice with 1X PBS and transferred to a glass slide and the cell morphology was observed by the fluorescence microscope (14).

Total protein assay

The cellular protein in the cell lysis solution was discharged according to the manufacturer's instructions (Pierce BCA Protein Assay Kit, Thermo Scientific, USA). In order to extract cellular protein by using the lysis cell method, 800 µl of the cell lysis solution (1% Triton X in PBS) was added in each well and the silk fibroin scaffolds were frozen at -70°C for 1 h and then thawed at room temperature for 1 h. This was repeated in 3 cycles. Following that, the solution was transferred to an Eppendorf tube and centrifuged at 12000 RPM for 10 min to remove the supernatant from the pellet. Measurement of the total protein synthesized by the cells in the silk fibroin scaffold was performed with absorbance at 562 nm at 7, 14, and 21 days. Bovine serum albumin was used for the standard curve in this experiment (15).

Histology analysis

Silk fibroin scaffold with cell culture on day 5 was fixed with 4% formaldehyde at 4°C for 24 h. The silk fibroin scaffolds in each group were immersed in paraffin. The paraffin sections were cut at 5 μm and placed on a glass slide and deparaffinized and hydrated in distilled water. The sample slide was stained with 2 types. At first, hematoxylin and eosin stain was used to observe cell migration, adhesion, and the extracellular matrix synthesized from the cells around the silk fibroin scaffold (16).

Statistical analysis

All data were shown as mean ± standard deviation. The samples were measured and statistically compared by one-way ANOVA and Tukey's HSD test (SPSS 16.0 software package). $p < 0.05$ was accepted as statistically significant.

Results and discussion

Structural formation of mimicked extracellular matrix

In this research a coating solution of collagen/decellularized pulp was prepared according to the above protocol before observation of its organization by AFM. To characterize the structure of the collagen/decellularized pulp was the preliminary demonstration before coating onto the silk fibroin scaffolds. Furthermore, this demonstration could relate to the arrangement of the collagen/decellularized pulp on the silk fibroin scaffolds. The structure of collagen/decellularized pulp is shown in Fig. 10. According to the structure formation illustrated in Fig. 10, all samples showed dendrite

formation of fibrils. Collagen without decellularized pulp organized predominantly into a dense branch structure. As reported previously, collagen molecules formed themselves into a fibril structure (17). Notably, collagen formed dendrite formation of fibrils when it was observed by AFM. This result can be explained by the disturbance of the collagen molecules by the sodium hypochlorite in the solution. Generally, sodium hypochlorite is a chemical reagent used for dental treatment. It has the important role of maintaining fibroblast viability and promotes healing of chronic wounds (18). Some reports demonstrated that sodium hypochlorite can change the hydroxyproline into pyrrole-2-carboxylic acid (19). Such forms of collagen might influence the organization into dendrite formation of fibrils.

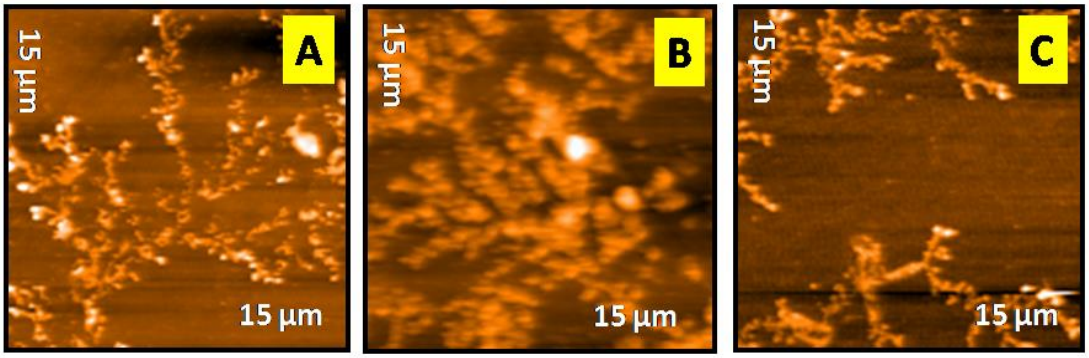

Figure. 10**.** AFM images of structure formation of coating solution: (A) decellularized pulp, (B) collagen, and (C) collagen/decellularized pulp.

Molecular organization analysis of modified silk fibroin scaffolds

To analyze molecular organization of coating solution, FTIR was used to characterize in this research. The results of molecular organization showed different wavenumbers of samples as Fig.11. For the collagen, as the previous, FTIR spectrum showed the important peak of -OH groups around 3500 cm^{-1} (20, 21) . In this research,

the -OH groups of collagen appeared at wavenumber around 3303 cm^{-1} that shifted to the low wavenumber. This indicated that –OH groups interacted with the other groups. Such interaction came from the self-assembly of collagen that molecules could organize themselves into the high order structure. For the coated silk fibroin scaffolds wave number of -OH groups shifted to the high wavenumber. This result indicated that -OH groups could vibrate freely in decellularized pulp and collagen/decellularized pulp that came from irregular organization of the components. Notably, in the case of decellularized pulp, it showed three peaks; 3416, 3472, and 3552 cm^{-1} that represented the combination of -OH groups in each component in decellularized pulp. For the collagen/decellularized pulp, it showed -OH groups around 3464 cm^{-1} that might be the merged peak of collagen and decellularized pulp. Furthermore, it demonstrated that -OH groups in collagen/decellularized pulp could vibrate freely.

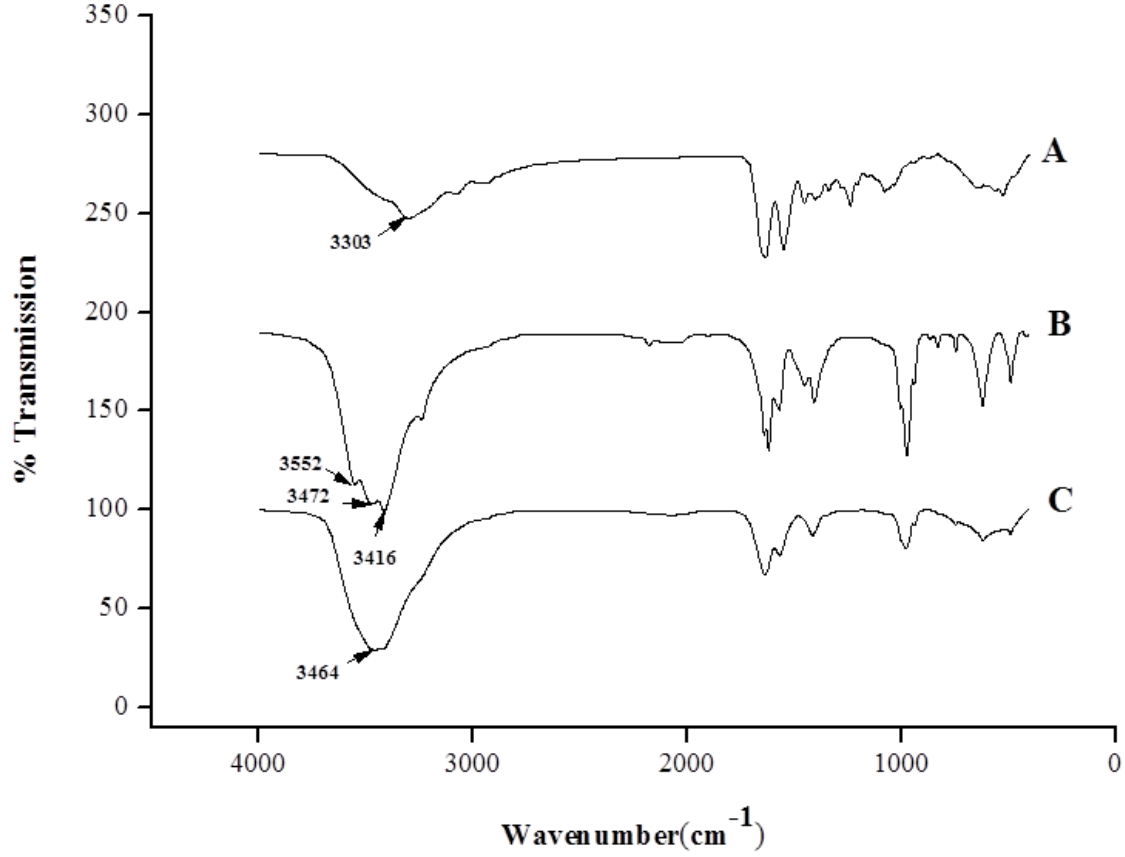

Figure. 11. FTIR spectra of collagen (A), decellularized pulp (B), and collagen/decellularized pulp.

Crystal structure analysis of modified silk fibroin scaffolds

The results of crystal structure showed different peaks of samples. The previous reports demonstrated that the regular crystal structure appeared sharp peak by XRD characterization and the broad peak represented amorphous or irregular structure (22). As the results of XRD analysis in this section, the silk fibroin scaffold and coated silk fibroin scaffolds showed the broad peak that represented the amorphous structure as a previous report (23).

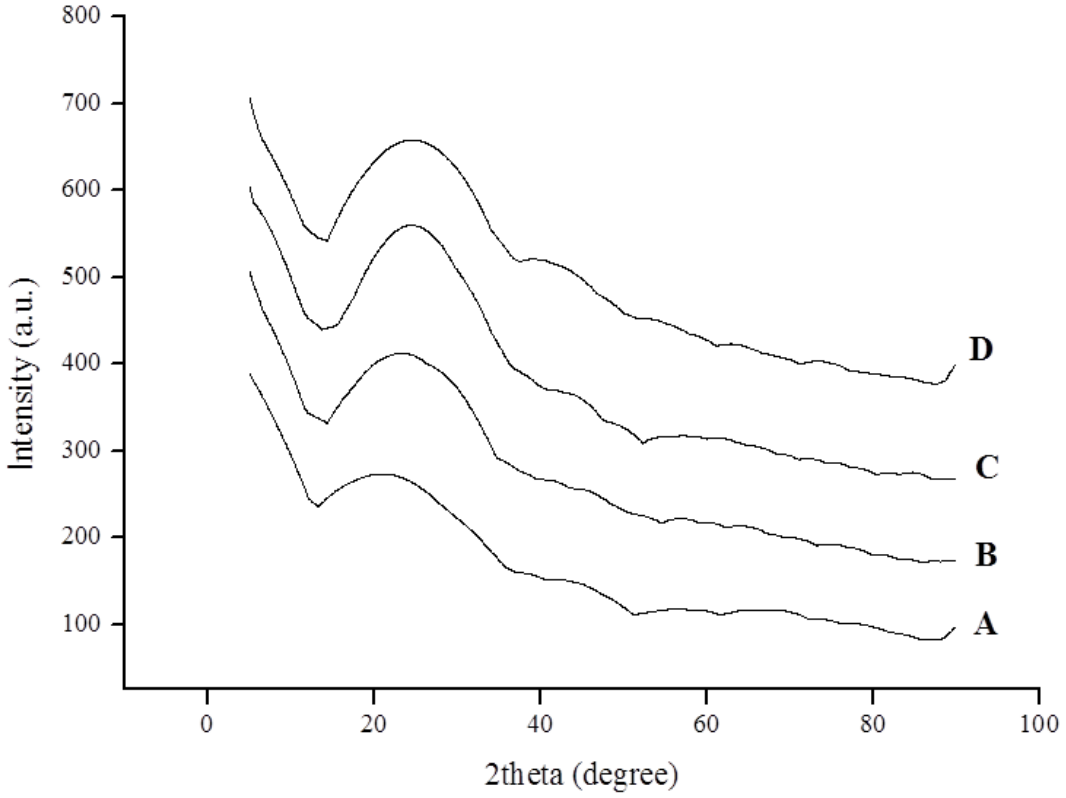

Figure. 12. XRD spectra of silk fibroin scaffold (A), silk fibroin scaffold coated with decellularized pulp (B), silk fibroin scaffold coated with collagen (C), silk fibroin scaffold coated with collagen/decellularized pulp (D).

Morphological analysis of modified silk fibroin scaffolds

In this research silk fibroin scaffolds were modified by coating solutions: collagen, decellularized pulp, and collagen/decellularized pulp. To start the modification, silk fibroin scaffolds were prepared by the freeze-dried technique before immersion into one of the coating solutions. Then, the immersed scaffolds were soaked in a buffer solution. Afterward the scaffolds were freeze-dried. The samples are shown in Fig. 13.

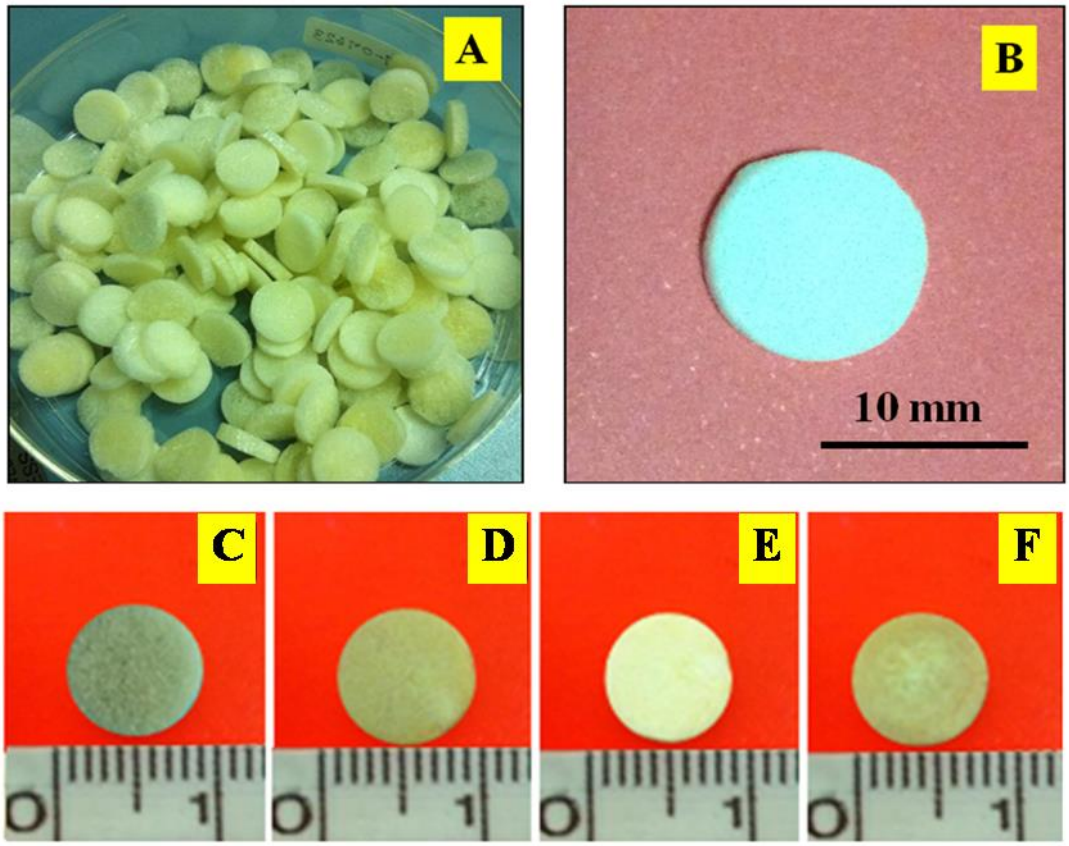

Figure. 13. Image of silk fibroin scaffolds: (A,C) before immersion(size 10 mm diameter and 2 mm thickness),Silk fibroin scaffold coated with decellularized pulp:(D) Silk fibroin scaffold coated with collagen:(E) Silk fibroin scaffold coated with collagen/decellulized pulp:(B,F).

Observations of the uptake of the coating solutions inside the silk fibroin scaffolds during immersing are shown in Fig. 14. Silk fibroin scaffolds with decellularized pulp, collagen, and collagen/decellularized pulp showed turbid and transparent parts distributed throughout the texture of the scaffold during the early period of the immersion. The turbid and transparent parts appeared to be merged into a homogenous texture. Obviously, the apparent homogenous texture in the scaffold showed the uptake of the solution inside the scaffold. For 60 min, the decellularized

pulp solution diffused into the whole texture of the silk fibroin scaffold (Fig 14-A3). For the silk fibroin scaffold with collagen and collagen/decellularized pulp, the apparent homogenous texture appeared throughout the inside of the silk fibroin scaffold at 240 min. It could be explained that collagen and collagen/decellularized pulp had a high viscosity when compared to decellularized pulp. This result demonstrated that the solution had the potential to modify silk fibroin scaffolds by the coating technique. After immersion of the silk fibroin scaffolds in the coating solution, they were soaked in PBS before freeze-drying. Then, the morphologies of the freeze-dried samplesof modified silk fibroin scaffolds were observed by SEM (Fig. 15 and Fig. 16).

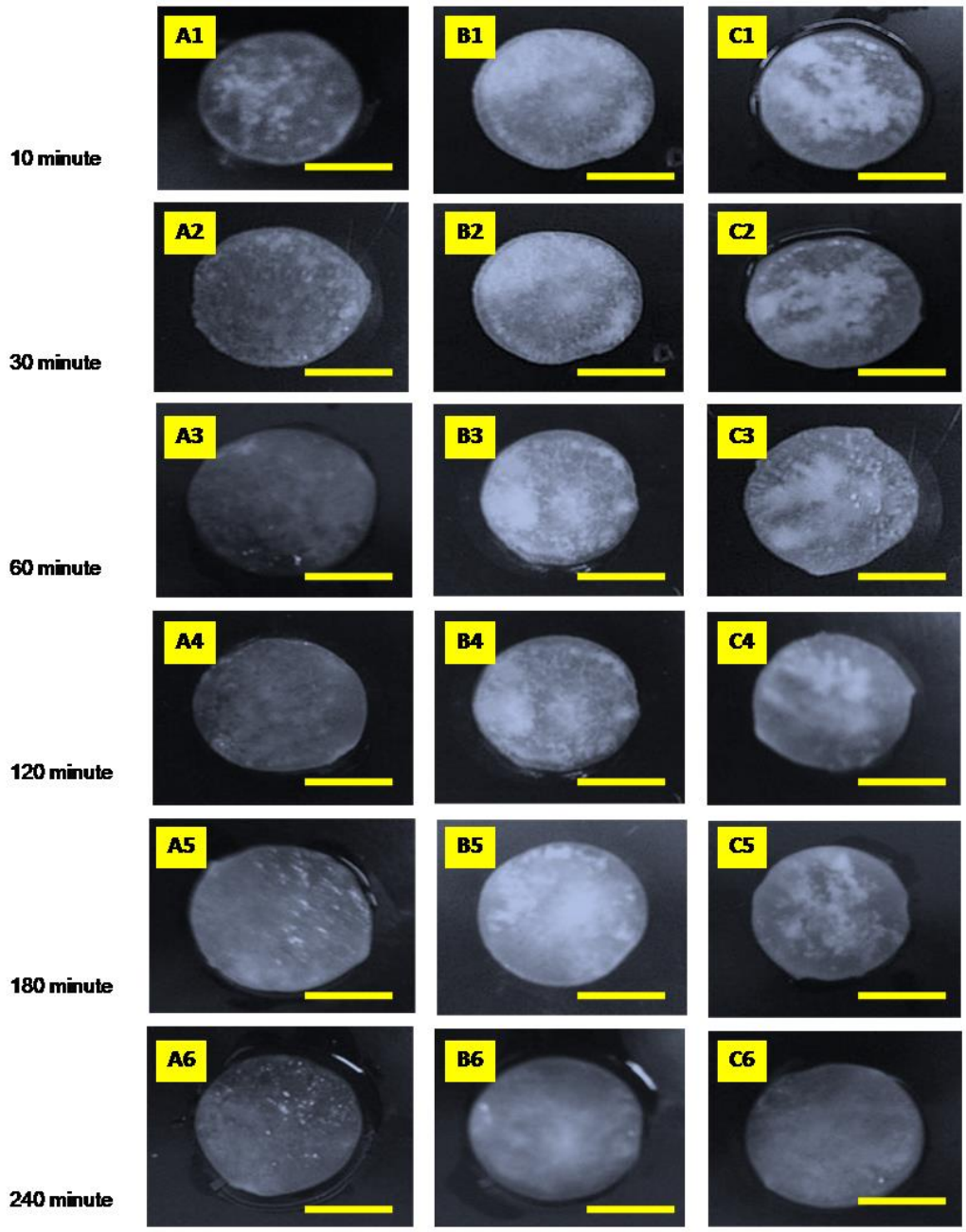

Figure. 14. Images of silk scaffolds after immersion in a coating solution at each time point of 10, 30, 60, 120, 180, and 240 min of decellularized, collagen, and collagen/decellularized solutions: (A1-A6) silk scaffold immersed with decellularized pulp solution, (B1-B6) silk scaffold immersed with collagen solution, (C1-C6) silk scaffold immersed with collagen/decellularized pulp solution. Scale bar: 5 mm.

The surface morphology of silk fibroin scaffold with and without modification showed a porous structure (Fig. 15A). For a silk fibroin scaffold without modification, it showed a smooth surface of the porous walls which had an interconnective porous structure. Significantly, this interconnective porous structure is suitable to support cell adhesion and migration (24). Interestingly, cells can connect with each other in the pores. Furthermore, the pores are suitable for media flow in and out of the silk fibroin scaffold. A porous silk fibroin scaffold can easily remove waste (24). Notably, the morphologies of modified silk fibroin scaffolds with collagen (Fig. 15C) and collagen/decellularized pulp (Fig. 15D) solutions, showed the fibril structure deposited at the inner pores of the silk fibroin scaffolds. This fibril structure might be formed according to the results from AFM observation. Notably, there were no deposited fibril structures in the decellularized pulp solution. This result indicates that the decellularized pulp might be detached from the surface of silk fibroin scaffolds while soaking in the buffer solution.

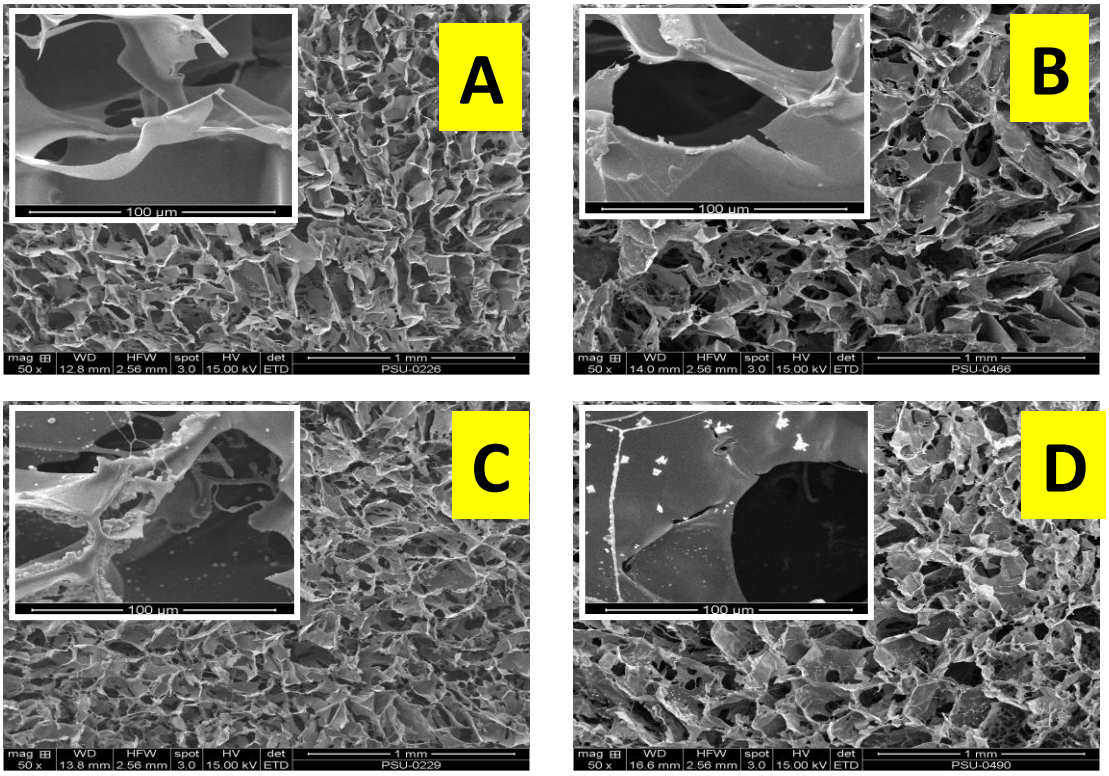

Figure. 15. Surface morphology of the scaffolds observed by scanning electron microscope (SEM) with different magnification. The wall surface is shown at 500x and connective pore size was shown at 50x. (A) surface morphology of silk scaffold without coating, (B) surface morphology of silk scaffold coated with decellularized pulp, (C) surface morphology of silk scaffold coated with collagen, (D) surface morphology of silk scaffold coated with collagen/decellularized pulp. Scale bars are shown in the micrographs.

To confirm the deposition of decellularized pulp and collagen/decellularized pulp solution inside the porous scaffolds, cross sections of the silk fibroin scaffolds were observed by SEM (Fig. 16). Unlike the surface morphology of modified silk fibroin scaffold, the cross-section morphology showed a deposited fibril structure inside the pores of the silk fibroin scaffolds for all coating solutions. As illustrated in the morphologies in Fig. 16, the fibrils organized themselves into a network

structure that was deposited on the pore walls of the silk fibroin scaffold. It demonstrated that decellularized, collagen, and collagen/decellularized solution have the potential for use as a coating solution for modification of the silk fibroin scaffolds. Interestingly, these results indicate that solutions of collagen, decellularized pulp, and collagen/decellularized pulp had the ability to mimic a network structure as in an extracellular matrix.

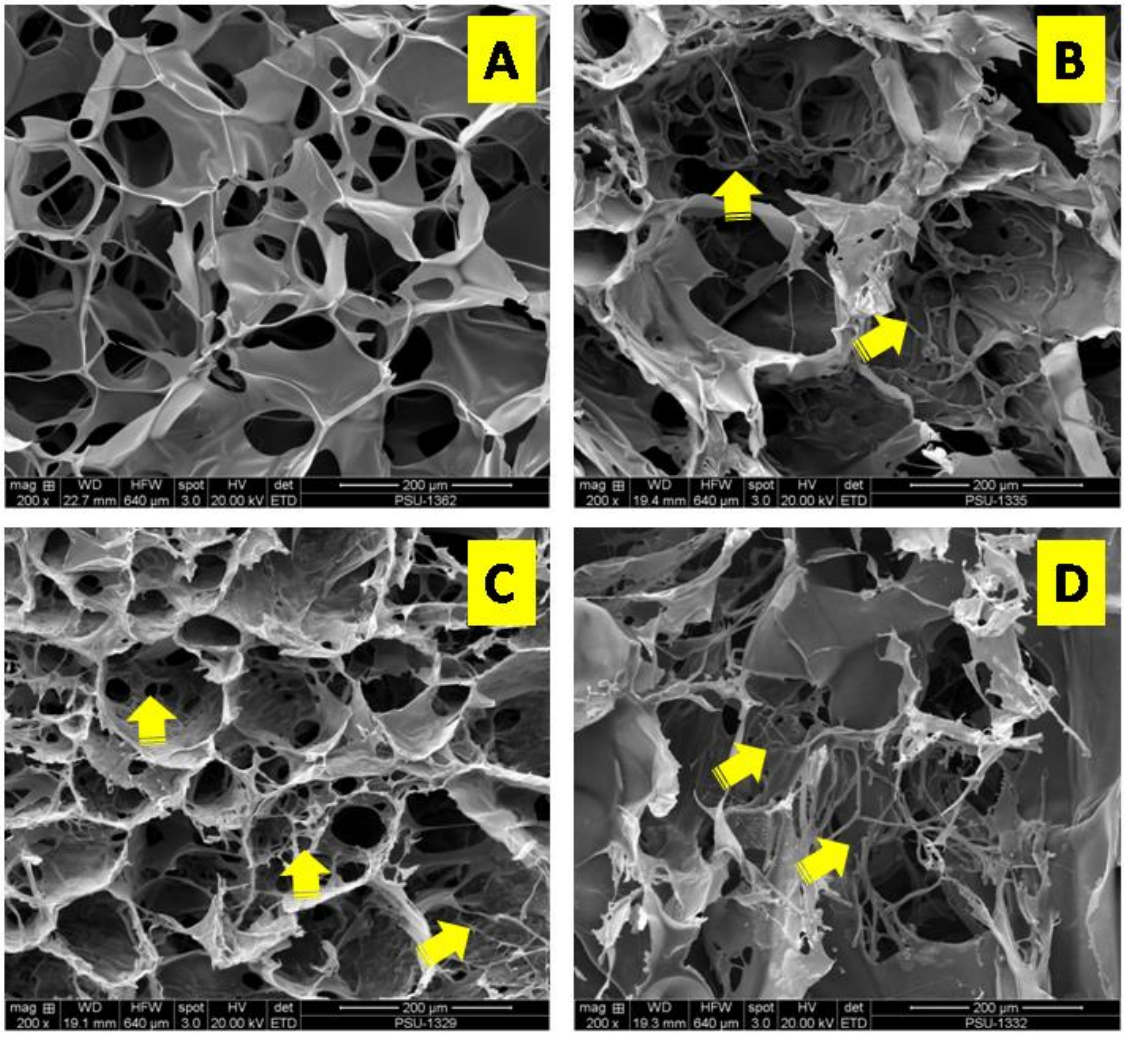

Figure. 16. Cross section morphology of scaffolds observed by scanning electron microscope (SEM): (A) silk scaffold without coating, (B) silk scaffold coated with decellularized pulp, (C) silk scaffold coated with collagen, (D) silk scaffold coated with

collagen/decellularized pulp. Scale bars are shown in the micrographs. Yellow arrow showed fibril structure.

Pore size measurement

In this research, the ImageJ software (1.48v) was used to measure the pore size in each group. The pore distribution of the scaffolds was analyzed from the SEM images. The pore size of the scaffolds in every group was a randomized area. The average pore size of the silk scaffold in all groups is shown in Table 3. The mean pore size of the silk scaffolds was 132.06 ± 3.74μm which was the biggest pore size of all the groups but not significantly different. A minimum pore size of 100 μm with interconnective pores is normally required for a cell culture system that can support the cell size and migration (24).

Table. 3 Average pore size of silk scaffold in each group. ImageJ software measured the silk scaffolds. Values are average ± standard deviation (N=25).

Groups	Pore size
A: Silk scaffold	132.06 ± 3.74μm
B: Silk scaffold coating with decellularized pulp	126.85 ± 2.72μm
C: Silk scaffold coating with collagen	127.94 ± 1.98μm
D: Silk scaffold coating with collagen and decellularized Pulp	125.83 ± 1.98μm

Weight increase of the modified scaffolds

To confirm the existence of collagen and collagen/decellularized pulp on silk fibroin scaffold, the percentage of weight increase was analyzied. The results in Fig. 17 show that the modified silk fibroin scaffolds had a significantly increased weight than the silk fibroin scaffold without modification. It demonstrated that decellularized pulp, collagen, and collagen/decellularized pulp could deposit and exist in the silk fibroin scaffolds. Notably, modified silk fibroin scaffolds with collagen showed a significantly increased weight compared to either silk scaffold modified decellularized pulp and collagen/decellularized pulp. Significantly, the results indicate that the solution of decellularized pulp, collagen, and collagen/decellularized pulp can adhere on silk fibroin scaffolds. These results support the previous results by SEM.

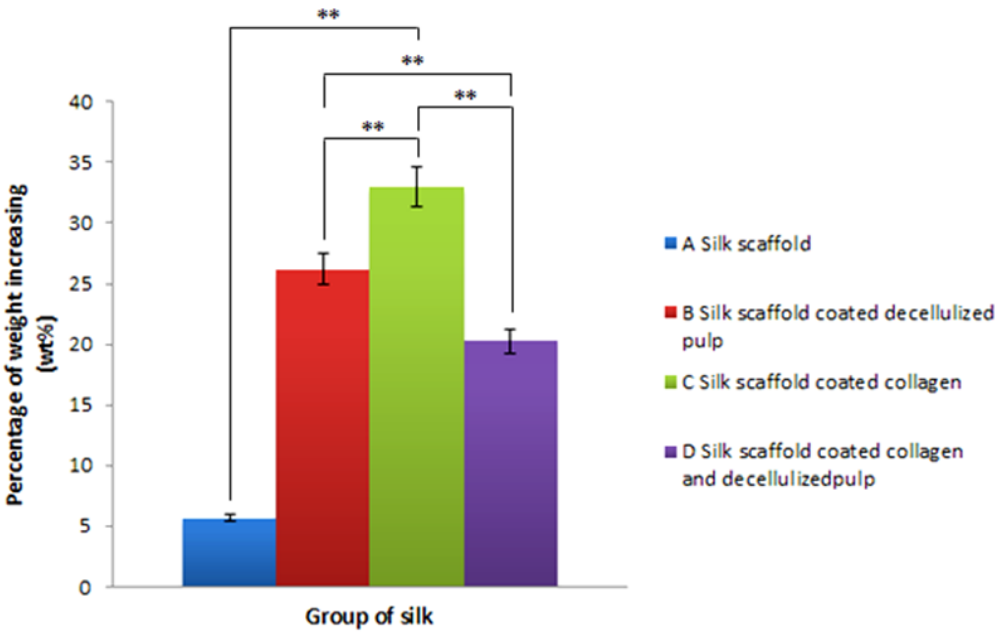

Figure. 17. Weight increase in percentage of deposition of decellularized pulp, collagen and combination of collagen with decellularized pulp. (** $p < 0.01$)

Swelling ratio analysis

Scaffold in all groups were swollen in different percentage, in silk scaffold and silk coated collagen and decellulized pulp can be more obviously swell than other groups. Fig. 18B-C were stable in shape more than silk scaffold and silk coated collagen and decellulized pulp (Fig. 18B-C). The scaffold non coating showed the high water binding capacity and this property plays an important role in tissue regeneration. (25)

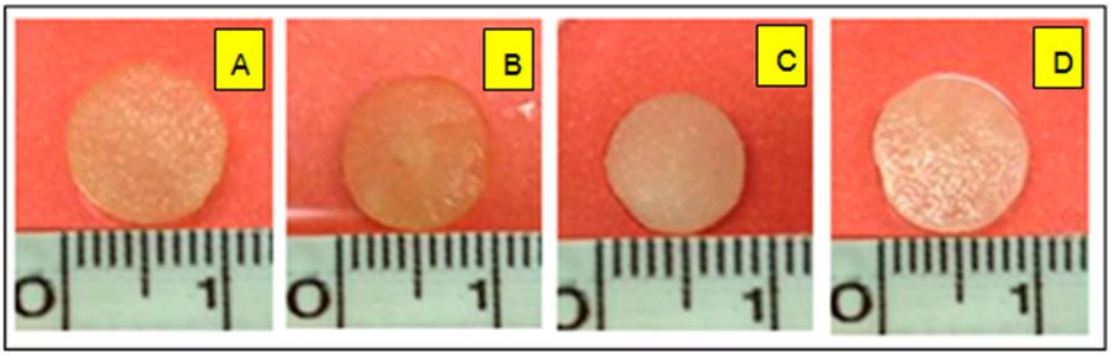

Figure. 18. Image of silk scaffolds: (A) After immersion in PBS, Silk coated decellularized pulp: (B) after immersion in PBS, Silk coated collagen: (C) after immersion in PBS, Silk coated collagen and decellulize pulp: (D) after immersion in PBS.

About swelling properties, silk scaffold was revealed the highest water binding capacity and significantly different with both silk scaffold coated with decellularized pulp and silk scaffold coated with decellularized pulp/collagen as Fig. 19. The coating collagen, and collagen/decellularized pulp on the silk scaffold surface seem to be decreasing the swelling ratio. As the morphological structure of scaffolds, it showed that silk fibroin scaffolds coated with collagen, and collagen/decellularized pulp

had fibril network structure in the porous. Such fibril network effected on decreasing of swelling ratio. This result was similar to the previous study that the swelling property of sponge-like matrice dependent on the network porous structure and microstructure of scaffold (26).

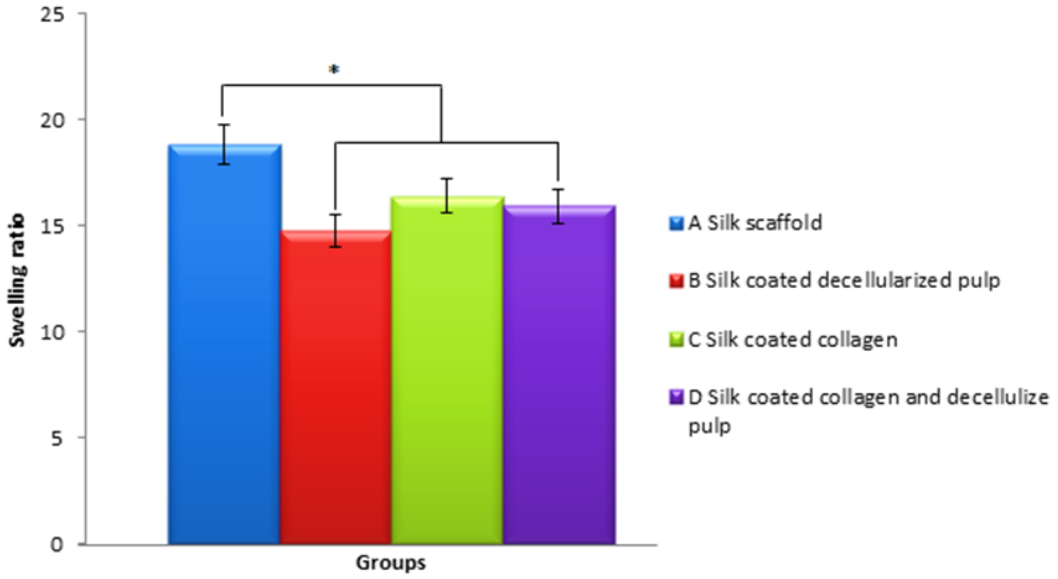

Fig. 19. Showed the swelling ratio of scaffold in each group. (* $p < 0.05$)

Mechanical testing analysis

As the results in mechanical testing, they showed that silk fibroin scaffold and silk fibroin coated with decellularized pulp had higher stress at maximum load and Young's modulus than silk fibroin scaffold coated with collagen and collagen/decellularized pulp. The results indicated that coating solution affected on mechanical properties of silk fibroin scaffolds. The coated samples showed smaller pore size that sample without coating. Such small pore size could retain lower amount of water than large pore size as the results in porous measurement and swelling ratio

analysis. The water in the porous scaffold could resist the compressive force during testing in the wet state. Therefore, the scaffold that could hold the high amount water in porous structure , showed the high stress and Young's modulus.

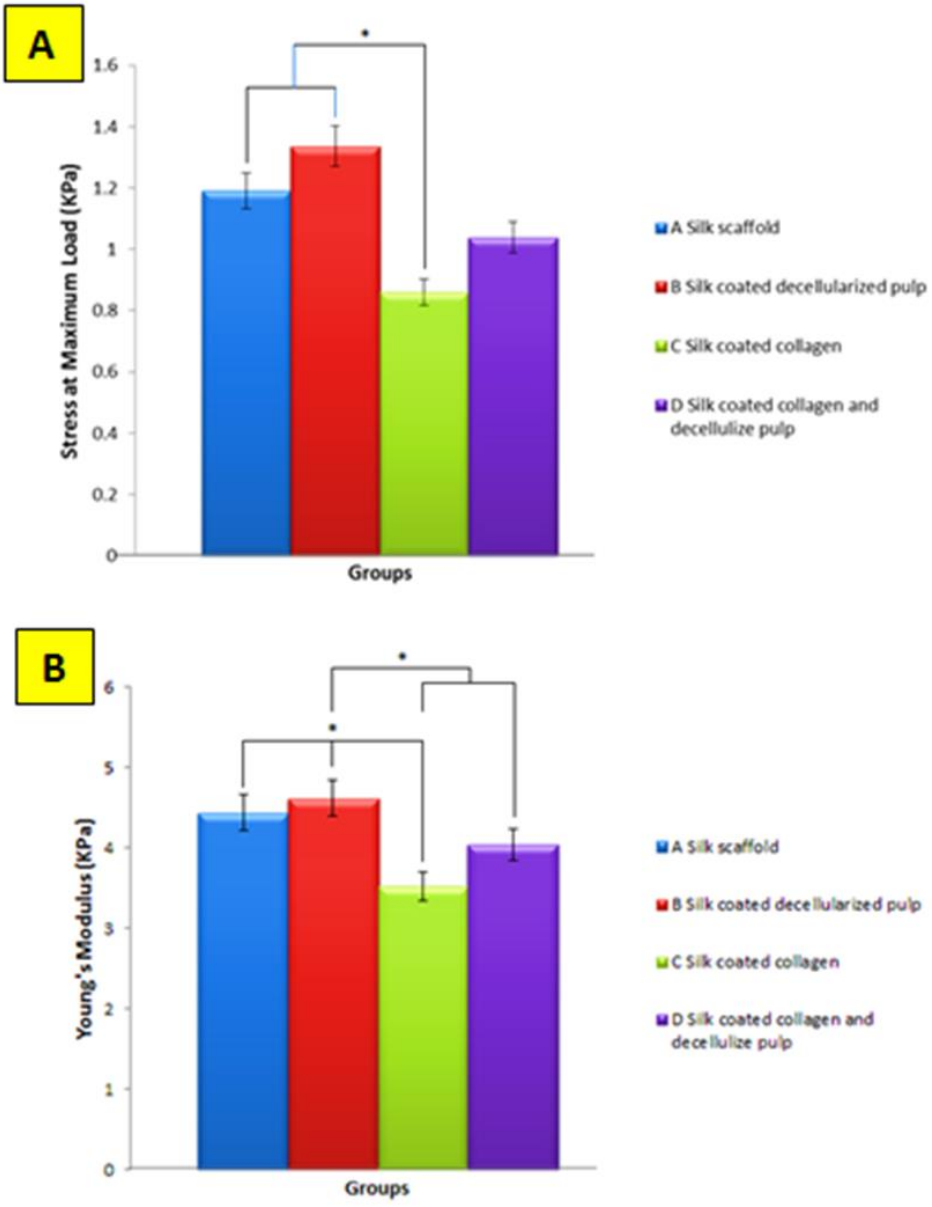

Figure. 20. Image of mechanical properties of scaffold in each group. The stress at maximum load of scaffold (A), The Young's Modulus (KPa) properties (B).

Cell proliferation

PrestoBlue™ was used to evaluate cell proliferation on days 1, 3, 5, and 7. The proliferation of osteoblast cells continuously increased from day 1 to day 5 and became lower on culture day 7 among all groups. On day 1, the silk scaffold modified by decellularized pulp was significantly higher in cell numbers than the silk scaffold without modification (Fig. 21). On day 3, all groups showed a similar behavior of cell proliferation, except the silk scaffold modified with collagen/decellularized pulp which was significantly higher than the other groups. On day 5 all groups became low, but the silk scaffold modified with decellularized pulp was significantly different than the other groups. On day 7, all groups had higher cell proliferation than the silk scaffold without modification.

Significantly, the results of cell proliferation indicated that decellularized pulp had an important role of inducing cell proliferation because the decellularized pulp had components of extracellular matrix. Importantly, the extracellular matrix can enhance cell proliferation (27). Notably, modified silk fibroin scaffold with collagen/decellularized pulp showed the potential to enhance cell proliferation. A previous report demonstrated that collagen acted as an extracellular matrix to induce cell attachment (28). Therefore, to combine collagen with decellularized pulp can synergize cell adhesion and proliferation. Interestingly, from these results, collagen/decellularized pulp might be formed as reconstructed extracellular matrix that has the biofunctionalities of native extracellular matrix. Hence, such reconstructed extracellular matrix has the effect of a high cell proliferation rate.

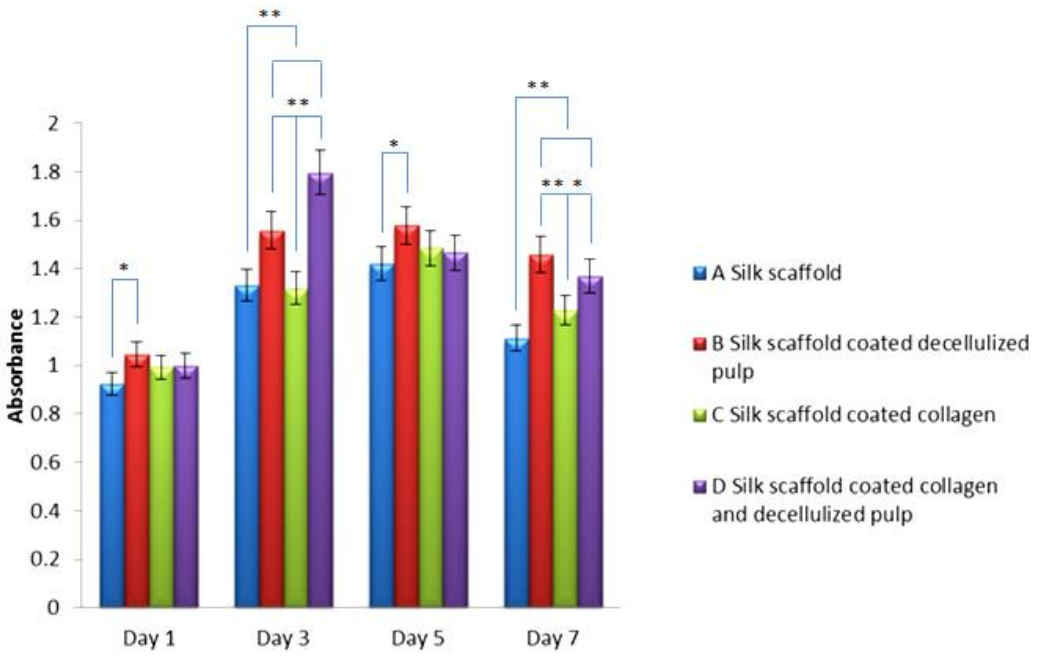

Figure. 21 Cell proliferation on different coating solutions in silk fibroin scaffold. Cell proliferation was evaluated based on the associative number of metabolically active osteoblast cells in each scaffold group identified by the PrestoBlue™ assay. The symbol (*) represents significant changes in resazurin activity of osteoblasts ($p < 0.05$), (**) ($p < 0.01$).

Fluorescein Diacetate (FDA)

To observe the cell morphology in scaffolds, osteoblasts were stained by FDA. Afterward, all samples were observed by a fluorescence microscope (Fig 22). The green luminance showed the nucleus of the osteoblasts. The osteoblasts were able to attach to the surface of silk scaffolds (Fig. 22). Notably, the cells in the modified silk scaffold with collagen/decellularized pulp arranged themselves into a dense aggregation. This result indicates that collagen/decellularized pulp can promote cell adhesion. Interestingly, cell adhesion might have come from the reconstructed extracellular matrix of collagen/decellularized pulp as previously explained.

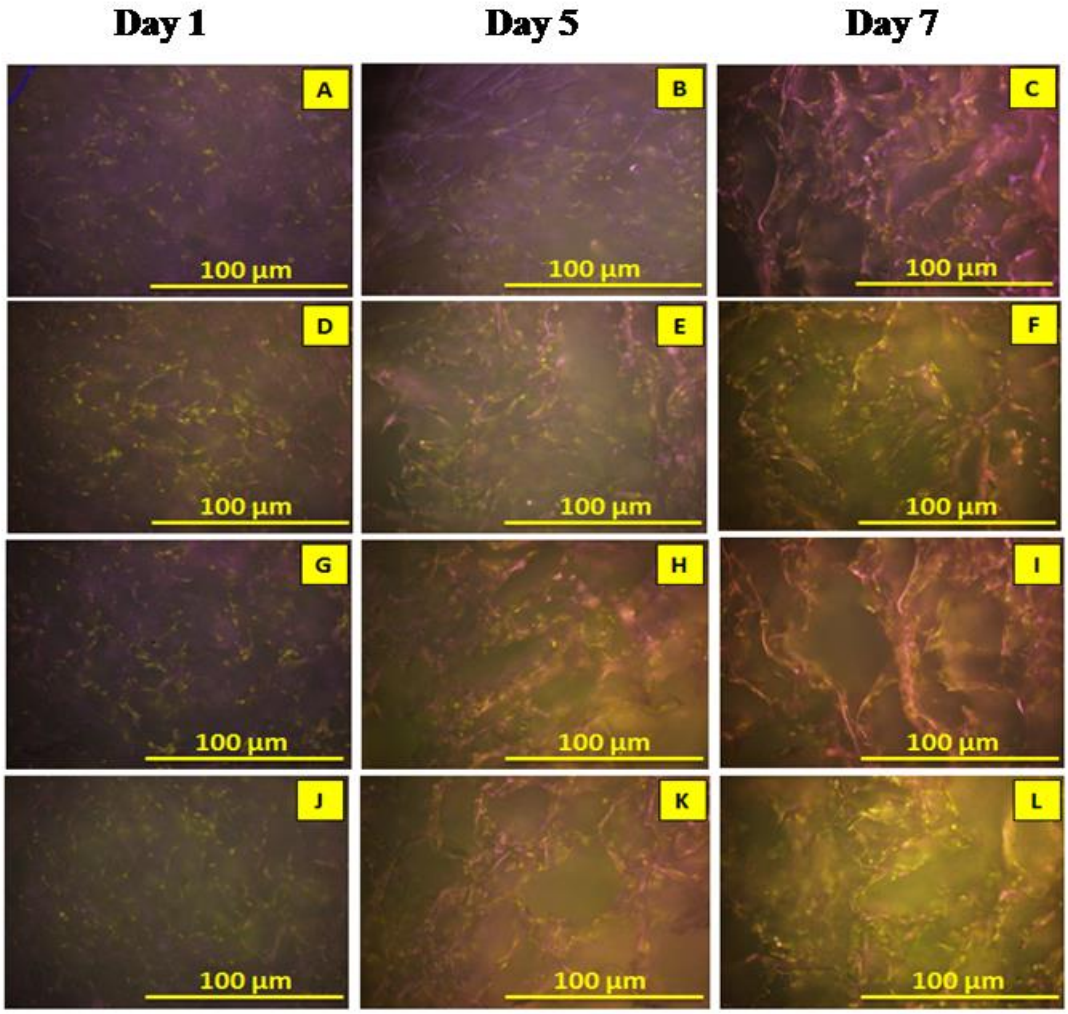

Figure. 22 Fluorescence image of the obvious cells and interconnections of osteoblast cells on the silk scaffold (FDA label, green brightness). A) silk scaffold, B) silk scaffold coated with decellularized pulp, C) silk scaffold coated with collagen, D) silk scaffold coated with collagen/decellularized pulp.

Bicinchoninic acid (BCA) analysis

Analysis of the protein during cell culturing was determined by BCA analysis. The total protein content on days 7, 14, and 21 are shown in Fig. 23. For days 7 and 14, the modified silk scaffold with collagen had a higher protein content than all groups. As previously reported, this demonstrated that the osteoblasts start protein

synthesizing on day 7 (29). Therefore, at days 7 and 14 the modified silk scaffold with collagen showed higher protein content than the other samples. These results indicate that the protein content at days 7 and 14 came from two main parts: 1) coated collagen on the scaffold and 2) secreted collagen from the osteoblasts. So, it can confirm the previous results that the protein content in the modified scaffold with collagen is higher than the other samples.

Interestingly, the protein content at day 21 of the modified silk fibroin scaffold with collagen/decellularized pulp is predominantly higher than the other samples. On day 21, the silk fibroin scaffold coated with collagen/decellularized pulp and the silk fibroin scaffold coated with decellularized pulp continuously showed higher protein synthesizing. On the other hand, protein synthesizing in the silk fibroin scaffold and silk scaffold coated with collagen became low at day 21. These results demonstrated that the coated components on modified silk fibroin scaffolds with collagen/decellularized pulp had a unique role in promoting protein synthesizing (Fig. 23). It indicated that the biofunctionalities of collagen and decellularized pulp could synergize protein.

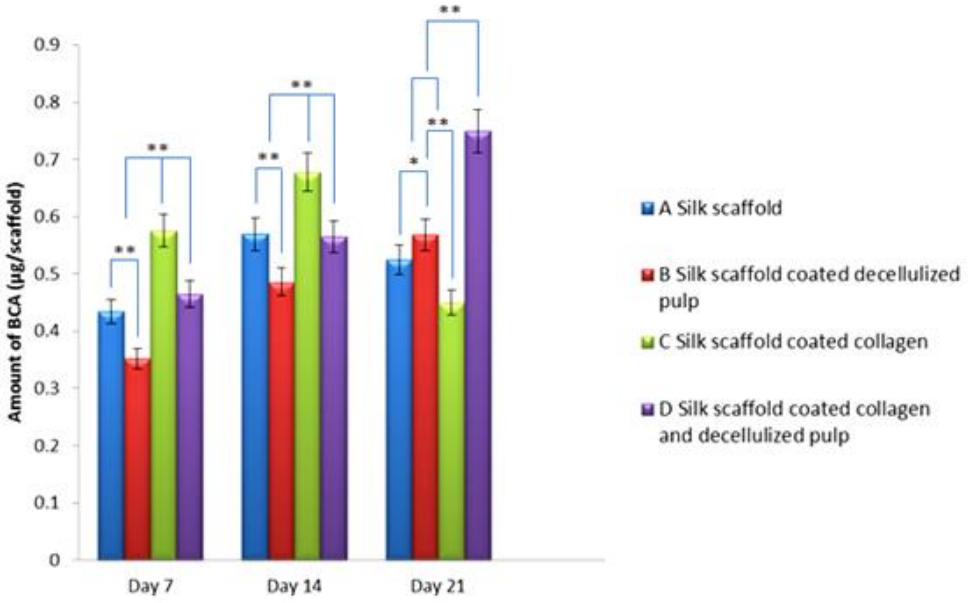

Figure. 23 Total protein content of osteoblast cells (MG63) on silk scaffold. Protein synthesis was evaluated by using the Pierce BCA protein assay. The symbol (*) represents significant changes in protein activity of osteoblasts ($p < 0.05$), (**) ($p < 0.01$).

Histological analysis

Osteoblast cells showed a good distribution throughout the silk scaffold in all groups. In Fig. 24, the red arrows point at the silk scaffold and the yellow arrows point at the osteoblast cells attached to the silk scaffold. The silk coated with decellularized pulp (Fig. 24B), collagen (Fig. 24C), and collagen/decellularized pulp (Fig. 24D) showed more osteoblast cells attached to the surface of the silk scaffold and the cells filled the pores of the scaffolds. The shape of the osteoblast cells was flat on the silk scaffold surface and the blue color indicates the nucleus that is located at the center of the cytoplasm. These results indicated that modified silk fibroin scaffold could induce cell adhesion.

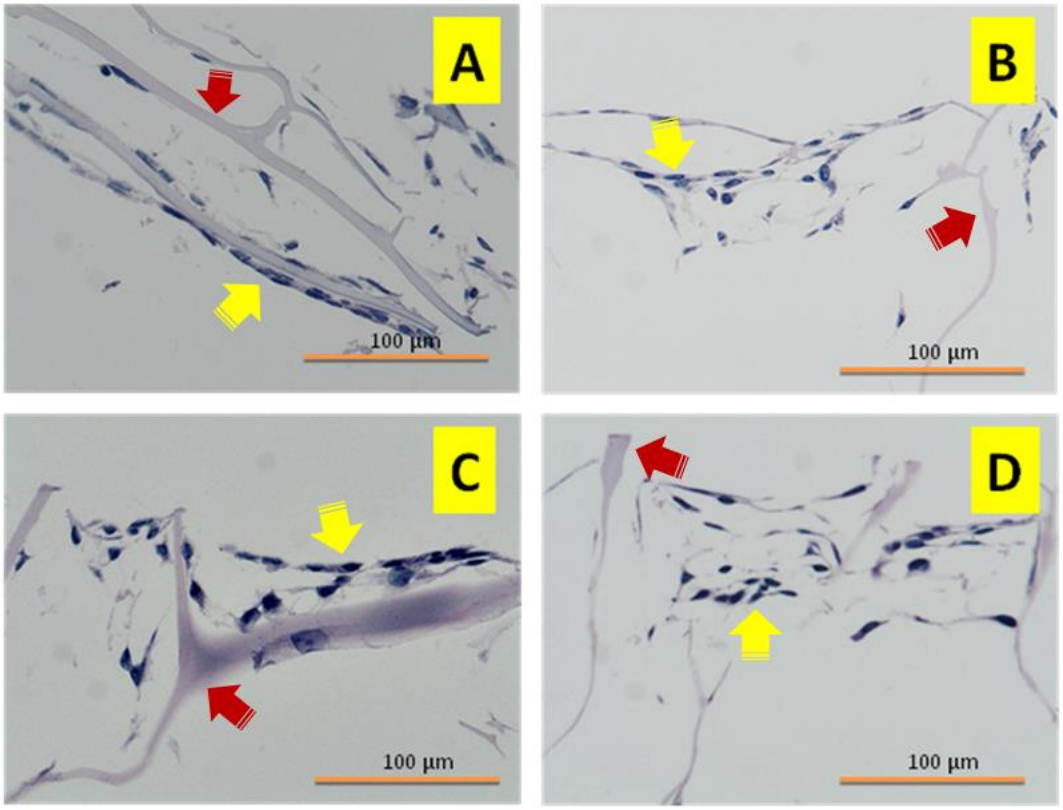

Figure. 24 Hematoxylin and eosin staining of cross sections on day 5 (A, B, C, D). The red arrows show the silk scaffold in each group. The yellow arrows show the osteoblast cells attached to the silk scaffold in all groups; A) silk scaffold, B) silk scaffold coated with decellularized pulp, C) silk fibroin coated with collagen, D) silk fibroin coated with collagen/decellularized. Scale bar: 100 µm.

Conclusion

This research demonstrated that the use of collagen, decellularized pulp, and collagen/decellularized pulp solutions for scaffold modification is attractive and is a potential approach to enhance the biofunctionalities of silk fibroin scaffolds. The solutions could organize themselves into fibrils that deposited in the pores of the silk fibroin scaffolds. More importantly, the results indicated that the fibrils in modified silk fibroin scaffolds can induce biofunctionalities including cell proliferation, cell viability, and

protein synthesis. Furthermore, the histological analysis demonstrated that cells could adhere well to the modified silk fibroin scaffolds. Interestingly, it indicated that the modified silk fibroin scaffolds coated with collagen/decellularized pulp had a unique structure and demonstrated biofunctionalities. The structure and biofunctionalities could enhance the performance of modified silk fibroin scaffold. Eventually from these results, it can be deduced that modified silk fibroin scaffold coated with collagen/decellularized pulp has promise for use in bone tissue engineering particularly in cleft palate.

Reference

1. G. Chang, H.-J. Kim, D. Kaplan, G. Vunjak-Novakovic, R. A. Kandel, Porous silk scaffolds can be used for tissue engineering annulus fibrosus. Eur Spine J. 16; 2007: 1848-1857.
2. Le-Ping Yan, Joana Silva-Correia, Cristina Correia, Sofia G Caridade, Emanuel M Fernandes, Rui A Sousa, Joao F Mano, Joaquim M Oliveira, Ana L Oliveira, Rui L Reis. Bioactive macro/micro porous silk fibroin/nano-sized calcium phosphate scaffolds with potential for bone-tissue-engineering applications. Nanomedicine. 8; 2013: 359-378.
3. Yong Zhao, R.Z. Legeros, Jing Chen. Initial Study on 3D Porous Silk Fibroin Scaffold: Preparation and Morphology. Bioceramics Development and Applications. 1; 2011: 1-3.
4. Phanat Kittiphattanabawon, Soottawat Benjakul, Wonnop Visessanguan, Hideki Kishimura, Fereidoon Shahidi. Isolation and Characterisation of collagen from the skin of brownbanded bamboo shark (Chiloscyllium punctatum). Food Chemistry. 119; 2010: 1519–1526.
5. Samantha B. Traphagen, Nikos Fourligas, Joanna Xylas, Sejuti Sengupta, David Kaplan, Irene Georgakoudi, Pamela C. Yelick. Characterization of Natural, Decellularized and Reseeded Porcine Tooth Bud Matrices. Biomaterials. 33; 2012: 5287-5296.
6. A. Gigante, S. Manzotti, C. Bevilacqua, M. Orciani, R. Di Primio, M. Mattioli-Belmonte. Adult mesenchymal stem cells for bone and cartilage engineering: effect of scaffold materials. European Journal of Histochemistry. 52; 2008: 169-174.
7. Chen K, Sahoo S, He P, Ng KS, Toh SL, Goh JC. A Hybrid Silk/RADA-Based Fibrous Scaffold with TripleHierarchy for Ligament Regeneration. Tissue Eng: Part A. 18; 2012: 1399-1409.
8. Naresh Kasoju, Dana Kubies, Marta M. Kumorek, Jan Krız, Eva Fabryova, Lud ka Machova, Jana Kovarova, Frantisek Rypacek. Dip TIPS as a Facile and Versatile Method for Fabrication of Polymer Foams with Controlled Shape Size and Pore Architecture for Bioengineering Applications. PLoS ONE. 9; 2014: 1-16.

9. Pengfei He, Sambit Sahoo, Kian Siang Ng, Kelei Chen, Siew Lok Toh, James Cho Hong Goh. Enhanced osteoinductivity and osteoconductivity throughhydroxyapatite coating of silk-based tissue-engineeredligament scaffold. Biomedical Materials Research Part A. 101A; 2013: 555-566.
10. Nicholas Guziewicza, Annie Besta, Bernardo Perez-Ramireza, and David L. Kaplanb. Lyophilized Silk Fibroin Hydrogels for the Sustained Local Delivery of Therapeutic Monoclonal Antibodies. Biomaterials. 32; 2011: 2642–2650.
11. Xiaochen Liu, Minzhi Zhao, Jingxiong Lu, Jian Ma, Jie Wei, Shicheng Wei. Cell responses to two kinds of nanohydroxyapatite with different sizes and crystallinities. International Journal of Nanomedicine. 7; 2012: 1239-1250.
12. Beom-Su Kim, Hyo Jin Kang, Jun Lee. Improvement of the compressive strength of a cuttlefish bone-derived porous hydroxyapatite scaffold via polycaprolactone coating. Journal of Biomedical Materials Research Part B: Applied Biomaterials. 101; 2013: 1302-1309.
13. Hairong Liu, Leilei Xia, Yao Dai, Man Zhao, Zheng Zhou, Hongbo Liu. Fabrication and characterization of novel hydroxyapatite/porous carbon composite scaffolds. Materials Letters. 66; 2011: 36–38.
14. Ting-Ting Li, Katrin Ebert, Jurgen Vogel, Thomas Groth. Comparative studies on osteogenic potential of micro- and nanofibre scaffolds prepared by electrospinning of poly(ε-caprolactone). Progress in Biomaterials. 2; 2013: 1-13.
15. Falguni Pati, Hemjyoti Kalita, Basudam Adhikari, Santanu Dhara. Falguni Pati, Hemjyoti Kalita, Basudam Adhikari, Santanu Dhara. Osteoblastic cellular responses on ionically crosslinked chitosan-tripolyphosphate fibrous 3-D mesh scaffolds. Journal of Biomedical Materials research Part A. 101A; 2013: 2526-2537.
16. Michael B. Keogh, Fergal J. O' Brien, Jacqueline S. Daly. A novel collagen scaffold supports human osteogenesis applications for bone tissue engineering. Cell and Tissue Research. 340; 2010: 169–177.
17. David E. Birk, Emanuel I. Zycband, Donald A. Winkelmann, Robert L. Trelstad. Collagen fibrillogenesis in situ: Fibril segments are intermediates in matrix assembly. Proc. Nati. Acad. Sci. USA. 86; 1989: 4549-4553.
18. Century Pharmaceuticals, Inc., Diluted Dakin's Solution Support for Antisepsis of Chronic Wounds.

19. J. A. Beeley, H. K. Yip, A. G. Stevenson. Conservative dentistry: Chemochemical caries removal: a review of the techniques and latest developments. British Dental Journal. 188; 2000: 427-430.
20. John A., Hong L., Ikada Y., Tabata Y. A trial to prepare biodegradable collagen-hydroxyapatite composites for bone repair. J Biomater Sci Polym Ed. 12; 2001: 689-705.
21. Olena S. Rabotyagova, Peggy Cebe, David L. Kaplan. Collagen Structural Hierarchy and Susceptibility to Degradation by Ultraviolet Radiation. Mater Sci Eng C Mater Biol Appl. 28; 2008: 1420–1429.
22. Mitra Naeimi, Mohammadhossein Fathi, Mohammad Rafienia, Shahin Bonakdar. Silk Fibroin-Chondroitin Sulfate-Alginate Porous Scaffolds: Structural Properties and In Vitro Studies. J. APPL. POLYM. SCI. 131; 2014: 1-9.
23. Mehdi Farokhi, Fatemeh Mottaghitalab, Jamshid Hadjati, Ramin Omidvar, Mohammad Majidi, Amir Amanzadeh, Mahmoud Azami, Seyed Mohammad Tavangar, Mohammad Ali Shokrgozar, Jafar Ai. Structural and Functional Changes of Silk Fibroin Scaffold Due to Hydrolytic Degradation. J. APPL. POLYM. SCI. 131; 2013: 1-8.
24. Ung-Jin Kim, Jaehyung Park, Hyeon Joo Kim, Masahisa Wada, David L. Kaplan. Three-dimensional aqueous-derived biomaterial scaffolds from silk fibroin. Biomaterials. 26; 2005: 2775–2785.
25. Le-Ping Yan, Ying-Jun Wang, Li Ren, Gang Wu, Sofia G. Caridade, Jia-Bing Fan, Ling-Yun Wang, Pei-Hong Ji, Joaquim M. Oliveira, Joao T. Oliveira, Joao F. Mano, Rui L. Reis. Genipin-cross-linked collagen/chitosan biomimetic scaffolds for articular cartilage tissue engineering applications. Journal of Biomedical Materials Research Part A. 95A; 2010: 465-475.
26. Si-Nae Park, Jong-Chul Park, Hea Ok Kim, Min Jung Song, Hwal Suh. Characterization of porous collagen/hyaluronic acid scaffold modified by 1-ethyl-3-(3-dimethylaminopropyl) carbodiimide cross-linking. Biomaterials. 23; 2002: 1205–1212.
27. Goldberg M, Smith J. Cells and Extracellular Matrices of Dentin and Pulp: A Biological Basis For Repair and Tissue Engineering. Crit Rev Oral Biol Med. 15; 2004: 13-27.

28. Gang Zhou, Guimin Zhang, Zhe Wu, Yongzhao Hou, Ming Yan, Haifeng Liu, Xufeng Niu, A. Ruhan, Yubo Fan. Research on the Structure of Fish Collagen Nanofibers Influenced Cell Growth. Journal of Nanomaterials. 2; 2013: 1-6.
29. S. I. Dworetzky, E. G. Fey, S. Penmant, J. B. Lian, J. L. Stein, G. S. Stein. Progressive changes in the protein composition of the nuclear matrix during rat osteoblast differentiation. Proc. Natl. Acad. Sci. 87; 1990: 4605-4609.

CHAPTER 4

Biofunctional mimicked silk fibroin scaffolds coated with reconstructed extracellular matrix of decellularized pulp/fibronectin as clues for maxillofacial bone tissue engineering in bone defect from oral cancer

Abstract

Oral cancer is a disease that leads to bone loss in the maxillofacial area. To replace bone loss by advanced biomaterials is a challenge for materials scientists and maxillofacial surgeons. In this research, biofunctional mimicked silk fibroin scaffolds were created as an advanced biomaterial for bone substitution. Silk fibroin scaffolds were fabricated by freeze-drying before coating with three different components: decellularized pulp, fibronectin, and decellularized pulp/fibronectin. The structure formation of the coating components and the morphology of the coated scaffolds were observed by atomic force microscope and scanning electron microscope, respectively. Existence of the coating components in the scaffolds was proved by the increase in weight. The coated scaffolds were seeded by MG-63 osteoblasts and cultured. Testing of the biofunctionalities included cell viability, calcium content, alkaline phosphatase activity (ALP), mineralization, and a histological analysis. The results demonstrated that the coating components existed in the scaffolds after coating. The coating components organized themselves into aggregations of globular structure. They were deposited and arranged themselves into clusters of aggregations with a fibril structure in the porous

walls of the scaffolds. The results showed that coated scaffolds with decellularized pulp/fibronectin were suitable for cell viability since the cells could attach and spread into most of the pores of the scaffold. Furthermore, the scaffolds could induce calcium synthesis, mineralization, and ALP activity. The results indicated that coated silk fibroin scaffolds with decellularized pulp/fibronectin hold promise for use in bone tissue engineering in bone defect from oral cancer.

Materials and Methods

Preparation of silk fibroin scaffolds

The degummed silk fibroin was obtained by boiling in 0.02 M Na_2CO_3 for 30 minutes. The silk sericin was removed after rinsing 3 times with distilled water. It was dried in a hot air oven at 60 °C for 24 h and the degummed silk fibroin was then dissolved in 9.3 M LiBr at 70 °C for 3 h (1). The purified silk fibroin was obtained after dialyzing with distilled water for 3 days (2). The purified silk fibroin was centrifuged at 3000 RPM at 4 °C for 5 minutes to separate the dregs from the solution. The concentration was adjusted to yield a 3% (w/v) and kept at 4 °C until further use. The solution was placed in 48-well plates to mold the 3D scaffolds. The freeze-drying method fabricated the porous silk fibroin scaffolds. All scaffolds were cut into discs (10 mm diameter x 2 mm thickness).

Preparation of decellularized pulp

We collected teeth from children who were 6-10 years old and then segmented the teeth in half to harvest the pulp tissue. Collagenase and dispase were used to digest the pulp for 1 hour. The solution was separated from the debris using a centrifuge at 37 °C and washed with phosphate-buffered saline (PBS) 2 times. Finally, the solution was filtered to obtain the decellularized pulp and the freeze-drying process was used for water sublimation (3).

Modification of silk fibroin scaffolds

The 4 groups of solutions are shown in Table 4. The decellularized pulp was prepared at a concentration of 0.1 mg/ml in 0.1% sodium hypochlorite. Fibronectin was prepared at a concentration of 0.1 mg/ml in deionized water. A combination of decellularized pulp and fibronectin was prepared at a ratio of 50:50. After soaking the SF scaffolds in each solution for 4 h, they were put in 1X PBS for 30 min. The freeze-drying method attached the ECM to the SF scaffolds.

Table 4. Groups of coated silk fibroin scaffolds with different ECMs

Group	Detail
A	Silk fibroin scaffold
B	Coated silk fibroin scaffold with decellularized pulp
C	Coated silk fibroin scaffold with fibronectin
D	Coated silk fibroin scaffold with decellularized pulp/fibronectin

Scanning Electron Microscopy (SEM) Observation

Scanning electron microscope (SEM) (Quanta400, FEI, Czech Republic) was used to observe the morphology and characterization of the SF scaffolds that were coated with the solutions. The samples were pre-coated with gold using a gold sputter coating machine (SPI Supplies, Division of Structure Probe, Inc., Westchester, PA, USA).

Atomic Force Microscopy Observation

A sample of coating solution from each group was dropped onto a glass slide, smeared, and soaked in PBS for 30 min. When the slides were dry, the morphology and structure using atomic force microscopy was observed (Nanosurf EasyScan 2 AFM, Switzerland).

Cell culturing of MG-63 osteoblasts

MG-63 osteoblasts were seeded in each scaffold with 1×10^6 cells and maintained in an alpha-MEM medium (α-MEM: Gibco®, Invitrogen™, Carlsbad, CA, USA) with the addition of 1% penicillin/streptomycin, 0.1% Fungizone, and 10% fetal bovine serum at 37 °C in a humidified 5% CO_2/95% air incubator. The medium was changed every 3-4 days (4). An osteogenic medium (OS: 20 mM b-glycerophosphate, 50 μM ascorbic acid, and 100 nM dexamethasone; Sigma-Aldrich) was used for osteoblast differentiation of the MG-63 osteoblast cells (5).

Calcium content assay

Calcium colorimetric assays (Calcium Colorimetric Assay Kit, BioVision Inc., Milpitas, CA, USA) was used to determine the calcium level secreted from the osteoblast cells. The cells were cultured on SF scaffolds at 7, 14, and 21 days (6). The cells were then lysed by adding 1% Triton X in each well. The SF scaffolds were frozen at -70 °C for 50 min and then thawed at room temperature for 1 h. This was repeated 3 times. The solutions were transferred to Eppendorf tubes and centrifuged at 20,000 RPM for 10 min to remove the supernatant from the pellets (7). The supernatant (30 µl) was placed in 96-well plates and the volume was adjusted to 50 µl with distilled water. Next 90 µl of Chromogenic Reagent and then 60 µl of the Calcium Assay Buffer were added to each well and mixed gently. The reaction was incubated for 5-10 min at room temperature and protected from light. The optical density was measured at 575 nm.

Alkaline Phosphatase (ALP) assay

The cells were cultured for 7, 14, and 21 days (Sung Eun Kim) for ALP analysis. The SF scaffolds in each group were washed twice with PBS. To extract the cellular proteins, 800 µl of cell lysis solution (1% Triton X in PBS) was added in each well. The SF scaffolds were frozen at -70 °C for 1 hour and then thawed at room temperature for 1 hour. This was repeated 3 times. The solutions were transferred to Eppendorf tubes and centrifuged at 20,000 RPM for 10 min to remove the supernatant from the pellets. The alkaline phosphatase Colorimetric Assay Kit (Abcam®, Cambridge, UK) was used to detect the ALP activity of the cells in the SF scaffolds. The

phosphatase substrate in the kit used *p*-nitrophenyl phosphate that turned to a yellow color when dephosphorylated by the ALP.

Mineralization assay

Alizarin red staining assay was used for mineralization of the nodules. The alizarin red technique detected calcium deposits on the SF scaffolds in each group. The cells in the SF scaffold were cultured for 14 days and then washed twice with PBS. The cells were fixed with 4% formaldehyde and 1 ml of alizarin red solution (2 gm in 100 ml of distilled water and pH adjusted to 4.1- 4.3) was added. After 20 min at room temperature in the dark, the alizarin red solution was carefully removed from the SF scaffolds and the SF scaffolds were washed four times with distilled water. Mineralization nodules were observed under a microscope (8).

Histology

The cell-cultured SF scaffolds were fixed with 4% formaldehyde at 4 °C for 24 h and samples taken on day 5 for cell morphology and on day 14 for detection of calcium. The SF scaffolds in each group were immersed in paraffin and the paraffin sections were cut at 5μ and placed on a glass slide. The sections were then deparaffinized and hydrated in distilled water. The sample slides were stained in 2 ways. Firstly, hematoxylin and eosin (H&E) stain was used to observe cell migration and adhesion on the SF scaffold. Secondly, von Kossa staining was used to detect calcium deposits that were secreted from the osteoblast cells.

Statistical analysis

The samples were measured and statistically compared by one-way ANOVA followed by Tukey's HSD test (SPSS 16.0 software package). Statistical significance was defined as $*p < 0.05$, and $**p < 0.01$.

Results and discussion

Characterization of reconstructed formation of decellularized pulp/fibronectin

In this research, silk fibroin scaffolds were prepared by the freeze-drying process. The silk fibroin scaffolds were formed into 3D porous scaffolds that were cut into discs (10 mm diameter by 2 mm thickness). The silk fibroin scaffolds were white with a consistent pore size (Figure 25).

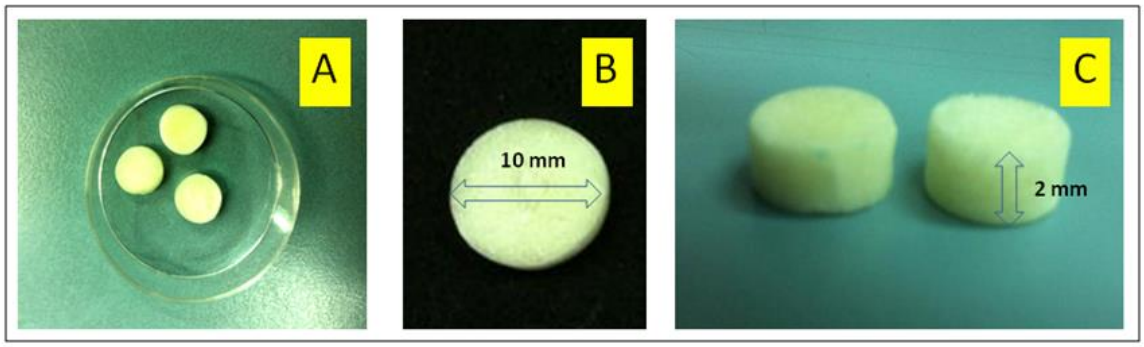

Figure 25. Silk fibroin scaffolds after freeze-drying and cut into discs (10 mm diameter x 2 mm thickness).

Before coating the silk fibroin scaffolds, the organization of the reconstructed decellularized pulp/fibronectin was observed by AFM (Figure 26). It was demonstrated that decellularized pulp without fibronectin organized themselves into a connected aggregation of globular structure (Figure 26A). This globular structure might

be the fragments of ECM during dissolution with sodium hypochlorite. In the case of fibronectin, there was an aggregation of globular structure that was connected into a dendrite structure (Figure 26B). In the case of decellularized pulp with fibronectin, both components organized themselves into an aggregation of a large dendrite structure (Figure 26C). As previously reported, the fibronectin acted as the binding component in the ECM (9). This indicated that fibronectin might connect with the fragments of the ECM. Furhermore, fibronectin plays the role of reconstructing the fragments of the ECM into a large dendrite structure. The decellularized pulp/fibronectin organized themselves into a more complicated structure than the decellularized pulp or fibronectin.

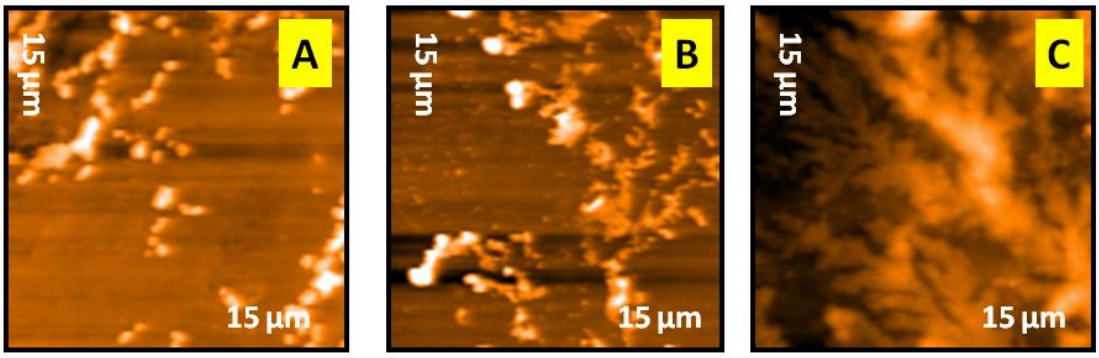

Figure 26. Structure formation from AFM: (A) Decellularized pulp, (B) Fibronectin, (C) Decellularized pulp/fibronectin.

Morphological analysis of modified silk fibroin scaffolds

The images of SEM observation of the surface of the silk fibroin scaffolds in each group are shown in Figure 3. The surface of the silk fibroin scaffold showed a smooth and interconnective pore size that supported cell adhesion (Figure 27A). Moreover, the cells could connect with other cells which was suitable for media flow in and out of the silk fibroin scaffold. The decellularized pulp showed some small

fibrils that covered the surface of the pores in the scaffold (Figure 27B). Those small fibrils might be the organized fragments of ECM components. Fibronectin showed a globular structure that covered the surface of the pores in the in scaffold (Figure 27C). Finally, decellularized pulp with fibronectin showed predominant fibers that covered most of the areas of the porous surface (Figure 27D). Interestingly, decellularized pulp with fibronectin could synergize the reconstruction into a complicated structure.

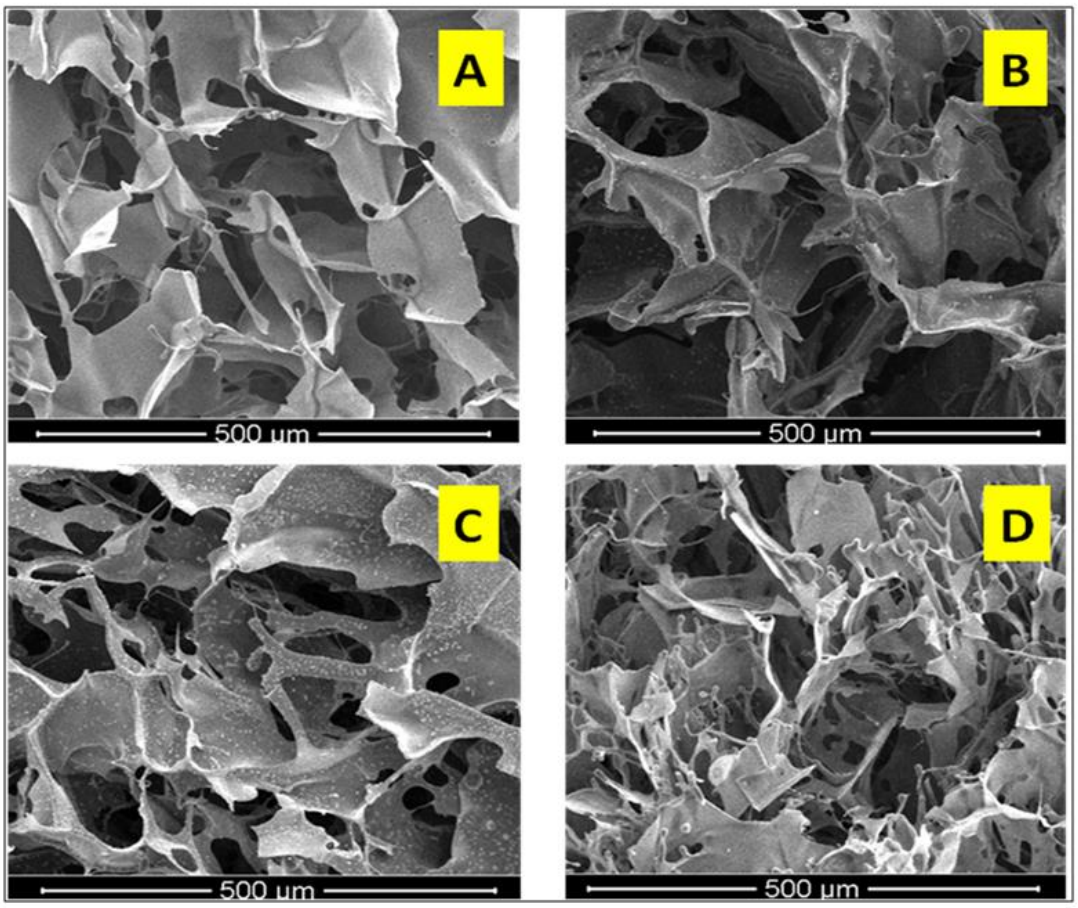

Figure 27. SEM images of surface morphology: (A) Silk scaffold, (B) Coated silk fibroin scaffold with decellularized pulp, (C) Coated silk fibroin scaffold with fibronectin, (D) coated silk fibroin scaffold with decellularized pulp/fibronectin.

The cross-section morphology of the coated silk fibroin scaffolds was observed by SEM (Figure 28). Smooth surfaces and regular pore sizes were found in the silk fibroin scaffolds (Figures 28A, B). In the case of decellularized pulp without fibronectin, the fibril structure of ECM fragments were attached to the surface and made rough properties on the surface (Figures 28C, D). The fibronectins arranged themselves into a small globular structure that covered the surface of the pores (Figures 28E, F). Finally, decellularized pulp/fibronectin organized themselves into a globular and fibril structure that adhered to the surface (Figures 28G, H).

Notably, the coated silk fibroin scaffolds with decellularized pulp, fibronectin, and decellularized pulp/fibronectin showed globular and fibril structures that attached in the pores. Those structures appeared in the surface and cross-section morphology of the coated silk fibroin scaffolds. Interestingly, the results of the surface and cross-section morphology demonstrated that decellularized pulp/fibronectin could reconstruct into a complicated structure. This complicated structure showed the globules connected with the fibril structure. The complicated structure of the reconstructed decellularized pulp/fibronectin might be clues to induce bone tissue regeneration. However, to confirm this hypothesis, cell experiments were undertaken.

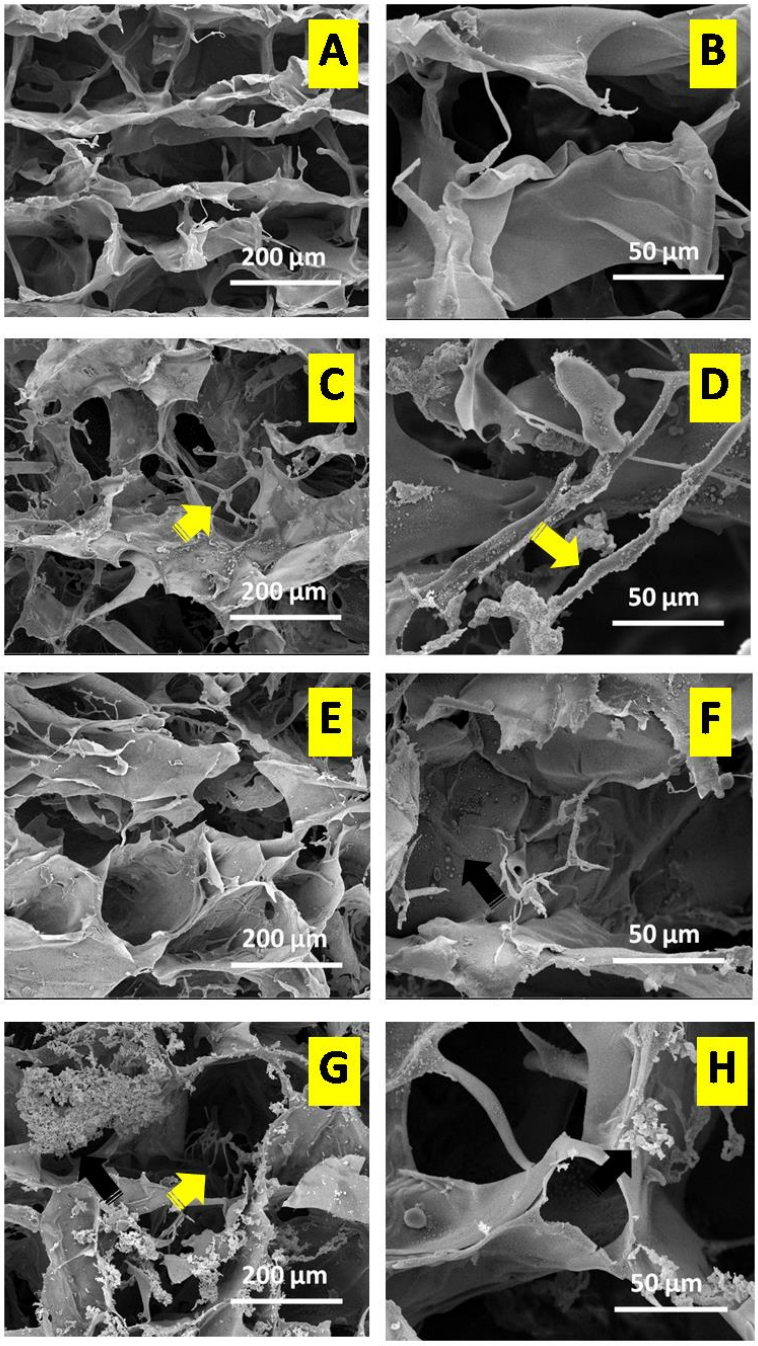

Figure 28. SEM images of cross-section morphology: (A, B) silk scaffolds, (C, B) coated silk fibroin scaffolds with decellularized pulp, (E, F) coated silk fibroin scaffolds with fibronectin, (G, H) coated silk fibroin scaffolds with decellularized pulp/fibronectin; Yellow arrow, rod structure; Black arrow, aggregation of globular structure.

Percentage of weight increase

Confirmation of the existence of decellularized pulp, fibronectin, and decellularized/fibronectin in the silk fibroin scaffolds was performed by an analysis of the increase in weights after coating. The coated silk fibroin scaffold with decellularized pulp/fibronectin showed the highest weight increase (Figure 29). The coated silk fibroin scaffold with decellularized pulp showed a lower weight increase than the coated silk fibroin with fibronectin but there was no significant difference. The increase in weight demonstrated that the decellularized pulp, fibronectin, and decellularized pulp/fibronectin had the potential to adhere to the surface of the silk fibroin scaffolds. In particular, decellularized pulp/fibronectin was the predominant component to adhere to the porous surface of the silk fibroin scaffolds.

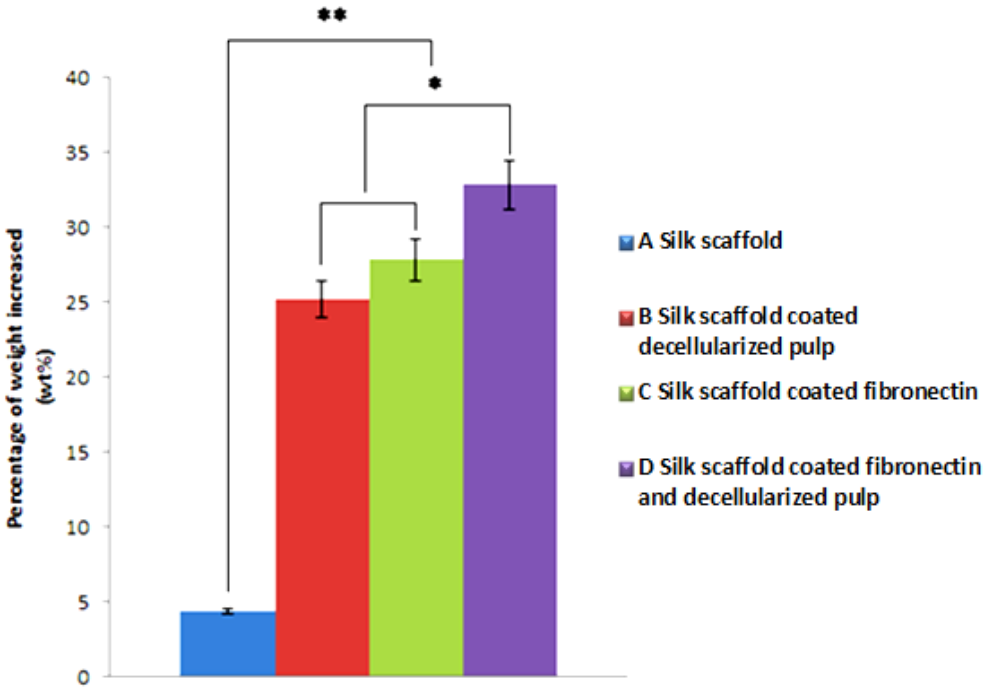

Figure 29. Weight increases in percentages of deposition of decellularized pulp, fibronectin, and decellularized pulp/fibronectin. (* $p < 0.05$)

Cell viability assay

Cell viability was analyzed to demonstrate the performance of the coated silk fibroin scaffolds. A green luminance indicated the cell viability on the scaffolds and that the MG-63 osteoblast cells could grow in all groups (Figure 30). The highest efficiency to promote cell proliferation and attachment was demonstrated on the silk fibroin scaffold with decellularized pulp/fibronectin (Figure 30D). This indicated that the reconstructed decellularized pulp/fibronectin acted as an important clue to induce cell adhesion and proliferation.

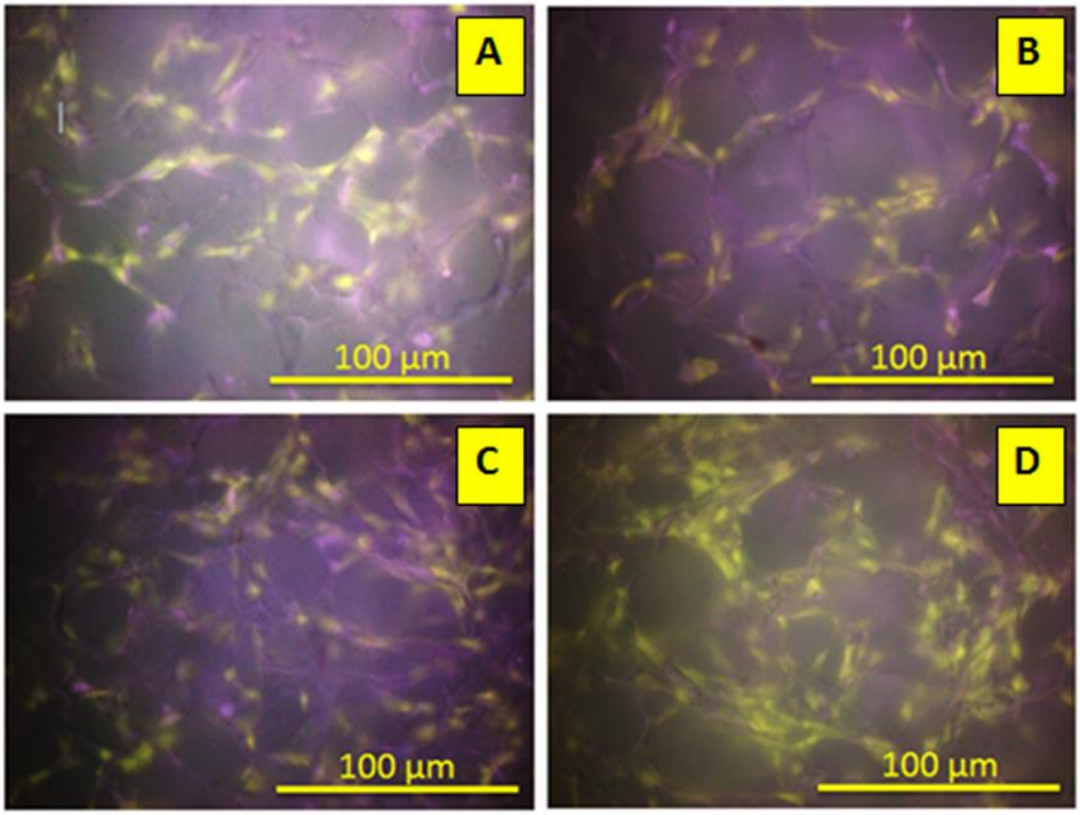

Figure 30. FDA cell staining on the scaffold (Green luminance): (A) Silk fibroin scaffold, (B) Coated silk fibroin scaffold with decellularized pulp, (C) Coated silk fibroin scaffold with fibronectin, (D) Coated silk fibroin scaffold with decellularized pulp/fibronectin.

Calcium content analysis

The performance of the coated silk fibroin scaffolds with decellularized pulp/fibronectin was tested with MG-63 osteoblasts. The calcium content was analyzed from the calcium synthesis of the osteoblasts. Mineralization as measured by matrix calcium content on days 7 to day 21, tended to show that calcium synthesis progressively increased (Figure 31). The coated silk fibroin scaffolds with decellularized pulp/fibronectin continued with the highest increase from day 7 to day 21. Interestingly, the decellularized pulp/fibronectin, showed higher calcium content than the others at

every time point. This indicated that the reconstruction of decellularized pulp/fibronectin played a role as a clue to induce calcium synthesis from the osteoblasts.

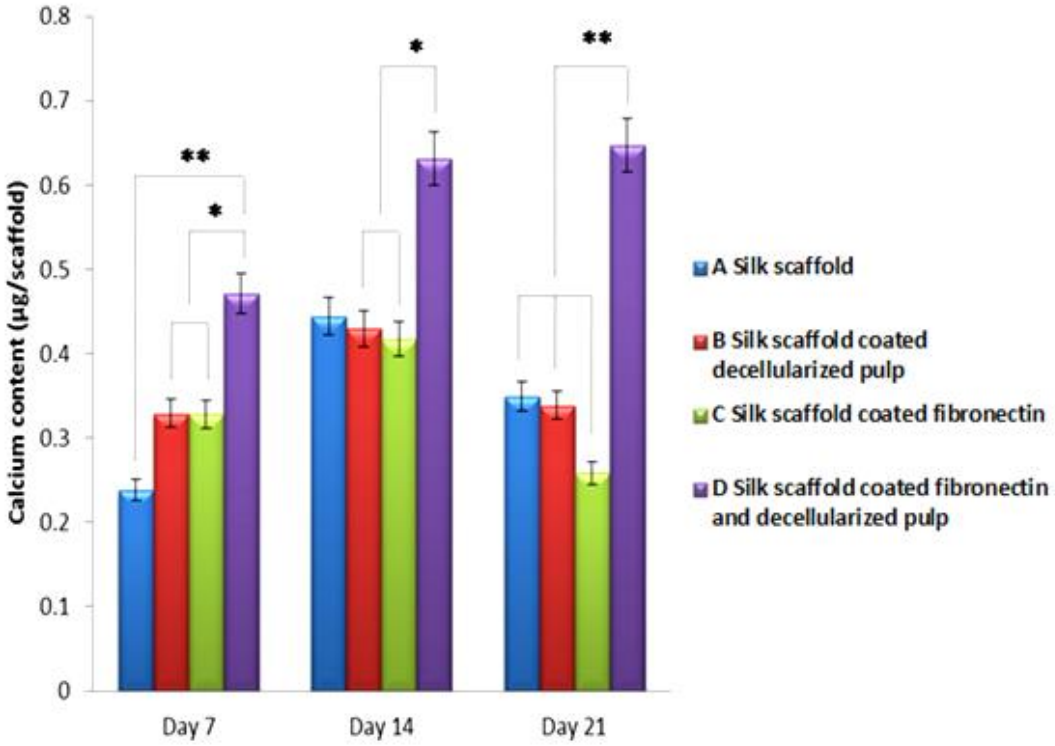

Figure 31. The calcium content values in SF scaffolds from MG-63 cell line at days 7, 14, and 21. ($p < 0.05$), (**) ($p < 0.01$).

Alkaline phosphatase (ALP) activity analysis

The ALP activity analysis measured the quality of the MG-63 osteoblast performance to differentiate from the pre-osteoblast cells to the mature cells. All groups of silk fibroin scaffolds revealed a progressive increase in ALP activity from day 7 to 21 (Figure 32). On day 7, the coated silk fibroin scaffold with decellularized pulp/fibronectin indicated that the MG-63 osteoblasts were osteo-induced and showed the highest ALP activity value. The silk fibroin scaffolds coated with fibronectin showed a higher ALP activity than the coated silk fibroin with decellularized pulp and the silk fibroin scaffolds.

On day 14, all groups continued to increase in ALP activity. The coated silk fibroin scaffolds with decellularized pulp increased ALP activity faster than the coated silk fibroin scaffolds with fibronectin and the silk fibroin scaffolds. All of those scaffolds showed less ALP activity than the coated silk fibroin scaffolds with decellularized pulp/fibronectin. The last period, the coated silk fibroin scaffold with decellularized pulp/fibronectin revealed the highest ALP activity value.

The results demonstrated that decellularized pulp/fibronectin could induce the osteo-induction of pre-osteoblasts to the mature stage. Fibronectin induced cell adhesion, extension, and migration adsorption of osteoblasts (10). Decellularized pulp has many components of the ECM which include collagen, fibronectin, and versican which acted as important clues for MG-63 osteoblasts to induce tissue regeneration (11). Therefore, the reconstructed ECM of decellularized pulp/fibronectin in this research showed the role as important clues for bone tissue engineering.

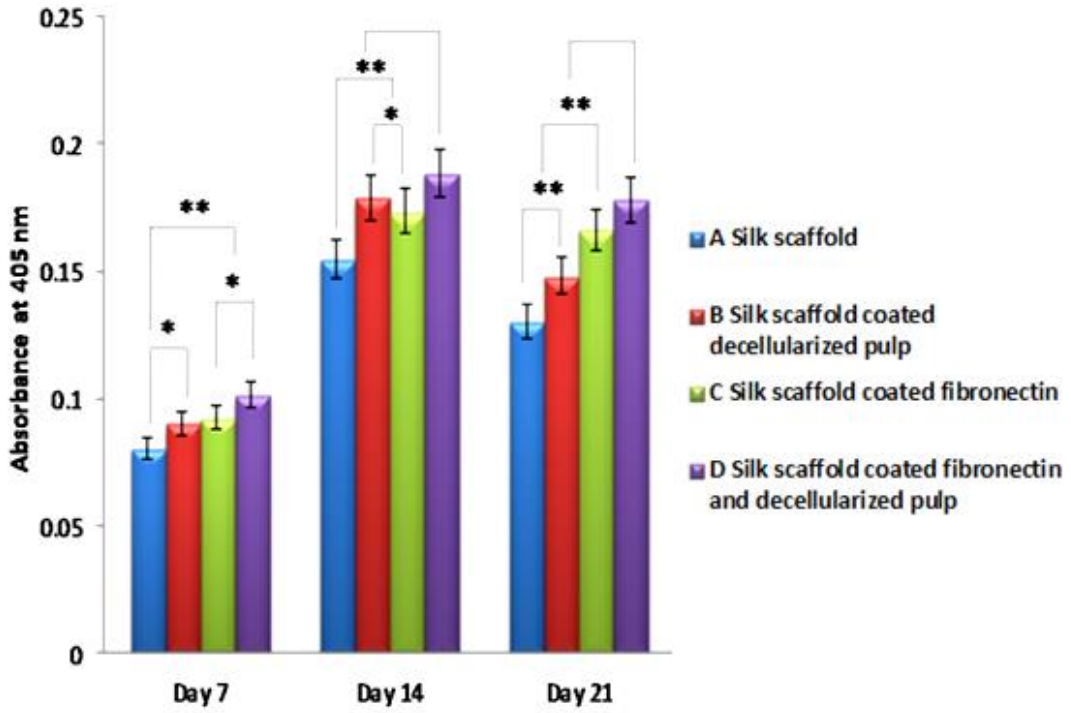

Figure 32. ALP activity from MG-63 osteoblast cells on days 7, 14, and 21. ($p < 0.05$), (**) ($p < 0.01$).

Nodule formation and mineralization analysis

Nodule formation was observed at day 14 after cell seeding. Alizarin red was used to check the osteogenic differentiation state of the cells that can synthesize ECM mineralization. The osteoblast cells showed osteogenesis in all groups of silk fibroin scaffolds (Figure 33). The red color indicated calcium production from the MG-63 osteoblasts and the calcium deposited on the silk fibroin scaffolds. The results showed red clusters that were distributed in the scaffolds. Importantly, the MG-63 osteoblast cells could produce calcium in all sample groups. The intensive red clusters in the coated silk fibroin scaffold with decellularized pulp/fibronectin showed the highest amount of deposited calcium. This indicated that the coated silk fibroin scaffold with

decellularized pulp/fibronectin was suitable for bone tissue engineering because the MG-63 osteoblast cells were spread throughout the silk fibroin scaffold and could produce calcium.

The results demonstrated that the reconstructed ECM of decellularized pulp/fibronectin acted as an important clue for MG-63 osteoblasts to induce calcium synthesis for bone tissue engineering.

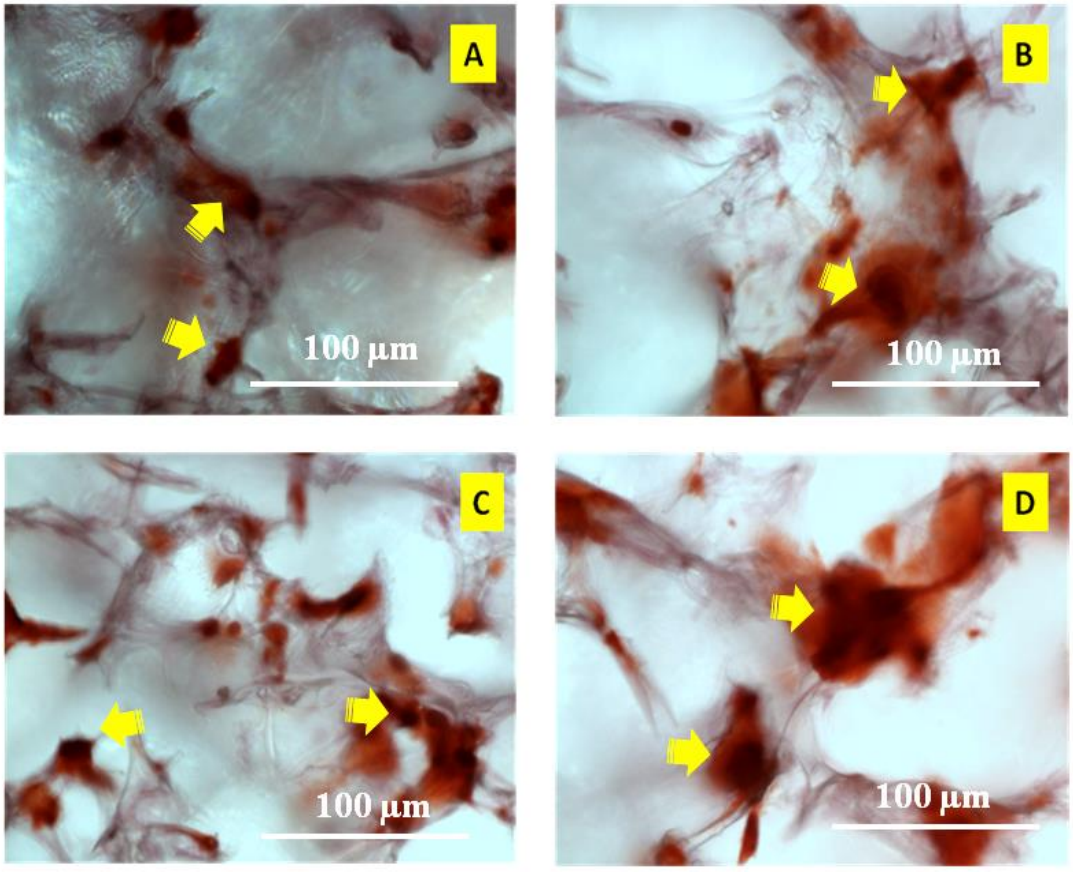

Figure 33. Alizarin red staining of SF scaffolds on day 14: (A) Silk fibroin scaffold, (B) Coated silk fibroin scaffold with decellularized pulp, (C) Coated silk fibroin scaffold with fibronectin, (D) Coated silk fibroin scaffold with decellularized pulp/fibronectin. The yellow arrows show the cluster of calcium.

Histological analysis

H&E staining

Histological analysis was used to observe the morphology and to explain the organization of the cells on the cell cultured silk fibroin scaffolds. The MG-63 osteoblast cells could spread thoroughly on the surface of the silk fibroin scaffolds in all groups (Figure 34). The MG-63 osteoblast cells could attach and migrate into the pores particularly onto the wall surface of the silk fibroin scaffolds. The coated silk fibroin scaffolds with decellularized pulp/fibronectin demonstrated that the cells could attach and spread throughout most of the areas of the scaffold (Figure 34D). The organization of the cells on the scaffolds from the histological analysis showed the same result as in Figure 30D.

Importantly, the results demonstrated that the coated silk fibroin scaffolds with decellularized pulp/fibronectin had the clues to enhance cell attachment and migration. The good cell attachment and migration on the scaffolds are suitable criteria to induce regeneration of new bone tissue (12).

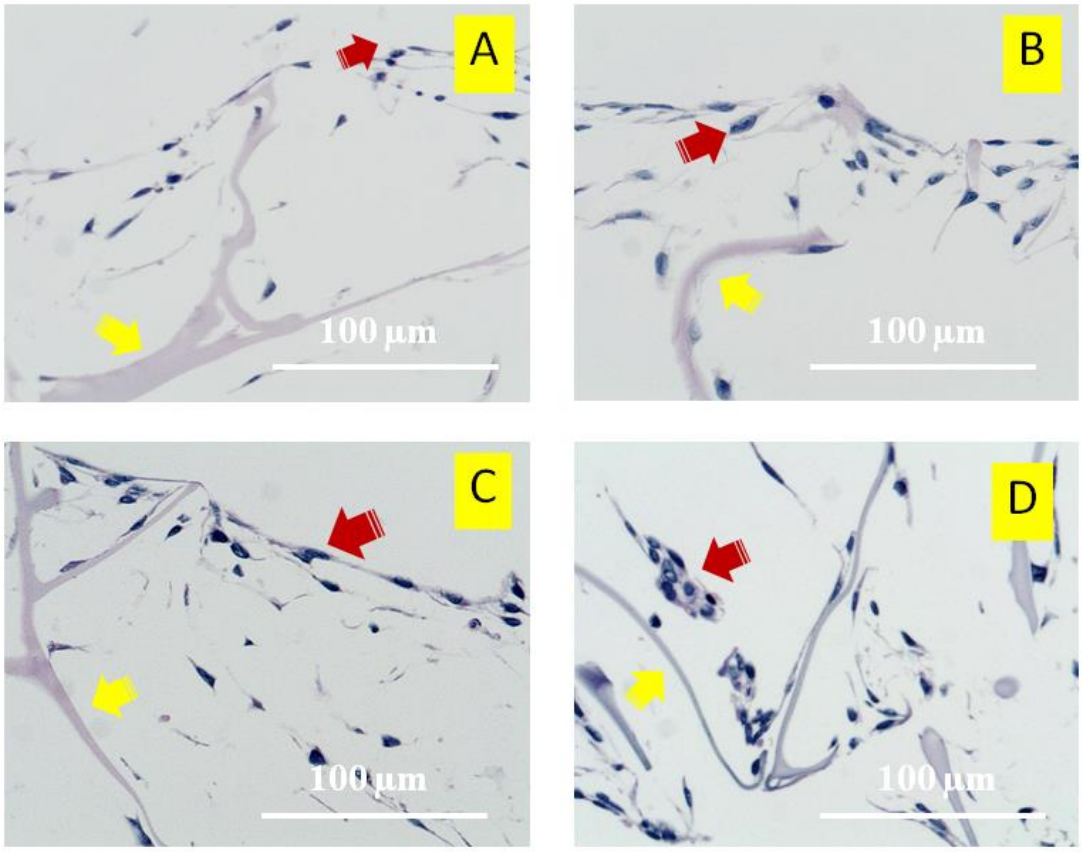

Figure 34. Representative histology (H&E) of cross-sections on day 5: (A) Silk fibroin scaffold, (B) Coated silk fibroin scaffold with decellularized pulp, (C) Coated silk fibroin scaffold with fibronectin, (D) Coated silk fibroin scaffold with decellularized pulp/fibronectin; Yellow arrows show the silk scaffold in each group; Red arrows show the osteoblast cells attached to the silk scaffolds in each group.

Von Kossa staining

Von Kossa staining was used to confirm mineralization of the extracellular matrix (13) secreted by the MG-63 osteoblast cells. In all groups of samples, the MG-63 osteoblast cells could proliferate and migrate on the silk fibroin scaffold (Figure 35). Moreover, the synthesis of calcium-containing salts such as calcium phosphate suggested the behavior of bone regeneration. The black color

(yellow arrows) revealed the calcium that was secreted from the MG-63 osteoblast cells and stained by von Kossa. The silk fibroin scaffolds coated with decellularized pulp/fibronectin expressed a lot of osteoblast cells (white arrows) attached to the silk surface (Figure 35D). The other groups, silk fibroin scaffold without coating, coated silk fibroin scaffold with decellularized pulp, and coated silk fibroin scaffold with fibronectin, showed both cell attachment and calcium synthesis (Figure 35A-C). The results of the von Kossa staining indicated that all groups of silk fibroin could induce cell attachment and calcium synthesis. The coated silk fibroin with decellularized pulp/fibronectin showed more cells in the scaffold. Not only could decellularized pulp/fibronectin induce calcium synthesis from the cells, it could promote cell adhesion. Therefore, the results of von Kossa staining demonstrated that the reconstructed extracellular matrix of decellularized pulp/fibronectin acted as suitable clues to promote bone regeneration.

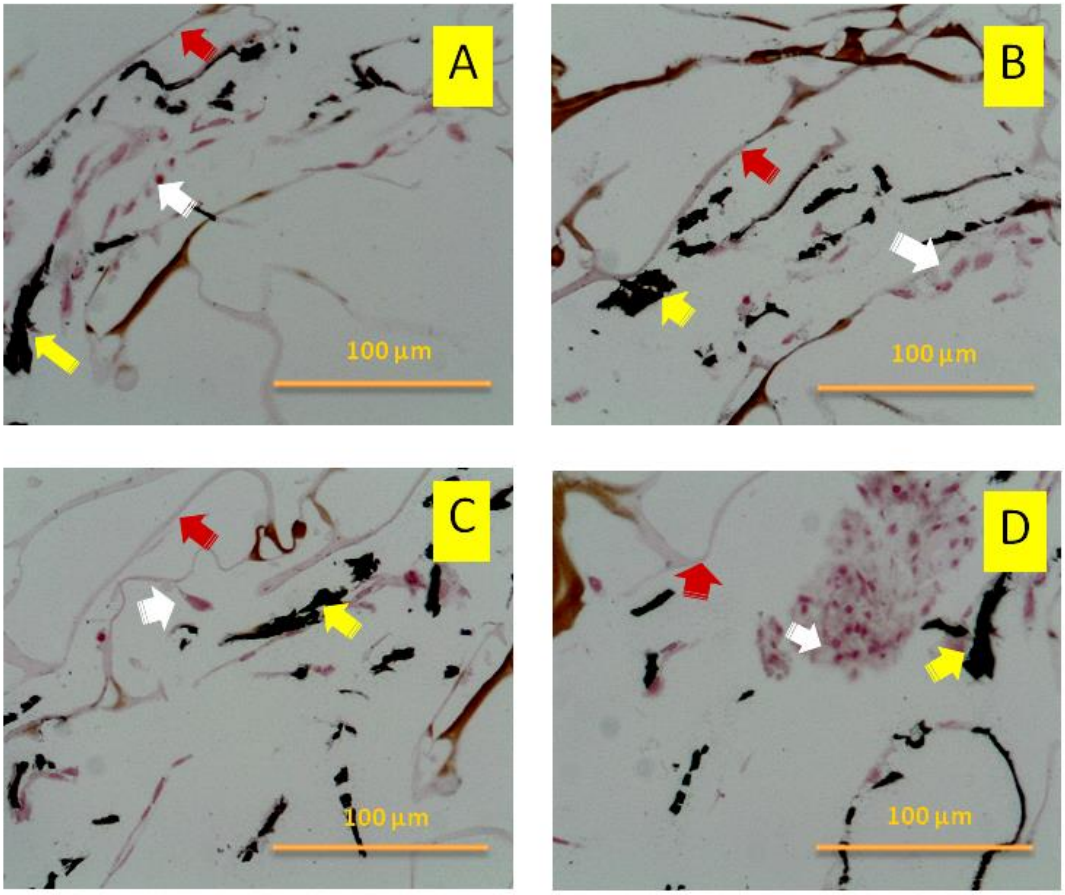

Figure 35. Histological sections of scaffold structures stained with von Kossa after day 14: (A) Silk fibroin scaffold, (B) Coated silk fibroin scaffold with decellularized pulp, (C) Coated silk fibroin scaffold with fibronectin, (D) Coated silk fibroin scaffold with decellularized pulp/fibronectin; White arrows, osteoblasts in scaffold; Yellow arrows, clusters of calcium; Red arrows, scaffold

Conclusion

In this research, coated silk fibroin scaffolds with reconstructed extracellular matrix of decellularized pulp/fibronectin were proposed as a biomaterial to replace bone defect from oral cancer at the maxillofacial area. The results demonstrated that the reconstructed extracellular matrix could attach to the porous walls of silk fibroin

scaffolds. The reconstructed extracellular matrix organized themselves into fibrils with an aggregation of a globular structure. Obviously, coated silk fibroin scaffolds with decellularized pulp/fibronectin played an important role as the clue to induce cell adhesion, proliferation, and calcium synthesis which can lead to promotion of bone tissue regeneration. The predominant biofunctionalities of a coated silk fibroin scaffold with decellularized pulp/fibronectin holds promise as a scaffold to replace bone defects in oral cancer. Nevertheless, to prove the performance for inhibition of cancer cell proliferation, the scaffolds need in vivo or ex vivo testing.

Reference

1. G. Chang, H.J. Kim, D. Kaplan, G. Vunjak-Novakovic, R. A. Kandel. Porous silk scaffolds can be used for tissue engineering annulus fibrosus. Eur Spine J. 16; 2007: 1848-1857.

2. Yong Zhao, R. Z Legeros, Jing Chen. Initial Study on 3D Porous Silk Fibroin Scaffold: Preparation and Morphology. Bioceramics Development and Applications. 1; 2011: 1-3.

3. Samantha B. Traphagen, Nikos Fourligas, Joanna Xylas, Sejuti Sengupta, David Kaplan, Irene Georgakoudi, Pamela C. Yelick. Characterization of Natural, Decellularized and Reseeded Porcine Tooth Bud Matrices. Biomaterials. 33; 2012: 5287-5296.

4. Xiaochen Liu, Minzhi Zhao, Jingxiong Lu, Jian Ma, Jie Wei, Shicheng Wei. Cell responses to two kinds of nanohydroxyapatite with different sizes and crystallinities. Int J Nanomedicine. 7; 2012: 1239-1250.

5. Beom-Su Kim, Hyo Jin Kang, Jun Lee. Improvement of the compressive strength of a cuttlefish bone-derived porous hydroxyapatite scaffold via polycaprolactone coating. Journal of Biomedical Materials Research Part B: Applied Biomaterials. 101; 2013: 1302-1309.

6. Sung Eun Kim, Sang-Hun Song, Young Pil Yun, Byung-Joon Choi, Il Keun Kwon, Min Soo Bae, Ho-Jin Moon, Yong-Dae Kwon. The effect of immobilization of heparin and bone morphogenic protein-2 (BMP-2) to titanium surfaces on in flammation and osteoblast function, Biomaterials. 32; 2010: 1-8.

7. Hong Ji. Lysis of Cultured Cells for Immunoprecipitation. Cold Spring Harbor Laboratory Press. 2010; 2010: 1-5.

8. Yu-Hsiung Wang, Yaling Liu, Peter Maye, David W. Rowe. Examination of Mineralized Nodule Formation in Living Osteoblastic Cultures Using Fluorescent Dyes. Biotechnol Prog. 22; 2006: 1697–1701.

9. Jaroslava Halper, Michael Kjaer. Basic Components of Connective Tissues and Extracellular Matrix: Elastin, Fibrillin, Fibulins, Fibrinogen, Fibronectin, Laminin, Tenascins and Thrombospondins. Advances in Experimental Medicine and Biology. 802; 2014: 31-47.

10. D. M. Rivera-Chacon, M. Alvarado-Velez, C.Y. Acevedo-Morantes, S.P. Singh, E. Gultepe, D. Nagesha, S. Sridhar, J.E. Ramirez-Vick. Fibronectin and vitronectin promote human fetal osteoblast cell attachment and proliferation on nanoporous titanium surfaces. J Biomed Nanotechnol. 9; 2013: 10 92–1097.

11. Goldberg M, Smith J. Cells and Extracellular Matrices of Dentin and Pulp: A Biological Basis For Repair and Tissue Engineering. Crit Rev Oral Biol Med. 15; 2004: 13-27.

12. Susmita Bose, Mangal Roy, Amit Bandyopadhyay. Recent advances in bone tissue engineering scaffolds. Trends Biotechnol. 30; 2012: 546-554.

13. Alexandra Ivan, V. Ordodi, Ada Cean, Daniela E. Ilie, Carmen Panaitescu, Gabriela Tanasie. Comparative study of the differentiation potential of rat bone marrow mesenchymal stem cells and rat muscle-derived stem cells. Arch Biol Sci. 65; 2013: 1307-1315.

14. William D. Norris, John G. Steelef, Graham Johnson, P. Anne Underwood. Serum enhancement of human endothelial cell attachment to and spreading on collagens I and IV does not require serum fibronectin or vitronectin. Journal of Cell Science 1990;95:255-262.

15. Amr M. Moursi, Caroline H. Damsky, Jonathan Lull, Deborah Zimmerman, Stephen B. Doty, Shin-ichi Aota and Ruth K. Globus. Fibronectin regulates calvarial osteoblast differentiation. Journal of Cell Science 1996;109:1369-1380.

16. Christina W. Chenga, Loran D. Solorioa, Eben Alsberg. Decellularized Tissue and Cell-Derived Extracellular Matrices as Scaffolds for Orthopaedic Tissue Engineering. Biotechnol Adv 2014;32:462-484.

17. Yuanyuan Zhang, Yujiang He, Shantaram Bharadwaj, Nevin Hammam, Kristen Carnagey, Regina Myers, Anthony Atala, Mark Van Dyke. Tissue-specific

extracellular matrix coatings for the promotion of cell proliferation and maintenance of cell phenotype. Biomaterials 2009;30:4021–4028.

CHAPTER 5

A biofunctional modified silk fibroin scaffold with mimic reconstructed extracellular matrix of decellularized pulp/collagen/fibronectin for bone tissue engineering in alveolar bone resorption

Abstract

Alveolar bone resorption is a critical problem that generate after bone losing. To use the bone grafting from another site is used to surgery. In this research,the modified silk fibroin scaffold with mimic reconstructed extracellular matrix of recellularized pulp/collagen/fibronectin was proposed for bone tissue engineering in alvelolar bone resorption. Silk fibroin scaffolds were fabricated by freeze-drying before modified by coating with decellularized pulp/collagen/fibronectin solution. The extracellular matrix reconstruction of decellularized pulp/collagen/fibronectin and morphological structure of modified silk fibroin was observed by Atomic Force Microscope (AFM) and Scanning Electron Microscope (SEM), respectively. Biofunctionalities were evaluated by cell viability, alkaline phophatase activity (ALP activity), calcium content, and mineralization analysis. The results showed that decellularized pulp/collagen/fibronectin could organized themselves into dense structure of dendrite structure and adhered in the silk fibroin scaffold into fibrillar network. For biofunctionalities , the modified silk fibroin scaffold showed the good cell adhesion and spreading. on the surface. Furthermore, the modified silk fibroin scaffold had the higher calcium content, ALP activity, and mineralization than silk fibroin without modification.

As the results, it could be deduced that the modified silk fibroin scaffold with mimic reconstructed extracellular matrix with decellularized pulp/collagen/fibronectin is promising for bone tissue engiuneering in alveolar bone resorption.

Materials and methods

Preparation of silk fibroin scaffolds

The silk fibroin solution was extracted follow Chang et al. 2007, the degummed silk fibroin was dissolved in 9.3 M lithium bromide and continue to dialyzed in distill water for 72 h. The concentration of silk fibroin solution was adjusted for 3% (w/v) (1, 2) and then poured into 48 well plates. The freeze drying method was used for water evaporation from silk fibroin scaffold, finally cut to 10 mm in diameter and 2 mm thickness.

Preparation of type I collagen

Type I collagen was extracted from the skin of brown banded bamboo shark (Chiloscylliumpunctatum). Preparation type I collagen was followed Kittiphattanabawon et al. 2010 (3). Briefly, Shark skin with size 1.0×1.0 cm^2 was mixed with 0.1 M NaOH. Next, the deproteinised skin was soaked in 0.5 M acetic acid for 48 h to get filtering mixture of the collagen solution, then NaCl to a final concentration of 2.6 M and 0.05 M Tris (hydroxymethyl) aminomethane at pH7.5 were added. Collagen pellet was collected using a refrigerated centrifuge. The pellet was dissolved with

minimum volume of 0.5 M acetic acid. To get for more purified collagen, the collagen solution was dialyzed with 0.1 M acetic acid for 12 h, and 48 h with distilled water. Freeze dried method was used for removing water and the samples were kept at -20 °C until used.

Preparation of decellularized pulp

The pulp used in this study was collected from teeth of children 6-10 years old, which segmented in half for harvesting pulp tissue. Collagenase and dispase were used to digest pulp for 1 h. At 37 °C, solutions were separated from pellet by using the centrifugation method and washed with PBS (Phosphate-Buffered Saline) for 2 times. Finally, the solution was filtered to get the decellularize pulp and freeze drying machine was used for water sublimation (4).

Modification of silk fibroin scaffolds

The study was designed into 2 groups as shown in table 5. In group of silk scaffold coated decellulized pulp, collagen and fibronectin group, the decellulized pulp powder was dissolved in 0.1 % sodium hypochlorite at ratio 0.1 mg/ml, the collagen powder dissolved in 0.1 M acetic acid at ratio 0.1 mg/ml and fibronectin dissolved in distilled deionized water with ratio 0.1 mg/ml. This solution was combined with balance ratio at 50:50. Then, scaffold was soaked in 1X PBS for 30 minutes and used freeze drying method.

Table 5. Groups of silk scaffold

Groups	Detail
A	**Silk scaffold**
B	**Modified silk scaffold coated with decellulized pulp/collagen/fibronectin**

Scanning Electron Microscopy (SEM) Observing

Scanning electron microscope (Quanta400, FEI, Czech Republic) has been used for observing morphology and characterization of SF scaffold that was coated with a special solution. The samples were pre-coated with gold using a gold sputter coater machine (SPI supplies, Division of STRUCTURE PROBE Inc., Westchester, PA USA).

Atomic Force Microscopy Observing

The special coating solution from each group was dropped into glass slide, smeared and soaked in PBS for 30 min. When the slides were dried, morphology and structure were observed by using atomic force microscopy.

MG-63 cell culture

MG-63 cells were cultured in 75 cm^2 flask with alphaMEM medium (α-MEM, Gibco™, Invitrogen, Carlsbad, CA) with the addition of 1% penicillin/streptomycin, 0.1% fungizone and 10% fetal bovine serum (FBS) at 37 °C in a humidified 5% of CO_2

and 95% air incubator. The MG-63 cells were seeded at ratio 5×10^5 cell per scaffold, the medium was changed every 3-4 day during cell culture. The osteogenic medium (OS; 10 mM b-glycerophosphate, 50 mg/ml ascorbic acid, and 100 nM dexamethasone; SigmaAldrich) was used for osteoblast differentiation of MG-63 (5).

Cell viability assay

Cell viability was investigated by Fluorescein Diacetate (FDA, Sigma) staining after day 3. The scaffolds were transferred to a new 48 well plates, added 1 ml of fresh medium. Then, added 5 µl FDA solution (5 mg FDA/ml in acetone) was added and incubated for 5 min at 37 °C. The scaffolds were moved to a glass support slide and observed by the fluorescence microscope (6).

Alkaline phosphatase activity analysis

The alkaline phosphatase (ALP) activity was used for measuring the osteogenic differentiation of MG-63 grown on the various scaffold types. After cell culture at day 7, 14 and 21, the scaffold was washed with PBS twice and then 1 ml of 0.02% Triton® X-100 was added on the scaffold to lysis cell. The solution was removed to 1.5 ml tube, the sample was centrifuged at 20,000 rpm at 4 °C for 10 min, and the supernatant was removed to new 1.5 ml tube (7). The cell lysate solution was used for ALP activity according to manufacture's instructions (Abcam®, Cambridge, UK). The 50 µl of assay buffer containing 5 mM p-nitrophenol phosphate, a phosphatase substrate that can turn yellow when dephosphorylated by ALP, was mixed with cell lysate solution and

incubated at room temperature. The reaction was stopped by adding 20 µl of NaOH, and then measured at 405 nm.

Calcium content analysis

The calcium value that synthesized from the MG-63 osteoblast cell was measured with Calcium colorimetric assays (Calcium colorimetric assay, Biovision). The 30 µl of lysate solution was added in 96 well plates, adjusted the final volume to 50 µl with dH_2O and followed by adding 90 µl of of the Chromogenic Reagent, 60 µl of the Calcium Assay Buffer and mixed gently. The reaction was incubated for 5-10 min at room temperature, protected from light and measured the OD at 575 nm.

Alizarin Red S staining for Mineralized Matrix

Cell were fixed with 4% formaldehyde and the 40 mM, of alizarin red S (Sigma-Aldrich) at pH 4.2 was used for staining calcium nodule deposition with 10 min incubation (8).

Von kossa staining

After cell culture on day 14, the scaffolds were transferred to 48 well plates and washed twice with PBS, used 4% formaldehyde to cell fixation at 4 $^{\circ}$C, 24 h. Scaffolds were immersed in paraffin, cut paraffin sections at 5µm and placed on a glass slide, then deparaffinized and hydrated to distilled water. The sample slide was stained

with the von kossa staining to investigate the deposits of calcium synthesized from the MG-63 osteoblast cell.

Statistical analysis

All data were shown as mean±standard deviation. The samples (n=5) were measured and statistically compared by T-test (SPSS 16.0 software package). $p < 0.05$ was accepted as statistically significant.

Results and discussion

Structural formation of mimicked extracellular matrix

Before coating silk fibroin scaffold with reconstructed ECM of decellularized pulp/collagen/fibronectin, the structural formation of reconstructed ECM was observed by AFM. As the results of AFM image in Fig 36, it demonstrated that decellularized pulp/collagen/fibronectin organized themselves into the dense structure of dendrite structure. Such dendrite structure showed the complicate structure. To evaluate the performance of decellularized pulp/collagen/fibronectin, solution for coating in the silk fibroin scaffold must be observed with scanning electron microscope (SEM) in the next section.

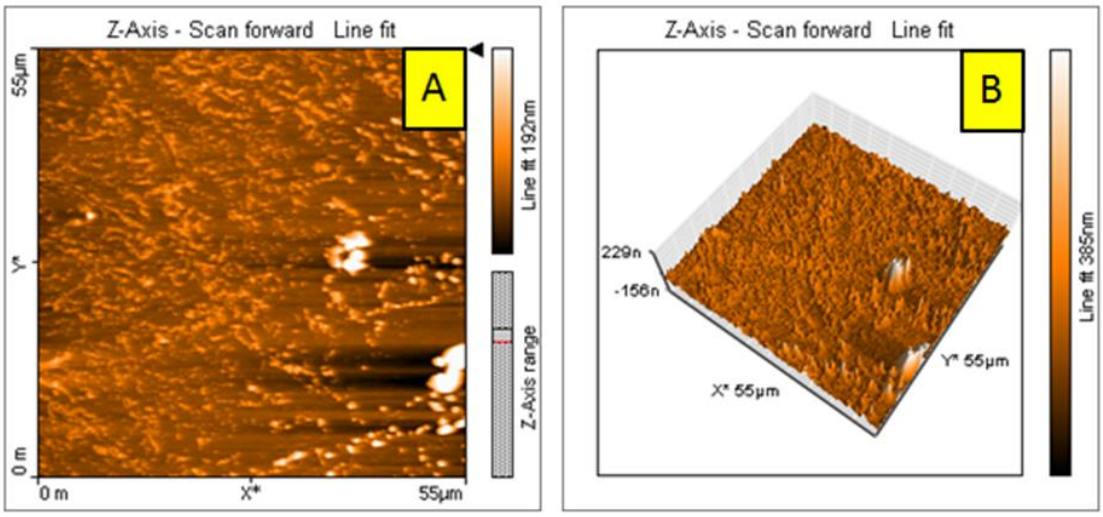

Figure 36.The 2 dimensions; (A) and 3 dimensions; (B) AFM analysis of the combination of decellulized pulp/collagen/fibronectin fibril forming.

Morphological analysis of modified silk fibroin scaffolds

The silk fibroin scaffold after coating showed the white color more than silk fibroin scaffold. The white color obtained from the combination of decellulized pulp, collagen, and fibronectin fibril as Fig. 37.

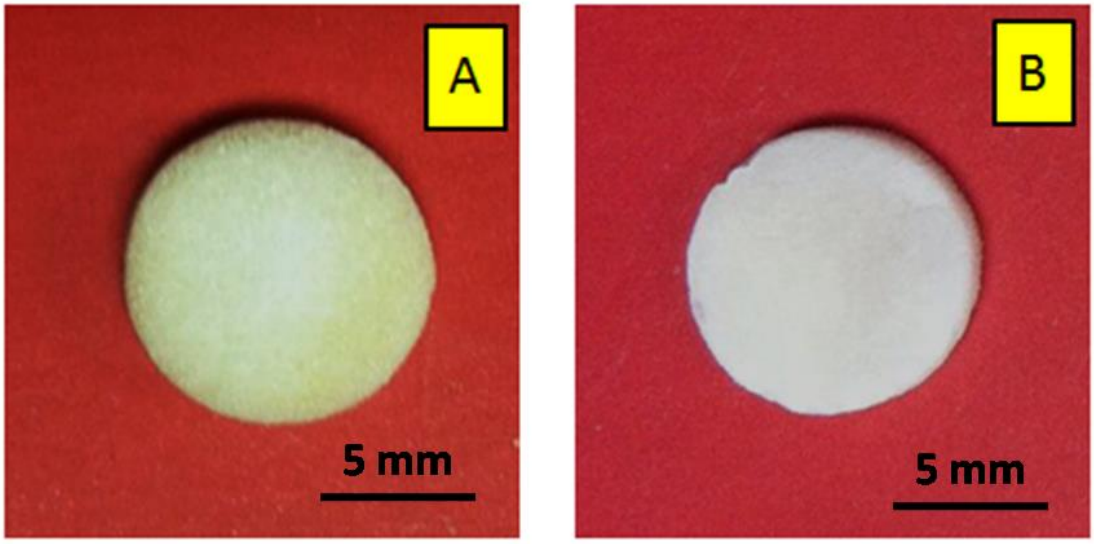

Figure 45. Silk fibroin scaffold after freeze drying and cut in size 10 diameter and 2 thicknesses; (A). Silk fibroin scaffold after modified with decellulized pulp/collagen/ fibronectin; (B).

The surface morphological structure of modified silk fibroin with decellularized pulp/collagen/fibronectin was observed by SEM. In the silk fibroin scaffold indicated the interconnective pore size and smooth surface, it has enough area for cell proliferation, migration and attachment (9) (Fig. 38A). Predominantly, the modified silk fibroin with decellulized pulp/collagen/fibronectin showed rougher surface with the interconnective pore size. Notably, there were fibrillar network that adhered to surface of the silk fibroin scaffold. That fibrillar network showed structure as native extracellular matrix (10). As the surface morphological structure of modified silk fibroin scaffold, it demonstrated that the fibrillar network structure came from the reconstruction of decellularized pulp/collagen/fibronectin.

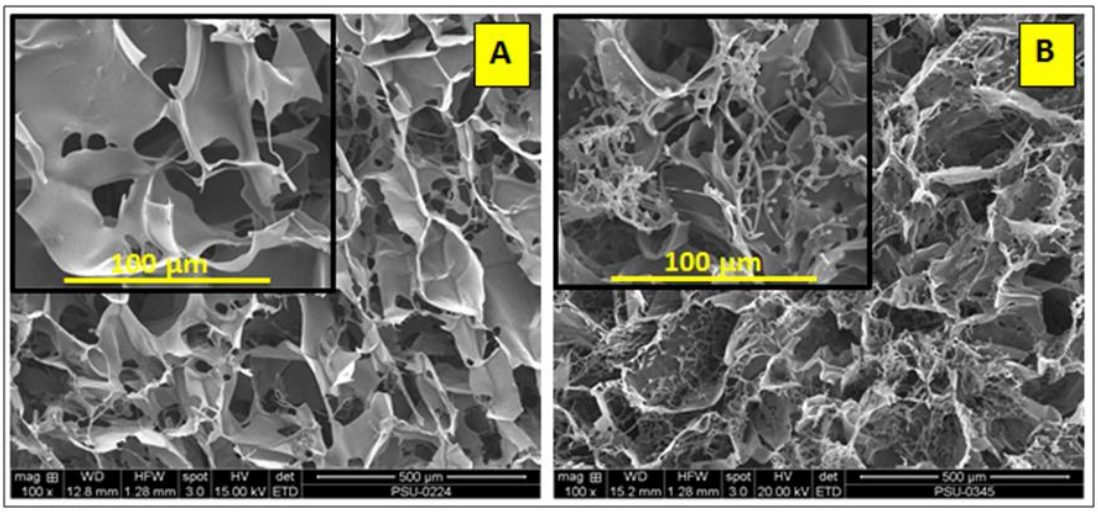

Figure 38. The SEM analysis showed the surface morphology of silk fibroin scaffold; (A) and the modified silk fibroin scaffold with decellulized pulp/collagen/fibronectin; (B).

To vindicate the performance of decellularized pulp/collagen/fibronectin as a performance coating solution for silk fibroin modification, it also needed to observe cross-section morphological structure of a modified silk fibroin scaffold. When consider morphological structure of cross-section area in the modified silk fibroin scaffold with decellulized pulp/collagen/fibronectin, it obviously showed the fibrillar network that adhered in the pores of scaffold as Fig.39B. Clearly, this result indicated the decellulized pulp/collagen/fibronectin could diffuse into the porous of scaffold and reconstruct their structure as extracellular matrix. Notably, the pore size of the modified silk fibroin scaffold with decellulized pulp/collagen/fibronectin was smaller than the silk fibroin scaffold.

Remarkably, as the morphological structure of modified silk fibroin scaffold with decellulized pulp/collagen/fibronectin, it indicated that those fibrillar network showed structure as native extracellular matrix. This results vindicated that those fibrillar network came from reconstructed extracellular matrix of decellulized pulp/collagen/fibronectin. As the previous report, it demonstrated that fibrillar network structure had the role to enhance cell adhesion, migration, and proliferation (11). Therefore, these results showed that the fibrillar network structure might act as the clues to induce bone tissue engineering. However, to clearify this hypothesis, cell experiments and biofunctional testing were undertaken.

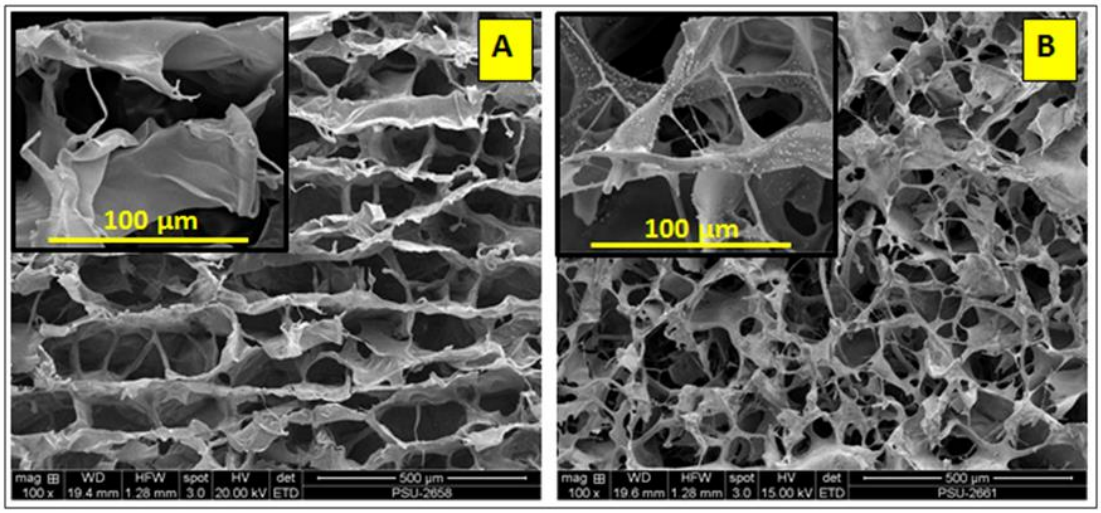

Figure 39. The SEM analysis showed the cross-section morphology of silk fibroin scaffold; (A) and the modified silk fibroin scaffold with decellulized pulp, collagen and fibronectin; (B).

Cell viability assay (day3)

To proof performance of the reconstructed extracellular matrix as clue for bone tissue engineering, MG-63 osteoblasts were cultured in scaffolds and cell viability was analyzed. As the results of cell viability in Fig.40, at the day 3 the MG-63 osteoblast could grow in silk fibroin and coated silk fibroin. Cells could migrate and adhere on the scaffold. Notably, the cells attached to almost all layers of scaffold on the superficial surface. Especially, cells on modified silk fibroin with decellulized pulp/collagen/fibronectin predominantly showed cell adhesion and proliferation. Clearly, such unique cell adhesion and proliferation came from the clues of reconstructed extracellular matrix that showed the influential regulator of the cell functions and differentiation.

Principally, extracellular matrix provided a suitable environment for the cell *in vitro* and acted as native scaffold for tissue tissue engineering (12). The components of extracellular matrix showed the function as the clue to induce tissue engineering (13). Furthermore, fibronectin had the important role to induce cell adhesion and spreading. For collagen, it could enhance cell adhesion (14). Obviously, as the result of cell viability, it indicated that the reconstructed extracellular matrix of decellulized pulp/collagen/fibronectin showed the important clues to support cell adhesion, spreading that is a suitable criteria to enhance bone tissue engineering.

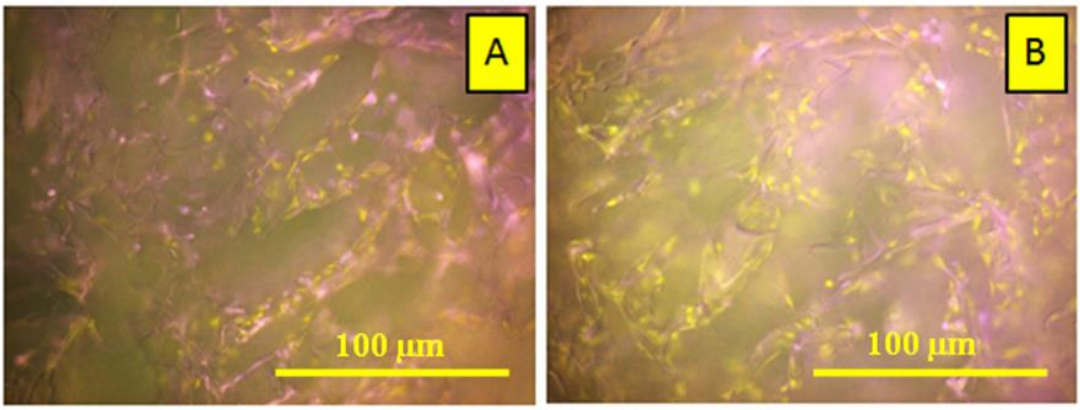

Figure 40. The fluorescent images indicated cell viability on the scaffold. A) The green luminance (FDA-labeled) was the MG-63 osteoblast cell attachment on silk fibroin scaffold, B) The modified silk fibroin with decellulized pulp/collagen/fibronectin showed more MG-63 osteoblast cell migration.

Alkaline phosphatase activity analysis

ALP activity analysis was used for measuring quality of MG-63 osteoblast that showed the performance for differentiation of pre-osteoblastic cells into mature osteoblast. The ALP assay was used for early MG-63 osteoblas differentiation

on culture days 7, 14 and 21 as Fig.49. The ALP activity in modified silk fibroin scaffold with decellulized pulp/collagen/fibronectin increased from day 7 to 21. For silk fibroin scaffold, ALP activity started to increase at day 7 to 14. Then, the ALP activity decreased at day 21. As the result, it demonstrated that modified silk fibroin scaffold with decellulized pulp/collagen/fibronectinshowed the predominant ALP activity of the MG-63 osteoblast.

As the previous reports, they indicated that collagen, fibronectin, decellularized tissue play important role in differentiation of osteoblasts (15,16). As the result of ALP activity, it was in the same way as the previous report that decellularized pulp, collagen, and fibronection could induce biofunctionallities of scaffold. Interestingly, the result of ALP activity indicated that reconstructed extracellular matrix of decellularized pulp/collagen/fibronectin could activate differentiation of osteoblast that lead to enhancing of bone tissue engineering.

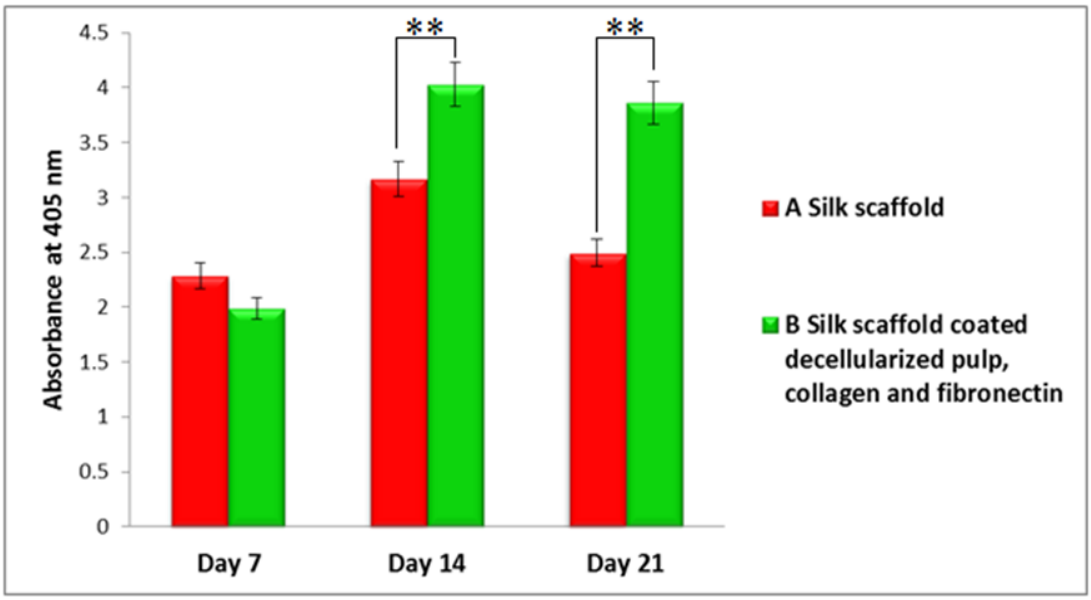

Figure 41.The ALP activity among different groups of silk firoin scaffold at day 7, 14 and 21. The symbol (*) represents significant changes in ALP activity of MG-63 osteoblast ($p < 0.05$), (**) ($p < 0.01$).

Calcium content analysis

Analysis of calcium content during cell culturing was the biofunctionallity test of coated silk fibroin scaffold with decellularized pulp/collagen/fibronectin in this section. As the result, it demonstrated that the calcium deposition ratio in both groups increased between day 7 to 14 and going down on day 21 of cell culture as Fig. 42. At day 7 and 14, modified silk fibroin scaffold with decellularlized pulp/collagen/fibronectin showed a higher calcium value than silk fibroin scaffold. As the reports, they showed that fibronectin had the role to induce calcium content of osteoblast and tissue decellularlized ECM coatings on the plate revealed highly differentiation of the osteoblasts that lead to the increasing of calcium content (17). Significantly, as the result of calcium content, it showed that reconstructed extracellular matrix of decellularlized pulp/collagen/fibronectin could induce synthesized calcium from osteoblast that lead to enhance bone tissue engineering.

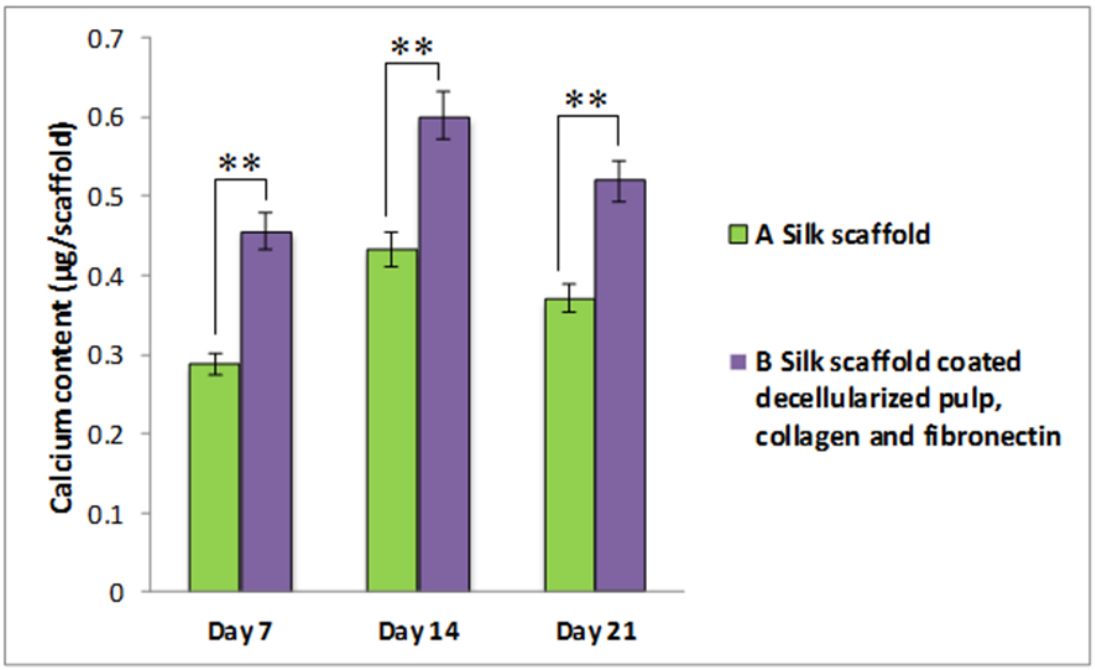

Figure 42. The calcium deposits on the different groups of the silk fibroin scaffold at day 7, 14 and 21. The symbol (*) represents significant changes in calcium activity of MG-63 osteoblast ($p < 0.05$), (**) ($p < 0.01$).

Nodule formation and mineralization analysis

To analyse the synthesized calcium from osteoblast that deposite in the scaffold, alizarin red was used to stain on calcim and observed by microscopy. Alizarin red staining was used for detecting the calcium on the scaffold on day 14 of osteogenic induction, the red color showed the calcium deposition that stained with alizarin red. The modified silk fibroin scaffold with decellulized pulp/collagen/fibronectin (Fig. 43B) indicated more calcium deposition when compared with silk fibroin scaffold. As the result, it demonstrated that reconstructed extracellular matrix of decellularlized pulp/collagen/fibronectin could promote calcium synthesis from osteoblast. The result

indicated that reconstructed extracellular matrix showed the performance could promote calcium synthesis.

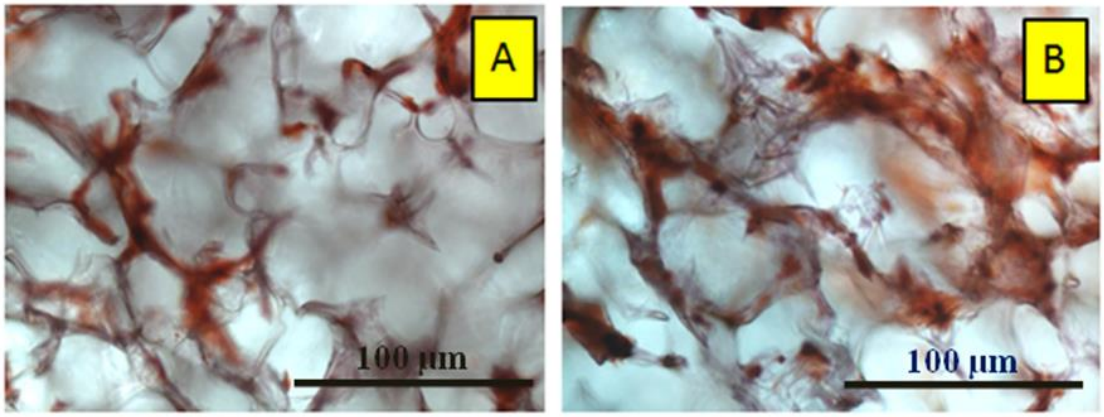

Figure 43.Alizarin red staining of silk fibroin scaffold on day 7. A) silk fibroin scaffold, B) Modified silk fibroin scaffold with decellulized pulp/collagen/fibronectin.

Von kossa staining

To clearify secreted mineral matrix on sample, Von Kossa staining was used to test with the scaffolds. Von Kossa staining performed on day 14 of osteogenic induction revealed the mineral matrix secrestion of MG-63 osteoblast cell that grown the silk fibroin scaffold. The modified silk fibroin scaffold with decellulized pulp/collagen/fibronectin (Fig. 44B) showed more mineral matrix (yellow arrow) when compared with silk fibroin scaffold (Fig. 44A). The MG-63 osteoblast cell (red arrow) was attached to the silk fibroin scaffold (blue arrow).

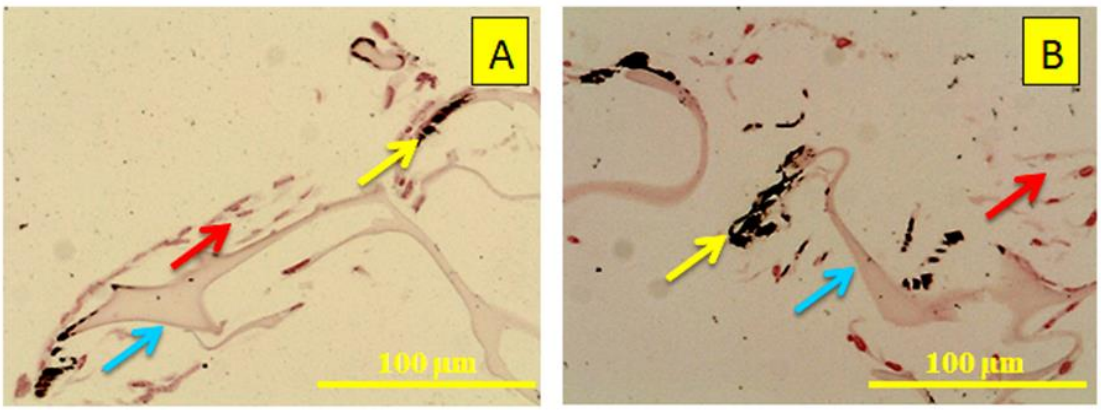

Figure 44.Histological sections of scaffold structures stained with von kossa after day 14. A) Silk fibroin scaffold, B) Modified scaffold with decellulized pulp/collagen/fibronectin.

Conclusion

In this research, a biofunctional modified silk fibroin scaffold with mimic reconstructed extracellular matrix of decellularized pulp/collagen/fibronectin was proposed to use for bone tissue engineering in alveolar bone resorption. The morphological structure, biofunctionalities of the modified scaffold was evaluated in this research. As the results, they demonstrated that decellularized pulp/collagen/fibronectin could form reconstructed extracellular matrix into fibrillar network structure. Such reconstructed extracellular matrix showed the suitable morphological structure and biofunctionalities to induce cell adhesion, calcium synthesis and deposition, secreted mineral on silk fibroin scaffold. Predominantly, the results demonatrated that those modified silk fibroin scaffold showed the suitable performance and promised to used for bone tissue engineering in alveolar bone resorption.

Reference

1. G. Chang, H.-J. Kim, D. Kaplan, G. Vunjak-Novakovic, R. A. Kandel. Porous silk scaffolds can be used for tissue engineering annulus fibrosus. Eur Spine J 2007;16:1848-1857.

2. Yong Zhao, R.Z. Legeros, Jing Chen. Initial Study on 3D Porous Silk Fibroin Scaffold: Preparation and Morphology. Bioceramics Development and Applications 2011;1:1-3.

3. Phanat Kittiphattanabawon, Soottawat Benjakul, Wonnop Visessanguan, Hideki Kishimura, Fereidoon Shahidi. Isolation and Characterisation of collagen from the skin of brownbanded bamboo shark (Chiloscyllium punctatum). Food Chemistry 2010;119:1519–1526.

4. Samantha B. Traphagen, Nikos Fourligas, Joanna Xylas, Sejuti Sengupta, David Kaplan, Irene Georgakoudi, Pamela C. Yelick. Characterization of Natural, Decellularized and Reseeded Porcine Tooth Bud Matrices. Biomaterials 2012;33:5287-5296.

5. Beom-Su Kim, Hyo Jin Kang, Jun Lee. Improvement of the compressive strength of a cuttlefish bone-derived porous hydroxyapatite scaffold via polycaprolactone coating. Journal of Biomedical Materials Research Part B: Applied Biomaterials 2013;101:1302-1309.

6. Ting-Ting Li, Katrin Ebert, Jurgen Vogel, Thomas Groth. Comparative studies on osteogenic potential of micro- and nanofibre scaffolds prepared by electrospinning of poly(ε-caprolactone). Progress in Biomaterials 2013;2:1-13.

7. Hong Ji. Lysis of Cultured Cells for Immunoprecipitation. Cold Spring Harbor Laboratory Press 2010;2010:1-5.

8. Yu-Hsiung Wang, Yaling Liu, Peter Maye, David W. Rowe. Examination of Mineralized Nodule Formation in Living Osteoblastic Cultures Using Fluorescent Dyes. Biotechnol Prog 2006;22:1697–1701.

9. Qiu Li Loh, BEng, Cleo Choong. Three-Dimensional Scaffolds for Tissue Engineering Applications: Role of Porosity and Pore Size. Tissue Engineering: Part B 2013;19:485-502.

10. Martijn de Wild, Wim Pomp, Gijsje H. Koenderink. Thermal Memory in Self-Assembled Collagen Fibril Networks. Biophysical Journal 2013;105:200-210.

11. Johanna Soikkeli, Piotr Podlasz, Miao Yin, Pirjo Nummela, Tiina Jahkola, Susanna Virolainen, Leena Krogerus, Paivi Heikkila, Karl von Smitten, Olli Saksela, Erkki Holtta. Metastatic Outgrowth Encompasses COL-I, FN1, and POSTN Up-Regulation and Assembly to Fibrillar Networks Regulating Cell Adhesion, Migration, and Growth. The American Journal of Pathology 2010;117:387-403.

12. Yong Guo, Chun-qiu Zhang, Qiang-cheng Zeng, Rui-xin Li, Lu Liu, Qin-xin Hao, Cai-hong Shi, Xi-zheng Zhang and Yu-xian Yan. Mechanical strain promotes osteoblast ECM formation and improves its osteoinductive potential. BioMedical Engineering OnLine 2012;11:1-10.

13. Wendell Q Sun, Hui Xu, Maryellen Sandor, Jared Lombardi. Process-induced extracellular matrix alterations affect the mechanisms of soft tissue repair and regeneration. Journal of Tissue Engineering 2013;4:1-13.

14. William D. Norris, John G. Steelef, Graham Johnson, P. Anne Underwood. Serum enhancement of human endothelial cell attachment to and spreading on collagens I and IV does not require serum fibronectin or vitronectin. Journal of Cell Science 1990;95:255-262.

15. Amr M. Moursi, Caroline H. Damsky, Jonathan Lull, Deborah Zimmerman, Stephen B. Doty, Shin-ichi Aota and Ruth K. Globus. Fibronectin regulates calvarial osteoblast differentiation. Journal of Cell Science 1996;109:1369-1380.

16. Christina W. Chenga, Loran D. Solorioa, Eben Alsberg. Decellularized Tissue and Cell-Derived Extracellular Matrices as Scaffolds for Orthopaedic Tissue Engineering. Biotechnol Adv 2014;32:462-484.

17. Yuanyuan Zhang, Yujiang He, Shantaram Bharadwaj, Nevin Hammam, Kristen Carnagey, Regina Myers, Anthony Atala, Mark Van Dyke. Tissue-specific extracellular matrix coatings for the promotion of cell proliferation and maintenance of cell phenotype. Biomaterials 2009;30:4021–4028.

CHAPTER 6

Modified silk fibroin scaffolds coated with a reconstructed collagen/fibronectin for bone tissue engineering in alveolar bone resorption: morphological structure and biological functionalities

Abstract

Alveolar bone resorption is a critical problem of patients who have been without teeth over an extended period of time. Bone tissue engineering was chosen for alveolar bone resorption. This research proposes to use a modified silk fibroin scaffold with reconstructed collagen/fibronectin as a bone graft. Silk fibroin scaffolds were fabricated by freeze-drying before modification by coating with reconstructed collagen/fibronectin. The structural formation of the reconstructed collagen/fibronectin and the morphological structure of the modified silk fibroin were observed by atomic force microscopy (AFM) and scanning electron microscopy (SEM), respectively. MG-63 osteoblast cells were cultured on the modified scaffolds before biological functionality testing for cell proliferation, viability, ALP activity, histology, and mineral matrix deposition. The results of the morphological structure of the modified silk fibroin scaffolds showed aggregation of globular structures on the porous surface that could induce cell proliferation, viability, ALP activity, spreading, and mineral matrix deposition. The results demonstrated that the modified silk fibroin scaffolds had good performance for bone tissue engineering and showed promise for bone grafting in alveolar bone resorption.

Materials and methods

Preparation of silk fibroin scaffolds

A silk fibrin scaffold was obtained from the freeze-drying method. Degummed silk fibroin was dissolved in 9.3 M LiBr for 4 h. A dialysis membrane was used for 72 hours to remove the LiBr from the silk fibroin. The water was changed every 3 hours on the first day and then prepared silk solution at yielding a 3% (w/v) solution (1). To fabricate the 3D silk fibroin scaffold, pure silk fibroin was poured into 48 well plates and frozen at -20°C for 24 h before freeze-drying. The 3D silk fibroin scaffolds were cut into discs with a diameter of 10 mm and a thickness of 2 mm.

Preparation of type I collagen

Brownbanded bamboo shark skin was used to extract type I collagen. The skin was cut into pieces each of 1 × 1 cm^2 in size. The non-collagen was removed from the skin with 0.1 M NaOH and the skin was separated from the solution by filtering. The skin was soaked in 0.5 M acetic acid for 48 h. The skin was removed and placed in a solution adjusted to 2.6 M NaCl and 0.05 M tris-(hydroxymethyl) aminomethane. The collagen was centrifuged in a refrigerated centrifuge to collect the collagen. The dregs of the collagen were dissolved with 0.5 M acetic acid in a minimum volume. Dialysis was used to purify the collagen using 0.1 M acetic acid for 12 h and distilled water for 48 h. Finally, the collagen was frozen at -20°C. The freeze-drying continued until the water was completely evaporated (2).

Modification of silk fibroin scaffolds

The 3D silk scaffolds were coated with a combination coating solution that included collagen type I and fibronectin (fibronectin from bovine plasma, Sigma-Aldrich). There were 2 groups with different solutions (Table 6).

Table 6. Experiment groups.

Groups	Detail
A	Silk fibroin scaffold
B	Collagen/fibronectin-coated silk fibroin scaffold

Scanning Electron Microscopy (SEM) Observation

The 3D silk fibroin scaffolds in both groups were coated with gold/palladium with a gold sputtering machine (JEOL, JFC-1200 Fine Coater, Japan) before observation of the structure characterization and morphology of the collagen and fibronectin compound that covered the silk fibroin scaffold surface under a scanning electron microscope (HITACHI, S-3400, Japan).

Atomic Force Microscopy Observation

The collagen and fibronectin compound solution was dropped onto a glass slide, equalized, and immersed in a PBS solution for 30 min. The glass slide was

dried at room temperature. The morphology characterization and structure were observed using atomic force microscopy.

Cell Culturing

MG-63 osteoblast cells were seeded in each scaffold with 1×10^{6} cells and maintained in an alpha-MEM medium (α-MEM, GibcoTM, Invitrogen, Carlsbad, CA) with the addition of 1% penicillin/streptomycin, 0.1% fungizone, and 10% fetal bovine serum at 37°C in a 5% CO_2 and 95% air-humidified incubator. The medium was changed every 3-4 days. An osteogenic supplements (OS) medium (OS; 20 mM b-glycerophosphate, 50 μM ascorbic acid, and 100 nM dexamethasone; Sigma-Aldrich) was used for osteoblast differentiation of the MG-63 osteoblast cells (3).

Cell proliferation assay (PrestoBlue™ on Days 1, 3, 5, and 7)

PrestoBlue™ assay, based on resazurin reagent, was used for observation of cell proliferation. The live cells reacted with resazurin and changed color from purple to red in the cytoplasm. The MG-63 was cultured on day 1, 3, 5, and 7 for the cell proliferation assay. The scaffolds in both groups were washed twice with PBS, then PrestoBlueTM was added to the scaffold with the complete medium at a ratio of 1:10 by volume. The incubation time of about 1 h at 37°C was used to detect the cell proliferation rate. The wavelength absorbance at 600 nm emission was used for measurement.

Cell viability (Fluorescence Microscope on Day 7)

Cell viability efficiency on the scaffolds in all groups was observed with fluorescein diacetate (FDA). The FDA hue was an embedded glow in the extracellular matrix and cellular clusters. The FDA powder was dissolved in acetone at a ratio of 5 mg/ml. Into each well that contained the scaffold with 1 ml of fresh complete medium, 5 µl of the FDA solution was added. The scaffold was kept away from light at 37°C for 5 min. The scaffolds in all groups were washed with PBS several times and the cells were monitored under a fluorescence microscope (4).

ALP activity analysis

The osteoblast cells (MG-63) were cultured for 7, 14, and 21 days for investigation of alkaline phosphatase (ALP) activity. The scaffolds were washed with PBS and added 1% Triton™ x for cell fission. The scaffolds were frozen at -70°C for about 1 h and then allowed to thaw at room temperature for about 1 h and repeated for 3 cycles to separate the solution for ALP activity measurement. The Alkaline Phosphatase Colorimetric Assay Kit (Abcam PLC, Cambridge, UK) was used to detect ALP activity. The method followed the manufacture's instructions.

Histology

The osteoblast cells (MG-63) were cultured for about 7 days in an OS medium to detect cell attachment and migration on the scaffold. The cells were cultured for 14 days to monitor calcium synthesis from the cells. The cells on the scaffolds were

fixed with 4% formaldehyde at 4°C for 24 h. The scaffolds in each group were immersed in paraffin and then cut into 5 μ sections. The sample slides were stained with hematoxylin and eosin and von Kossa.

Statistical analysis

The samples were measured and statistically compared by independent samples t-tests. Statistical significance was defined at $p < 0.05$.

Results and discussion

Structural formation of reconstructed extracellular matrix

The structural characterization of reconstructed collagen type I/fibronectin is shown in Fig. 45. As the Fig.45, fibronectin/collagen organized themselves into aggregation of globular structure that covered the porous surface of the silk fibroin scaffold. The results demonstrated that reconstructed collagen/fibronectin organized themselves into a non-complete extracellular matrix.

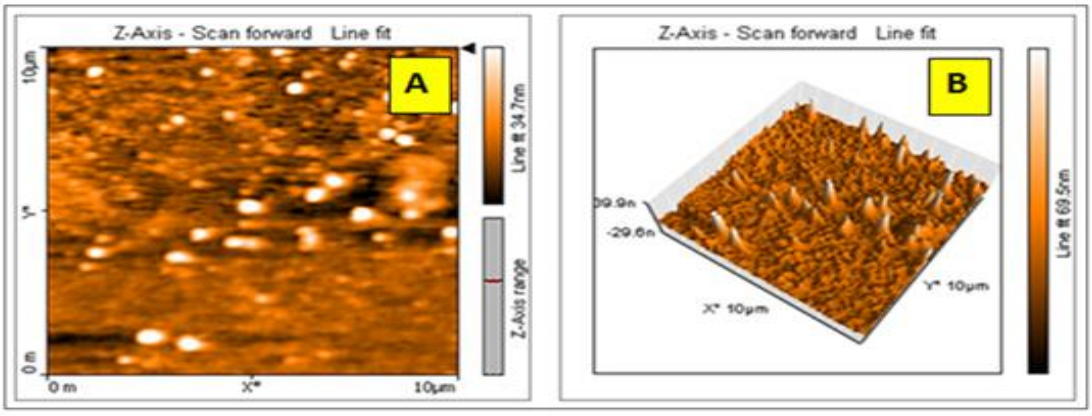

Figure 45. AFM image of coating solution structure of collagen. Network of fibronectin/collagen compound; (A). 2D network of fibronectin/collagen compound; (B).

Morphological structure of mimicked silk fibroin scaffolds

The color of the collagen/fibronectin coated silk scaffold was found to be whiter than the silk scaffold without the coating (Fig. 46). The white color was obtained from the combination of fibronectin and collagen.

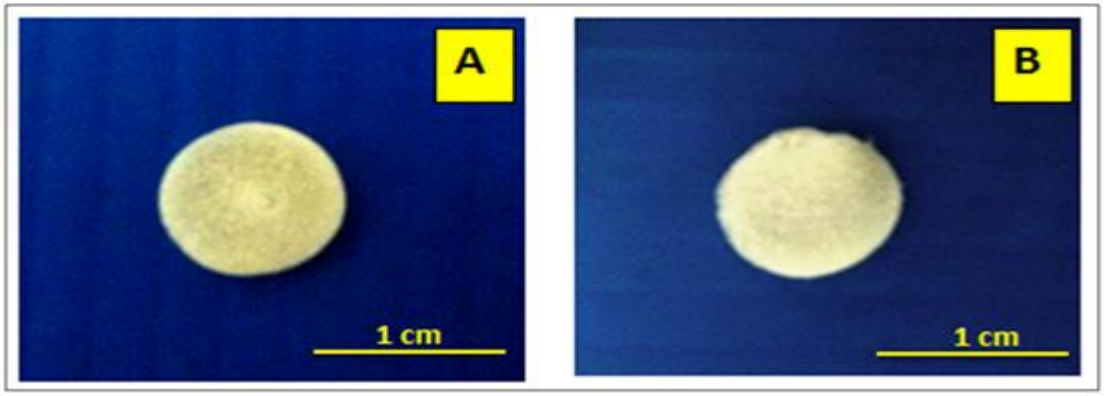

Figure 46. Photographs of the scaffolds. Silk scaffold without coating solution; (A). Collagen/fibronectin-coated silk scaffold; (B).

A smooth surface was found in the silk scaffold (Fig. 47A) and a rough surface was displayed on the silk coated with collagen and fibronectin. Both groups showed an interconnective pore size that supported cell attachment and migration, assistance on the flow of nutrients, and the release of waste (5). This indicated that collagen and fibronectin reconstructed into an incomplete morphological structure of an extracellular matrix. The covered surface showed a roughness that could induce cell adhesion, proliferation, and mineral matrix deposition on a silk fibroin scaffold.

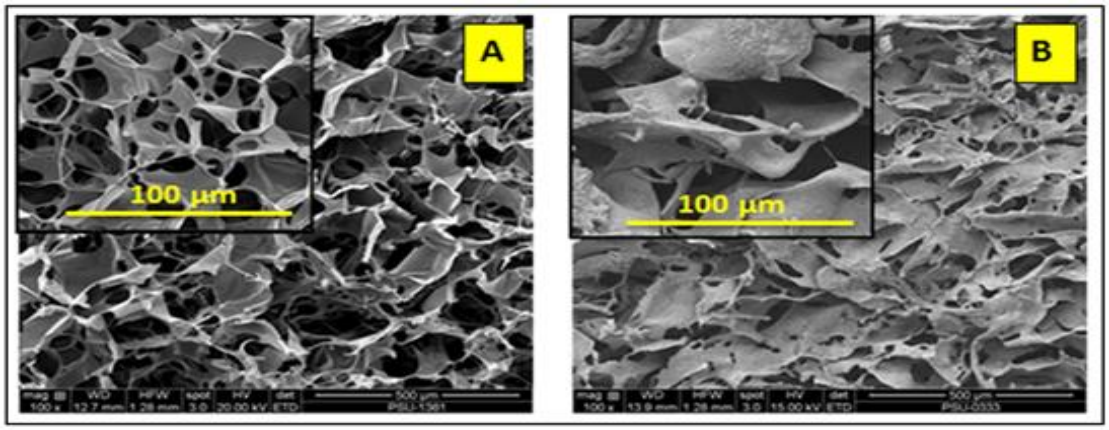

Figure 47. Scanning electron microscopy image of scaffolds. Smooth surface of silk scaffold; (A). Collagen/fibronectin compound network that covered the surface of the silk scaffold; (B)

Cell proliferation

Osteoblast cell (MG-63) proliferation continually increased at every time point in both groups except for the silk scaffold on day 7 (Fig. 48). From day 1 to day 5, the silk scaffold group revealed a higher cell proliferation rate than the silk coated with collagen and fibronectin, but it was not significantly different. On day 7, the cell proliferation rate of the silk coated with reconstructed collagen/fibronectin was higher than the silk scaffold without the coating. The fibronectin formation with collagen could express a great increase in the number of cells.

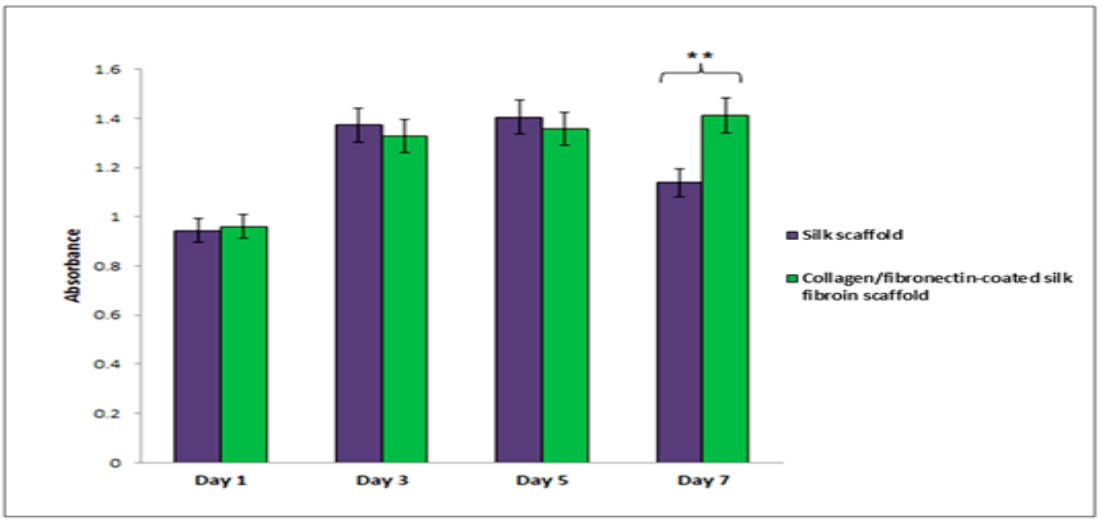

Figure 48. Cell proliferation rate at days 1, 3, 5, and 7 on the scaffold base on PrestoBlue™ assay. The symbol (**) represents significant conversion of the resazurin-based PrestoBlue™ metabolic assay ($p < 0.05$).

Cell viability

The green luminance from the FDA labeling on the MG-63 osteoblasts cell revealed cell viability on the surface of scaffold. The MG-63 cells showed good attachment and migration covering the surface area in the silk coated collagen/fibronectin scaffold group (Fig. 49B) more than the silk scaffold not in the coated group (Fig. 49A). This indicated that collagen and fibronectin improved the cell activity and stimulated cell proliferation.

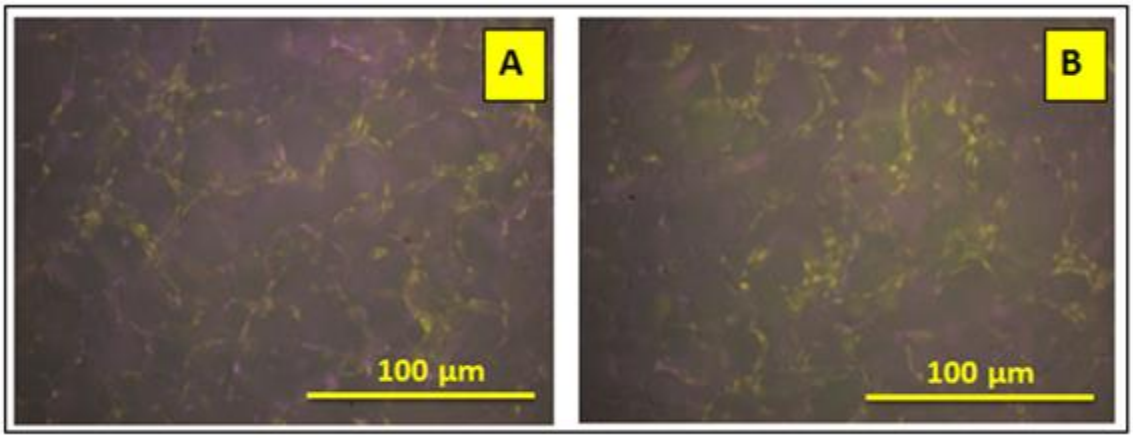

Figure 49. Cell viability on the scaffold with FDA labeling. Silk scaffold; (A). Collagen/fibronectin-coated silk; (B).

ALP activity analysis

The mineralization during cell culturing was analyzed from the ALP activity. The ALP assay was used for early cell differentiation analysis on days 7, 14, and 21. Both groups showed a progressive increase of ALP activity from day 7 to day 21. There was significantly higher ALP activity in the collagen/fibronectin-coated silk group than the silk scaffold at every time point (Fig. 50). The collagen/fibronectin coating on the surface of the silk scaffold increased the ALP activity and synthesis by the MG-63 osteoblasts.

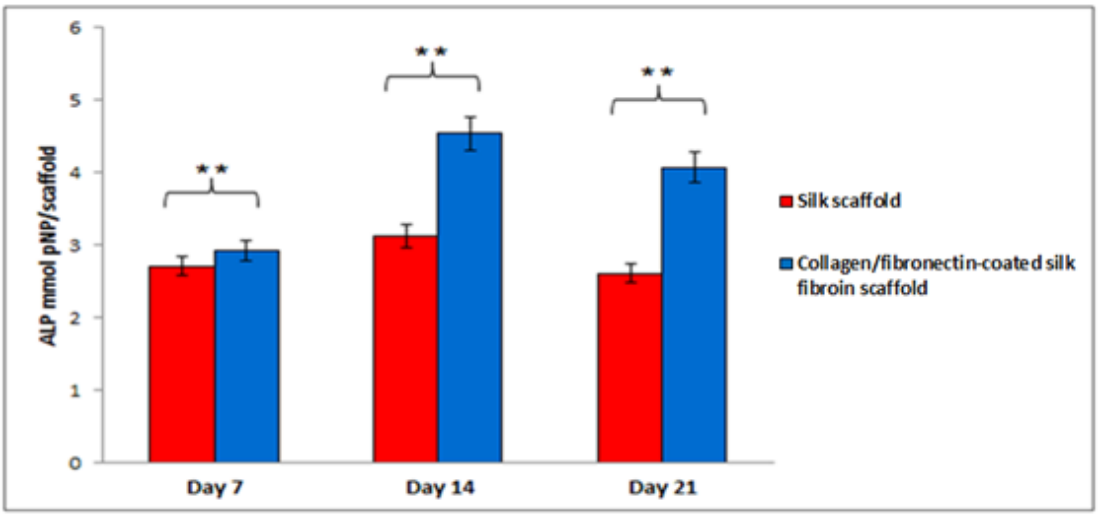

Figure 50. ALP activity from the MG-63 cells at days 7, 14, and 21 of culture. The symbol (**) represents significant changes in resazurin activity of the osteoblasts (p < 0.01).

Histological analysis with hematoxylin and eosin staining

The MG-63 osteoblast cells (blue arrows) showed the morphology characterization attachment on the silk fiber (red arrows) (Fig. 51). The MG-63 cells were well expanded and adhered to the scaffold at both the surface and inner zone. There was no difference in the size and shape between the two groups.

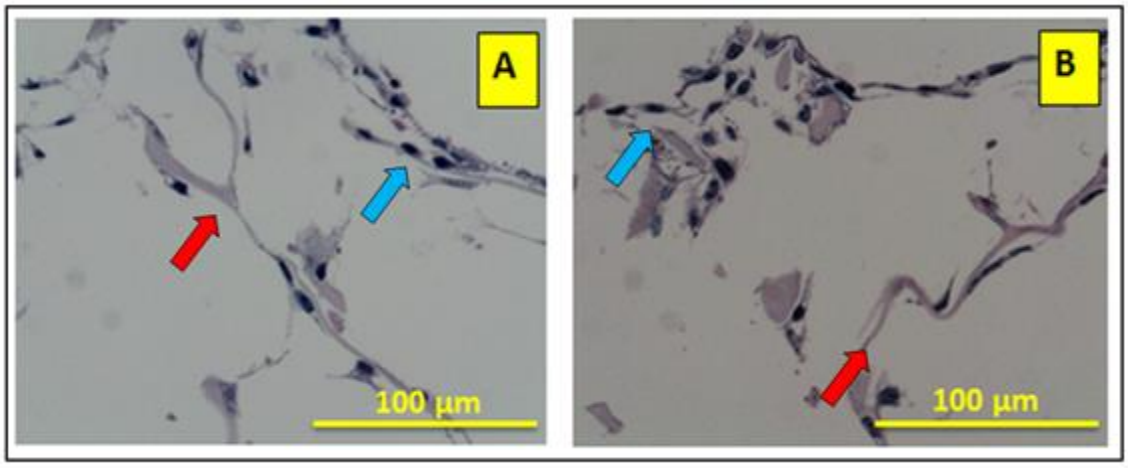

Figure 51. Hematoxylin and eosin staining on the scaffold at day 7. Silk scaffold; (A). Collagen/fibronectin-coated silk; (B).

Mineralized matrix deposition analysis by Von Kossa staining

Von Kossa staining was used to detect deposits of a mineralized matrix. The dark brown areas (blue arrows) indicated a mineralized matrix synthesized from the osteoblast cells. The long dark brown lines (red arrows) showed the scaffold area covered with a mineralized matrix secreted from the cells. The osteoblast cells indicated efficiency on attachment to both the surface and pores and a great amount of synthesized mineralization.

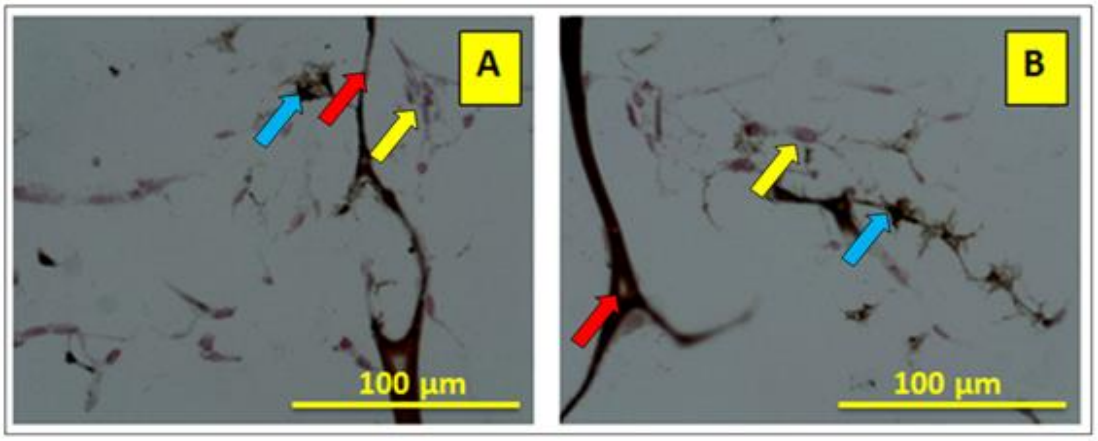

Figure 52. Von Kossa staining on scaffold at day 14. Silk scaffold; (A). Collagen/fibronectin-coated silk; (B).

Discussion

In this research, a modified silk fibroin scaffold with reconstructed collagen/fibronectin was used for bone tissue engineering in alveolar resorption. The silk fibroin scaffold coated with collagen and fibronectin can improve the biofunctionalities. Such interaction disturbed fibrillation of collagen type I (6). Hence, fibronectin/collagen compound did not form triple helical collagen fibrils after soaked in PBS. Clearly, as in previous reports, fibronectin could bind with collagen molecules at a binding site (7). Fibronectin disturbed self-assembly of collagen into fibrils (6). Therefore, the reconstructed collagen/fibronectin showed non-fibril structure on the porous surface of the scaffold as Fig. 29.

Interestingly, reconstructed collagen/fibronectin organized themselves into a rough surface that came from small global aggregation and the microrough

surface stimulated the differentiation function of the cells. Importantly, the rough surface promoted osteoblast proliferation, ALP activity, and osteocalcin expression (6).

The reconstructed collagen/fibronectin arranged into a suitable microenvironment for cell growth and migration. (7). In osteoblast differentiation, fibronectin played an important role in the cells with integrin interaction (8). The collagen intergrin receptor alpha 2 beta 1 as a binding site for fibronectin (9) provided stable adhesion and osteoblast differentiation (10). Remarkably, the morphology of the cells in all groups showed that the cytoplasm spread out to adhere to the surface of the scaffold. Fibronectin bound to collagen could stimulate cell migration and cell enhancement (11). Collagen type I and fibronectin were important in forming calcified structures and osteoblast differentiation. Collagen type I is the main component (90%) of bone and some studies suggested that collagen was necessary in scaffolding for mineralization. Collagen and fibronectin were found to encourage calcification (12). The modified silk fibroin scaffold with reconstructed collagen/fibronectin has good performance for bone tissue engineering and has promise for bone grafting in alveolar bone resorption.

Reference

1. Biman B.Mandal, Sonia Kapoor, Subhas C.Kundu. Silfibroin/polyacrylamide semi-interpenetrating network hydrogels for controlled drug release. Biomaterials. 30; 2009: 2826-2836.
2. Ting-Ting Li, Katrin Ebert, Jurgen Vogel, Thomas Groth. Comparative studies on osteogenic potential of micro- and nanofibre scaffolds prepared by electrospinning of poly(ε-caprolactone). Progress in Biomaterials. 2; 2013: 1-13.
3. Ung-Jin Kim, Jaehyung Parka, Hyeon Joo Kima, Masahisa Wada, David L. Kaplan. Three-dimensional aqueous-derived biomaterial scaffolds from silk fibroin. Biomaterials. 26; 2005: 2775-2785.
4. John A. Mcdonald, Diane G. Kelley, Thomas J. Broekelmann. Role of Fibronectin in Collagen Deposition : Fab' to the Gelatin-binding Domain of Fibronectin Inhibits Both Fibronectin and Collagen Organization in Fibroblast Extracellular Matrix. Cell Biology. 19; 1982: 485-492.
5. Bette J. Dzamba, Hong Wu, Rudolf Jaenisch, Donna M. Peters. Fibronectin Binding Site in Type I Collagen Regulates Fibronectin Fibril Formation. J Cell Biol. 121; 1993: 1165-1172.
6. Chang G, Kim HJ, Kaplan D, Vunjak-Novakovic G, Kandel RA. Porous silk scaffolds can be used for tissue engineering annulus fibrosus. European Spine Journal. 16; 2007: 1848-1857.
7. Candace D. Gildner, Daniel C. Roy, Christopher S. Farrar, Denise C. Hocking. Opposing effects of collagen I and vitronectin on fibronectin fibril structure and function. Matrix Biol. 34; 2014: 33-45.
8. Sujin Lee, Dong-Sung Lee, Ilsan Choi, Le B. Hang Pham, Jun-Hyeog Jang. Design of an Osteoinductive Extracellular Fibronectin Matrix Protein for Bone Tissue Engineering. Int. J. Mol. 16; 2015: 7672-2682.
9. Roberto Pacifici, Cristina Basilico, Jesse Roman, Mary M. Zutter, Samuel A. Santoro, Ruth McCracken. Collagen-induced Release of Interleukin 1 from Human Blood Mononuclear Cells Potentiation by Fibronectin Binding to the $\alpha_5\beta_1$ Integrin. J. Clin Invest. 2; 2005: 119-125.

10. Benjamin G. Keselowskya, David M. Collard, Andres J. Garcıia. Surface chemistry modulates focal adhesion composition and signaling through changes in integrin binding. Biomaterials. 25; 2004: 5947-5954.
11. Carlos A. Sevilla, Diane Dalecki, Denise C. Hocking. Regional Fibronectin and Collagen Fibril Co-Assembly Directs Cell Proliferation and Microtissue Morphology. PLoS One. 8; 2013: 1-17.
12. Karol E. Watson, Farhad Parhami, Victoria Shin, Linda L. Demer. Fibronectin and Collagen I Matrixes Promote Calcification of Vascular Cells in Vitro, Whereas Collagen IV Matrix Is Inhibitory. Arteriosclerosis, Thrombosis, and Vascular Biology. 18; 1998: 1964-1971.

Bioinspired, Biomimetic and Nanobiomaterials

Modified silk and chitosan scaffolds with collagen assembly for osteoporosis

–Manuscript Draft–

Manuscript Number:	BBN-D-15-00006
Full Title:	Modified silk and chitosan scaffolds with collagen assembly for osteoporosis
Article Type:	Research Article
Keywords:	Silk fibroin, Chitosan, Collagen, Bone tissue engineering, Osteoporosis
Corresponding Author:	Jirut Meesane, Dr.Ing Institute of Biomedical Engineering Hat-Yai, Songkhla THAILAND
Corresponding Author Secondary Information:	
Corresponding Author's Institution:	Institute of Biomedical Engineering
Corresponding Author's Secondary Institution:	
First Author:	Jirut Meesane, Dr.Ing
First Author Secondary Information:	
Order of Authors:	Jirut Meesane, Dr.Ing
	Supaporn Sangkert, B.Sc
	Suttatip Kamonmattayakul, Ph.D
	Chai Lin, Ph.D
Order of Authors Secondary Information:	
Abstract:	Currently, there are many patients who suffer from osteoporosis. Osteoporosis is a disease that leads to bone defect. Severe cases of bone defect from osteoporosis need an operation using a performance scaffold for bone tissue engineering. Therefore, to build a performance scaffold for bone defect from osteoporosis is the target of this research. Samples of silk fibroin and chitosan were fabricated into porous scaffolds before modification by coating with collagen self-assembly. The structure and morphology of the samples were characterized and observed by Fourier transform infrared (FTIR) spectroscopy, atomic force nicroscope (AFM) and scanning electron microscope (SEM). For biological functionality analysis, MC3T3-E1 osteoblasts were cultured on the samples. Afterward, biodegradation, cell proliferation, viability and mineralization were analyzed. The results demonstrated that collagen organized into a fibril structure covering the pores of the scaffold. The modified scaffolds showed low degradability, high cell proliferation, viability and mineralization. The results demonstrated that the modified scaffolds with a coating of mimicked collagen self-assembly had good performce and showed promise for bone tissue engineering in osteoporosis.
Suggested Reviewers:	Ruth Cameron, Ph.D University of Cambridge rec11@cam.ac.uk She has many experiences in the field of matereials for medicne that relate to this aricle.
	Jan Czernuszka, Ph.D University of Oxford jan.czernuszka@materials.ox.ac.uk He is the person who have experiences and hold many research about biomaterials. Therefore,his expertise relate to this article.
	Gwendolen Reilly, Ph.D University of Sheffield g.reilly@sheffield.ac.uk

Manuscript with author contact details

Modified silk and chitosan scaffolds with collagen assembly for osteoporosis

[1]Supaporn Sangkert (B.Sc), M.Sc.student, [2]Suttatip Kamonmattayakul (Ph.D), Associate Professor, [3]Chai Wen Lin (Ph.D), Associate Professor, [1*]Jirut Meesane (Dr.-Ing), Assitant Professor

[1]Biological Materials for Medicine Research Unit, Institute of Biomedical Engineering, Faculty of Medicine, Prince of Songkla University, Hat Yai, Songkhla, Thailand, 90110

[2]Department of Preventive Dentistry, Faculty of Dentistry, Prince of Songkla University, Hat Yai, Songkhla, Thailand, 90110

[3]Department of General Dental Practice and Oral and Maxillofacial Imaging, Faculty of Dentistry, University of Malaya, Kualalumpur, Malaysia

Tel: 66-74-558866 Fax: 66-74-446728 *Correspondence author e-mail: jirutmeesane999@yahoo.co.uk

ABSTRACT

Currently, there are many patients who suffer from osteoporosis. Osteoporosis is a disease that leads to bone defect. Severe cases of bone defect from osteoporosis need an operation using a performance scaffold for bone tissue engineering. Therefore, to build a performance scaffold for bone defect from osteoporosis is the target of this research. Samples of silk fibroin and chitosan were fabricated into porous scaffolds before modification by coating with collagen self-assembly. The structure and morphology of the samples were characterized

and observed by Fourier transform infrared (FTIR) spectroscopy, atomic force nicroscope (AFM) and scanning electron microscope (SEM). For biological functionality analysis, MC3T3-E1 osteoblasts were cultured on the samples. Afterward, biodegradation, cell proliferation, viability and mineralization were analyzed. The results demonstrated that collagen organized into a fibril structure covering the pores of the scaffold. The modified scaffolds showed low degradability, high cell proliferation, viability and mineralization. The results demonstrated that the modified scaffolds with a coating of mimicked collagen self-assembly had good performce and showed promise for bone tissue engineering in osteoporosis.

Keywords: Silk fibroin, Chitosan, Collagen, Bone tissue engineering, Osteoporosis

1. Introduction

A report shows that osteoporosis is the major disease of public health problems (1). About 200 million women around the world have bone loss from osteoporosis that causes more than 8.9 million fractures annually (2). The patients who are confronted with osteoporosis must take medications, for example raloxifene which is a synthetic estrogen receptor modulator (SERM) to preserve the bone; however, its side effects are harmful (3). Another way to cure the patient is surgery (4). In some cases the patients need biomaterials for bone substitution (5). Therefore, to create performance materials for osteoporosis is a challenging issue.

Currently, bone tissue engineering has been used for bone diseases that need performance materials substitution. The aim of bone tissue engineering (TE) is the repair of damaged tissue and regeneration of new tissue. The popular approach for bone tissue engineering is to seed and culture cells in a porous scaffold before transplant into the target tissue site. The

porous scaffold acts as a biodegradable substituted material that has the role of a template for cell adhesion. The cells are then induced to be new tissue (6). The properties of the scaffold should be biocompatible, bioresorbable and have a controllable degradation rate to match the tissue growth. The surface of the scaffold has the proper chemistry for cell attachment, proliferation, and differentiation. The scaffold properties need to be three-dimensional and highly porous with interconective pores for nutrient and metabolic waste transport (7).

Silk fibroin (SF) is the protein obtained from the silk worm, *Bombyx mori*. The main amino acids are glycine (43%), alanine (30%) and serine (12%) (8). SF demonstrates excellent properties that include biocompatibility, great mechanical properties and biodegradable and SF can fabricate in various forms (9). The porous scaffold was suitable for bone tissue engineering because the cells can proliferate, migrate and attach to the surface of the interconnecting pores of the scaffold (10,11).

Chitosan is a semi-crystalline polysaccharide. A deacetylated form of chitin is obtained from the cell wall of fungi and the shells of crabs, shrimps and the bony plates of squids and cuttlefish. Pure chitosan has the properties of biocompatibility, biodegradation and can be prepared in many forms (12). Because of its unique properties chitosan has been used as scaffolds for bone tissue engineering (13).

Collagen is a fibril protein composed of a triple helix of the peptide molecule. The main amino acids in the peptide molecule are glycine, alanine and proline. Predominantly, the fibril structure and amino sequence of arginylglycylaspartic acid in collagen can induce cell adhesion and tissue regeneration (14,15). The unique biofunctionality of collagen lends itself to be used as material for tissue regeneration. To mimick collagen self-assembly is an

attractive technique that can reconstruct the fibril structure of collagen as an extracellular matrix (ECM) (16). Importantly, collagen fibril is the structure that can enhance cell adhesion and proliferation (17). Therefore, to use the mimicry of collagen self-assembly for scaffold modification was chosen for this research.

Due to the advantages of silk fibroin, chitosan, and collagen, they were selected as materials to build a performance porous scaffold for bone tissue engineering in this research. Silk fibroin and chitosan were fabricated into porous scaffolds before modification by coating with mimicked collagen self-assembly that can organize into a fibril structure. The structure, morphology, and biofunctionality of the modified scaffold was considered. Eventually, the aim of this research is to create a performance scaffold that hold promise for bone tissue engineering in osteoporosis.

2. Materials and methods

2.1 Materials

2.1.1 Preparation of silk fibroin scaffolds

Degummed silk fibrin was extracted by boiling the cocoons for 30 min in 0.02 M Na_2CO_3 to remove sericin, the glue like protein that holds the fibers together. The degummed silk fibroin was dried in a hot oven (14). A 9.3 M lithium bromide solution was used to dissolve the silk fibroin. The solution was then subjected to dialysis to remove the lithium bromide (15). The silk fibroin solution was adjusted to 3% (w/v) and poured into 48 well plates for the forming of 3-dimensional silk fibroin after the freeze-dried method (14).

2.1.2 Preparation of type I collagen

The skin of the brown banded bamboo shark, *Chiloscyllium punctatum*, was used for collagen extraction that followed the report of P. Kittiphattanabawon et al. 2010 (16). Briefly, the shark skin was cut into small sizes, combined with 0.1M NaOH to remove the none collagen proteins. The skin continued to soak in 0.5 M acetic acid for 48 h. The collagen solution was filtered and then the final concentration of NaCl was adjusted to 2.6 M and 0.05 M of tris(hydroxymethyl)aminomethane at pH 7.5. The collagen solution was centrifuged using a refrigerated centrifuge machine. Then the collagen pellet was collected and dissolved in a minimum volume of 0.5 M acetic acid. The collagen solution was subjected to dialysis with 0.1 M acetic acid for 12 h and 48 h in distilled water. The freeze-dried method was used for removal of the water and kept at -20°C until use.

2.1.3 Preparation of chitosan scaffold

Sufficient chitosan powder (Marine Bio Resources Co., Ltd, Shrimp Chitosan) was dissolved in 0.1 M acetic acid for a 2% concentration and mixed continuously in a magnetic stirrer for 24 h. The chitosan solution was poured into 48 well plates and then kept at -20°C for overnight. The freeze-drying method was used to fabricate 3D chitosan scaffolds (17). After that they were cut into 10 mm diameter and 2 mm thick pieces.

2.1.4 Modification of silk fibroin and chitosan scaffolds

This study designed the scaffolds into 4 groups: 1) non-coated silk fibroin scaffolds without collagen, 2) coated silk fibroin scaffolds with collagen, 3) non-coated chitosan scaffolds with collagen and 4) coated chitosan scaffolds with collagen. 0.1 mg/ml collagen solution was used for coating (Table 1). To coat with the collagen solution, silk fibroin and chitosan scaffolds were immersed in a collagen solution for 4 hours at 37°C. Afterwards, the

immersed scaffolds were soaked in 1xPBS for 30 minutes to form self-assembly of collagen. These scaffolds were kept at -20°C for overnight before freeze-drying.

Table 1

2.2 Methods

2.2.1 Self-assembly of collagen type I

Collagen solution was mixed with PBS to observe self-assembly. The optical density (OD) at 313 nm was used to identify the form of the collagen fibrils (18). The OD of the mixed collagen solution was measured every 5 minutes for 30 minutes. The OD of each time point was plotted into a kinetic curve to explain the collagen self-assembly.

2.2.2 Atomic Force Microscopy Observing

A sample of the collagen solution at a concentration of 0.1 mg/ml was dropped and smeared onto a glass slide. After soaking in 1xPBS for 30 minutes, the glass slide was dried at room temperature. Then, the coated glass slide with collagen was observed for self-assembly formation of the collagen by atomic force microscopy (Nanosurf easyScan 2 AFM, Switzerland).

2.2.3 Fourier transform infrared (FTIR) spectroscopy

The chemical functional group of collagen was obtained using a FTIR spectrometer (EQUINOX 55, Bruker, Ettlingen, Germany). The internal reflection crystal (Pike Technologies, Madison, WI, USA), made of zinc selenide, had a 45° angle of incidence of the IR beam. The spectra were acquired at a resolution of 4 cm^{-1}. The spectral data analysis used the OPUS 3.0 data collection software program (Bruker, Ettlingen, Germany). To

characterise the chemical function groups of collagen self-assembly, the mixed collagen with PBS as in the previous experiment was freeze-dried before preparation into KBr discs and measured by FTIR.

2.2.4 Scanning Electron Microscopy (SEM) Observing

All groups of scaffolds were observed for morphology, surface and pore size by a scanning electron microscope (Quanta400, FEI, Czech Republic). The samples were pre-coated with gold using a gold sputter coater machine (SPI supplies, Division of STRUCTURE PROBE Inc., Westchester, PA USA).

2.2.5 Degradation

Lysozyme powder was mixed with PBS into solution at 4 mg/ml (pH = 7.4) before incubation at 37°C (19). The scaffolds were immersed in that solution. The scaffolds were then removed from the solution, rinsed and freeze-dried. The freeze-dried scaffolds were weighed at different time points: 1, 2, and 4 weeks. Afterward, the percentage of weight loss was calculated.

2.3 Cell culture

MC3T3-E1 osteoblast cells were seeded in each scaffold with 1×10^5 cells and maintained in an alpha-MEM medium (α-MEM, GibcoTM, Invitrogen, Carlsbad, CA) with the addition of 1% penicillin/streptomycin, 0.1% fungizone and 10% fetal bovine serum (FBS) at 37°C in a humidified 5% of CO_2 and 95% air incubator (20). The medium was changed every 3-4 days. An osteogenic medium (OS; 20 mM b-glycerophosphate, 50 μM ascorbic acid, and 100 nM dexamethasone; SigmaAldrich) was used for osteoblast differentiation of the MC3T3-E1 osteoblast cells (21).

2.3.1 Cell Proliferation

The measurement of cell proliferation was performed on days 3, 5 and 7 (22). Following the manufacturer's protocol, the scaffold was washed two times with 1xPBS and fresh media of 100 µl and 10 µl of 12 mM MTT (3-[4,5-dimethylthiazol-2-yl]-2,5-dimethyl tetrazolium bromide, and 5 mg/ml) were added into the cells/scaffolds, respectively. Afterward, the cells/scaffolds were incubated for 2 hours at 37ºC. Then, 50 µl of dimethyl sulfoxide was added to each cells/scaffolds and incubated for 10 minutes. The solutions were moved to 96 well plates and measurements continued by monitoring the light absorbance at 540 nm.

2.3.2 Cell viability

On day 3, the MC3T3-E1 osteoblast cells in the scaffolds were stained with fluorescein diacetate (FDA). The FDA attached to the extracellular matrix and cellular clusters. The FDA was dissolved with acetone at a concentration of 5 mg/ml. The medium was removed and replaced with 1 ml of fresh medium, then 5 µl of the FDA was added. The scaffolds were kept away from light for 5 minutes. The scaffolds were washed twice with 1xPBS and moved to a glass slide and the cell morphology was observed by a fluorescence microscope (23).

2.3.3 Alizarin red staining

The calcium synthesis of the MC3T3-E1 osteoblast cells was inspected by alizarin red staining. On days 7, the scaffolds were washed with 1xPBS and the cells were fixed with 4% formaldehyde before the addition of 1 ml of alizarin red solution (2 g in 100 ml of distilled water to adjust the pH to 4.1-4.3) for 20 min at room temperature in the dark (24). The alizarin red was removed carefully from 48 well plates and the scaffolds were washed with

distilled water until the red color disappeared. Afterward, that scaffolds were observed by light microscope.

2.3.4 Statistical analysis

All data were shown as mean ± standard deviation. The samples were measured and statistically compared by one-way ANOVA and Tukey's HDS test (SPSS 16.0 software package). $P< 0.05$ was accepted as statistically significant.

3. Results and discussion

3.1 Self assembly of collagen fibril

Before coating scaffolds, self-assembly of collagen was monitored by measuring the absorbance at a wavelength of 313 nm at each time point. Then, the absorbances were plotted into a kinetic curve (Fig. 1). The curve represented self-assembly of collagen fibrils (25). We monitored the collagen self-assembly in solution for 30 min that corresponded to the coating time of collagen on the scaffolds. The absorbance value increased with time (Fig. 1). During the time from 5 minutes to 30 minutes, the group absorbance was higher at each time point which meant collagen fibrils were forming in the solution. In this study, it showed that collagen type I solution 0.1 mg/ml (0.1 M acetic acid, pH 2.88) was mixed PBS with ratio 1:1 for neutralization. Under these conditions, collagen molecules organized and aggregated into the fibril structure (26). Notably, it indicated that the collagen organized into the fibril structure during the time of coating.

Fig. 1.

3.2 Collagen self assembly by AFM observing

Neutralized collagen solution was dripped and dried on a glass slide to observe the structure formation by AFM of the collagen fibrils in the coating. The collagen fibrils organized themselves into small branches (Fig. 2). Interestingly, this indicated that the neutralized collagen solution had performed coating that could mimic the fibril structure as an extracellular matrix. Notably, the mimicked collagen fibril could induce cell adhesion and proliferation (27). Nevertheless, to confirm the fibril structure of collagen, the neutralized collagen solution was freeze-dried before characterization by FTIR in the next section.

Fig. 2.

3.3 FTIR analysis

The freeze-dried neutralized collagen solution was characterized by FTIR to demonstrate the fibril structure of the collagen coating. Principally, the FTIR technique detected the vibration characteristics of the chemical functional groups of collagen. A specific wavenumber (cm^{-1}) range of IR radiation was absorbed by the chemical functional group (28). The amide A band of collagen was found at 3292 cm^{-1}, this was the general band associated with the N–H stretching vibration and indicated the existence of hydrogen bonds. When the NH group of peptides formed the hydrogen bond, the absorbance shifted to a lower wavenumber. The amide B was observed at 2921–2925cm^{-1}. The amide I of collagen was found at 1631 cm^{-1}. This band was due to C=O stretching vibration. Importantly, the FTIR results indicated that the collagen could organize into fibril structures (29). Therefore, these results confirmed the previous explanation that collagen could form into a fibril structure in the coating.

Fig. 3.

3.4 Scanning electron microscopy analysis

After clarification that the collagen could arrange into a fibril structure, the coating solution was used for silk fibroin and chitosan scaffolds. For coating, silk fibroin and chitosan scaffolds were immersed in a collagen solution at pH 3 before soaking in PBS. Then, those scaffolds were freeze-dried before observation of the morphology by SEM. Interestingly, the morphology of the scaffolds showed that the coated scaffolds of silk fibroin and chitosan had deposited a fibril network structure of collagen inside the pores (Fig. 4). Therefore, the results from the SEM indicate that collagen could form a fibril network structure as a mimicked extracellular matrix that deposited inside the pores of the scaffolds. Importantly, the mimicked extracellular matrix might induce cell adhesion and proliferation as according to a previous report (30). Besides the suitable structure for cell adhesion and proliferation, it is important to determine the biodegradation of scaffolds in tissue engineering. Biodegradation and cell experiments were undertaken to vindicate those issues,.

Fig. 4.

3.5 Analysis of scaffold degradation

The scaffolds in all groups showed a changed shape. The silk scaffold revealed the surface and margin areas that were digested with lysozyme (Fig. 5A). The surface area of the silk scaffold coated collagen group collapsed but maintained a good shape (Fig. 5B) when compared with the other groups. The chitosan scaffold was broken after digestion and the surface and margin areas were digested (Fig. 5C). The coated chitosan scaffold with collagen showed the most digestion in the marginal zone and the surface area collapsed after digestion (Fig. 5D). Both silk and chitosan scaffolds coated with collagen showed slow degradation compared to the non-coated scaffolds. The triple helix structure of collagen coated on the

scaffold surface was the cause of difficult degradation. The silk fibroin scaffold coated with collagen showed the least amount of degradation. These results illustrated the same explanation as previously reported that the molecules of the enzyme had less opportunity to contact the scaffold (31). Furthermore, the literature was reported that the silk fibroin could extend biodegradability of the scaffolds (32).

Fig. 5.

The silk fibroin scaffold with and without modification had more stability from biodegradtion than the modified and non-modified chitosan scaffold. Importantly, the results indicated that collagen could improve biodegradation of scaffolds. Interestingly, silk fibroin and chitosan scaffolds better tolerated the enzyme activity after coating (Fig. 6). The results of biodegradtion indicated that the coated scaffolds with mimicked collagen self-assembly had the performance for bone tissue engineering. However, to confirm the performance of those modified scaffolds experiments to determine cell proliferation, viability, and mineralization were undertaken.

Fig. 6.

3.6 Cell proliferation

Figure 7 showed the MTT assay in cell proliferation on the scaffolds. The results showed that the OD values increased from day 3 to 5 and then decreased on day 7 of the cell culture. On day 3, OD value of the silk fibroin scaffold was higher than the chitosan scaffold. The coated scaffold with mimicked collagen self-assembly had directly improved cell proliferation. The cell proliferation of the silk fibroin and chitosan scaffolds after coating with mimicked

collagen self-assembly showed good performance for bone tissue engineering. Cell proliferation in all groups of the scaffold increased on day 5 which demonstrated that the cells adhered and proliferated in all groups. Notably, the collagen coated silk fibroin scaffold and the collagen coated chitosan scaffold showed the highest cell proliferations on day 7. The results indicated that collagen promoted cell proliferation and adhesion. The literature reported that collagen had the important role of inducing cell migration and differentiation (33).

Fig. 7.

3.7 Fluorescein Diacetate (FDA)

The MC3T3-E1 cells adhered in all groups to the scaffolds. The bright green indicated the cell viability and morphology thoroughly on the surface. The coated scaffolds with mimicked collagen self-assembly showed a lot of cells compared to the non-coated scaffolds. The cells arranged and expanded themselves on the surface of the coated scaffolds. This demonstrated that the coated scaffolds with mimicked collagen self-assembly could enhance cell viability. However, to confirm the performance of scaffolds for bone tissue engineering, the presence calcium in the scaffold was analyzed and observed in the next section.

Fig. 8.

3.8 Alizarin red

To confirm the presence of calcium that was secreted from the MC3T3-E1 cells, the scaffolds were stained with Alizarin red. Afterward, the stained scaffolds were observed by microscope. Calcium nodules were found in all groups of scaffolds (Fig. 9). The results

showed that the MC3T3-E1 cells could grow in the scaffolds and secret calcuim onto the scaffolds. The staining with alizarin red indicated a high amount of calcium deposition. The coated scaffolds could induce calcium synthesis from the MC3T3-E1 cells. Notably, in the coated silk fibroin, the calcium deposition was more intensive than the coated chitosan scaffold. The results demonstrated that the coated scaffolds with mimicked collagen self-assembly had the performance for bone tissue engineering particularly in the coated silk fibroin scaffold.

Fig. 9.

4. Conclusion

The use the modified scaffolds by coatings with mimicked collagen self-assembly for tissue engineering was proposed in this research for osteoporosis treatment in the case of bone defect. The results of this research indicated that collagen organized into assembled fibril structures in the pores of the coated scaffolds. The fibril structures showed performance as an extracellular matrix that could induce biogical functionalities of coated scaffolds. Predominantly, the coated silk fibroin and chitosan scaffolds with collagen self-assembly had good biological functionalities: stability from biodegradation, good cell proliferation, viability and mineralization. Importantly, it can be deduced that the modified scaffolds by coating with mimicked collagen self-assembly had the proformance for bone tissue engineering and showed promise for use in osteoporosis treatment.

ACKNOWLEDGEMENT

This work was financially supported by grant no. EC 50-042-25-2-3 from the Faculty of Medicine, Prince of Songkla University. Many thanks to the Biological Materials for Medicine (BMM) Research Unit and Queen Sirikit Sericulture Centre, Narathiwat, for silk supporting.

REFERENCES

1. O. Strom.; F. Borgstrom.; John A. Kanis.; Juliet Compston.; Cyrus Cooper.; Eugene V. McCloskey.; Bengt Jonsson. Osteoporosis: burden, health care provision and opportunities in the EU. Arch Osteoporos. 2011, 6, 59-155.
2. Kanis JA. on behalf of the World Health Organization Scientific Group (2007) Assessment of osteoporosis at the primary health-care level. Technical Report. World Health Organization Collaborating Centre for Metabolic Bone Diseases, University of Sheffield, UK. 2007: Printed by the University of Sheffield.
3. Jill Waalen. Current and emerging therapies for the treatment of osteoporosis. Journal of Experimental Pharmacology. 2010, 2, 121-134.
4. Julie A. Sterling.; Scott A. Guelcher. Biomaterial Scaffolds for Treating Osteoporotic Bone. Curr osteoporos Rep. 2014, 12, 48-54.
5. Marc Bohner. Resorbable biomaterials as bone graft substitutes. Materialstoday. 2010, 13, 24-30.
6. Fergal J. O'Brien. Biomaterials & scaffolds for tissue engineering. Materialstoday. 2011, 14, 88-95.
7. Xiaoming Li.; Rongrong Cui.; Lianwen Sun.; Katerina E. Aifantis.; Yubo Fan.; Qingling Feng.; Fuzhai Cui.; Fumio Watari. 3D-Printed Biopolymers for Tissue Engineering Application. International Journal of Polymer Science. 2014, 2014, 1-13.
8. Yongzhong Wang.; Dominick J. Blasioli.; Hyeon-Joo Kim.; Hyun Suk Kim.; David L. Kaplan. Cartilage tissue engineering with silk scaffolds and human articular chondrocytes. Biomaterials. 2006,27, 4434–4442.
9. Cristina Correia.; Sarindr Bhumiratana.; Le-Ping Yan.; Ana L. Oliveira.; Jeffrey M. Gimble.; Danielle Rockwood.; David L. Kaplan.; Rui A. Sousa.; Rui L. Reis.; Gordana Vunjak-Novakovic. Development of silk-based scaffolds for tissue engineering of bone from human adipose-derived stem cells. Acta Biomaterialia. 2012,8, 2483–2492.

10. Boonlom Thavornyutikarn.; Nattapon Chantarapanich.; Kriskrai Sitthiseripratip.; George A. Thouas.; Qizhi Chen. Bone tissue engineering scaffolding: computer-aided scaffolding techniques. Prog Biomater. 2014, 3, 61–102.
11. Murphy CM.; Haugh MG.; O'Brien FJ. The effect of mean pore size on cell attachment, proliferation and migration in collagen-glycosaminoglycan scaffolds for tissue engineering. Biomaterials. 2010, 31, 461-6.
12. Nitar New.; Tetsuya Furuike.; Hiroshi Tamura. The Mechanical and Biological Properties of Chitosan Scaffolds for Tissue Regeneration Templates Are Significantly Enhanced by Chitosan from Gongronella butleri. Materials. 2009, 2, 374-398.
13. Ana Rita Costa-Pinto.; Rui L. Reis.; Nuno M. Neves. Scaffolds Based Bone Tissue Engineering: The Role of Chitosan. Tissue engineering: Part B. 2011, 17, 1-17.
14. Lisa D. Muiznieks.; Fred W. Keeley. Molecular assembly and mechanical properties of the extracellular matrix: A fibrous protein perspective. Biochimica et Biophysica Acta (BBA) - Molecular Basis of Disease. 2013, 1832, 866-875.
15. Shizuka Yamada.; Kohei Yamamoto.; Takeshi Ikeda.; Kajiro Yanagiguchi.; Yoshihiko Hayashi. Potency of Fish Collagen as a Scaffold for Regenerative Medicine. BioMed Research International. 2014, 2014, 1-8.
16. Blayne A. Roeder.; Klod Kokini.; Jennifer E. Sturgis.; J. Paul Robinson.; Sherry L. Voytik-Harbin. Tensile Mechanical Properties of Three-Dimensional Type I Collagen Extracellular Matrices With Varied Microstructure. Transactions of the ASME. 2002, 124, 214-222.
17. Timothy Douglas.; Sascha Heinemann.; Ute Hempel.; Carolin Mietrach.; Christiane Knieb.; Susanne Bierbaum.; Dieter Scharnweber.; Hartmut Worch. Characterization of collagen II fibrils containing biglycan and their effect as a coating on osteoblast adhesion and proliferation. J Mater Sci: Mater Med. 2008, 4, 1653-1660.
18. Rucsanda C. Preda.; Gary Leisk.; Fiorenzo Omenetto.; David L. Kaplan. Bioengineered Silk Proteins to Control Cell and Tissue Functions. Protein nanotechnology. 2012, 996, 19-41.
19. G. Chang; H.-J. Kim.; D. Kaplan.; G. Vunjak-Novakovic.; R. A. Kandel. Porous silk scaffolds can be used for tissue engineering annulus fibrosus. Eur Spine J. 2007, 16, 1848-1857.
20. Phanat Kittiphattanabawon.; Soottawat Benjakul.; Wonnop Visessanguan.; Hideki Kishimura.; Fereidoon Shahidi. Isolation and Characterisation of collagen from the skin

of brownbanded bamboo shark (Chiloscyllium punctatum). Food Chemistry. 2010, 119, 1519–1526.

21. Stephanie Tully-Dartez.; B.S., Henry E. Cardenas.; Ping-Fai Sidney Sit. Pore Characteristics of chitosan scaffolds studied by electrochemical impedance spectroscopy. Tissue engineering; Part C. 2010, 16, 339-343.
22. Barbara R. Williams.; Robert A. Gelman,; Donald C. Poppke.; Karl A. Piez. Collagen Fibril Formation. The journal of biological chemistry. 1978, 253, 6578-6585.
23. Zhe Zhang.; Huifei Cui. Biodegradability and Biocompatibility Study of Poly(Chitosan-g-lactic Acid) Scaffolds. Molecules. 2012, 17, 3243-3258.
24. Damla Cetin.; A. Sera Kahraman.; Menemse Gumusderelioglu. Novel Scaffolds Based on Poly(2-hydroxyethyl methacrylate) Superporous Hydrogels for Bone Tissue Engineering. Journal of Biomaterials Science. 2011, 22, 1157–1178.
25. E. Birmingham.; G.L. Niebur.; P.E. McHugh.; G. Shaw.; F.P. Barry.; L.M. McNamara. Osteogenic differentiation of mesenchymal stem cells is regulated by osteocyte and osteoblast cells in a simplified bone niche. European Cells and Materials. 2012,23, 13-27.
26. Fariba Mansourizadeh.; Asadollah Asadi.; Shahrbanoo Oryan.; Ali Nematollahzadeh.; Masoumeh Dodel.; Mehdi Asghari-Vostakolaei. PLLA/HA Nano composite scaffolds for stem cell proliferation and differentiation in tissue engineering. Molecular Biology Research Communications. 2013, 2, 1-10.
27. Ting-Ting Li.; Katrin Ebert.; Jurgen Vogel.; Thomas Groth. Comparative studies on osteogenic potential of micro- and nanofibre scaffolds prepared by electrospinning of poly(ε-caprolactone). Progress in Biomaterials. 2013, 2, 1-13.
28. Stein GS.; Lian JB. Molecular mechanisms mediating developmental and hormone-regulated expression of genes in osteoblasts: an integrated relationship of cell growth and differentiation. In: Noda M, editor. Cellular and molecular biology of bone. Tokyo: Academic Press. 1993, 47–95.
29. Barbara R. Williams.; Robert A. Gelman.; Donald C. Poppke.; Karl A. Piez. Collagen Fibril Formation. The journal of biological chemistry. 1978, 253, 6578-6585.
30. Nima Saeidi.; Edward A. Sander.; Jeffrey W. Ruberti. Dynamic shear-influenced collagen self-assembly. Biomaterials. 2009, 30, 6581–6592.
31. Deok-Ho Kim.; Paolo P. Provenzano.; Chris L. Smith.; Andre Levchenko. Matrix nanotopography as a regulator of cell function. JCB: Review. 2012, 197, 351-360.
32. Benedicto de Campos Vidal.; Maria Luiza S. Mello. Collagen type I amide I band infrared spectroscopy. Micron. 2011, 42, 283–289.

33. Phanat Kittiphattanabawon.; Soottawat Benjakul.; Wonnop Visessanguan.; Hideki Kishimura.; Fereidoon Shahidi. Isolation and Characterisation of collagen from the skin of brownbanded bamboo shark (Chiloscyllium punctatum). Food Chemistry. 2010, 119, 1519–1526.
34. Victor Hernandez-Gordillo.; Jean Chmielewski. Mimicking the extracellular matrix with functionalized, metal-assembled collagen peptide scaffold. Bioomaterials. 2014, 35, 7363-7373.
35. Jutamas Ratanavaraporn.; Siriporn Damrongsakkul.; Neeracha Sanchavanakit.; Tanom Banaprasert.; Sorada Kanokpanont. Comparison of Gelatin and Collagen Scaffolds for Fibroblast Cell Culture. Journal of Metals. Materials and Minerals. 2006, 16, 31-36.
36. Nandana Bhardwaj.; Subhas C. Kundu. Silk fibroin protein and chitosan polyelectrolyte complex porous scaffolds for tissue engineering applications. Carbohydrate Polymers. 2011, 85, 325–333.
37. Cox, T. R.; J. T. Erler. Remodeling and homeostasis of the extracellular matrix: implications for fibrotic diseases and cancer. Dis. Model. Mech. 2011, 14, 165–178.

Figure and Table captions

Table 1 Groups of scaffolds.

Group	Detail
A	Silk fibroin scaffold
B	Coated silk fibroin scaffold with collagen
C	Chitosan scaffold
D	Coated chitosan scaffold with collagen

Figure and Table captions

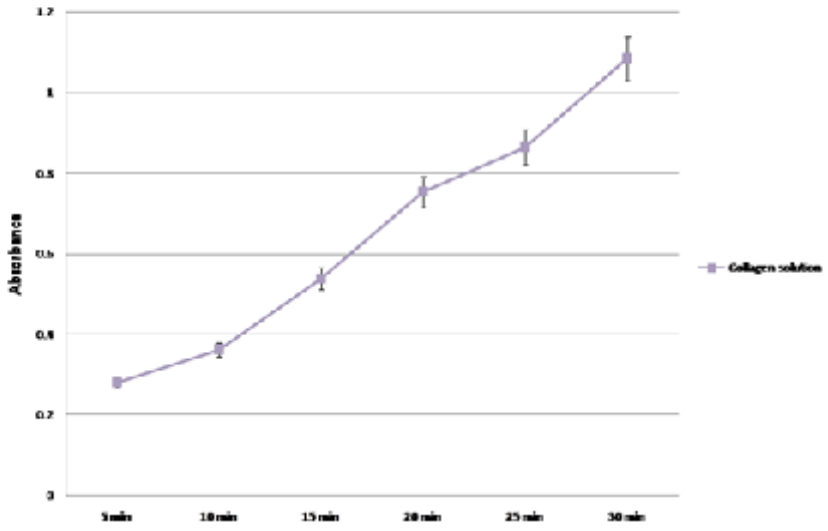

Fig. 1. Kinetic curve of self-assembly of collagen measured by absorbance at 313 nm vs. time (min).

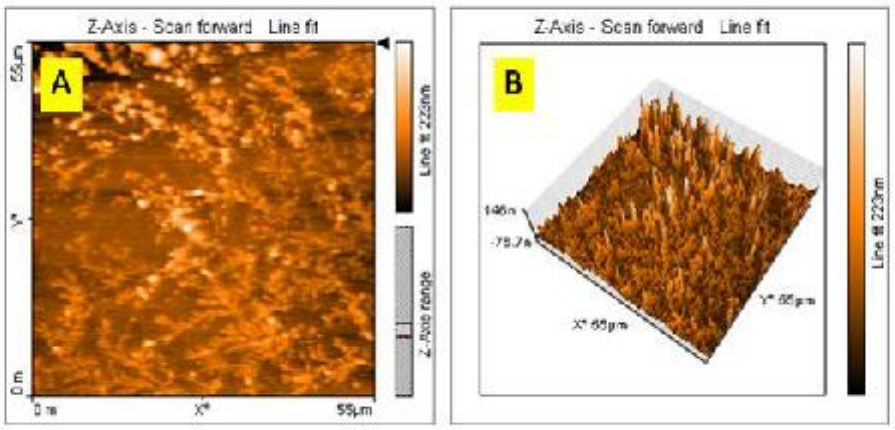

Fig. 2. Self-assembly of collagen into fibrils observed by AFM.

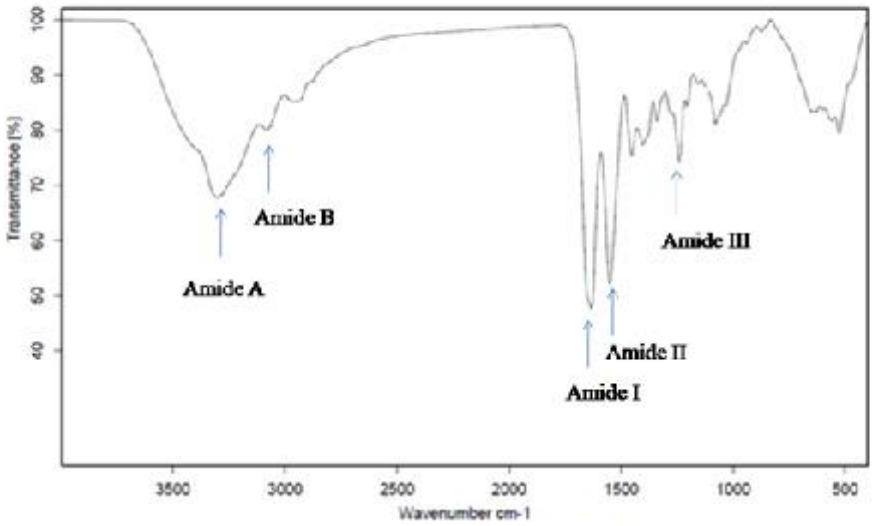

Fig. 3. Fourier transform infrared spectrum of collagen fibrils after freeze-drying.

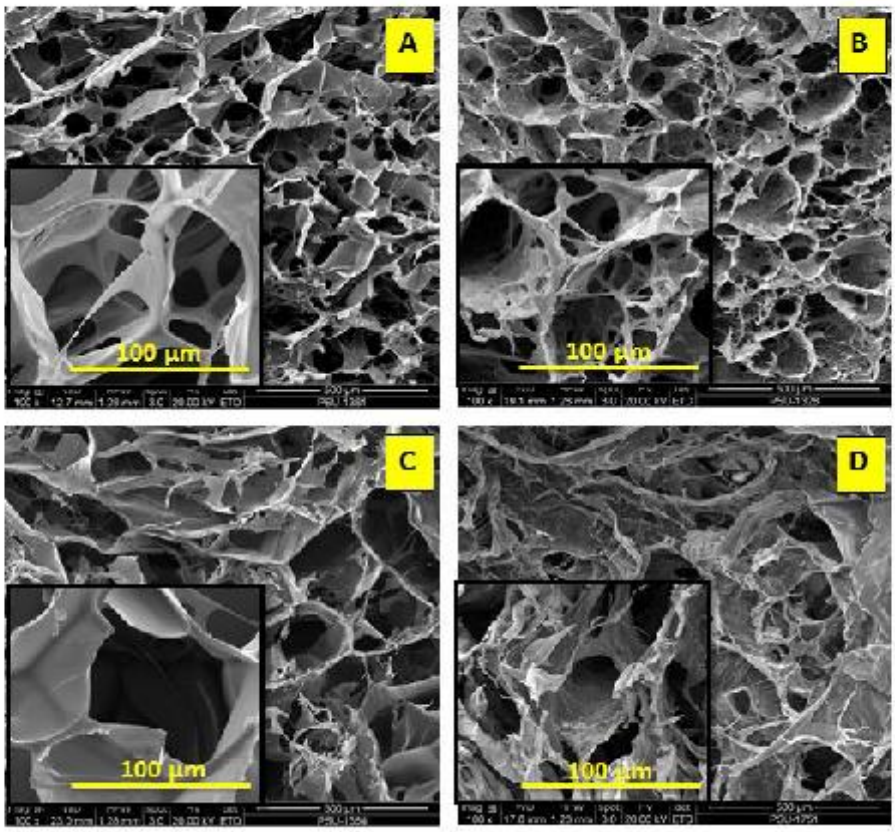

Fig. 4. Morphology and surface of scaffold in each group observed by scanning electron microscopy (SEM): A) silk fibroin scaffold, B) collagen coated silk fibroin scaffold, C) chitosan scaffold, D) collagen coated chitosan scaffold.

Fig. 5. Scaffolds after degradation with lysozyme at 4 weeks: A) silk fibroin scaffold, B) collagen coated silk fibroin scaffold, C) chitosan scaffold, D) collagen coated chitosan.

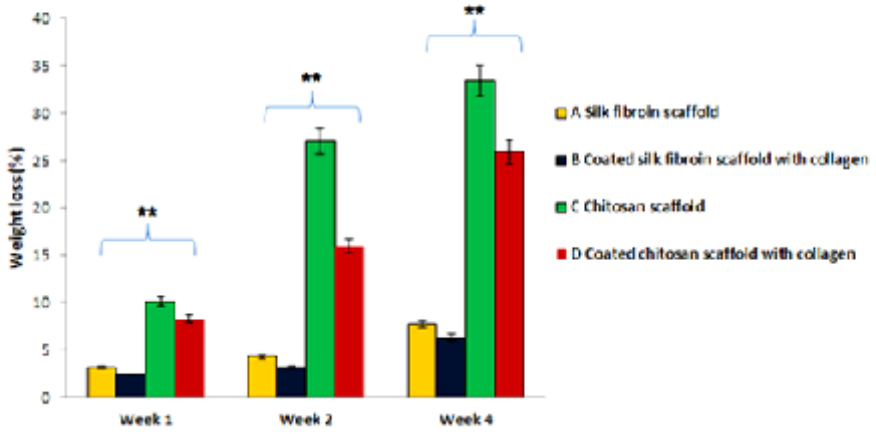

Fig. 6. Degradation of scaffold after digestion with lysozyme at weeks 1, 2 and 4.

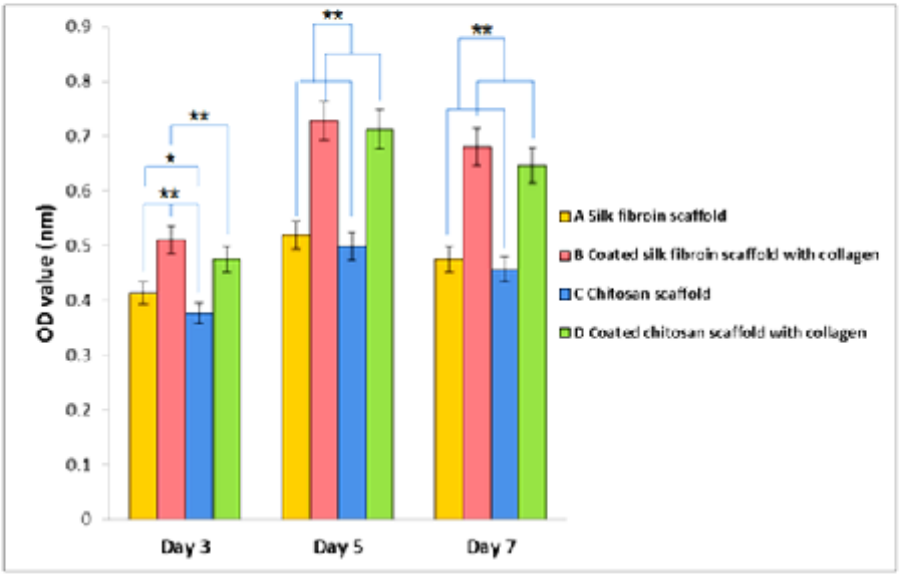

Fig. 7. MTT assay of MC3T3-E1 grown on various scaffolds at days 3, 5 and 7.

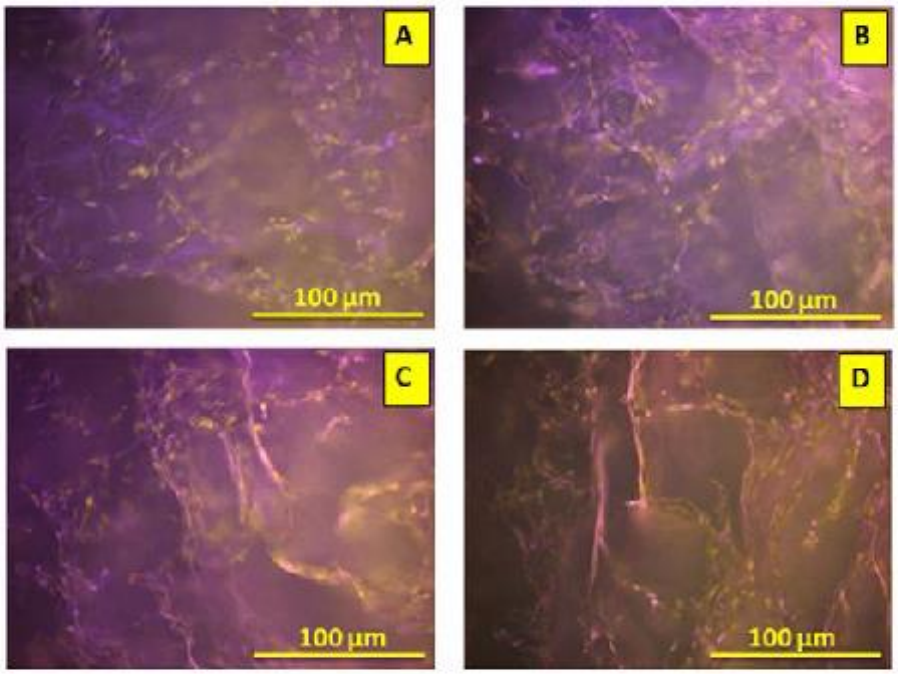

Fig. 8. Fluorescence image showed the viability (bright green) of MC3T3-E1 attached to the scaffolds in all groups: A) silk fibroin scaffold, B) collagen coated silk fibroin, C) chitosan scaffold, D) collagen coated chitosan.

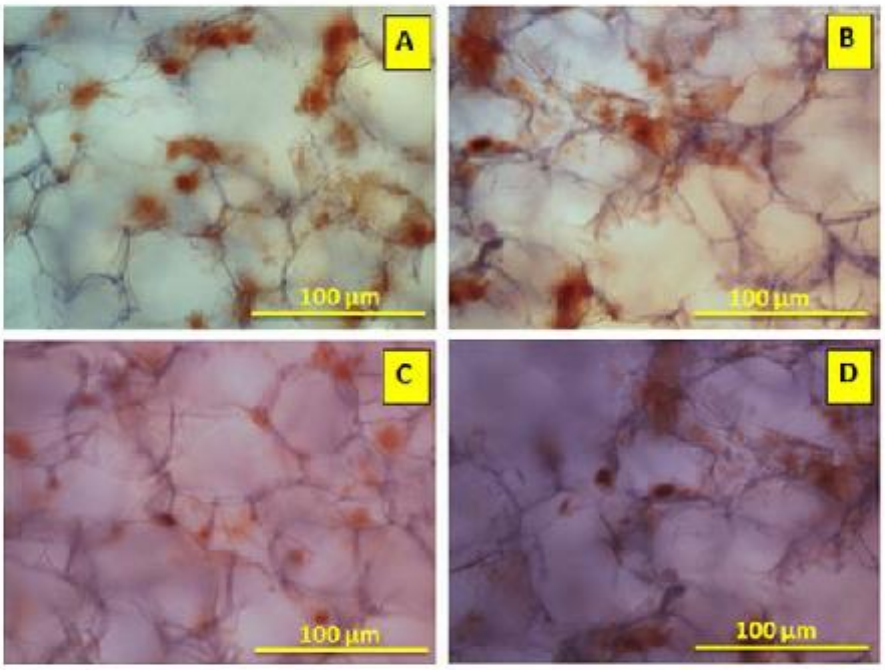

Fig. 9. Alizarin red staining of the scaffolds at day 7 of cell culture under OS media conditions. The red indicates calcium deposits on the scaffold: A) silk fibroin scaffold, B) collagen coated silk fibroin scaffold, C) chitosan scaffold, D) collagen coated chitosan scaffold.

Modified silk fibroin scaffolds with collagen/decellularized pulp for bone tissue engineering in cleft palate: morphological structures, and biofunctionalities

Supaporn Sangkert[1], Jirut Meesane1*, Suttatip Kamonmattayakul[2], Chai Wen Lin[3]

[1]Biological Materials for Medicine Research Unit, Institute of Biomedical Engineering, Faculty of Medicine, Prince of Songkla University, Hat Yai, Songkhla, Thailand, 90110

[2]Department of Preventive Dentistry, Faculty of Dentistry, Prince of Songkla University, Hat Yai, Songkhla, Thailand, 90110

[3]Department of General Dental Practice and Oral and Maxillofacial Imaging, Faculty of Dentistry, University of Malaya, Kuala Lumpur, Malaysia

*Correspondence author e-mail: jirutmeesane999@yahoo.co.uk

ABSTRACT

Cleft palate is a congenital malformation that generates a maxillofacial bone defect around the mouth area. To create performance scaffolds for bone tissue engineering in cleft palate is an issue that was proposed in this research. Because of its good biocompatibility, high stability, and non-toxicity, silk fibroin was selected as the scaffold of choice in this research. Silk fibroin scaffolds were prepared by freeze-drying before immerging in a solution of collagen, decellularized pulp, and collagen/decellularized pulp. Then, the immersed scaffolds were freeze-dried. Structural organization in solution was observed by Atomic Force Microscope (AFM). The molecular organization of the solutions and crystal structure of the scaffolds were characterized by Fourier transform infrared (FT-IR) and X-ray diffraction

(XRD), respectively. The weight increase of the modified scaffolds and pore size were determined. The morphology was observed by a scanning electron microscope (SEM). Mechanical properties were tested. Biofunctionalities were considered by seeding osteoblasts in silk fibroin scaffolds before analysis of the cell proliferation, viability, total protein assay, and histological analysis. The results demonstrated that dendrite structure of the fibrils occurred in those solutions. Molecular organization of the components in solution arranged themselves into an irregular structure. The fibrils were deposited in the pores of the modified silk fibroin scaffolds. The modified scaffolds showed a beta-sheet structure. The morphological structure affected the mechanical properties of the silk fibroin scaffolds with and without modification. Following assessment of the biofunctionalities, the modified silk fibroin scaffolds could induce cell proliferation, viability, and total protein particularly in modified silk fibroin with collagen/decellularized pulp. Furthermore, the histological analysis indicated that the cells could adhere in modified silk fibroin scaffolds. Finally, it can be deduced that modified silk fibroin scaffolds with collagen/decellularized pulp had the performance for bone tissue engineering and a promise for cleft palate treatment.

Keywords; Silk fibroin, Tissue engineering, Collagen, Decellularized pulp, Osteoblast

INTRODUCTION

Cleft palate is a congenital malformation that develops from a defect in facial development. This defect includes bone loss around the mouth. Cleft palate causes dysfunction of the mouth, for instance, problematic verbal and speech development, and abnormal suction during breast sucking (1). To treat cleft palate, patients need to have an operation. However, incomplete bone tissue regeneration often occurs post-operatively. Therefore, creating a potential approach to complete the bone regeneration is a challenge for cleft palate.

Bone tissue engineering is the process of regeneration of functional tissue. Bone tissue engineering can treat bone tissue defects from disease (2). Principally, tissue engineering is an interdisciplinary field that includes three disciplines: material engineering, cell technology, and biomaterials (3). Biomaterials for tissue engineering scaffolds are especially important to induce bone tissue regeneration (4).

Silk fibroin (SF) is a protein that is produced by the *Bombyx mori* silkworm. The main proteins of silk fibroin include the amino acids glycine (43%), alanine (30%), and serine (12%) (5). Importantly, silk fibroin can arrange into three forms: 1) random coil, 2) alpha helix, and 3) crystalline β-sheet. The properties of silk fibroin are slow degradation, biocompatibility, low immunogenicity and toxicity, and good mechanical properties. Silk-based biomaterials were used as tissue engineering scaffolds in skeletal tissue like bone, cartilage, connective skin, and ligament tissue (6). Particularly in bone tissue engineering, the silk fibroin scaffold is a suitable choice because it has stability during bone tissue regeneration (7).

Collagen is a natural protein that is the main component in the extracellular matrix (ECM) in tissue. Especially in bone tissue, collagen acts as the template for calcium phosphate deposition. More specifically, collagen can enhance the stability and strength of the bone (8). Collagen is a popular material for tissue regeneration because collagen has biofunctionalities that cells can recognize. Such functionalities can enhance cell adhesion that leads to inducing tissue regeneration (9).

Pulp is the tissue located in teeth that has an ECM in its texture (10). Generally, this ECM plays a significant role as a native scaffold for bone tissue regeneration (11). Some reports demonstrated the performance of ECM from different sources for bone tissue regeneration (12). Normally, isolating ECM is an important step before it is used for tissue

regeneration. Therefore, decellularized tissue is an attractive approach which has been used to isolate ECM. However, the use of decellularized pulp in bone tissue engineering has been rarely reported. Hence, the use of decellularized pulp is the proposed novel choice for bone tissue engineering in this research.

Due to the attractiveness of collagen and decellularized pulp, we developed a high performance silk fibroin scaffold by modification with collagen/decellularized pulp for application in cleft palate. To hybridize collagen with decellularized pulp was considered and prepared in a solution. Silk fibroin scaffolds were coated with that solution. The characterization of the morphological structure and biofunctionalities were considered in this research. The eventual aim of this research was to enhance the biofunctionalities of a porous silk scaffold with collagen/decellularized pulp for bone tissue engineering in cleft palate.

MATERIALS AND METHODS

Preparation of silk fibroin scaffolds

Silk fibrin scaffolds were prepared by boiling the cocoons for 30 min in 0.02 M Na_2CO_3 and then rinsed with distilled water to extract the sericin. The silk was dried in a hot air oven at 60°C for 24 h. The silk was dissolved in a 9.3 M LiBr solution at 70°C for 3 h and then a silk solution was prepared yielding a 3% (w/v) solution (13). After dissolving the silk fibroin, it was centrifuged for 20 min at 9000 RPM at 4°C (14). The silk solution was purified by dialyzing against distilled water for 3 days (15). The silk fibroin solution was stored at 4°C until further use. Preparation of the 3D silk scaffold for experiment followed five steps. First, the silk fibroin solution was poured in 48 well plates. Second, the silk fibroin solution was freeze-dried to generate the porosity. Third, the porous silk scaffolds were treated by immersion in 70% (v/v) methanol for 30 min. Fourth, porous silk scaffolds were freeze-dried again. Finally, all scaffolds were cut into a diameter of 10 mm and 2 mm in thickness.

Preparation of type I collagen

Type I collagen was extracted from the skin of brown banded bamboo shark (*Chiloscyllium punctatum*). The preparation of type I collagen followed the report of P. Kittiphattanabawon et al. 2010 (16). Briefly, shark skin (1.0 × 10 cm^2) was mixed with 0.1 M NaOH. Next, the deproteinized skin was soaked in 0.5 M acetic acid for 48 h. After filtering the mixture to get the collagen solution, NaCl was added to a final concentration of 2.6 M and 0.05 M Tris (hydroxymethyl) aminomethane at pH 7.5. The pellet was dissolved in a minimum volume of 0.5 M acetic acid and the collagen pellet was collected following refrigerated centrifugation. For a more purified collagen solution, dialysis was performed with 0.1 M acetic acid for 12 h and 48 h with distilled water. The freeze-dried method was used to remove the water and it was kept at -20°C for later use.

Preparation of decellularized pulp

We collected teeth pulp from children who were 6 to 10 years old and segmented the teeth in half to harvest the pulp tissue. Collagenase and dispase were used to digest the pulp into solution for 1 h. The solution was separated from the debris pellet by using a centrifuge at 37°C. Then, the solution was washed with PBS (phosphate-buffered saline) 2 times. Finally the solution was filtered to get the decellularized pulp and used the freeze-drying machine for water sublimation (17).

Modification of silk fibroin scaffolds

For modification of silk fibroin scaffolds, we designed the silk fibroin scaffolds into 4 groups that were modified with different coating solutions (Table 1). For coated silk scaffolds in the decellularized pulp group, the decellularized pulp powder was dissolved in 0.1% sodium hypochlorite to a concentration of 0.1 mg/ml. In the case of coated silk scaffolds with

collagen, the collagen powder was dissolved in 0.1 M acetic acid to a concentration of 0.1 mg/ml (18). For coated silk scaffolds with collagen/decellularized pulp, the previous collagen and decellularized pulp were mixed together to obtain a 50:50 ratio. The collagen, decellularized pulp, and collagen/decellularized pulp were used as the coating solutions to modify the scaffolds. To modify the scaffolds, the silk fibroin scaffolds were immersed into the coating solutions for 240 min. Then, the immersed scaffolds were soaked in 1X PBS for 30 min before they were freeze-dried (19).

Table 1 Groups of silk scaffolds coated with the coating solutions.

Group	Detail
A	Silk scaffold
B	Silk coated decellularized pulp
C	Silk coated collagen
D	Silk coated collagen and decellularized pulp

Pore size measurement

The ImageJ software (1.48v) was used to measure the pore size in each group. The pore distribution of the scaffolds was analyzed from SEM images. The pore size of the scaffolds in each group was a randomized area (n=25) to calculate the average pore size (20).

Weight increase of the modified scaffolds

The weight increase of the modified scaffolds was measured by the percentage deposition of components in the coating solution on the scaffolds. All groups of silk scaffold

were weighed before and after coating (n=5). The difference in the weights showed the increased percentages of the components from the coating solutions that attached onto the silk scaffolds (21). The calculation for the percentage deposition of components in the coating solution onto the scaffold (w/w, %) was $(W_t - W_p) / W_t \times 100\%$, where W_t = weight of the coated scaffold and W_p = weight of scaffold.

Swelling testing

The silk scaffolds in all groups were soaked in PBS at 37℃ for 24 hours. After removal of excess PBS by contact with a plastic surface, the swollen samples were weighed immediately. The swelling ratios were calculated using the equation $(W_s - W_d)/W_d$, where W_s and W_d are the weights of the swollen scaffold and the dry scaffold, respectively (22).

Mechanical properties testing

The mechanical properties of the scaffolds in the wet phase were investigated using the Universal Testing Machine (Lloyd model LRX-Plus, Lloyd Instrument Ltd., London, UK). In this study all groups of scaffolds were cut into a diameter of 10 mm and a thickness of 5 mm. The testing machine used a static load cell of 10 N at a rate of 2 mm/min and stopped at a strain of 40%.

Fourier transform infrared (FT-IR) characterization

The molecular organization of the silk fibroin scaffolds and the silk fibroin scaffolds coated with decellularized pulp, collagen, and collagen/decellularized pulp were analyzed by FT-IR. The samples were analyzed as a KBr pellet in a FT-IR spectrophotometer using the EQUINOX 55 (Bruker Optics, Germany) in the range of 4000-400 cm^{-1}.

X-ray diffraction (XRD) characterization

The crystal structure of the silk fibroin scaffolds and silk fibroin scaffolds coated with decellularized pulp, collagen, and collagen/decellularized pulp were analyzed by XRD (X'Pert MPD (PHILIPS, Netherlands). Samples were put in the XRD instrument and the diffraction patterns were measured over a 2 θ range of 5-90 θ with a step size of 0.05 θ and time per step of 1 s.

Scanning Electron Microscopy (SEM) Observations

A scanning electron microscope (Quanta400, FEI, Czech Republic) was used to observe the morphology and characterization of the SF scaffold that was coated with a special solution. The samples were pre-coated with gold using a gold sputter coater machine (SPI Supplies, Division of STRUCTURE PROBE Inc., Westchester, PA USA).

Atomic Force Microscopy Observations

The coating solution for each group was dropped into a glass slide, smeared and soaked in PBS for 30 min. When the slides were dried, the morphology and structure were observed by using atomic force microscopy (Nanosurf easyScan 2 AFM, Switzerland).

Cell culture experiments

The MG-63 cell line was cultured in alpha-MEM medium (α-MEM, Gibco™, Invitrogen, Carlsbad, CA) with the addition of 1% penicillin/streptomycin, 0.1% fungizone and 10% fetal bovine serum (FBS) at 37°C in a humidified CO_2 (5%) and air (95%) incubator. The MG-63 was seeded with a 5 $\times 10^5$/silk scaffold and the medium was changed every 3-4 days (23). The osteogenic medium (10 mM b-glycerophosphate, 50 mg=mL ascorbic acid, and 100 nM dexamethasone; Sigma-Aldrich) was used for osteoblast differentiation of MG-63 (24).

Cell proliferation assay (PrestoBlue: Day 1, 3, 5, and 7)

To observe the cell proliferation, PrestoBlue assay was used based on resazurin reagent. When the live cells go through the reducing process in the cytoplasm they will react with the resazurin to form resorufin to produce a purple or red color. The measurement of cell proliferation was performed according to the manufacturer's instructions (PrestoBlue® Cell Viability Reagent, Invitrogen, USA) and measured at 1, 3, 5, and 7 days (25). Silk fibroin scaffolds from each group were washed twice with 1X PBS and then 1/10th volume of PrestoBlue reagent was added directly into the complete media and incubated for 1 hour at 37°C and the proliferation rate of the cells was measured by monitoring the wavelength absorbance at 600 nm emission. The untreated cell group was used for the negative control.

Cell viability (Fluorescence Microscope on Day 3)

Cell viability on silk fibroin scaffold in each group was evaluated by fluorescence microscope. The live cells on the SF scaffold were stained by fluorescein diacetate (FDA). The application of the FDA was to attach to the cells and embed them into the ECM and cellular clusters. FDA was dissolved in acetone at 5 mg/ml. Next the media was removed by replacement of fresh 1 ml medium and then 5 µl of the FDA was added to each well and kept in the dark at 37°C for 5 min. The silk fibroin scaffold was washed twice with 1X PBS and transferred to a glass slide and the cell morphology was observed by the fluorescence microscope (26).

Total protein assay

The cellular protein in the cell lysis solution was discharged according to the manufacturer's instructions (Pierce BCA Protein Assay Kit, Thermo Scientific, USA). In order to extract cellular protein by using the lysis cell method, 800 µl of the cell lysis solution

(1% Triton X in PBS) was added in each well and the silk fibroin scaffolds were frozen at -70°C for 1 hour and then thawed at room temperature for 1 hour. This was repeated in 3 cycles. Following that, the solution was transferred to an Eppendorf tube and centrifuged at 12000 RPM for 10 min to remove the supernatant from the pellet. Measurement of the total protein synthesized by the cells in the silk fibroin scaffold was performed with absorbance at 562 nm at 7, 14, and 21 days. Bovine serum albumin was used for the standard curve in this experiment (27).

Histology analysis

The silk fibroin scaffolds with cell cultures on day 5 were fixed with 4% formaldehyde at 4°C for 24 h. The silk fibroin scaffolds in each group were immersed in paraffin. The paraffin sections were cut at 5μ and placed on a glass slide and deparaffinized and hydrated in distilled water. The sample slides were stained with 2 types of stain. At first, hematoxylin and eosin stain was used to observe cell migration, adhesion, and the ECM synthesized from the cells around the silk fibroin scaffold (28).

Statistical analysis

All data were shown as mean ± standard deviation. The samples were measured and statistically compared by one-way ANOVA and Tukey's HSD test (SPSS 16.0 software package). $P < 0.05$ was accepted as statistically significant.

RESULTS AND DISCUSSION

Structural formation of mimicked extracellular matrix

In this research a coating solution of collagen/decellularized pulp was prepared according to the above protocol before observation of its organization by AFM. To characterize the structure of the collagen/decellularized pulp was the preliminary demonstration before coating onto the silk fibroin scaffolds. Furthermore, this demonstration could relate to the arrangement of the collagen/decellularized pulp on the silk fibroin scaffolds. The structure of collagen/decellularized pulp showed dendrite formation of fibrils (Fig. 1). Collagen without decellularized pulp organized predominantly into a dense branch structure. As reported previously, collagen molecules formed themselves into a fibril structure (29). Notably, collagen formed dendrite formation of fibrils when it was observed by AFM. This result can be explained by the disturbance of the collagen molecules by the sodium hypochlorite in the solution. Generally, sodium hypochlorite is a chemical reagent used for dental treatment. Sodium hypochlorite maintains fibroblast viability and promotes healing of chronic wounds (30). Some reports demonstrated that sodium hypochlorite can change hydroxyproline into pyrrole-2-carboxylic acid (31). Such forms of collagen might influence the organization into dendrite formation of fibrils.

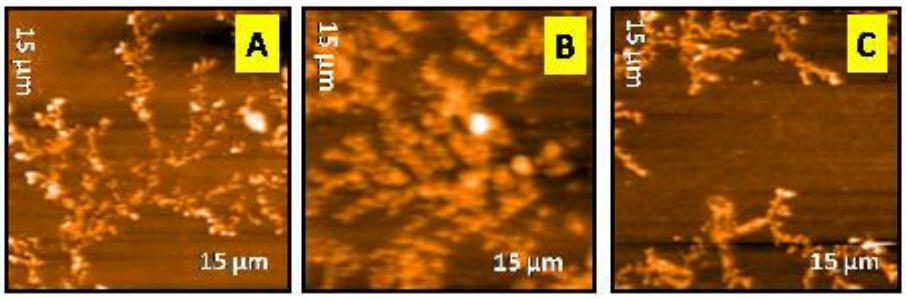

Fig. 1. AFM images of structure formation of coating solution: (A) decellularized pulp, (B) collagen, and (C) collagen/decellularized pulp.

Molecular organization analysis of modified silk fibroin scaffolds

FTIR was used to analyze the molecular organization of the coating solutions for characterization in this research. The results of the molecular organization showed different wavenumbers of the samples (Fig. 2). As previously mentioned for the collagen, the FTIR spectrum showed the important peak of -OH groups at 3500 cm^{-1} (32,33) . In this research, the -OH groups of collagen appeared at a wavenumber of 3303 cm^{-1} that shifted to a lower wavenumber. This indicated that the –OH groups interacted with the other groups. This interaction came from the self-assembly of the collagen molecules which showed that they could organize themselves into a higher order structure. The wave number of the -OH groups in the coated silk fibroin scaffolds shifted to a higher wavenumber. This result indicated that the -OH groups could vibrate freely in the decellularized pulp and collagen/decellularized pulp that came from an irregular organization of the components. The decellularized pulp showed three peaks at 3416, 3472, and 3552 cm^{-1} which represented the combination of -OH groups in each component of the decellularized pulp. The collagen/decellularized pulp showed -OH groups at 3464 cm^{-1} that possibly was the merged peak of collagen and decellularized pulp. Furthermore, it demonstrated that the -OH groups in the collagen/decellularized pulp could vibrate freely.

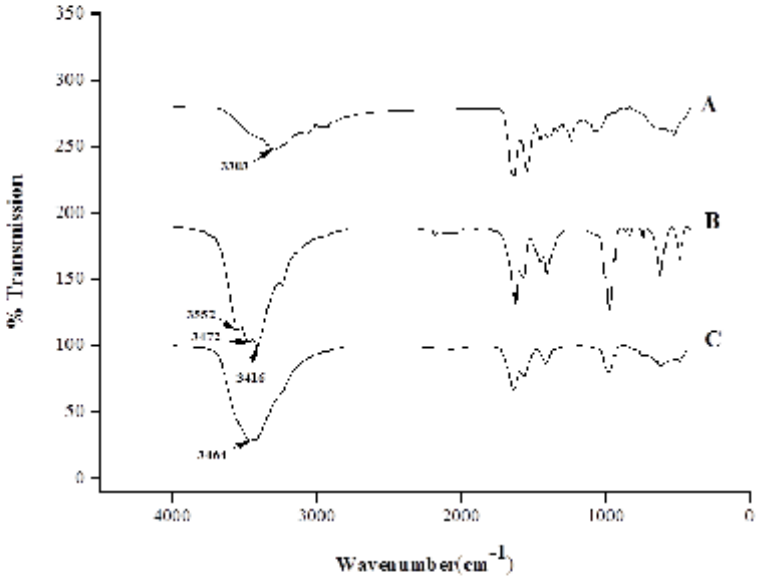

Fig. 2. FTIR spectra: (A) collagen, (B) decellularized pulp, and (C) collagen/decellularized pulp.

Crystal structure analysis of modified silk fibroin scaffolds

For an analysis of the crystal structure of silk fibroin scaffolds, the peak of NaCl deposited during coating was subtracted. The results showed different peaks in the crystal structures of the silk fibroin scaffolds (Fig. 3). Interestingly, the peaks that showed at around 20 degrees represented the beta-sheet conformation of silk fibroin as reported in previous literature (34). As a result, the peaks of the silk fibroin scaffold and the coated silk fibroin scaffolds appeared at around 20 degrees. This indicated that the silk fibroin scaffold and the coated silk fibroin scaffolds could organize into a beta-sheet structure.

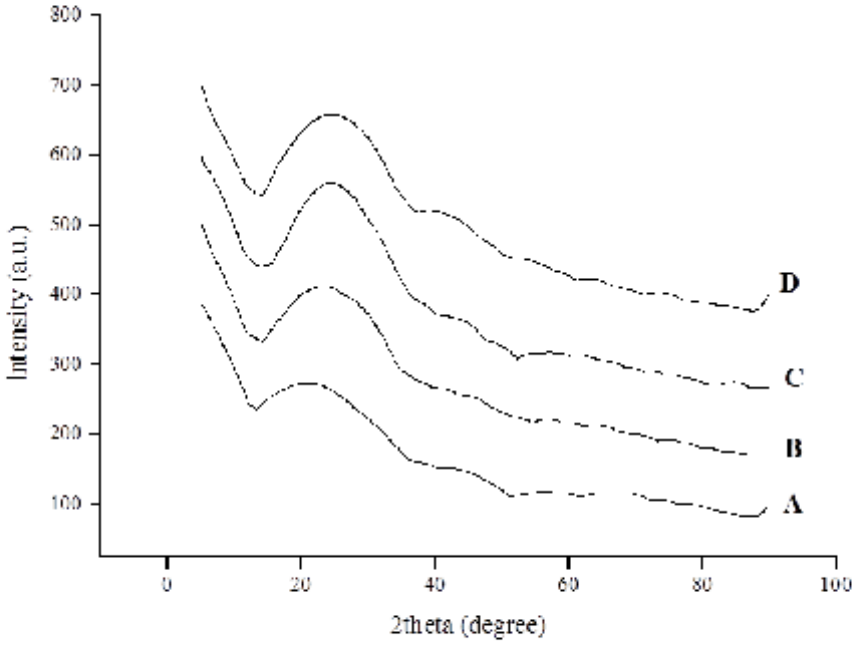

Fig. 3. XRD spectra: (A) silk fibroin scaffold, (B) silk fibroin scaffold coated with decellularized pulp, (C) silk fibroin scaffold coated with collagen, and (D) silk fibroin scaffold coated with collagen/decellularized pulp.

Morphological analysis of modified silk fibroin scaffolds

In this research silk fibroin scaffolds were modified by these coating solutions: collagen, decellularized pulp, and collagen/decellularized pulp. To start the modification, silk fibroin scaffolds were prepared by the freeze-dried technique before immersion into one of the coating solutions. Then, the immersed scaffolds were soaked in a buffer solution and then freeze-dried. The samples are shown in Fig. 4.

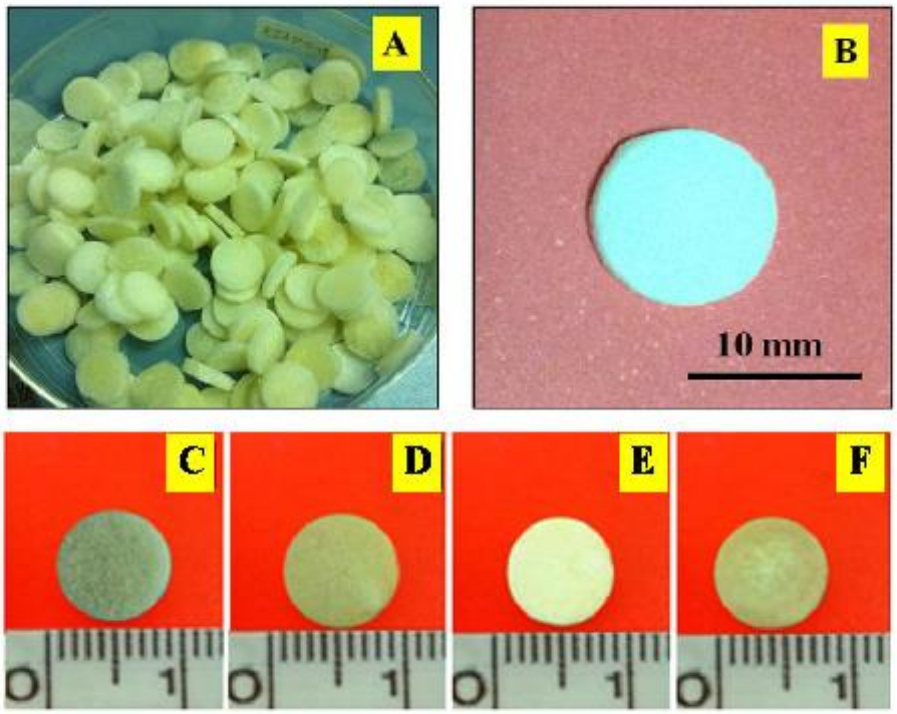

Fig. 4. Images of silk fibroin scaffolds: (A,C) before immersion (10 mm diameter x 2 mm thickness), (D) silk fibroin scaffold coated with decellularized pulp, (E) silk fibroin scaffold coated with collagen, (B,F) silk fibroin scaffold coated with collagen/decellularized pulp.

Observations of the uptake of the coating solutions inside the silk fibroin scaffolds during immersing are shown in Fig. 5. Silk fibroin scaffolds with decellularized pulp, collagen, and collagen/decellularized pulp showed turbid and transparent parts distributed throughout the texture of the scaffold during the early period of the immersion. The turbid and transparent parts appeared to be merged into a homogenous texture. Obviously, the apparent homogenous texture in the scaffold showed the uptake of the solution inside the scaffold. At 60 min, the decellularized pulp solution had diffused into the whole texture of the silk fibroin scaffold (Fig 5-A3). For the silk fibroin scaffolds with collagen and

collagen/decellularized pulp, the apparent homogenous texture appeared throughout the inside of the silk fibroin scaffold at 240 min. It could be explained that collagen and collagen/decellularized pulp had higher viscosities when compared to decellularized pulp. This result demonstrated that the solution had the potential to modify silk fibroin scaffolds by the coating technique. After immersion of the silk fibroin scaffolds in the coating solution, they were soaked in PBS before freeze-drying. Then, the morphologies of the freeze-dried modified silk fibroin scaffolds were observed by SEM (Fig. 6 and Fig. 7).

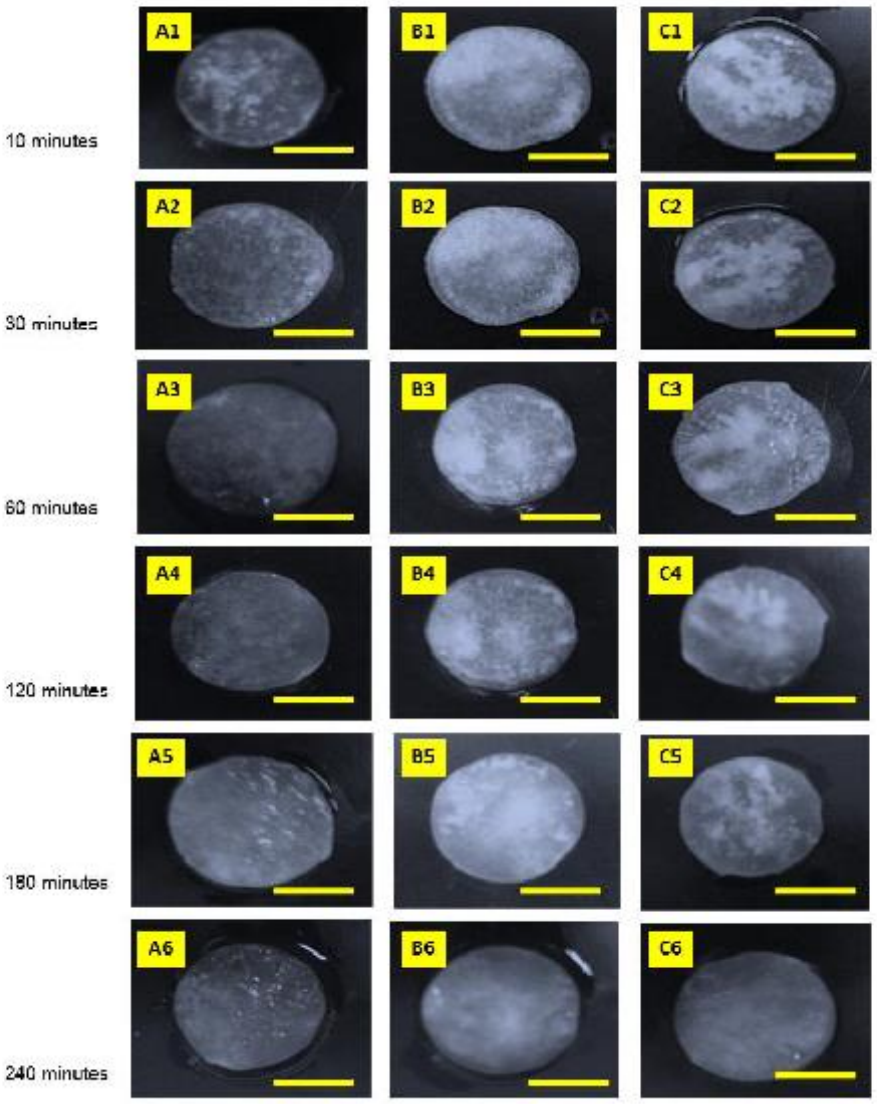

Fig. 5. Images of silk scaffolds after immersion in a coating solution at each time point of 10, 30, 60, 120, 180, and 240 minutes of decellularized, collagen, and collagen/decellularized solutions: (A1-A6) silk scaffold immersed with decellularized pulp solution, (B1-B6) silk scaffold immersed with collagen solution, (C1-C6) silk scaffold immersed with collagen/decellularized pulp solution. Scale bar: 5 mm.

The surface morphology of silk fibroin scaffolds with and without modification showed porous structures (Fig. 6). The silk fibroin scaffold without modification showed a smooth surface of the porous walls which had an interconnective porous structure. This interconnective porous structure is suitable to support cell adhesion and migration (35). Interestingly, cells could connect with each other in the pores. Furthermore, the pores are suitable for media flow in and out of the silk fibroin scaffold. A porous silk fibroin scaffold can easily remove waste (35). Notably, the morphologies of modified silk fibroin scaffolds with collagen (Fig. 6C) and collagen/decellularized pulp (Fig. 6D) solutions, showed the fibril structure deposited at the inner pores of the silk fibroin scaffolds. This fibril structure might be formed according to the results from AFM observation. Notably, there were no deposited fibril structures in the decellularized pulp solution. This result indicates that the decellularized pulp possibly detached from the surface of silk fibroin scaffolds while soaking in the buffer solution.

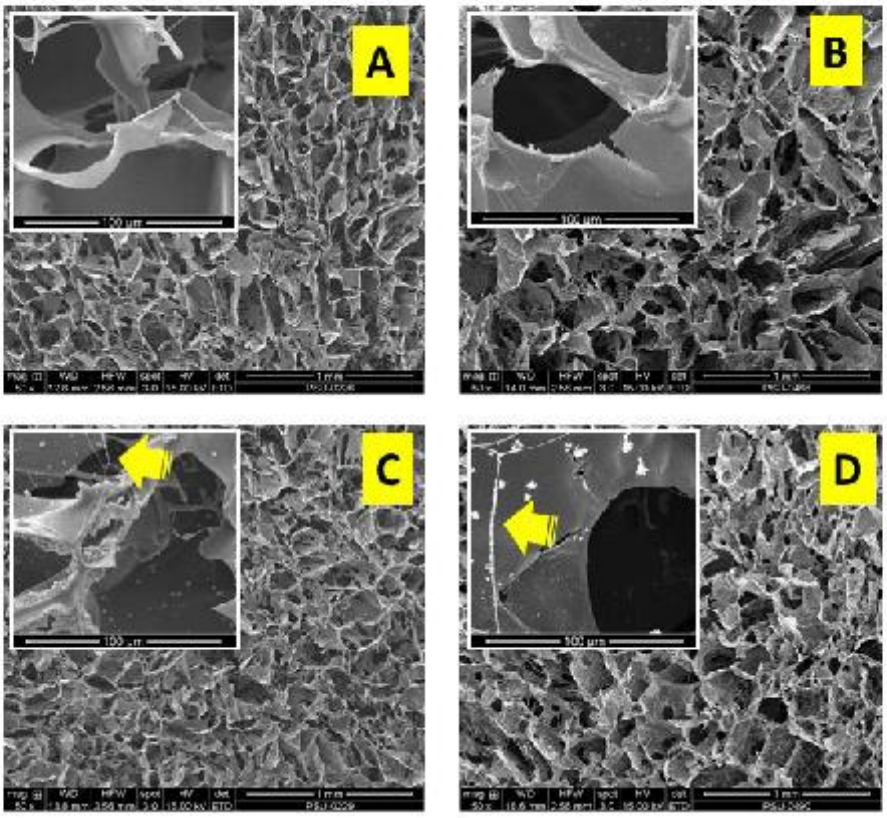

Fig. 6. Surface morphology of the scaffolds observed by scanning electron microscope (SEM) with different magnification. The wall surface is shown at 500x and connective pore size is shown at 50x. (A) surface morphology of silk scaffold without coating, (B) surface morphology of silk scaffold coated with decellularized pulp, (C) surface morphology of silk scaffold coated with collagen, (D) surface morphology of silk scaffold coated with collagen/decellularized pulp. Scale bars are shown in the micrographs. Yellow arrows show fibril structure.

Cross sections of the silk fibroin scaffolds were observed by SEM to confirm the deposition of decellularized pulp and collagen/decellularized pulp solutions inside the porous scaffolds (Fig. 7). Unlike the surface morphology of modified silk fibroin scaffold, the cross-section morphology showed a deposited fibril structure inside the pores of the silk fibroin

scaffolds for all coating solutions. The fibrils organized themselves into a network structure that was deposited on the pore walls of the silk fibroin scaffold. It demonstrated that decellularized, collagen, and collagen/decellularized solution have the potential for use as a coating solution for modification of the silk fibroin scaffolds. These results indicate that solutions of collagen, decellularized pulp, and collagen/decellularized pulp had the ability to mimic a network structure as in an ECM.

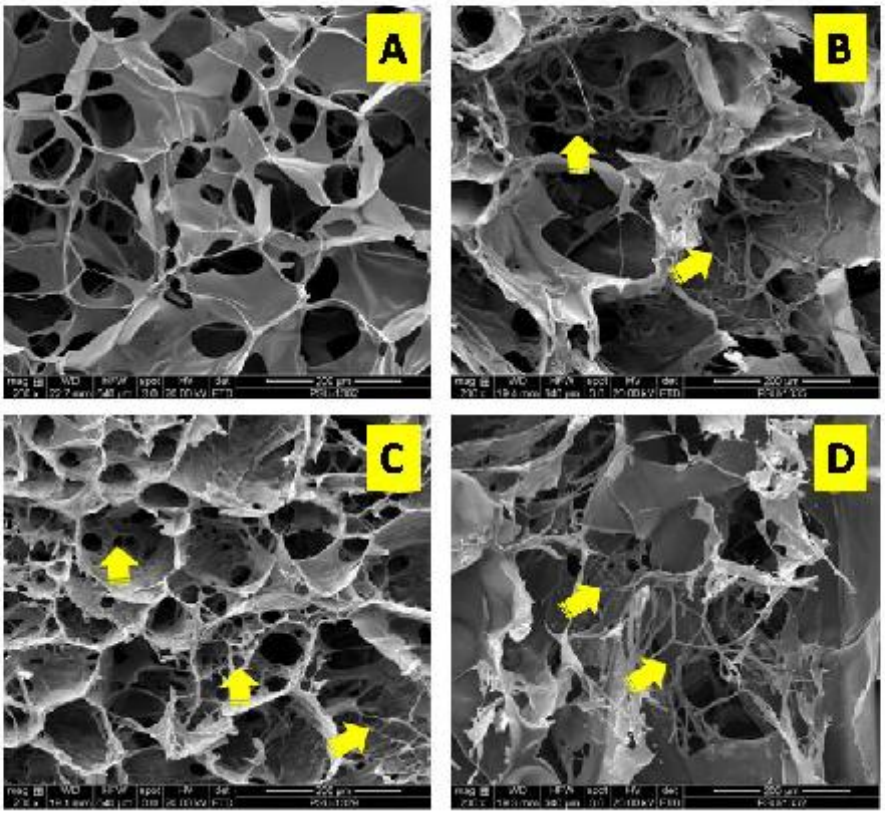

Fig. 7 Cross section morphology of scaffolds observed by scanning electron microscope (SEM): (A) silk scaffold without coating, (B) silk scaffold coated with decellularized pulp, (C) silk scaffold coated with collagen, (D) silk scaffold coated with collagen/decellularized pulp. Scale bars are shown in the micrographs. Yellow arrows show fibril structure.

Pore size measurement

In this research, the ImageJ software (1.48v) was used to measure the pore size in each group. The pore distribution of the scaffolds was analyzed from the SEM images. The pore size of the scaffolds in every group was a randomized area. The average pore sizes of the silk scaffolds in all groups are shown in Table 2. The mean pore size of the silk scaffolds was 132.06 ± 3.74µm which was the biggest pore size of all the groups but not significantly different. A minimum pore size of 100 µm with interconnective pores is normally required for a cell culture system that can support the cell size and migration (35).

Table 2 Average pore size of silk scaffold in each group. ImageJ software measured the silk scaffolds. Values are average ± standard derivation (N=25).

Groups	Pore size
A: Silk scaffold	132.06 ± 3.74µm
B: Silk scaffold coating with decellularized pulp	126.85 ± 2.72µm
C: Silk scaffold coating with collagen	127.94 ± 1.98µm
D: Silk scaffold coating with collagen and decellularized pulp	125.83 ± 1.98µm

Weight increase of the modified scaffolds

To confirm the existence of collagen and collagen/decellularized pulp on silk fibroin scaffold, the percentage of weight increase was analyzed. The results showed that the modified silk fibroin scaffolds had a significantly increased weight than the silk fibroin scaffold without modification (Fig. 8). It demonstrated that decellularized pulp, collagen, and collagen/decellularized pulp could deposit and exist in the silk fibroin scaffolds. The modified silk fibroin scaffolds with collagen showed a significantly increased weight compared to either silk scaffold modified decellularized pulp and collagen/decellularized pulp. The results indicate that the solutions of decellularized pulp, collagen, and collagen/decellularized pulp can adhere onto the silk fibroin scaffolds. These results support the previous results by SEM.

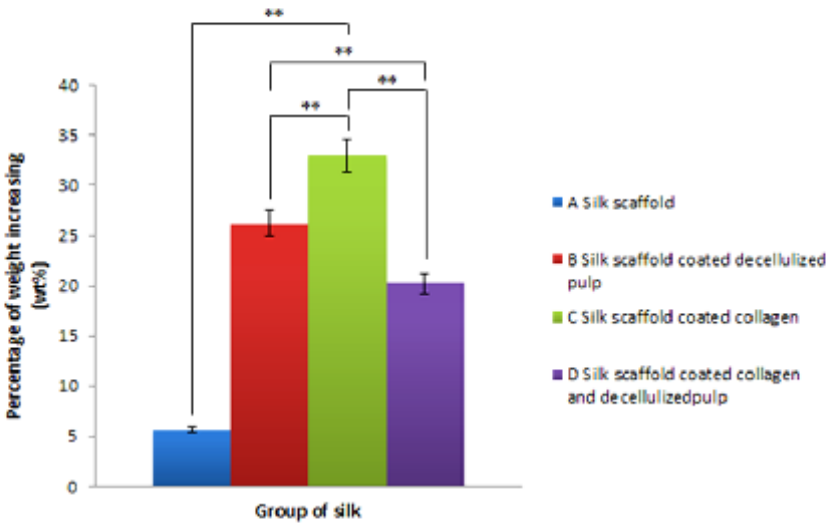

Fig. 8. Weight increase in percentage of deposition of decellularized pulp, collagen, and combination of collagen with decellularized pulp. (** $p < 0.01$)

Swelling ratio analysis

The scaffolds in all groups were swollen in different percentages. The uncoated scaffold showed a higher water binding capacity. This property plays an important role in tissue regeneration. (36). The silk scaffold revealed the highest water binding capacity and was significantly different than both the silk scaffold coated with decellularized pulp and the silk scaffold coated with collagen/decellularized pulp (Fig. 9). The collagen coating, and collagen/decellularized pulp on the silk scaffold surfaces seemed to decrease in the swelling ratio. The morphological structures of the silk fibroin scaffolds coated with collagen and the scaffolds coated with collagen/decellularized pulp had fibril network structures in the pores. These fibril networks decreased the swelling ratios. The results were similar to a previous study that reported the swelling property of the sponge-like matrices was dependent on the network porous structure and microstructure of the scaffold (37).

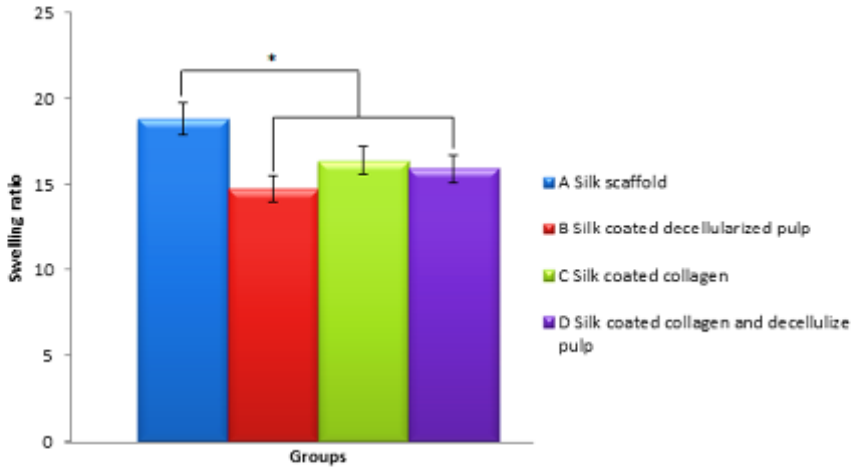

Fig. 9. Scaffold swelling ratios in each group.

Mechanical testing analysis

The results in mechanical testing showed that the silk fibroin scaffold and silk fibroin coated with decellularized pulp had higher stress values at the maximum load and higher Young's moduli than the silk fibroin scaffolds coated with collagen and collagen/decellularized pulp (Fig. 10). The results indicated that coating solutions affected the mechanical properties of the silk fibroin scaffolds. The coated samples showed smaller pore sizes than the samples without a coating. The small pore sizes retained smaller amounts of water than the large pore sizes according to the results in the pore measurement and swelling ratio analyses. The water in the porous scaffolds could resist the compressive force while testing in the wet state. Therefore, the scaffolds that could hold a higher amount of water in the porous structure showed higher stress values and Young's moduli. Notably, the silk fibroin scaffold coated with decellularized pulp showed the highest stress value and Young's moduli. The morphological structure of the decellularized pulp possibly reinforced the silk fibroin scaffold.

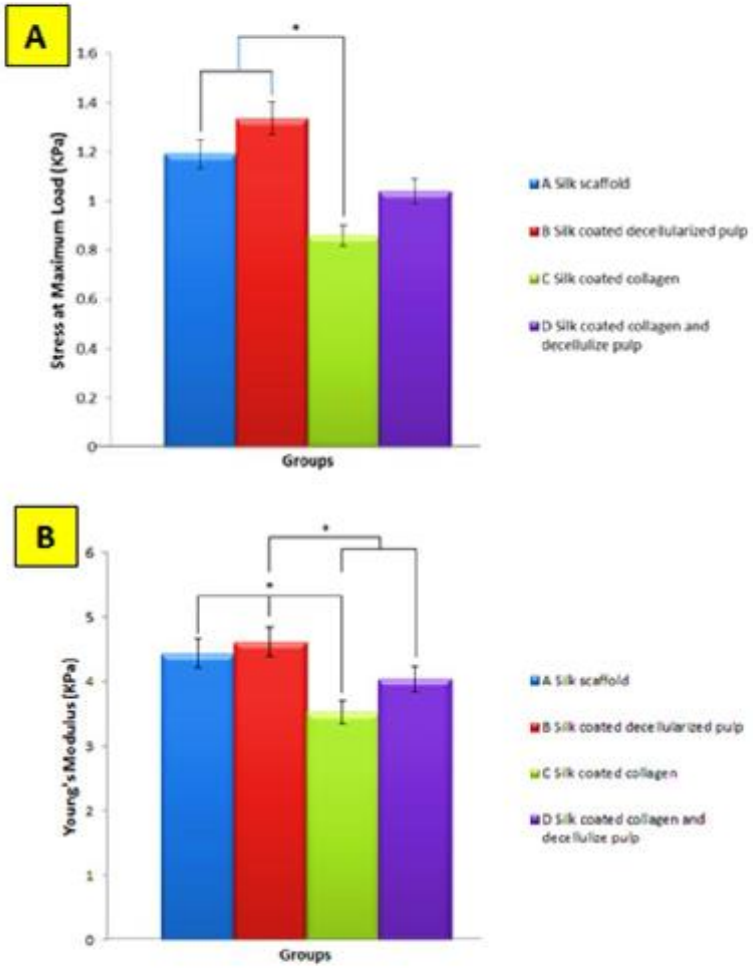

Fig. 10. Mechanical properties of the scaffolds in each group. (A) stress at maximum load of scaffold, (B) Young's modulus (KPa).

Cell proliferation

PrestoBlue™ was used to evaluate cell proliferation on days 1, 3, 5, and 7. The proliferation of osteoblast cells continuously increased from day 1 to day 5 and became lower on culture day 7 among all groups. On day 1, the silk scaffold modified by decellularized pulp was significantly higher in cell numbers than the silk scaffold without modification (Fig. 11). On day 3, all groups showed a similar behavior of cell proliferation, except the silk scaffold modified with collagen/decellularized pulp which was significantly higher than the other groups. On day 5 all groups became low, but the silk scaffold modified with decellularized pulp was significantly different than the other groups. On day 7, all groups had higher cell proliferation than the silk scaffold without modification.

Significantly, the results of cell proliferation indicated that decellularized pulp induced cell proliferation because the decellularized pulp had components of ECM. Importantly, the ECM could enhance cell proliferation (38). Modified silk fibroin scaffold with collagen/decellularized pulp showed the potential to enhance cell proliferation. A previous report demonstrated that collagen acted as an ECM to induce cell attachment (39). Therefore, to combine collagen with decellularized pulp can synergize cell adhesion and proliferation. From these results, collagen/decellularized pulp might be formed as reconstructed ECM that has the biofunctionalities of native ECM. Hence, such reconstructed ECM has the effect of a high cell proliferation rate.

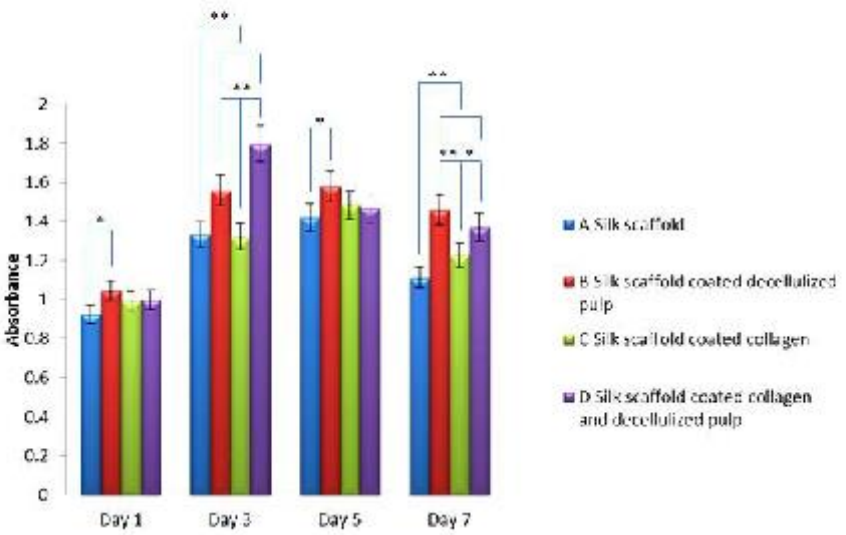

Fig. 11. Cell proliferation on different silk fibroin scaffolds. Cell proliferation was evaluated based on the associative number of metabolically active osteoblast cells in each scaffold group identified by the PrestoBlue™ assay. The symbol (*) represents significant changes in resazurin activity of osteoblasts ($P < 0.05$), (**) ($P < 0.01$).

Fluorescein Diacetate (FDA)

To observe the cell morphology in scaffolds, osteoblasts were stained by FDA. Afterward, all samples were observed by a fluorescence microscope. The green luminance showed the nucleus of the osteoblasts. The osteoblasts were able to attach to the surface of silk scaffolds (Fig. 12). The cells in the modified silk scaffold with collagen/decellularized pulp arranged themselves into a dense aggregation. This result indicated that collagen/decellularized pulp can promote cell adhesion. Cell adhesion might have come from the reconstructed ECM of collagen/decellularized pulp as previously explained.

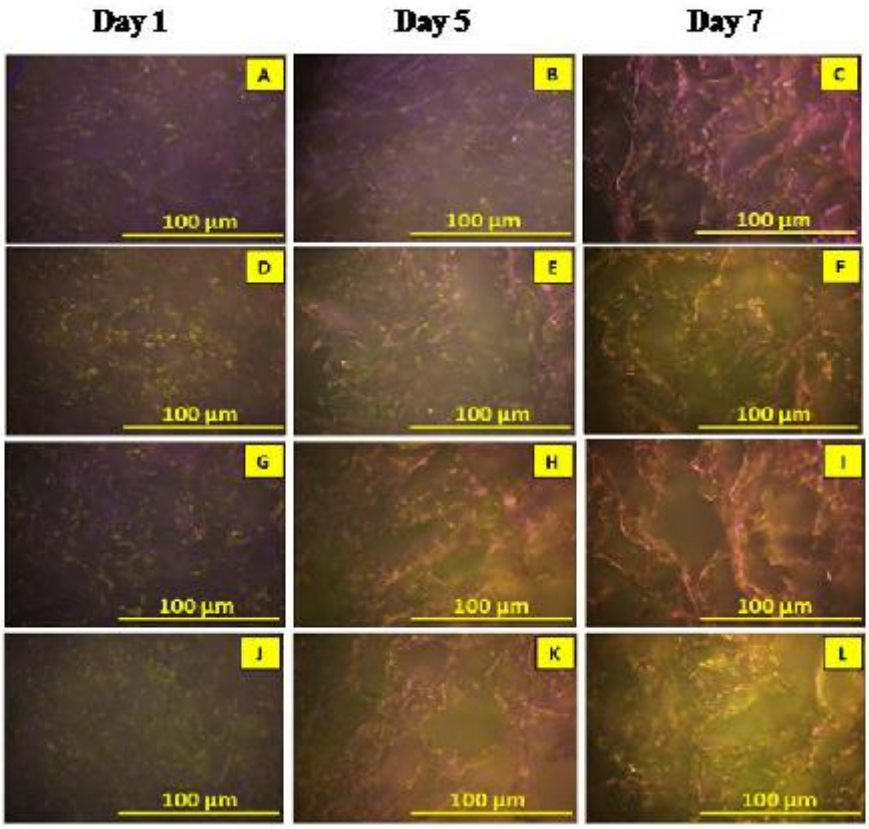

Fig. 12. Fluorescence images of the obvious cells and interconnections of the osteoblast cells on the silk scaffolds (FDA label, green brightness). (A-C) silk scaffold, (D-F) silk scaffold coated with decellularized pulp, (G-I) silk scaffold coated with collagen, (J-L) silk scaffold coated with collagen/decellularized pulp.

Bicinchoninic acid (BCA) analysis

Analysis of the total protein content during cell culturing was determined by BCA analysis on days 7, 14, and 21 (Fig. 13). For days 7 and 14, the modified silk scaffold with collagen had the highest protein content than the other groups. As previously reported, this

demonstrated that the osteoblasts start synthesizing protein on day 7 (40). Therefore, at days 7 and 14 the modified silk scaffold with collagen showed higher protein content than the other samples. These results indicate that the protein content at days 7 and 14 came from two main parts: 1) coated collagen on the scaffold and 2) secreted collagen from the osteoblasts. This confirmed the previous results that the protein content in the modified scaffold with collagen is higher than the other samples. The protein content at day 21 of the modified silk fibroin scaffold with collagen/decellularized pulp was predominantly higher than the other samples. On day 21, the silk fibroin scaffold coated with collagen/decellularized pulp and the silk fibroin scaffold coated with decellularized pulp continuously showed higher synthesizing of protein. On the other hand, protein synthesizing in the silk fibroin scaffold and silk scaffold coated with collagen became low at day 21. These results demonstrated that the coated components on modified silk fibroin scaffolds with collagen/decellularized pulp had a unique role in promoting the synthesizing of protein. It indicated that the biofunctionalities of collagen and decellularized pulp could synergize protein.

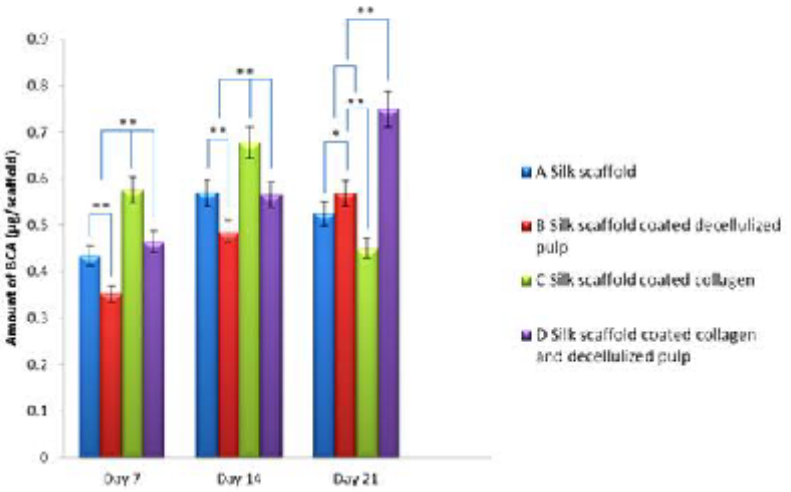

Fig. 13. Total protein content of osteoblast cells (MG63) on silk scaffold. Protein synthesis was evaluated by using the Pierce BCA protein assay. The symbol (*) represents significant changes in protein activity of osteoblasts ($P < 0.05$), (**) ($P < 0.01$).

Histological analysis

Osteoblast cells showed a good distribution throughout the silk scaffold in all groups. In Fig. 14, the red arrows point at the silk scaffold and the yellow arrows point at the osteoblast cells attached to the silk scaffold. The silk coated scaffolds with decellularized pulp (Fig. 14B), collagen (Fig. 14C), and collagen/decellularized pulp (Fig. 14D) showed more osteoblast cells attached to the surface of the silk scaffold and the cells filled the pores of the scaffolds. The shape of the osteoblast cells was flat on the silk scaffold surface and the blue color indicates the nucleus that is located at the center of the cytoplasm. These results indicated that modified silk fibroin scaffold could induce cell adhesion.

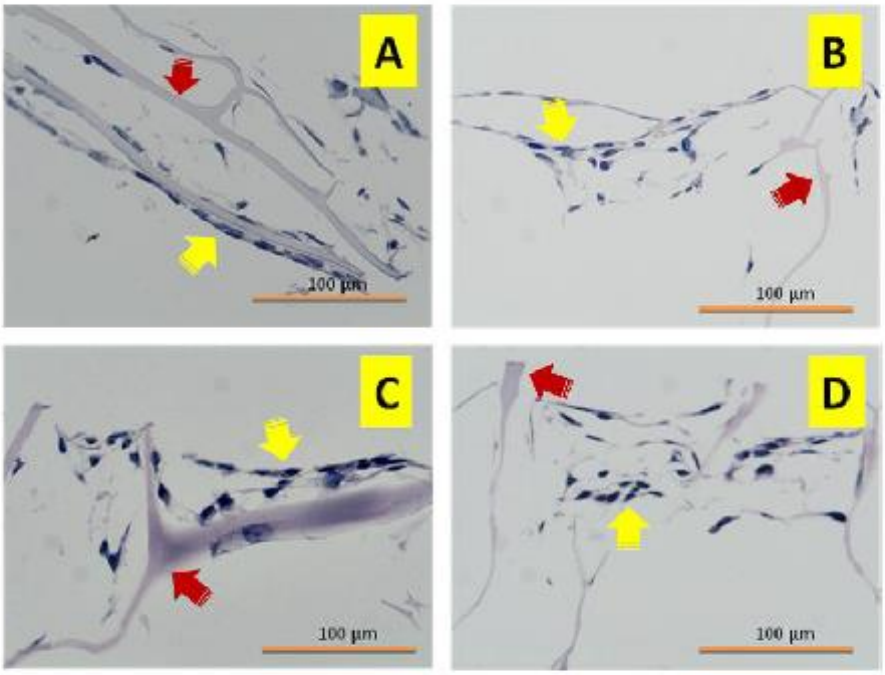

Fig. 14. Hematoxylin and eosin staining of cross sections on day 5 (A, B, C, D); the red arrows show the silk scaffold in each group, the yellow arrows show the osteoblast cells attached to the silk scaffold in all groups: (A) silk scaffold, (B) silk scaffold coated with decellularized pulp, (C) silk fibroin coated with collagen, (D) silk fibroin coated with collagen/decellularized pulp. Scale bar: 100 µm.

CONCLUSION

This research demonstrated that the use of collagen, decellularized pulp, and collagen/decellularized pulp solutions for scaffold modification is attractive and is a potential approach to enhance the biofunctionalities of silk fibroin scaffolds. The solutions could organize themselves into fibrils that deposited in the pores of the silk fibroin scaffolds. More importantly, the results indicated that the fibrils in modified silk fibroin scaffolds can induce biofunctionalities including cell proliferation, cell viability, and protein synthesis. Furthermore, the histological analysis demonstrated that cells could adhere well to the

modified silk fibroin scaffolds. Interestingly, it indicated that the modified silk fibroin scaffolds coated with collagen/decellularized pulp had a unique structure and demonstrated biofunctionalities. The structure and biofunctionalities could enhance the performance of modified silk fibroin scaffold. Eventually, it can be deduced from these results that modified silk fibroin scaffolds coated with collagen/decellularized pulp has promise for use in bone tissue engineering particularly in cleft palate.

ACKNOWLEDGEMENT

This work was financially supported by grant no. EC 50-042-25-2-3 from the Faculty of Medicine, Prince of Songkla University. Many thanks to the Biological Materials for Medicine (BMM) Research Unit and Queen Sirikit Sericulture Centre, Narathiwat, for silk supporting.

REFERENCES

1. P. A. Zuk, Tissue Engineering Craniofacial Defects With Adult Stem Cells? Are We Ready Yet. Pediatric Research. 63(2008)478-486.
2. G. M. de Peppoa, I. Marcos-Campos, D. John Kahler, D. Alsalman, L. Shang, G. Vunjak-Novakovic, D. Marolt, Engineering bone tissue substitutes from human induced pluripotent stem cells. PNAS. 110(2013)8680–8685.
3. R. Langer, J. P. Vacanti, Tissue Engineering. Science. 260(1993)920-926.
4. F. J. O'Brien, Biomaterials & scaffolds for tissue engineering. 14(2011)88-95.
5. Z. Zhao, Y. Li, M.B. Xie. Silk Fibroin-Based Nanoparticles for Drug Delivery. Int J Mol Sci. 16(2015)4880-4903.
6. Y. Wang, D. J. Blasioli, H.J. Kim, H.S. Kim, D.L. Kaplan, Cartilage tissue engineering with silk scaffolds and human articular chondrocytes. Biomaterials. 27(2006)4434–4442.
7. B.Kundu, R.Rajkhowa, S.C. Kundu, X. Wang, Silk fibroin biomaterials for tissue regenerations. Advanced Drug Delivery Reviews. 65(2013)457–470.

8. T. Matsuura, K. Tokutomi, M. Sasaki, M. Katafuchi, E. Mizumachi, H. Sato, Distinct Characteristics of Mandibular Bone Collagen Relative to Long Bone Collagen: Relevance to Clinical Dentistry. BioMed Research International. 2014(2014)1-9.

9. G.E. Davis, Affinity of integrins for damaged extracellular matrix: αvβ3 binds to denatured collagen type I through RGD sites. Biochemical and Biophysical Research Communications 182(1992)1025-1031.

10. M.Goldberg, J. Smith, Cells and Extracellular Matrices of Dentin and Pulp: A Biological Basis For Repair and Tissue Engineering. Crit Rev Oral Biol Med. 15(2004)13-27.

11. L.Cen, W.Liu, L. Cui, W. Zhang, Y. Cao, Collagen Tissue Engineering: Development of Novel Biomaterials and Applications. Pediatric Research. 63(2008)492-496.

12. S. Yamada, K. Yamamoto, T. Ikeda, K. Yanagiguchi, Y. Hayashi, Potency of Fish Collagen as a Scaffold for Regenerative Medicine. BioMed Research International. (2014)1-9.

13. G. Chang, H.-J. Kim, D.L. Kaplan, G. Vunjak-Novakovic, R. A. Kandel, Porous silk scaffolds can be used for tissue engineering annulus fibrosus. Eur Spine J. 16(2007)1848-1857.

14. L.P. Yan, J. Silva-Correia, C. Correia, S.G. Caridade, E.M. Fernandes, R.A. Sousa, J.F. Mano, J.M. Oliveira, A.L. Oliveira, R.L. Reis, Bioactive macro/micro porous silk fibroin/nano-sized calcium phosphate scaffolds with potential for bone-tissue-engineering applications. Nanomedicine. 8(2013)359-378.

15. Y.Zhao, R.Z. Legeros, J. Chen, Initial Study on 3D Porous Silk Fibroin Scaffold: Preparation and Morphology. Bioceramics Development and Applications. 1(2011)1-3.

16. P. Kittiphattanabawon, S. Benjakul, W. Visessanguan, H. Kishimura, F. Shahidi, Isolation and Characterisation of collagen from the skin of brownbanded bamboo shark (Chiloscyllium punctatum). Food Chemistry. 119(2010)1519–1526.

17. S.B. Traphagen, N. Fourligas, J. Xylas, S. Sengupta, D. Kaplan, I. Georgakoudi, P. C. Yelick, Characterization of Natural, Decellularized and Reseeded Porcine Tooth Bud Matrices. Biomaterials. 33(2012)5287-5296.

18. A. Gigante, S. Manzotti, C. Bevilacqua, M. Orciani, R. Di Primio, M. Mattioli-Belmonte, Adult mesenchymal stem cells for bone and cartilage engineering: effect of scaffold materials. European Journal of Histochemistry. 52(2008)169-174.

19. K.Chen, S.Sahoo, P. He, K.S. Ng, S.L.Toh, J.L. Goh, A Hybrid Silk/RADA-Based Fibrous Scaffold with Triple Hierarchy for Ligament Regeneration. Tissue Eng: Part A. 18(2012)1399-1409.

20. N. Kasoju, D. Kubies, M.M. Kumorek, J. Kriz, E. Fabryova, L. Machova, J. Kovarova, F. Rypacek, Dip TIPS as a Facile and Versatile Method for Fabrication of Polymer Foams with Controlled Shape Size and Pore Architecture for Bioengineering Applications. PLoS ONE. 9(2014)1-16.

21. P. He, S. Sahoo, K.S. Ng, K. Chen, S.L. Toh, J.C.H. Goh, Enhanced osteoinductivity and osteoconductivity throughhydroxyapatite coating of silk-based tissue-engineeredligament scaffold. Biomedical Materials Research Part A. 101A(2013)555-566.

22. N. Guziewicza, A. Besta, B. Perez-Ramireza, D. L. Kaplanb. Lyophilized Silk Fibroin Hydrogels for the Sustained Local Delivery of Therapeutic Monoclonal Antibodies. Biomaterials. 32(2011)2642–2650.

23. X. Liu, M. Zhao, J. Lu, J. Ma, J. Wei, S. Wei, Cell responses to two kinds of nanohydroxyapatite with different sizes and crystallinities. International Journal of Nanomedicine. 7(2012)1239-1250.

24. B.S. Kim, H.J. Kang, J.Lee, Improvement of the compressive strength of a cuttlefish bone-derived porous hydroxyapatite scaffold via polycaprolactone coating. Journal of Biomedical Materials Research Part B: Applied Biomaterials. 101(2013)1302-1309.

25. H. Liu, L. Xia, Y. Dai, M. Zhao, Z. Zhou, H. Liu, Fabrication and characterization of novel hydroxyapatite/porous carbon composite scaffolds. Materials Letters. 66(2011)36–38.

26. T.T. Li, K. Ebert, J. Vogel, T. Groth, Comparative studies on osteogenic potential of micro- and nanofibre scaffolds prepared by electrospinning of poly(ε-caprolactone). Progress in Biomaterials. 2(2013)1-13.

27. F. Pati, H. Kalita, B. Adhikari, S. Dhara. F. Pati, H. Kalita, B. Adhikari, S. Dhara, Osteoblastic cellular responses on ionically crosslinked chitosan-tripolyphosphate fibrous 3-D mesh scaffolds. Journal of Biomedical Materials research Part A. 101A(2013)2526-2537.

28. M.B. Keogh, F.J. O' Brien, J. S. Daly, A novel collagen scaffold supports human osteogenesis applications for bone tissue engineering. Cell and Tissue Research. 340(2010)169–177.

29. D. E. Birk, E. I. Zycband, D.A. Winkelmann, R.L. Trelstad, Collagen fibrillogenesis in situ: Fibril segments are intermediates in matrix assembly. Proc. Nati. Acad. Sci. USA. 86(1989)4549-4553.

30. Century Pharmaceuticals, Inc., Diluted Dakin's Solution Support for Antisepsis of Chronic Wounds.

31. J. A. Beeley, H. K. Yip, A. G. Stevenson, Conservative dentistry: Chemochemical caries removal: a review of the techniques and latest developments. British Dental Journal. 188(2000)427-430.

32. A.John, L.Hong, Y.Ikada, Y.Tabata. A trial to prepare biodegradable collagen-hydroxyapatite composites for bone repair. J Biomater Sci Polym Ed. 12(2001)689-705.

33. O.S. Rabotyagova, P.Cebe, D.L. Kaplan, Collagen Structural Hierarchy and Susceptibility to Degradation by Ultraviolet Radiation. Mater Sci Eng C Mater Biol Appl. 28(2008)1420–1429.

34. M. Farokhi, F. Mottaghitalab, J. Hadjati, R. Omidvar, M. Majidi, A. Amanzadeh, M. Azami, S.M. Tavangar, M.A. Shokrgozar, J. Ai, Structural and Functional Changes of Silk Fibroin Scaffold Due to Hydrolytic Degradation. J. APPL. POLYM. SCI. 131(2013)1-8.

35. U.J. Kim, J. Park, H. J. Kim, M. Wada, D.L. Kaplan, Three-dimensional aqueous-derived biomaterial scaffolds from silk fibroin. Biomaterials. 26(2005)2775–2785.

36. L.P. Yan, Y.J. Wang, L.Ren, G.Wu, S.G.Caridade, J.B. Fan, L.Y. Wang, P.H. Ji, J.M. Oliveira, J.T. Oliveira, J.F. Mano, R.L. Reis. Genipin-cross-linked collagen/chitosan biomimetic scaffolds for articular cartilage tissue engineering applications. Journal of Biomedical Materials Research Part A. 95A(2010)465-475.

37. S.N. Park, J.C. Park, H.O.Kim, M.J.Song, H.Suh, Characterization of porous collagen/hyaluronic acid scaffold modified by 1-ethyl-3-(3-dimethylaminopropyl) carbodiimide cross-linking Biomaterials. 23(2002)1205–1212.

38. M.Goldberg, J. Smith, Cells and Extracellular Matrices of Dentin and Pulp: A Biological Basis For Repair and Tissue Engineering. Crit Rev Oral Biol Med. 15(2004)13-27.

39. G. Zhou, G. Zhang, Z. Wu, Y. Hou, M. Yan, H. Liu, X Niu, A. Ruhan, Y. Fan, Research on the Structure of Fish Collagen Nanofibers Influenced Cell Growth. Journal of Nanomaterials. 2(2013)1-6.

40. S.I. Dworetzky, E.G. Fey, S. Penmant, J.B. Lian, J.L. Stein, G.S. Stein, Progressive changes in the protein composition of the nuclear matrix during rat osteoblast differentiation. Proc. Natl. Acad. Sci. 87(1990)4605-4609.

Biofunctional mimicked silk fibroin scaffolds coated with reconstructed extracellular matrix of decellularized pulp/fibronectin as clues for maxillofacial bone tissue engineering in bone defect from oral cancer

Supaporn Sangkert[1], Suttatip Kamonmattayakul[2], Chai Wen Lin[3], Jirut Meesane[1*]

[1]Institute of Biomedical Engineering, Faculty of Medicine, Prince of Songkla University, Hat Yai, Songkhla, Thailand, 90110

[2]Department of Preventive Dentistry, Faculty of Dentistry, Prince of Songkla University, Hat Yai, Songkhla, Thailand, 90110

[3]Department of General Dental Practice and Oral and Maxillofacial Imaging, Faculty of Dentistry, University of Malaya, Kuala Lumpur, Malaysia

*Correspondence author e-mail: jirutmeesane999@yahoo.co.uk

Abstract: Oral cancer is a disease that leads to bone loss in the maxillofacial area. To replace bone loss by advanced biomaterials is a challenge for materials scientists and maxillofacial surgeons. In this research, biofunctional mimicked silk fibroin scaffolds were created as an advanced biomaterial for bone substitution. Silk fibroin scaffolds were fabricated by freeze-drying before coating with three different components: decellularized pulp, fibronectin, and decellularized pulp/fibronectin. The structure formation of the coating components and the morphology of the coated scaffolds were observed by atomic force microscope and scanning electron microscope, respectively. Existence of the coating components in the scaffolds was proved by the increase in weight. The coated scaffolds were

seeded by MG-63 osteoblasts and cultured. Testing of the biofunctionalities included cell viability, calcium content, alkaline phosphatase activity (ALP), mineralization, and a histological analysis. The results demonstrated that the coating components existed in the scaffolds after coating. The coating components organized themselves into aggregations of globular structure. They were deposited and arranged themselves into clusters of aggregations with a fibril structure in the porous walls of the scaffolds. The results showed that coated scaffolds with decellularized pulp/fibronectin were suitable for cell viability since the cells could attach and spread into most of the pores of the scaffold. Furthermore, the scaffolds could induce calcium synthesis, mineralization, and ALP activity. The results indicated that coated silk fibroin scaffolds with decellularized pulp/fibronectin hold promise for use in bone tissue engineering in bone defect from oral cancer.

Key Words: Silk fibroin, Bone tissue engineering, Fibronectin, Decellularized pulp, Oral cancer

INTRODUCTION

Oral cancer is a disease that is associated with rapid bone loss in the maxillofacial area that results from radiation treatments as well as tumor growth. To reduce morbidity associated with the disease, patients frequently require treatments consisting of tumor removal, reconstruction of the mandibular defect with vascularized bone from the fibula, and subsequent placement of dental implants [1]. To create high performance biomaterials for maxillofacial bone regeneration at the defect site is a challenge for the materials scientists and surgeons. Therefore, in this research, to create performance biomaterials for maxillofacial bone tissue engineering in bone defect from oral cancer was considered.

Tissue engineering is the performance approach to regenerate new tissue. Generally, there are three main parts for bone tissue engineering: the cells, growth factors, and scaffolds.

Scaffolds have been created and fabricated to enhance the performance for bone tissue engineering. In the case of bone defect from oral cancer, high performance and functional scaffolds were used to regenerate new tissue at the defect area [2]. Therefore, in this research performance scaffolds for maxillofacial bone tissue engineering were created and proposed to replace bone defect from oral cancer.

Silk fibroin (SF) is a protein available from the *Bombyx mori* silk worm. Most of the proteins of the silk include the amino acids glycine (43%), alanine (30%), and serine (12%) [3]. These proteins arrange into a crystalline β-sheet form in silk fiber [3]. Silk fibroin shows interesting properties such as slow degradation, biocompatibility, low immunogenicity and toxicity, and good mechanical properties (Young's modulus and tensile strength) [4-5]. Interestingly, silk-based biomaterials as tissue engineering scaffolds were used as parts of skeletal tissue like bone cartilage, connective tissue skin, and ligament [5]. Therefore, in this research, the silk fibroin scaffold was selected for fabrication into scaffolds for maxillofacial bone tissue engineering and proposed for use in bone defect from oral cancer. Nevertheless, to enhance the performance in bone tissue engineering, a silk fibroin scaffold needs modification to improve the biofunctionalities.

Interestingly, the modification of scaffolds with drugs, bioactive molecules, and critical clues for tissue regeneration was an effective method to treat bone defect from cancer [6]. Firstly, drugs were combined with scaffolds to kill cancer cells [7]. Secondly, bioactive molecules were added in scaffolds to inhibit proliferation of cancer cells [8]. Finally, critical clues were added in the scaffolds to induce tissue regeneration [9]. Importantly, for severe cases, the patients need surgery to remove the bone tissue defect and replace the defect with scaffolds that had clues added [10]. In this research, the modification of the scaffolds with clues that had the role of inducing tissue regeneration was selected for maxillofacial bone tissue engineering in bone defect from oral cancer.

The extracellular matrix (ECM) is the important clue to induce tissue regeneration. Some literature reported that the ECM from various tissues was used as a scaffold for tissue regeneration [11-12]. Those ECMs effectively induced tissue regeneration [13]. However, the use of ECM from decellularized pulp tissue was rarely reported. The components of ECM in pulp tissue are the main important clues for tissue regeneration, for instance collagen type I, collagen type II, and fibronectin [14]. The components of ECM were often damaged during the process of isolating ECM from tissue [15]. Therefore, to reconstruct ECM from decellularized pulp was the focus in this research.

Fibronectin is one component in ECM. There are many domains that can act as binding sites in this molecule. Fibronectin functions biologically as a binder molecule that can interact with the other components in ECM and growth factors [16]. Fibronectin acts as a clue to induce cell adhesion, proliferation, and mineralization in bone tissue regeneration [17]. Interestingly, some reports demonstrated that fibronectin could function biologically to inhibit the proliferation of cancer cells [18] after surgery. With the unique biological functions of fibronectin, we expected that fibronectin could induce reconstruction of an extracellular matrix from decellularized pulp and act as a bioactive molecule to inhibit recurrence of cancer during bone tissue regeneration.

The mimicking approach is an attractive method that was used often to create performance scaffolds. Some reports demonstrated that mimicked scaffolds as native extracellular matrix could enhance cell adhesion, proliferation, and differentiation [19]. The mimicking approach for bone tissue engineering was used for structural and biofunctional mimicking [20]. Mimicking the biofunctions of scaffolds is an interesting method to create performance scaffolds for bone tissue engineering. Therefore, in this research, we choose the mimicking approach to reconstruct ECM from decellularized pulp in combination with fibronectin as a coating on silk fibroin scaffolds.

Biofunctional mimicked silk fibroin scaffolds with important clues from decellularized pulp/fibronectin was proposed as a biomaterial for replacement of a bone defect area. The morphological structure and biofunctionalities of mimicked silk fibroin scaffolds were observed and analyzed in this research. The target was to create a performance scaffold that promises use for maxillofacial bone tissue engineering, particularly in a defect area from oral cancer.

MATERIALS AND METHODS

Preparation of silk fibroin scaffolds

The degummed silk fibroin was obtained by boiling in 0.02 M Na_2CO_3 for 30 minutes. The silk sericin was removed after rinsing 3 times with distilled water. It was dried in a hot air oven at 60 °C for 24 h and the degummed silk fibroin was then dissolved in 9.3 M LiBr at 70 °C for 3 h [21]. The purified silk fibroin was obtained after dialyzing with distilled water for 3 days [22]. The purified silk fibroin was centrifuged at 3000 RPM at 4 °C for 5 minutes to separate the dregs from the solution. The concentration was adjusted to yield a 3% (w/v) and kept at 4 °C until further use. The solution was placed in 48-well plates to mold the 3D scaffolds. The freeze-drying method fabricated the porous silk fibroin scaffolds. All scaffolds were cut into discs (10 mm diameter x 2 mm thickness).

Preparation of decellularized pulp

We collected teeth from children who were 6-10 years old and then segmented the teeth in half to harvest the pulp tissue. Collagenase and dispase were used to digest the pulp for 1 hour. The solution was separated from the debris using a centrifuge at 37 °C and washed with phosphate-buffered saline (PBS) 2 times. Finally, the solution was filtered to obtain the decellularized pulp and the freeze-drying process was used for water sublimation [23].

Modification of silk fibroin scaffolds

The 4 groups of solutions are shown in Table 1. The decellularized pulp was prepared at a concentration of 0.1 mg/ml in 0.1% sodium hypochlorite. Fibronectin was prepared at a concentration of 0.1 mg/ml in deionized water. A combination of decellularized pulp and fibronectin was prepared at a ratio of 50:50. After soaking the SF scaffolds in each solution for 4 h, they were put in 1X PBS for 30 minutes. The freeze-drying method attached the ECM to the SF scaffolds.

TABLE I. Groups of coated silk fibroin scaffolds with different ECMs

Group	Detail
A	Silk fibroin scaffold
B	Coated silk fibroin scaffold with decellularized pulp
C	Coated silk fibroin scaffold with fibronectin
D	Coated silk fibroin scaffold with decellularized pulp/fibronectin

Scanning Electron Microscopy (SEM) Observation

Scanning electron microscope (SEM) (Quanta400, FEI, Czech Republic) was used to observe the morphology and characterization of the SF scaffolds that were coated with the solutions. The samples were pre-coated with gold using a gold sputter coating machine (SPI Supplies, Division of Structure Probe, Inc., Westchester, PA, USA).

Atomic Force Microscopy Observation

A sample of coating solution from each group was dropped onto a glass slide, smeared, and soaked in PBS for 30 min. When the slides were dry, the morphology and structure using atomic force microscopy was observed (Nanosurf EasyScan 2 AFM, Switzerland).

Cell culturing of MG-63 osteoblasts

MG-63 osteoblasts were seeded in each scaffold with 1×10^6 cells and maintained in an alpha-MEM medium (α-MEM: Gibco®, Invitrogen™, Carlsbad, CA, USA) with the addition of 1% penicillin/streptomycin, 0.1% Fungizone, and 10% fetal bovine serum at 37 °C in a humidified 5% CO_2/95% air incubator. The medium was changed every 3-4 days [24]. An osteogenic medium (OS: 20 mM b-glycerophosphate, 50 µM ascorbic acid, and 100 nM dexamethasone; Sigma-Aldrich) was used for osteoblast differentiation of the MG-63 osteoblast cells [25].

Calcium content assay

Calcium colorimetric assays (Calcium Colorimetric Assay Kit, BioVision Inc., Milpitas, CA, USA) was used to determine the calcium level secreted from the osteoblast cells. The cells were cultured on SF scaffolds at 7, 14, and 21 days [26]. The cells were then lysed by adding 1% Triton X in each well. The SF scaffolds were frozen at -70 °C for 50 min and then thawed at room temperature for 1 h. This was repeated 3 times. The solutions were transferred to Eppendorf tubes and centrifuged at 20,000 RPM for 10 min to remove the supernatant from the pellets [27]. The supernatant (30 µl) was placed in 96-well plates and the volume was adjusted to 50 µl with distilled water. Next 90 µl of Chromogenic Reagent and then 60 µl of the Calcium Assay Buffer were added to each well and mixed gently. The reaction was

incubated for 5-10 minutes at room temperature and protected from light. The optical density was measured at 575 nm.

Alkaline Phosphatase (ALP) assay

The cells were cultured for 7, 14, and 21 days (Sung Eun Kim) for ALP analysis. The SF scaffolds in each group were washed twice with PBS. To extract the cellular proteins, 800 µl of cell lysis solution (1% Triton X in PBS) was added in each well. The SF scaffolds were frozen at -70 °C for 1 hour and then thawed at room temperature for 1 hour. This was repeated 3 times. The solutions were transferred to Eppendorf tubes and centrifuged at 20,000 RPM for 10 min to remove the supernatant from the pellets. The alkaline phosphatase Colorimetric Assay Kit (Abcam®, Cambridge, UK) was used to detect the ALP activity of the cells in the SF scaffolds. The phosphatase substrate in the kit used *p*-nitrophenyl phosphate that turned to a yellow color when dephosphorylated by the ALP.

Mineralization assay

Alizarin red staining assay was used for mineralization of the nodules. The alizarin red technique detected calcium deposits on the SF scaffolds in each group. The cells in the SF scaffold were cultured for 14 days and then washed twice with PBS. The cells were fixed with 4% formaldehyde and 1 ml of alizarin red solution (2 gm in 100 ml of distilled water and pH adjusted to 4.1- 4.3) was added. After 20 min at room temperature in the dark, the alizarin red solution was carefully removed from the SF scaffolds and the SF scaffolds were washed four times with distilled water. Mineralization nodules were observed under a microscope [28].

Histology

The cell-cultured SF scaffolds were fixed with 4% formaldehyde at 4 °C for 24 h and samples taken on day 5 for cell morphology and on day 14 for detection of calcium. The SF scaffolds in each group were immersed in paraffin and the paraffin sections were cut at 5μ and placed on a glass slide. The sections were then deparaffinized and hydrated in distilled water. The sample slides were stained in 2 ways. Firstly, hematoxylin and eosin (H&E) stain was used to observe cell migration and adhesion on the SF scaffold. Secondly, von Kossa staining was used to detect calcium deposits that were secreted from the osteoblast cells.

Statistical analysis

The samples were measured and statistically compared by one-way ANOVA followed by Tukey's HSD test (SPSS 16.0 software package). Statistical significance was defined as $*P < 0.05$, and $**P < 0.01$.

RESULTS AND DISCUSSION

Characterization of reconstructed formation of decellularized pulp/fibronectin

In this research, silk fibroin scaffolds were prepared by the freeze-drying process. The silk fibroin scaffolds were formed into 3D porous scaffolds that were cut into discs (10 mm diameter by 2 mm thickness). The silk fibroin scaffolds were white with a consistent pore size (Figure 1).

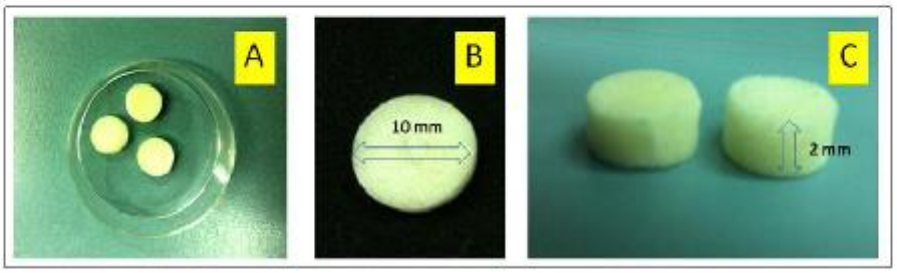

FIGURE 1. Silk fibroin scaffolds after freeze-drying and cut into discs (10 mm diameter x 2 mm thickness).

Before coating the silk fibroin scaffolds, the organization of the reconstructed decellularized pulp/fibronectin was observed by AFM (Figure 2). It was demonstrated that decellularized pulp without fibronectin organized themselves into a connected aggregation of globular structure (Figure 2A). This globular structure might be the fragments of ECM during dissolution with sodium hypochlorite. In the case of fibronectin, there was an aggreagtion of globular structure that was connected into a dendrite structure (Figure 2B). In the case of decellularized pulp with fibronectin, both components oragnized themselves into an aggregation of a large dendrite structure (Figure 2C). As previously reported, the fibronectin acted as the binding component in the ECM [29]. This indicated that fibronectin might connect with the fragments of the ECM. Furhermore, fibronectin plays the role of reconstructing the fragments of the ECM into a large dendrite structure. The decellularized pulp/fibronectin organized themselves into a more complicated structure than the decellularized pulp or fibronectin.

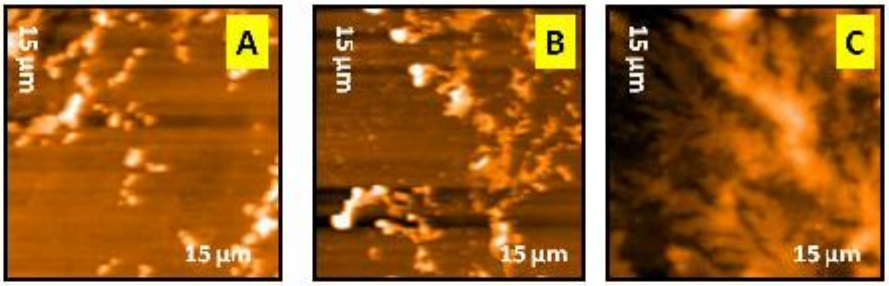

FIGURE 2. Structure formation from AFM: (A) Decellularized pulp, (B) Fibronectin, (C) Decellularized pulp/fibronectin.

Morphological analysis of modified silk fibroin scaffolds

The images of SEM observation of the surface of the silk fibroin scaffolds in each group are shown in Figure 3. The surface of the silk fibroin scaffold showed a smooth and interconnective pore size that supported cell adhesion (Figure 3A). Moreover, the cells could connect with other cells which was suitable for media flow in and out of the silk fibroin scaffold. The decellularized pulp showed some small fibrils that covered the surface of the pores in the scaffold (Figure 3B). Those small fibrils might be the organized fragments of ECM components. Fibronectin showed a globular structure that covered the surface of the pores in the in scaffold (Figure 3C). Finally, decellularized pulp with fibronectin showed predominant fibers that covered most of the areas of the porous surface (Figure 3D). Interestingly, decellularized pulp with fibronectin could synergize the reconstruction into a complicated structure.

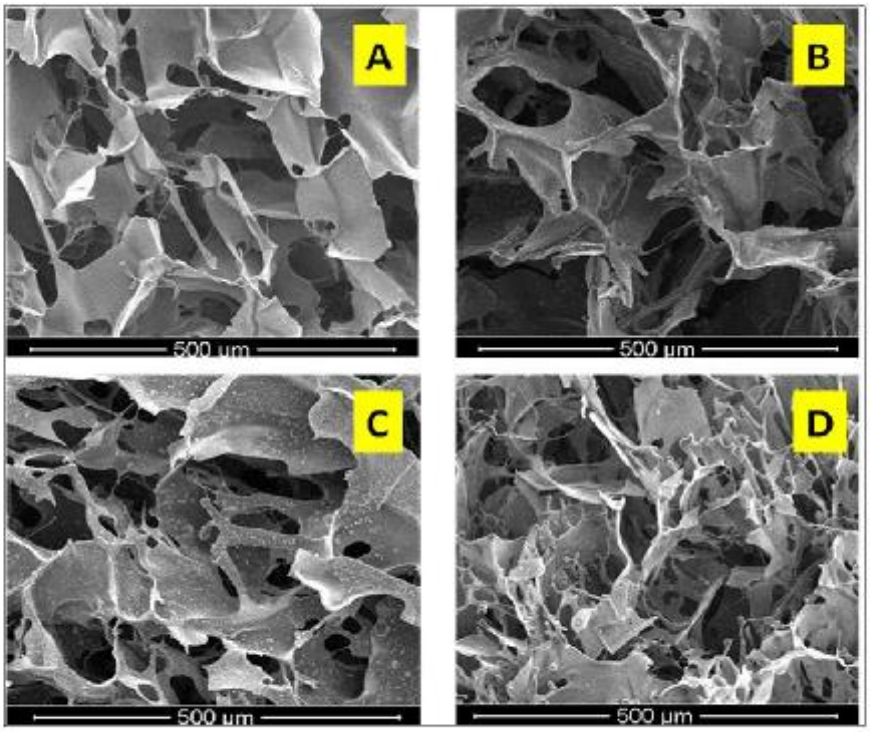

FIGURE 3. SEM images of surface morphology: (A) Silk scaffold, (B) Coated silk fibroin scaffold with decellularized pulp, (C) Coated silk fibroin scaffold with fibronectin, (D) coated silk fibroin scaffold with decellularized pulp/fibronectin.

The cross-section morphology of the coated silk fibroin scaffolds was observed by SEM (Figure 4). Smooth surfaces and regular pore sizes were found in the silk fibroin scaffolds (Figures 4A, B). In the case of decellularized pulp without fibronectin, the fibril structure of ECM fragments were attached to the surface and made rough properties on the surface (Figures 4C, D). The fibronectins arranged themselves into a small globular structure that covered the surface of the pores (Figures 4E, F). Finally, decellularized pulp/fibronectin organized themselves into a globular and fibril structure that adhered to the surface (Figures 4G, H).

Notably, the coated silk fibroin scaffolds with decellularized pulp, fibronectin, and decellularized pulp/fibronectin showed globular and fibril structures that attached in the pores. Those structures appeared in the surface and cross-section morphology of the coated silk fibroin scaffolds. Interestingly, the results of the surface and cross-section morphology demonstrated that decellularized pulp/fibronectin could reconstruct into a complicated structure. This complicated structure showed the globules connected with the fibril structure. The complicated structure of the reconstructed decellularized pulp/fibronectin might be clues to induce bone tissue regeneration. However, to confirm this hypothesis, cell experiments were undertaken.

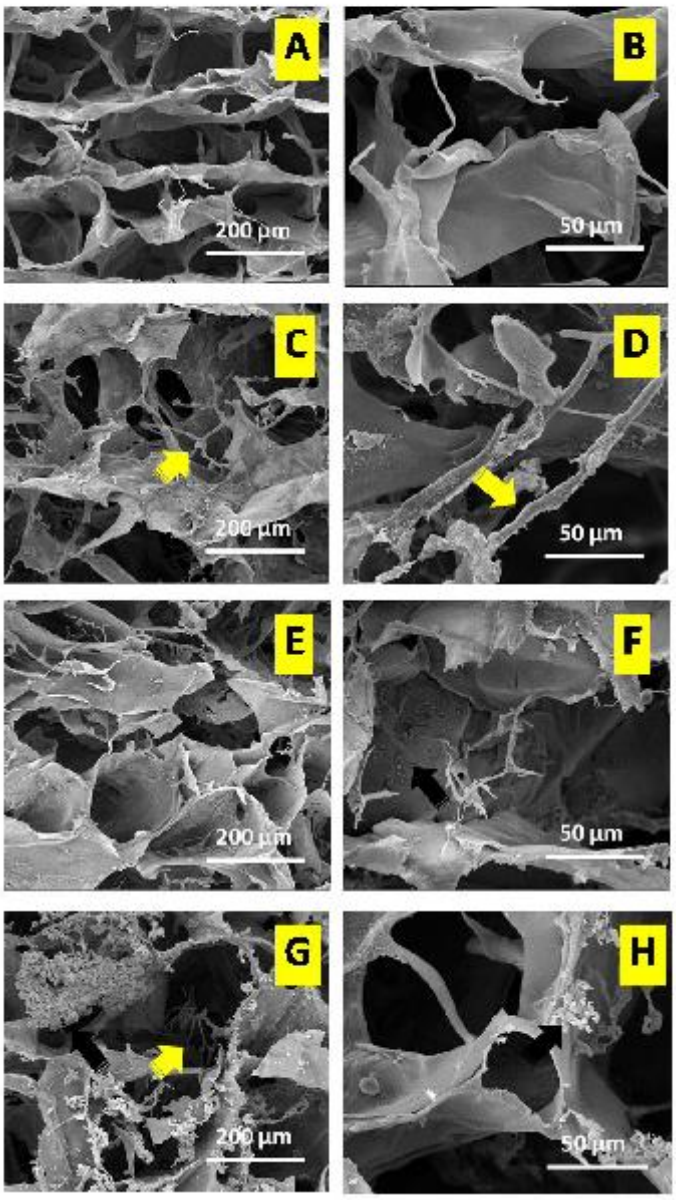

FIGURE 4. SEM images of cross-section morphology: (A, B) silk scaffolds, (C, B) coated silk fibroin scaffolds with decellularized pulp, (E, F) coated silk fibroin scaffolds with fibronectin, (G, H) coated silk fibroin scaffolds with decellularized pulp/fibronectin; Yellow arrow, rod structure; Black arrow, aggregation of globular structure.

Percentage of weight increase

Confirmation of the existence of decellularized pulp, fibronectin, and decellularized/fibronectin in the silk fibroin scaffolds was performed by an analysis of the increase in weights after coating. The coated silk fibroin scaffold with decellularized pulp/fibronectin showed the highest weight increase (Figure 5). The coated silk fibroin scaffold with decellularized pulp showed a lower weight increase than the coated silk fibroin with fibronectin but there was no significant difference. The increase in weight demonstrated that the decellularized pulp, fibronectin, and decellularized pulp/fibronectin had the potential to adhere to the surface of the silk fibroin scaffolds. In particular, decellularized pulp/fibronectin was the predominant component to adhere to the porous surface of the silk fibroin scaffolds.

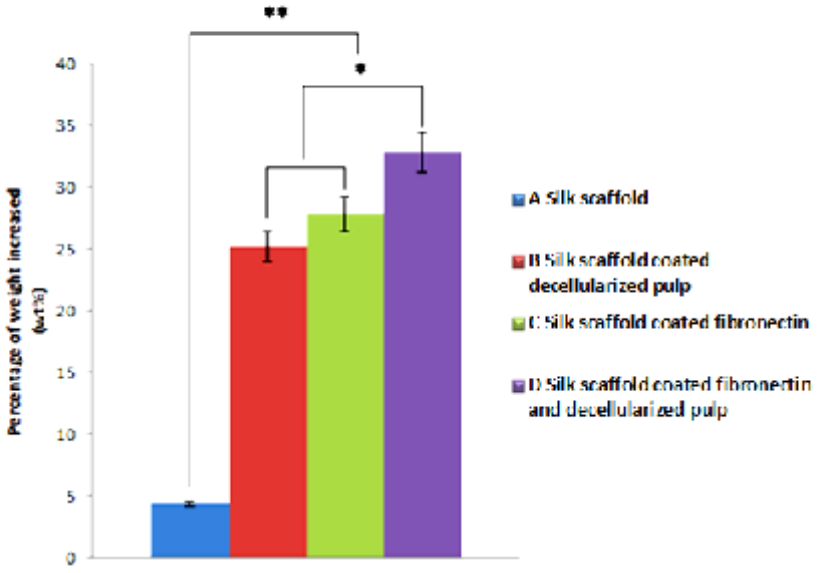

FIGURE 5. Weight increases in percentages of deposition of decellularized pulp, fibronectin, and decellularized pulp/fibronectin. (* $p < 0.05$)

Cell viability assay

Cell viability was analyzed to demonstrate the performance of the coated silk fibroin scaffolds. A green luminance indicated the cell viability on the scaffolds and that the MG-63 osteoblast cells could grow in all groups (Figure 6). The highest efficiency to promote cell proliferation and attachment was demonstrated on the silk fibroin scaffold with decellularized pulp/fibronectin (Figure 6D). This indicated that the reconstructed decellularized pulp/fibronectin acted as an important clue to induce cell adhesion and proliferation.

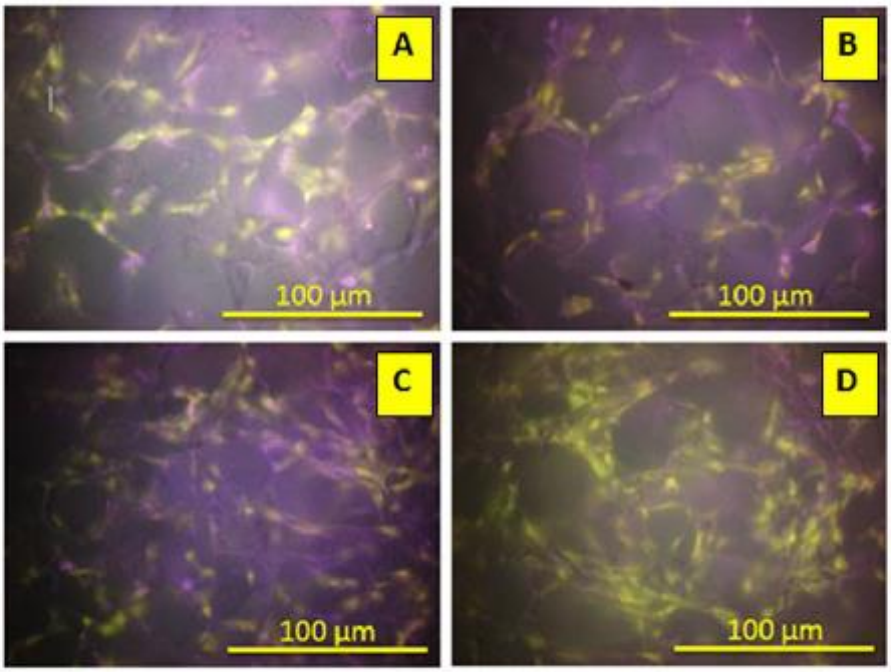

FIGURE 6. FDA cell staining on the scaffold (Green luminance): (A) Silk fibroin scaffold, (B) Coated silk fibroin scaffold with decellularized pulp, (C) Coated silk fibroin scaffold with fibronectin, (D) Coated silk fibroin scaffold with decellularized pulp/fibronectin.

Calcium content analysis

The performance of the coated silk fibroin scaffolds with decellularized pulp/fibronectin was tested with MG-63 osteoblasts. The calcium content was analyzed from the calcium synthesis of the osteoblasts. Mineralization as measured by matrix calcium content on days 7 to day 21, tended to show that calcium synthesis progressively increased (Figure 7). The coated silk fibroin scaffolds with decellularized pulp/fibronectin continued with the highest increase from day 7 to day 21. Interestingly, the decellularized pulp/fibronectin, showed higher calcium content than the others at every time point. This indicated that the reconstruction of decellularized pulp/fibronectin played a role as a clue to induce calcium synthesis from the osteoblasts.

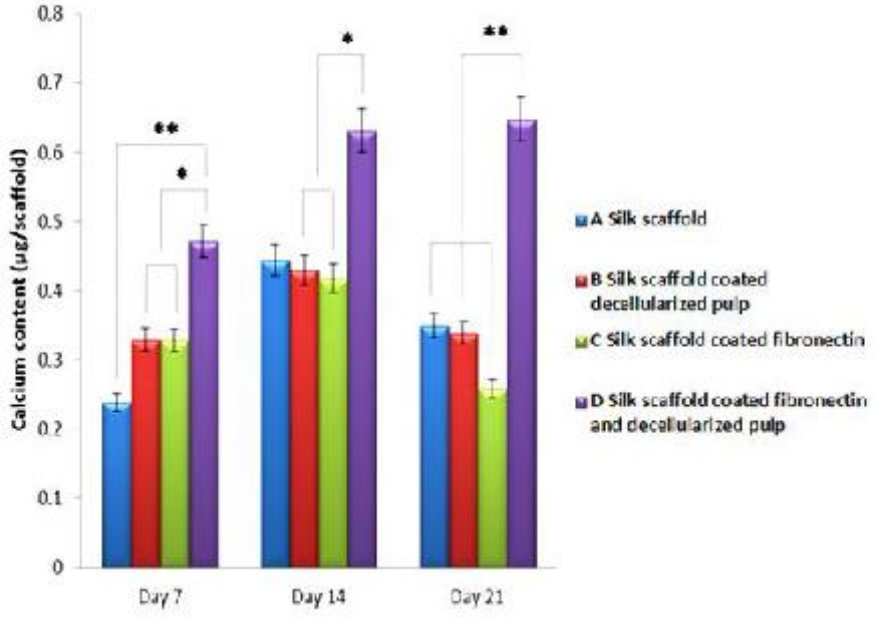

FIGURE 7. The calcium content values in SF scaffolds from MG-63 cell line at days 7, 14, and 21.

Alkaline phosphatase (ALP) activity analysis

The ALP activity analysis measured the quality of the MG-63 osteoblast performance to differentiate from the pre-osteoblast cells to the mature cells. All groups of silk fibroin scaffolds revealed a progressive increase in ALP activity from day 7 to 21 (Figure 8). On day 7, the coated silk fibroin scaffold with decellularized pulp/fibronectin indicated that the MG-63 osteoblasts were osteo-induced and showed the highest ALP activity value. The silk fibroin scaffolds coated with fibronectin showed a higher ALP activity than the coated silk fibroin with decellularized pulp and the silk fibroin scaffolds. On day 14, all groups continued to increase in ALP activity. The coated silk fibroin scaffolds with decellularized pulp increased ALP activity faster than the coated silk fibroin scaffolds with fibronectin and the silk fibroin scaffolds. All of those scaffolds showed less ALP activity than the coated silk fibroin scaffolds with decellularized pulp/fibronectin. The last period, the coated silk fibroin scaffold with decellularized pulp/fibronectin revealed the highest ALP activity value.

The results demonstrated that decellularized pulp/fibronectin could induce the osteo-induction of pre-osteoblasts to the mature stage. Fibronectin induced cell adhesion, extension, and migration adsorption of osteoblasts [30]. Decellularized pulp has many components of the ECM which include collagen, fibronectin, and versican which acted as important clues for MG-63 osteoblasts to induce tissue regeneration [31]. Therefore, the reconstructed ECM of decellularized pulp/fibronectin in this research showed the role as important clues for bone tissue engineering.

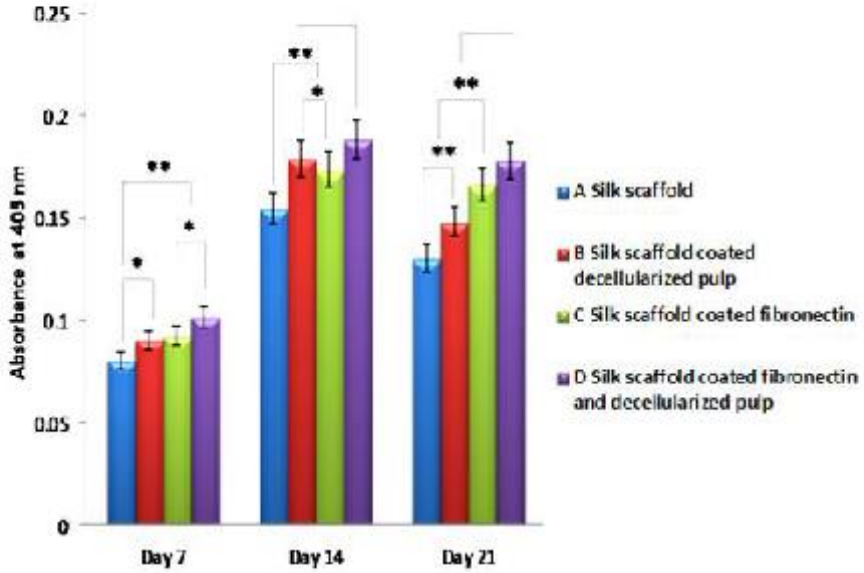

FIGURE 8. ALP activity from MG-63 osteoblast cells on days 7, 14, and 21.

Nodule formation and mineralization analysis

Nodule formation was observed at day 14 after cell seeding. Alizarin red was used to check the osteogenic differentiation state of the cells that can synthesize ECM mineralization. The osteoblast cells showed osteogenesis in all groups of silk fibroin scaffolds (Figure 9). The red color indicated calcium production from the MG-63 osteoblasts and the calcium deposited on the silk fibroin scaffolds. The results showed red clusters that were distributed in the scaffolds. Importantly, the MG-63 osteoblast cells could produce calcium in all sample groups. The intensive red clusters in the coated silk fibroin scaffold with decellularized pulp/fibronectin showed the highest amount of deposited calcium. This indicated that the coated silk fibroin scaffold with decellularized pulp/fibronectin was suitable for bone tissue engineering because the MG-63 osteoblast cells were spread throughout the silk fibroin scaffold and could produce calcium.

The results demonstrated that the reconstructed ECM of decellularized pulp/fibronectin acted as an important clue for MG-63 osteoblasts to induce calcium synthesis for bone tissue engineering.

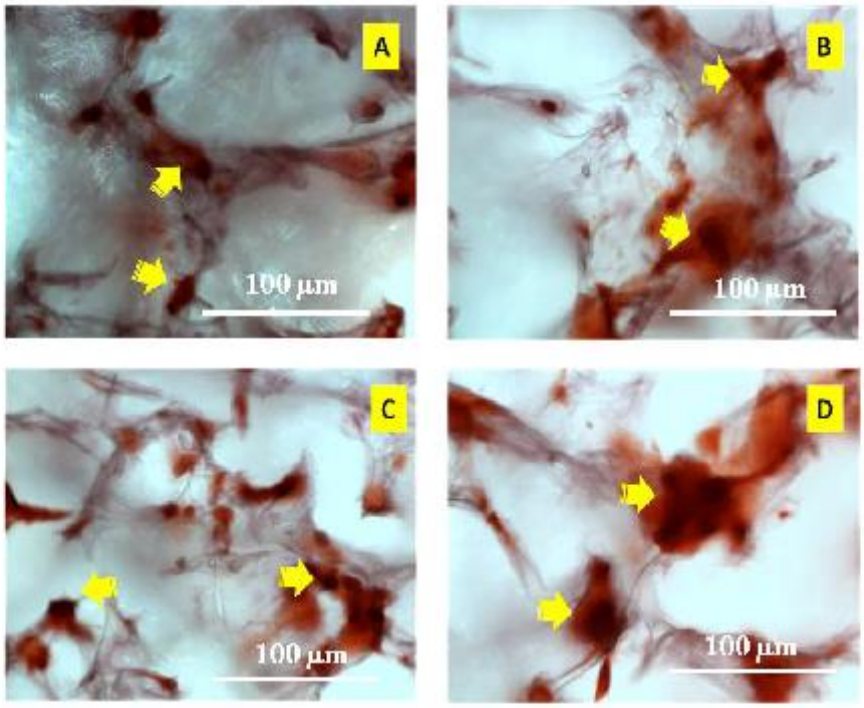

FIGURE 9. Alizarin red staining of SF scaffolds on day 14: (A) Silk fibroin scaffold, (B) Coated silk fibroin scaffold with decellularized pulp, (C) Coated silk fibroin scaffold with fibronectin, (D) Coated silk fibroin scaffold with decellularized pulp/fibronectin. The yellow arrows show the cluster of calcium.

Histological analysis

Histological analysis was used to observe the morphology and to explain the organization of the cells on the cell cultured silk fibroin scaffolds. The MG-63 osteoblast

cells could spread thoroughly on the surface of the silk fibroin scaffolds in all groups (Figure 10). The MG-63 osteoblast cells could attach and migrate into the pores particularly onto the wall surface of the silk fibroin scaffolds. The coated silk fibroin scaffolds with decellularized pulp/fibronectin demonstrated that the cells could attach and spread throughout most of the areas of the scaffold (Figure 10D). The organization of the cells on the scaffolds from the histological analysis showed the same result as in Figure 6D.

Importantly, the results demonstrated that the coated silk fibroin scaffolds with decellularized pulp/fibronectin had the clues to enhance cell attachment and migration. The good cell attachment and migration on the scaffolds are suitable criteria to induce regeneration of new bone tissue [32].

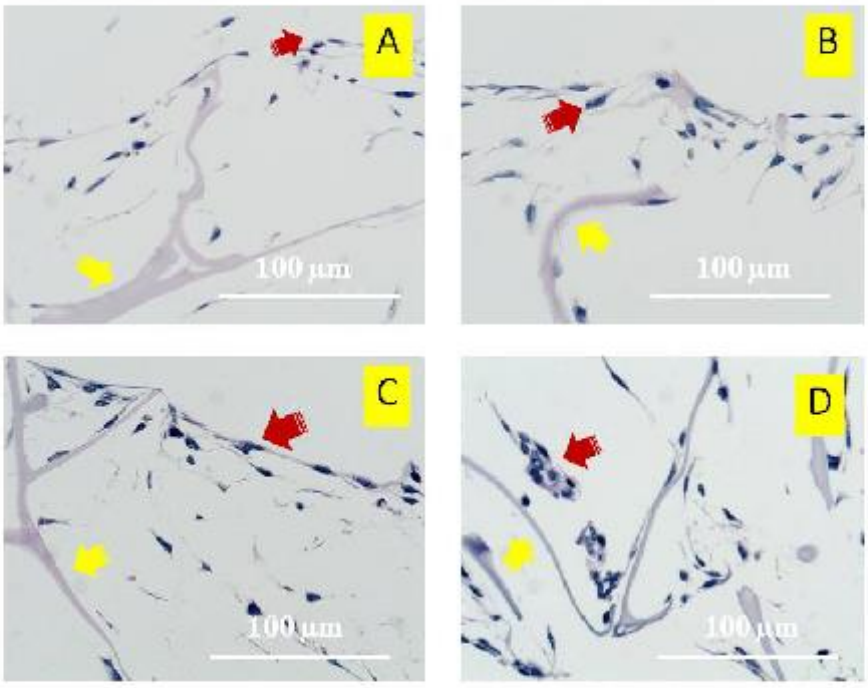

FIGURE 10. Representative histology (H&E) of cross-sections on day 5: (A) Silk fibroin scaffold, (B) Coated silk fibroin scaffold with decellularized pulp, (C) Coated silk fibroin scaffold with fibronectin, (D) Coated silk fibroin scaffold with decellularized pulp/fibronectin; Yellow arrows show the silk scaffold in each group; Red arrows show the osteoblast cells attached to the silk scaffolds in each group.

Von Kossa

Von Kossa staining was used to confirm mineralization of the extracellular matrix [33] secreted by the MG-63 osteoblast cells. In all groups of samples, the MG-63 osteoblast cells could proliferate and migrate on the silk fibroin scaffold (Figure 11). Moreover, the synthesis of calcium-containing salts such as calcium phosphate suggested the behavior of bone regeneration. The black color (yellow arrows) revealed the calcium that was secreted from the MG-63 osteoblast cells and stained by von Kossa. The silk fibroin scaffolds coated with decellularized pulp/fibronectin expressed a lot of osteoblast cells (white arrows) attached to the silk surface (Figure 11D). The other groups, silk fibroin scaffold without coating, coated silk fibroin scaffold with decellularized pulp, and coated silk fibroin scaffold with fibronectin, showed both cell attachment and calcium synthesis (Figure 11A-C). The results of the von Kossa staining indicated that all groups of silk fibroin could induce cell attachment and calcium synthesis. The coated silk fibroin with decellularized pulp/fibronectin showed more cells in the scaffold. Not only could decellularized pulp/fibronectin induce calcium synthesis from the cells, it could promote cell adhesion. Therefore, the results of von Kossa staining demonstrated that the reconstructed extracellular matrix of decellularized pulp/fibronectin acted as suitable clues to promote bone regeneration.

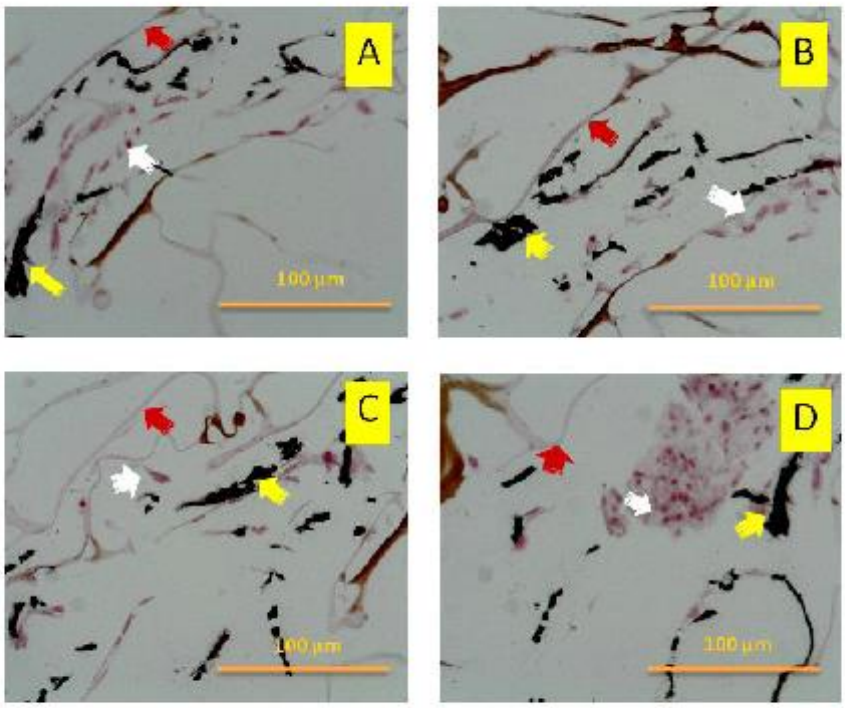

FIGURE 11. Histological sections of scaffold structures stained with von Kossa after day 14: (A) Silk fibroin scaffold, (B) Coated silk fibroin scaffold with decellularized pulp, (C) Coated silk fibroin scaffold with fibronectin, (D) Coated silk fibroin scaffold with decellularized pulp/fibronectin; White arrows, osteoblasts in scaffold; Yellow arrows, clusters of calcium; Red arrows, scaffold

CONCLUSION

In this research, coated silk fibroin scaffolds with reconstructed extracellular matrix of decellularized pulp/fibronectin were proposed as a biomaterial to replace bone defect from oral cancer at the maxillofacial area. The results demonstrated that the reconstructed extracellular matrix could attach to the porous walls of silk fibroin scaffolds. The reconstructed extracellular matrix organized themselves into fibrils with an aggregation of a globular structure. Obviously, coated silk fibroin scaffolds with decellularized pulp/fibronectin played an important role as the clue to induce cell adhesion, proliferation,

and calcium synthesis which can lead to promotion of bone tissue regeneration. The predominant biofunctionalities of a coated silk fibroin scaffold with decellularized pulp/fibronectin holds promise as a scaffold to replace bone defects in oral cancer. Nevertheless, to prove the performance for inhibition of cancer cell proliferation, the scaffolds need in vivo or ex vivo testing.

ACKNOWLEDGEMENT

This work was financially supported by grant no. EC 50-042-25-2-3 from the Faculty of Medicine, Prince of Songkla University. Many thanks to Institute of Biomedical Engineering and Queen Sirikit Sericulture Centre, Narathiwat, for silk supporting.

REFERENCES

1. J.A. Sterling, S.A. Guelcher, Biomaterial scaffolds for treating osteoporotic bone, Curr Osteoporos Rep 12 (2014) 48–54.
2. J.Nagy, L.Seres,P. Novak, K.Nagy, Osseointegration of dental implants after radiotherapy for oral cancer, Fogorv Sz 102 (2009) 7-11.
3. Z. Zhao, Y. Li, M.B. Xie, Silk Fibroin-Based Nanoparticles for Drug Delivery, Int. J. Mol. Sci 16 (2015) 4880-4903.
4. V. Kearns, A.C. MacIntosh, A. Crawford, P.V. Hatton, Silk-based Biomaterials for Tissue Engineering, Topics in Tissue Engineering 4 (2008) 1-19.
5. Y. Wang, D. J. Blasioli, H.J. Kim, H.S. Kim, D. L. Kaplan, Cartilage tissue engineering with silk scaffolds and human articular chondrocytes, Biomaterials 27 (2006) 4434–4442.
6. E. Andronescu, D. Ficai, A. Ficai, Multifunctional materials for bone cancer treatment, Int J Nanomedicine 9 (2014) 2713–2725.
7. P. S. Pramod, R. Shah, S. Chaphekar, N. Balasubramanian, M. Jayakannan, Polysaccharide nano-vesicular multidrug carriers for synergistic killing of cancer cells, Nanoscale 6 (2014) 11841-11855.

8. B. Hoeger, M. Diether, P. J.Ballester, M. Kohn, Biochemical evaluation of virtual screening methods reveals a cell active inhibitor of the cancer-promoting phosphatases of regenerating liver, Eur J Med Chem 88 (2014) 89-100.

9. K. Arvidson, B. M. Abdallah, L. A. Applegate, N. Baldini, E. Cenni, E. Gomez-Barrena, D. Granchi, M. Kassem, Y. T. Konttinen, K. Mustafa, D. P. Pioletti, T. Sillat, A. Finne-Wistrand, Bone regeneration and stem cells, Regenerative Medicine Review Series 15 (2011) 718-746.

10. A. Chatterjea, G. Meijer, C. van Blitterswijk, J. de Boer, Clinical Application of HumanMesenchymal Stromal Cells for Bone Tissue Engineering, Stem Cells International 2010 (2010) 1-12.

11. B. P. Chan, K. W. Leong, Scaffolding in tissue engineering: general approaches and tissue-specific considerations, Eur Spine J 17 (2008) 467–479.

12. S. S. Patnaik, B. Wang, B. Weed, J. A. Wertheim, J. Liao, Decellularized Scaffolds: Concepts, Methodologies, and Applications in Cardiac Tissue Engineering and Whole-Organ Regeneration, Tissue Regeneration: Where Nanostructure Meets Biology, Chapter: 3. World Scientific Company (2014) 77-124.

13. M. P. Prabhakaran, J. Venugopal, L. Ghasemi-Mobarakeh, D. Kai, G. Jin, S. Ramakrishna, Stem Cells and Nanostructures for Advanced Tissue Regeneration, Adv Polym Sci 246 (2012) 21–62.

14. S. P. H. Miyagi, I. Kerkis, C. M. da Costa Maranduba, C. M. Gomes, M. D. Martins, M. M. Marques, Expression of Extracellular Matrix Proteins in Human Dental Pulp Stem Cells Depends on the Donor Tooth Conditions, Journal of endodontics 36 (2010) 826-831.

15. P. M. Crapo, T. W. Gilbert, S. F. Badylak, An overview of tissue and whole organ decellularization processes, Biomaterials 32 (2011) 3233–3243.

16. B. Alberts, A. Johnson, J. Lewis, Molecular Biology of the Cell, 4th edition, New York: Garland Science, 2002.

17. M.Smitha, B.Ramesh, K.M. Pawan, T.Satish , Extracellular matrix protein mediated regulation of the osteoblast differentiation of bone marrow derived human mesenchymal stem cells, Differentiation 84 (2012) 185–192.

18. T. Ishikawa, S. Kokura, T. Enoki, N. Sakamoto, T. Okayama, M. Ideno, J. Mineno, K. Uno , N. Yoshida , K. Kamada , K. Katada, K. Uchiyama, O. Handa, T. Takagi, H. Konishi, N. Yagi, Y. Naito, Y. Itoh , T. Yoshikawa, Phase I Clinical Trial of Fibronectin CH296-Stimulated T Cell Therapy in Patients with Advanced Cancer, PLOS ONE 9 (2014) 1-9.

19. F. M. Watt, Extracellular matrix and cell shape, Trends in biochemical sciences 11 (1986) 482-485.

20. H. Geckil, F. Xu, X. Zhang, S. Moon, U. Demirci, Engineering hydrogels as extracellular matrix mimics, Nanomedicine 5 (2010) 469–484.

21. G. Chang, H.J. Kim, D. Kaplan, G. Vunjak-Novakovic, R. A. Kandel, Porous silk scaffolds can be used for tissue engineering annulus fibrosus, Eur Spine J 16 (2007) 1848-1857.

22. Y. Zhao, R. Z Legeros, J. Chen, Initial Study on 3D Porous Silk Fibroin Scaffold: Preparation and Morphology, Bioceramics Development and Applications 1 (2011) 1-3.

23. S. B. Traphagen, N. Fourligas, J. Xylas, S. Sengupta, D. Kaplan, I. Georgakoudi, P. C. Yelick, Characterization of Natural, Decellularized and Reseeded Porcine Tooth Bud Matrices, Biomaterials 33 (2012) 5287-5296.

24. X. Liu, M. Zhao, J. Lu, J. Ma, J. Wei, S. Wei, Cell responses to two kinds of nanohydroxyapatite with different sizes and crystallinities, Int J Nanomedicine 7 (2012) 1239-1250.

25. B.S. Kim, H. J. Kang, J. Lee, Improvement of the compressive strength of a cuttlefish bone-derived porous hydroxyapatite scaffold via polycaprolactone coating, Journal of Biomedical Materials Research Part B: Applied Biomaterials 101 (2013) 1302-1309.

26. S E. Kim, S.-H. Song, Y. P. Yun, B.J. Choi, K. Kwon, M. S. Bae, H.J. Moon, Y.D. Kwon, The effect of immobilization of heparin and bone morphogenic protein-2 (BMP-2) to titanium surfaces on in flammation and osteoblast function, Biomaterials 32 (2010) 1-8.

27. H. Ji, Lysis of Cultured Cells for Immunoprecipitation, Cold Spring Harbor Laboratory Press 2010 (2010) 1-5.

28. Y.H. Wang, Y. Liu, P. Maye, D. W. Rowe, Examination of Mineralized Nodule Formation in Living Osteoblastic Cultures Using Fluorescent Dyes, Biotechnol Prog 22 (2006) 1697–1701.

29. J. Halper, M. Kjaer, Basic Components of Connective Tissues and Extracellular Matrix: Elastin, Fibrillin, Fibulins, Fibrinogen, Fibronectin, Laminin, Tenascins and Thrombospondins, Advances in Experimental Medicine and Biology 802 (2014) 31-47.

30. D. M. Rivera-Chacon, M. Alvarado-Velez, C.Y. Acevedo-Morantes, S.P. Singh, E. Gultepe, D. Nagesha, S. Sridhar, J.E. Ramirez-Vick, Fibronectin and vitronectin promote human fetal osteoblast cell attachment and proliferation on nanoporous titanium surfaces, J Biomed Nanotechnol 9 (2013) 1092–1097.

31. M.Goldberg, J.Smith, Cells and Extracellular Matrices of Dentin and Pulp: A Biological Basis For Repair and Tissue Engineering, Crit Rev Oral Biol Med 15 (2004) 13-27.

32. S. Bose, M. Roy, A. Bandyopadhyay, Recent advances in bone tissue engineering scaffolds, Trends Biotechnol 30 (2012) 546-554.

33. A. Ivan, V. Ordodi, A. Cean, D. E. Ilie, C.Panaitescu, G. Tanasie, Comparative study of the differentiation potential of rat bone marrow mesenchymal stem cells and rat muscle-derived stem cells, Arch Biol Sci 65 (2013) 1307-1315.

*Manuscript

A biofunctional-modified silk fibroin scaffold with mimic reconstructed extracellular matrix of decellularized pulp/collagen/fibronectin for bone tissue engineering in alveolar bone resorption

Supaporn Seangkert[1], Suttatip Kamonmattayakul[2], Chai Wen Lin[3], Jirut Meesane[1*]

[1]Institute of Biomedical Engineering, Faculty of Medicine, Prince of Songkla University, Hat Yai, Songkhla, Thailand, 90110

[2]Department of Preventive Dentistry, Faculty of Dentistry, Prince of Songkla University, Hat Yai, Songkhla, Thailand, 90110

[3]Department of General Dental Practice and Oral and Maxillofacial Imaging, Faculty of Dentistry, University of Malaya, Kuala Lumpur, Malaysia

*Correspondence author e-mail: jirutmeesane999@yahoo.co.uk

Abstract

A modified silk fibroin scaffold with mimic reconstructed extracellular matrix of decellularized pulp/collagen/fibronectin was proposed for bone tissue engineering in alveolar bone resorption. Silk fibroin scaffolds were fabricated by freeze-drying before modification by coating in a decellularized pulp/collagen/fibronectin solution. The extracellular matrix reconstruction of the decellularized pulp/collagen/fibronectin and the morphology and biofunctionalities of the modified scaffolds were evaluated. The results showed that decellularized pulp/collagen/fibronectin organized into a dense dendrite structure and adhered in the scaffold in a fibrillar network. The modified scaffold showed predominant biofunctionalities and promise for bone tissue engineering in alveolar bone resorption.

Keywords: Silk fibroin, Tissue engineering, Fibronectin, Decellularized pulp, Bone tissue engineering, Alveolar bone resorption

1. Introduction

Generally, alveolar bone resorption is treated by bone graft from another area, for instance the fibula, scapula, iliac crest, or radius. Nevertheless, bone grafting outcomes include donor-area morbidity and prolonged treatment [1]. Therefore, to use scaffolds for bone tissue engineering is an interesting issue to solve those problems.

Bombyx mori silk fibroin has been used for biomaterial applications for several decades [2]. To create a high performance scaffold for bone tissue engineering, silk fibroin needs enhancement of the biofunctionalities to induce bone tissue regeneration.

Some reports demonstrated that mimicking by reconstruction from the components of an extracellular matrix (ECM) was an attractive method to maintain biofunctionality [3]. Interestingly, the use of ECM from decellularized pulp was rarely reported. Therefore, to reconstruct an ECM from decellularized pulp is the focus of this research.

Collagen is used as a signal to induce cell adhesion and proliferation for bone tissue regeneration [4]. Fibronectin has the important role of inducing mineralization [5]. Due to the biofunctionalities of collagen and fibronectin, they were selected for combination with decellularized pulp and reconstruction into an ECM.

In this research modification of silk fibroin scaffolds with reconstructed ECM of decellularized pulp/collagen/fibronectin was considered. The focus was on the morphology and biological functionalities related to bone tissue engineering in alveolar bone resorption.

2. Materials and methods

2.1 Preparation of silk fibroin scaffolds

The silk fibroin solution was prepared following G. Chang et al. 2007. The concentration of silk fibroin solution was adjusted to 3% (w/v) [6,7]. Then, the solution was poured into 48 well plates before freeze-drying. The samples were cut into discs of 10 mm in diameter and 2 mm in thickness.

2.2 Preparation of type I collagen

Type I collagen was extracted from the skin of the brown banded bamboo shark (*Chiloscyllium punctatum*). Preparation of the collagen followed P. Kittiphattanabawon et al. 2010 [8].

2.3 **Preparation of decellularized pulp**

This study collected teeth pulp from children 6-10 years old. The teeth were segmented in half to harvest the dental pulp tissue. Decellularized pulp was prepared following S. Traphagen et al. 2012 [9].

2.4 Modification of silk fibroin scaffolds

Two groups of scaffolds were used in this study: silk scaffold and modified silk scaffold coated with decellularized pulp/collagen/fibronectin. For the modified scaffold group, the decellularized pulp powder was dissolved in a solution of 0.1% sodium hypochlorite at a concentration of 0.1 mg/ml. The collagen was dissolved in 0.1 M acetic acid at a concentration of 0.1 mg/ml and the fibronectin was dissolved in distilled deionized water at a concentration of 0.1 mg/ml. Those solutions were mixed together at a volume ratio of 1:1:1. The scaffolds were soaked in 1X PBS for 30 minutes and then the freeze-drying method was used.

2.5 Scanning Electron Microscopy (SEM)

A scanning electron microscope (Quanta 400, FEI, Czech Republic) was used to observe the morphology and characterization of the scaffolds that were coated with the

special solution. The samples were pre-coated with gold using a gold sputter-coating machine (SPI supplies, Division of STRUCTURE PROBE Inc., Westchester, PA, USA).

2.6 Atomic Force Microscopy

A sample of the coating solution from each group was dropped onto a glass slide, smeared, and soaked in PBS for 30 min. When the slides were dry, the morphology and structure were observed by atomic force microscopy.

2.7 MG-63 cell culture

MG-63 cells were cultured in a 75 cm^3 flask with alpha-MEM medium (α-MEM, Gibco™, Invitrogen, Carlsbad, CA, USA) with the addition of 1% penicillin/streptomycin, 0.1% fungizone, and 10% fetal bovine serum at 37 °C in a humidified CO_2 (5%) and air (95%) incubator. The MG-63 cells were seeded at 5×10^5 per scaffold. The medium was changed every 3-4 days during the cell culture. An osteogenic medium (OS; 10 mM b-glycerophosphate, 50 mg=mL ascorbic acid, and 100 nM dexamethasone; Sigma-Aldrich) was used for osteoblast differentiation of the MG-63 cells [10] .

2.8 Alkaline phosphatase activity analysis

After cell culture at days 7, 14, and 21, the scaffolds were washed twice with PBS. Then, lysing of the cells followed Hong Ji 2010 [11]. The cell lysate solutions were used for the ALP activity according to the manufacturer's instructions (Abcam®, Cambridge, UK).

2.9 Calcium content analysis

The cell lysate solution from paragraph 2.8 was used to analyze the calcium content. The calcium value synthesized from the MG-63 osteoblast cells was measured with calcium colorimetric assays (Calcium colorimetric assay, Biovision).

2.10 Alizarin Red staining for mineralized matrix

The cells were fixed with 70% ethanol for 1 h and removed to -20 °C. Alizarin red S (40 mM, pH at 4.2; Sigma-Aldrich) was used to stain the calcium nodule deposition with a 10 min incubation period [12].

2.11 Von Kossa staining

After cell culture on day 14, the scaffolds were transferred to 48 well plates and washed twice with PBS and 4% formaldehyde was used for cell fixation at 4 °C for 24 h. The scaffolds were immersed in paraffin. The paraffin sections were cut at 5μ and placed on a glass slide, deparaffinized, and hydrated in distilled water. The sample slides were stained with von Kossa reagent to investigate the deposits of calcium synthesized from the MG-63 osteoblast cells[13].

2.12 Statistical analysis

All data were shown as mean±standard deviation. The samples (n=5) were measured and statistically compared by one-way ANOVA (SPSS 16.0 software package). A P value < 0.05 was accepted as statistically significant.

3. Results and discussion

3.1 Reconstructed ECM formation and morphological structure of scaffolds

The decellularized pulp/collagen/fibronectin organized into a dense structure of dendrites (Fig. 1A, B). The modified scaffold appeared whiter than the non-modified scaffold (Fig. 1C, D). The morphology of the non-modified scaffold showed pores that had a smooth surface (Fig. 2A, B). The pores of the modified scaffold had a fibrillar network (Fig. 2C, D) as a native ECM structure[14]. This result indicated that the fibrillar network was reconstructed ECM.

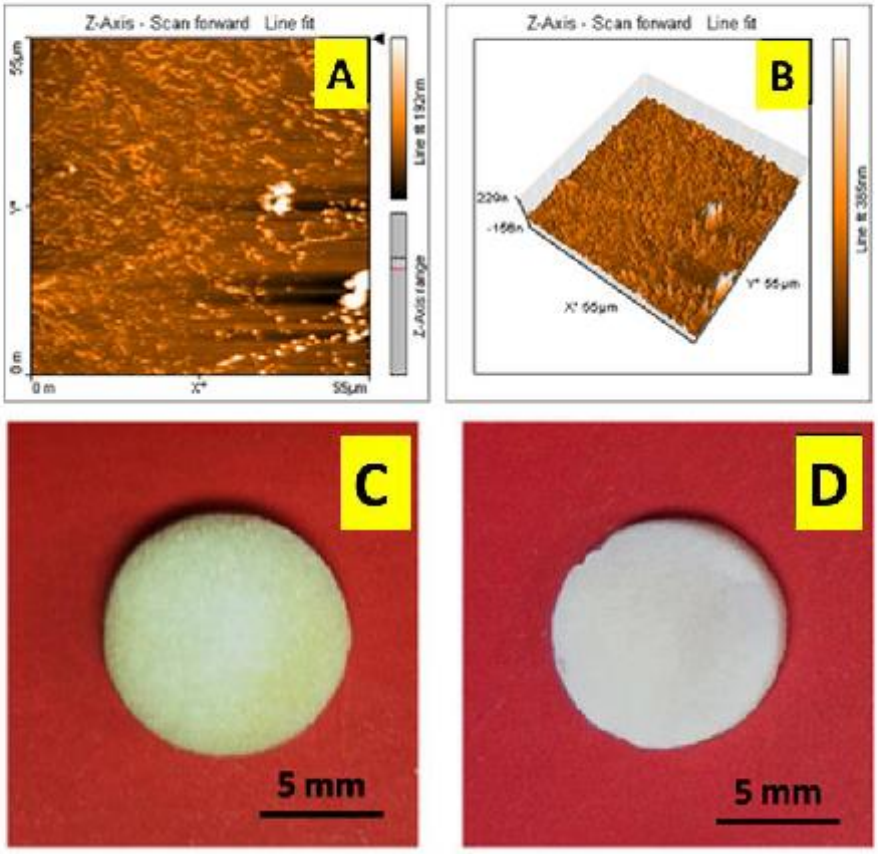

Fig. 1. AFM analysis of the combination of decellularized pulp/collagen/fibronectin fibril formation: (A) 2 dimensions and (B) 3 dimensions. (C) non-modified scaffold and (D) modified scaffold.

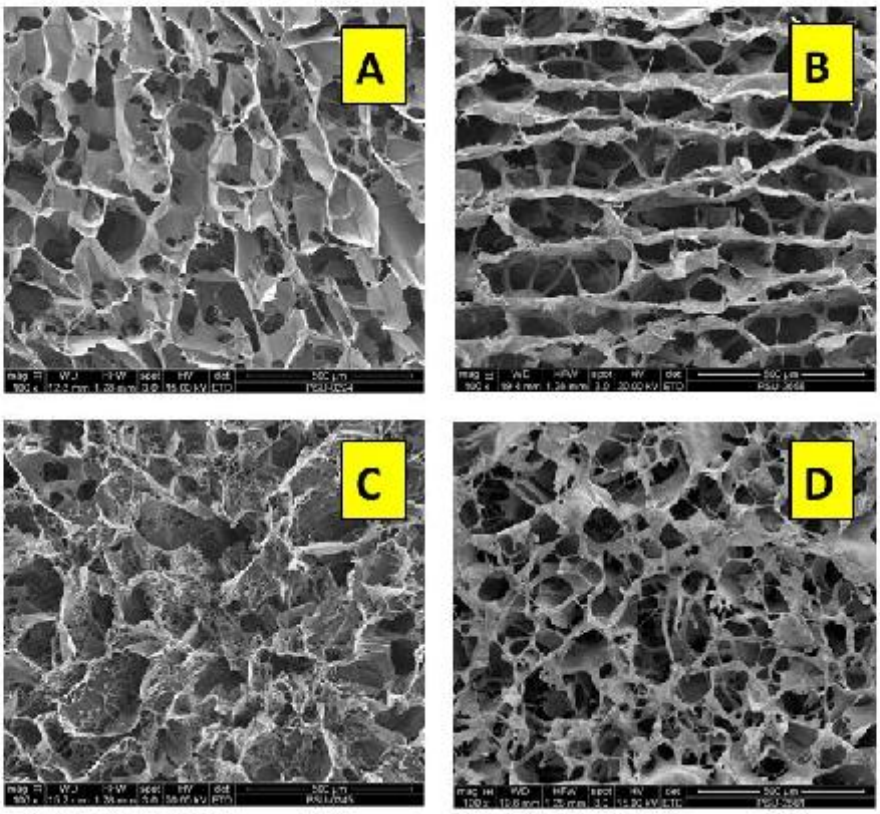

Fig. 2. SEM analysis showed the surface morphology of (A) non-modified scaffold and (C) modified scaffold. The cross-section morphology of (B) non-modified scaffold and (D) modified scaffold.

3.2 Alkaline phosphatase activity and calcium content analysis

The ALP assay was used for early MG-63 osteoblast differentiation on culture days 7, 14, and 21 (Fig. 3A). The ALP activity in the modified scaffold increased from day 7 to 21. The non-modified scaffold started to increase during days 7 to 14 and decreased at day 21. The modified scaffold showed predominant ALP activity of the MG-63 osteoblasts. The calcium deposition ratio in both groups increased between days 7 to 14 and went down on day 21 (Fig. 3B). At days 7 and 14, the modified scaffold had a higher calcium value than the

non-modified scaffold. The results showed that the reconstructed ECM could activate differentiation of the osteoblasts and induce the synthesis of calcium from the osteoblasts.

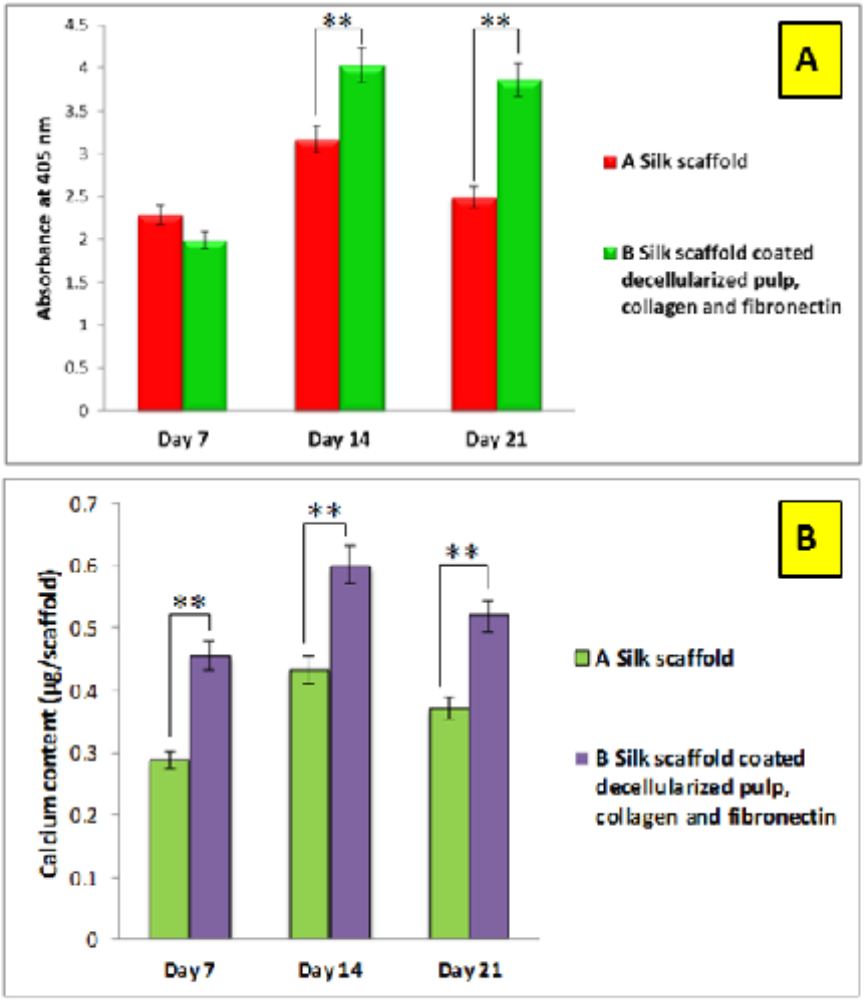

Fig. 3. (A) ALP activity among different groups of scaffold at day 7, 14, and 21. (B) Calcium deposits on the different groups of scaffold at day 7, 14, and 21. The symbol (*) represents significant changes in ALP and calcium activity of the MG-63 osteoblasts ($P < 0.05$), (**) ($P < 0.01$).

3.3 Calcium deposition and mineralization analysis

Alizarin red staining was used to detect the calcium on the scaffold on day 14 of osteogenic induction. The modified scaffold indicated more calcium deposition compared with the silk fibroin scaffold (Fig. 4B). The results demonstrated that the reconstructed ECM had the ability to promote calcium synthesis of the osteoblasts. Von Kossa staining performed on day 14 of osteogenic induction revealed mineral matrix secretion of the MG-63 osteoblast cells (red arrows) were attached to the scaffold (blue arrows).The modified scaffold (Fig. 4D) showed more mineral matrix (yellow arrows) compared with the non-modified scaffold (Fig. 4C).

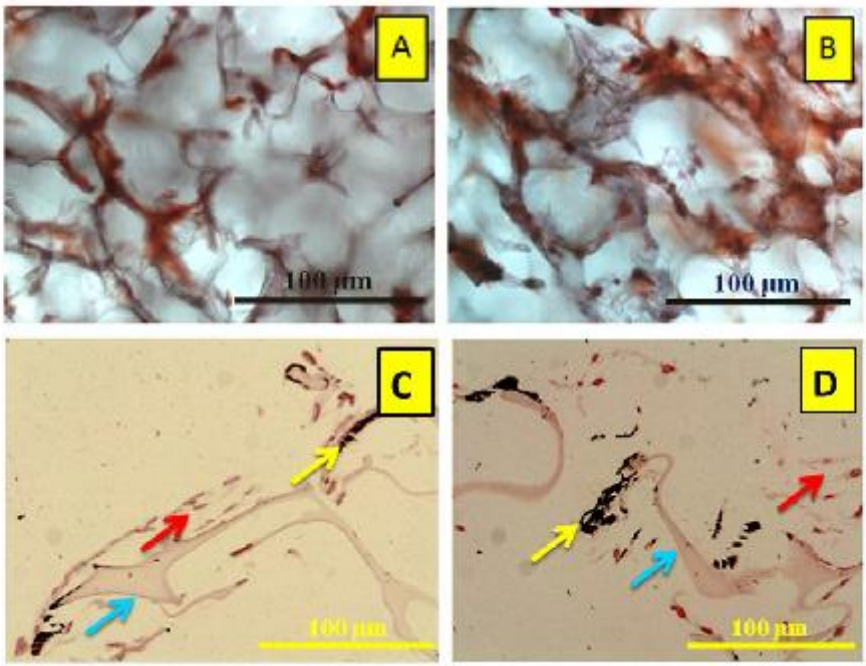

Fig. 4. Alizarin red staining of scaffold on day 7: (A) non-modified scaffold and (B) modified scaffold. Histological sections of scaffold structures stained with von Kossa after day 14: (C) non-modified scaffold and (D) modified scaffold.

4. Conclusion

A modified scaffold was proposed for use in bone tissue engineering in alveolar bone resorption. The morphological structure and biofunctionalities of the modified scaffold were evaluated. The results demonstrated that decellularized pulp/collagen/fibronectin formed a reconstructed ECM into a fibrillar network. This reconstructed ECM could enhance biofunctionalities of the scaffold. The results demonstrated that the modified scaffold showed promise for alveolar bone resorption treatment.

Acknowledgements

This work was financially supported by grant no. EC 50-042-25-2-3 from the Faculty of Medicine, Prince of Songkla University. Many thanks to the Biological Materials for Medicine (BMM) Research Unit and Queen Sirikit Sericulture Centre, Narathiwat, for supply of the silk.

References

1. Swapan Kumar Sarkar, Byong Taek Lee. Hard tissue regeneration using bone substitutes: an update on innovations in materials. The Korean Journal of Internal Medicine 2015;30:279-293.
2. Derya Aytemiz, Tetsuo Asakura. Application of Bombyx mori Silk Fibroin as a Biomaterial for Vascular Grafts. Biologically-Inspired Systems 2014;5:69-85.
3. Junmin Zhu, Roger E Marchant. Design properties of hydrogel tissue-engineering scaffolds. Expert Rev Med Devices 2012;8:607-626.
4. B. P. Chan, K. W. Leong. Scaffolding in tissue engineering: general approaches and tissue-specific considerations. Eur Spine J 2008;17:S467–S479.
5. Nileshkumar Dubey, Ricardo Bentini, Intekhab Islam, Tong Cao, Antonio Helio Castro Neto, Vinicius Rosa. Graphene: A Versatile Carbon-Based Material for Bone Tissue Engineering. Stem Cells International 2015;2015:1-12.
6. Akihide Kamegai, Toshi-ichiro Tanabe, Masahiko Mori. Laminin and fibronectin in bone formation induced by bone morphogenetic protein (BMP) in mouse muscle tissue. Journal of Bone and Mineral Metabolism 1994;12:31-41.
7. G. Chang, H.-J. Kim, D. Kaplan, G. Vunjak-Novakovic, R. A. Kandel. Porous silk scaffolds can be used for tissue engineering annulus fibrosus. Eur Spine J 2007;16:1848-1857.
8. Phanat Kittiphattanabawon, Soottawat Benjakul, Wonnop Visessanguan, Hideki Kishimura, Fereidoon Shahidi. Isolation and Characterisation of collagen from the skin of brownbanded bamboo shark (Chiloscyllium punctatum). Food Chemistry 2010;119:1519–1526.

9. Samantha B. Traphagen, Nikos Fourligas, Joanna Xylas, Sejuti Sengupta, David Kaplan, Irene Georgakoudi, Pamela C. Yelick. Characterization of Natural, Decellularized and Reseeded Porcine Tooth Bud Matrices. Biomaterials 2012;33:5287-5296.
10. Beom-Su Kim, Hyo Jin Kang, Jun Lee. Improvement of the compressive strength of a cuttlefish bone-derived porous hydroxyapatite scaffold via polycaprolactone coating. Journal of Biomedical Materials Research Part B: Applied Biomaterials 2013;101:1302-1309.
11. Hong Ji. Lysis of Cultured Cells for Immunoprecipitation. Cold Spring Harbor Laboratory Press 2010;2010:1-5.
12. Yu-Hsiung Wang, Yaling Liu, Peter Maye, David W. Rowe. Examination of Mineralized Nodule Formation in Living Osteoblastic Cultures Using Fluorescent Dyes. Biotechnol Prog 2006;22:1697–1701.
13 Lin Sun, Sara T. Parker, Daisuke Syoji, Xiuli Wang, Jennifer A. Lewis, David L. Kaplan. Direct-Write Assembly of 3D Silk/Hydroxyapatite Scaffolds for Bone Co-Cultures. Adv Healthc Mater 2012;1: 729–735.
14. Martijn de Wild, Wim Pomp, Gijsje H. Koenderink. Thermal Memory in Self-Assembled Collagen Fibril Networks. Biophysical Journal 2013;105:200-210.

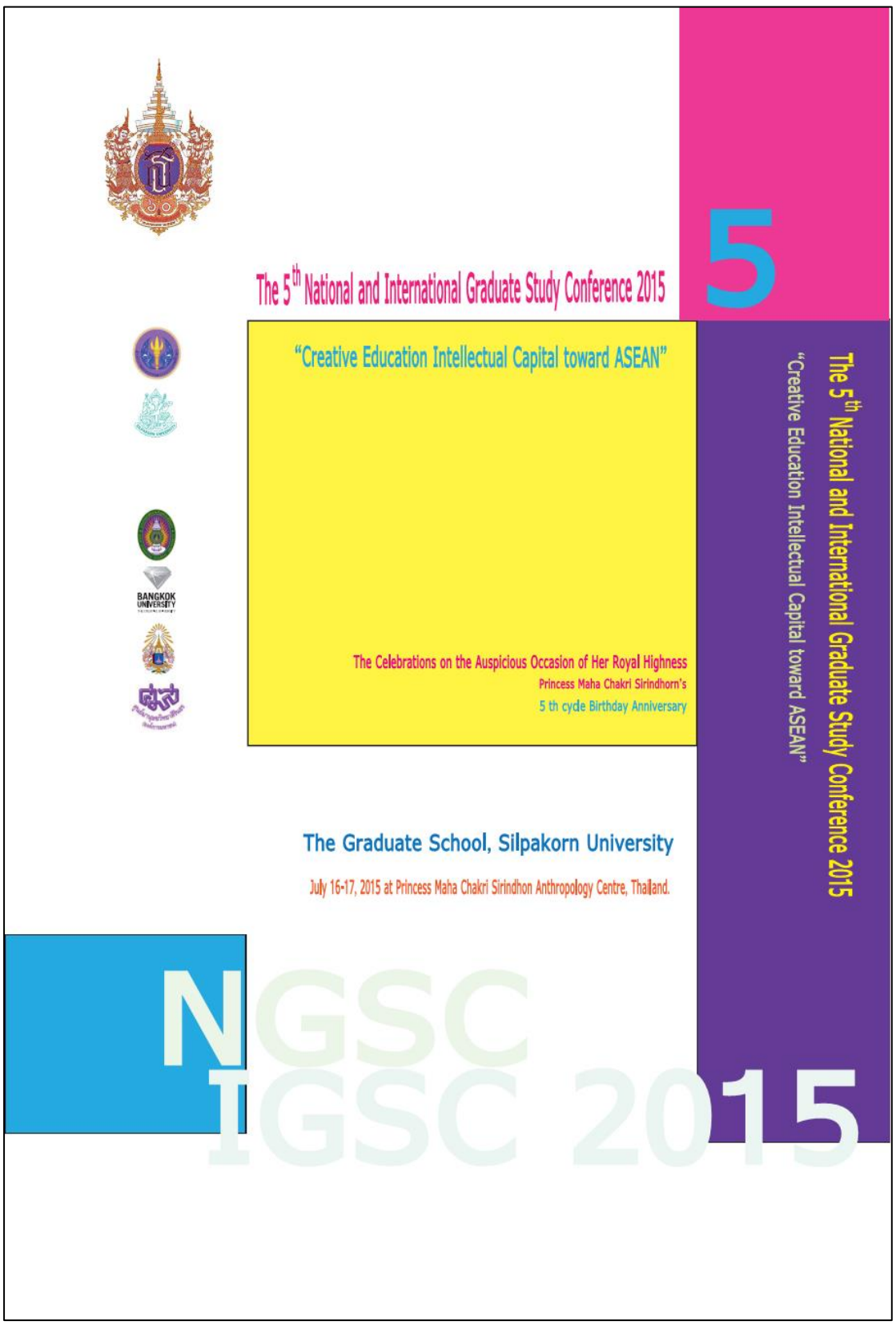
The 5th National and International Graduate Study Conference 2015
5
"Creative Education Intellectual Capital toward ASEAN"
The Celebrations on the Auspicious Occasion of Her Royal Highness
Princess Maha Chakri Sirindhorn's
5 th cycle Birthday Anniversary
The Graduate School, Silpakorn University
July 16-17, 2015 at Princess Maha Chakri Sirindhon Anthropology Centre, Thailand.
BANGKOK UNIVERSITY
The 5th National and International Graduate Study Conference 2015
"Creative Education Intellectual Capital toward ASEAN"
NGSC
IGSC 2015

Preface

The 5th International Silpakorn Graduate Study Conference 2015 (IGSC2015) "Creative Education: Intellectual Capital toward ASEAN " on July 16 – 17 2015 is going to be a major contribution of the Graduate Research and Creative to the community of graduate students researchers and artists. In addition, this is one of the the celebrations on the auspicious occasion of Her Royal Highness Princes Maha Chakri Sirindhorn's 5th cycle birthday anniversary 2nd April 2015.

We are proud to offer presentations from a number of participants from academic research institutes and organizations around the country and abroad. The IGSC 2015 conference program committee has done the great job in establishing an outstanding program which includes:

• Keynote speakers who is the deputy secretary-general of office of the higher education commission (Assoc. Prof. Soranit Siltharm,Ph.D.)

• Selected research papers to be presented in oral sessions.

• Poster sessions to engage and interact with researchers from several institutes.

We would like to thank the keynote, referee and committee who contributed for this conference. As well as experts who share the knowledge in research and creative works. In addition we would like to thank all staff of the Graduate School who organized this successful conference and also thank for the sponsors. We look forward to initiate the opportunity to work together to develop graduate education among universities and strengthen graduate research and creativity in future.

(Assoc. Prof. Panjai Tantatsanawong Ph.D.)

Dean of Graduate School, Silpakorn University

Modified silk fibroin scaffolds coated with a reconstructed collagen/fibronectin for bone tissue engineering in alveolar bone resorption: morphological structure and biological functionalities.

Supaporn Sangkert, Asst. Prof. Jirut Meesane, Assoc. Prof. Suttatip Kamonmattayakul, Assoc. Prof. Chai Wen Lin.
Biological Materials for Medicine Research Unit, Prince of Songkla University.

Abstract

Alveolar bone resorption is a critical problem of patients who have been without teeth over an extended period of time. Bone tissue engineering was chosen for alveolar bone resorption. This research proposes to use a modified silk fibroin scaffold with reconstructed collagen/fibronectin as a bone graft. Silk fibroin scaffolds were fabricated by freeze-drying before modification by coating with reconstructed collagen/fibronectin. The structural formation of the reconstructed collagen/fibronectin and the morphological structure of the modified silk fibroin were observed by atomic force microscopy (AFM) and scanning electron microscopy (SEM), respectively. MG-63 osteoblast cells were cultured on the modified scaffolds before biological functionality testing for cell proliferation, viability, ALP activity, histology, and mineral matrix deposition. The results of the morphological structure of the modified silk fibroin scaffolds showed aggregation of globular structures on the porous surface that could induce cell proliferation, viability, ALP activity, spreading, and mineral matrix deposition. The results demonstrated that the modified silk fibroin scaffolds had good performance for bone tissue engineering and showed promise for bone grafting in alveolar bone resorption.

Key word (s): Silk fibroin, Tissue engineering, Fibronectin, collagen

Introduction

Critical-sized bone defects from progressive resorption of the alveolar bone after tooth loss affects the structure and leads to a deformity. Normally, autograft, allograft, and xenograft are used for reconstruction and maintaining functionality of alveolar bone at the defect site. Generally, the popular approach for reconstruction is bone grafting from another site, for instance, the scapula, fibula, iliac crest, and radius. However, the disadvantages of that approach are limited ability, prolonged treatment in a hospital, and donor-site morbidity (1).

Tissue engineering is the process of generating new tissue. The main components of tissue engineering include scaffolds, growth factors, and cells (2). Currently, those components are used to create novel approaches to enhance tissue regeneration, especially scaffolds that are fabricated and modified into various types for different types of tissue. Generally, scaffolds with and without cell culturing are used for transplantation into the defective site of the bone (3-6). For bone tissue engineering in alveolar bone resorption, the scaffold can be divided into synthetic polymers and natural polymers. Synthetic polymers do not degrade and are used at load-bearing sites around the implantation area. Natural polymers are resorbable by the body and the tissue can heal itself completely. The scaffold is replaced by tissue regeneration (7). Importantly, the scaffolds for bone graft substitutes should be osteoinductive, osteoconductive, biocompatible with the structure, and should degrade similarly as bone. Providing a suitable environment for cell growth is necessary for scaffolds (8).

Currently, researchers and clinicians are interested in the biomaterials used in tissue engineering. Natural polymers have the ability to prevent chronic inflammation, immunological response, and toxicity. Presently, natural polymers are usually used in tissue engineering (eg, gelatin, collagen, fibrin, chitosan, hyaluronic acid and silk fibroin) (8).

Silk fibroin is a protein obtained from the silk worm, *Bombyx mori*. The main amino acid components are glycine (43%), alanine (30%), and serine (12%) (9). The excellent properties of silk are good mechanical properties, biocompatibility, and biodegradable (10). Moreover, silk fibroin can be fabricated into various forms such as fiber, porous, and thin film which were successfully used as tissue engineering scaffolds (11).

Guided bone regeneration in alveolar bone always uses sponge or gel forms that fit easily into the alveolar bone space (8). Silk fibroin porous scaffolds have a network structure with interconnective pores, good mechanical properties, and a suitable microenvironment with a surface area for cell attachment and extracellular matrix (ECM) deposition (12).

There is a lack of biological signals to promote cell proliferation, migration, and adhesion at the silk fibroin surface. A modified silk scaffold surface with integrin recognition sequence RGDS can improve cell attachment (13). Collagen and fibronectin are the components in an extracellular matrix that can organize into a complicated network structure. Importantly, collagen and fibronectin have shown to play the role as a substrate for cell residence and biological signals for tissue engineering (14). Generally, collagen is the material that was used often as a signal to induce cell adhesion and proliferation for bone tissue regeneration (15,16). Fibronectin has the important role of inducing mineralization during bone regeneration (17).

Considering the critical problem of alveolar bone resorption, the unique properties of silk fibroin and the predominant biological functions of collagen and fibronectin, this research considered modified silk scaffolds with reconstructed collagen/fibronectin into a extracellular matrix. This research focused on the morphological structure and biological functionalities related to bone tissue engineering in alveolar bone resorption.

Objective

1. To improve silk scaffold by the special coating solution.
2. To compare morphology, properties and functionalities of silk scaffold with and without special coating solution.
3. To develop silk scaffold for bone tissue engineering in alveolar bone resorption.

Research Methodology

Preparation of silk fibroin scaffolds

A silk fibrin scaffold was obtained from the freeze-drying method. Degummed silk fibroin was dissolved in 9.3 M LiBr for 4 h. A dialysis membrane was used for 72 hours to remove the LiBr from the silk fibroin. The water was changed every 3 hours on the first day and then prepared silk solution at yielding a 3% (w/v) solution (18). To fabricate the 3D silk fibroin scaffold, pure silk fibroin was poured into 48 well plates and frozen at -20°C for 24 hours before freeze-drying. The 3D silk fibroin scaffolds were cut into discs with a diameter of 10 mm and a thickness of 2 mm.

Preparation of type I collagen

Brownbanded bamboo shark skin was used to extract type I collagen. The skin was cut into pieces each of 1 × 1 cm^2 in size. The non-collagen was removed from the skin with 0.1 M NaOH and the skin was separated from the solution by filtering. The skin was soaked in 0.5 M acetic acid for 48 h. The skin was removed and placed in a solution adjusted to 2.6 M NaCl and 0.05 M tris-(hydroxymethyl) aminomethane. The collagen was centrifuged in a refrigerated centrifuge to collect the collagen. The dregs of the collagen were dissolved with 0.5 M acetic acid in a minimum volume. Dialysis purified the collagen using 0.1 M acetic acid for 12 h and distilled water for 48 h. Finally, the collagen was frozen at -20°C. The freeze-drying continued until the water had completely evaporated (19).

Modification of silk fibroin scaffolds

The 3D silk scaffolds were coated with a combination coating solution that included collagen type I and fibronectin (fibronectin from bovine plasma, Sigma-Aldrich). There were 2 groups with different solutions (Table 1).

Groups	Detail
A	**Silk fibroin scaffold**
B	**Collagen/fibronectin-coated silk fibroin scaffold**

Table 1. Experiment groups.

Scanning Electron Microscopy (SEM) Observation

The 3D silk fibroin scaffolds in both groups were coated with gold/palladium with a gold sputtering machine (JEOL, JFC-1200 Fine Coater, Japan) before observation of the structure characterization and morphology of the collagen and

fibronectin compound that covered the silk fibroin scaffold surface under a scanning electron microscope (HITACHI, S-3400, Japan).

Atomic Force Microscopy Observation

The collagen and fibronectin compound solution was dropped onto a glass slide, equalized, and immersed in a PBS solution for 30 min. The glass slide was dried at room temperature. The morphology characterization and structure were observed using atomic force microscopy.

Cell Culturing

MG-63 osteoblast cells were seeded in each scaffold with 1×10^6 cells and maintained in an alpha-MEM medium (α-MEM, GibcoTM, Invitrogen, Carlsbad, CA) with the addition of 1% penicillin/streptomycin, 0.1% fungizone, and 10% fetal bovine serum at 37°C in a 5% CO_2 and 95% air-humidified incubator. The medium was changed every 3-4 days. An osteogenic supplements (OS) medium (OS; 20 mM b-glycerophosphate, 50 µM ascorbic acid, and 100 nM dexamethasone; Sigma-Aldrich) was used for osteoblast differentiation of the MG-63 osteoblast cells (20).

Cell proliferation assay (PrestoBlue™ on Days 1, 3, 5, and 7)

PrestoBlue™ assay, based on resazurin reagent, was used for observation of cell proliferation. The live cells reacted with resazurin and changed color from purple to red in the cytoplasm. The MG-63 was cultured on day 1, 3, 5, and 7 for the cell proliferation assay. The scaffolds in both groups were washed twice with PBS, then PrestoBlue™ was added to the scaffold with the complete medium at a ratio of 1:10 by volume. The incubation time of about 1 hour at 37°C was used to detect the cell proliferation rate. The wavelength absorbance at 600 nm emission was used for measurement.

Cell viability (Fluorescence Microscope on Day 7)

Cell viability efficiency on the scaffolds in all groups was observed with fluorescein diacetate (FDA). The FDA hue was an embedded glow in the extracellular matrix and cellular clusters. The FDA powder was dissolved in acetone at a ratio of 5 mg/ml. Into each well that contained the scaffold with 1 ml of fresh complete medium, 5 µl of the FDA solution was added. The scaffold was kept away from light at 37°C for 5 min. The scaffolds in all groups were washed with PBS several times and the cells were monitored under a fluorescence microscope (21).

ALP activity analysis

The osteoblast cells (MG-63) were cultured for 7, 14, and 21 days for investigation of alkaline phosphatase (ALP) activity. The scaffolds were washed with PBS and added 1% Triton™ x for cell fission. The scaffolds were frozen at -70°C for about 1 hour and then allowed to thaw at room temperature for about 1 hour and repeated for 3 cycles to separate the solution for ALP activity measurement. The Alkaline Phosphatase Colorimetric Assay Kit (Abcam PLC, Cambridge, UK) was used to detect ALP activity. The method followed the manufacture's instructions.

Histology

The osteoblast cells (MG-63) were cultured for about 7 days in an OS medium to detect cell attachment and migration on the scaffold. The cells were cultured for 14 days to monitor calcium synthesis from the cells. The cells on the scaffolds were fixed with 4% formaldehyde at 4°C for 24 h. The scaffolds in each group were immersed in paraffin and then cut into 5 μ sections. The sample slides were stained with hematoxylin and eosin and von Kossa.

Statistical analysis

The samples were measured and statistically compared by independent samples t-tests. Statistical significance was defined at $p < 0.05$.

Results/conclusion

Structural formation of reconstructed extracellular matrix

The structural characterization of reconstructed collagen type I/fibronectin is shown in Fig. 1. As the Fig.1, fibronectin/collagen organized themselves into aggregation of globular structure that covered the porous surface of the silk fibroin scaffold. The results demonstrated that reconstructed collagen/fibronectin organized themselves into a non-complete extracellular matrix.

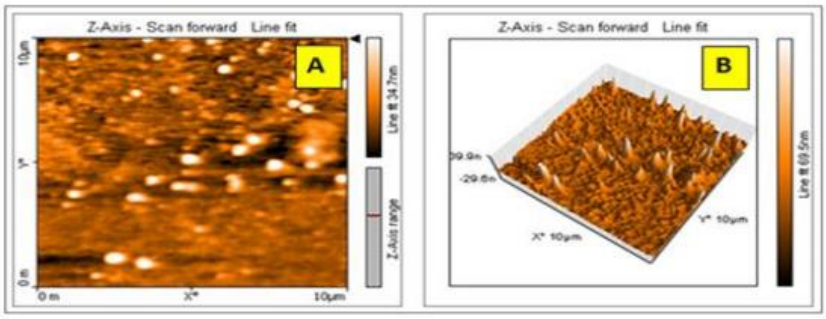

Figure 1. AFM image of coating solution structure of collagen. Network of fibronectin/collagen compound; (A). 2D network of fibronectin/collagen compound; (B).

Morphological structure of mimicked silk fibroin scaffolds

The color of the collagen/fibronectin coated silk scaffold was found to be whiter than the silk scaffold without the coating (Fig. 2). The white color was obtained from the combination of fibronectin and collagen.

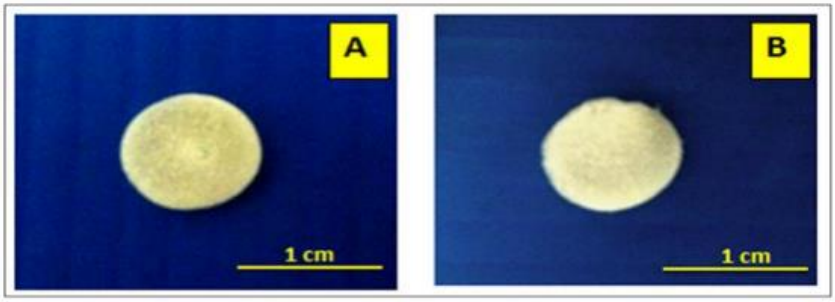

Figure 2. Photographs of the scaffolds. Silk scaffold without coating solution; (A). Collagen/fibronectin-coated silk scaffold; (B).

A smooth surface was found in the silk scaffold (Fig. 3A) and a rough surface was displayed on the silk coated with collagen and fibronectin. Both groups showed an interconnective pore size that supported cell attachment and migration, assistance on the flow of nutrients, and the release of waste (22). This indicated that collagen and fibronectin reconstructed into an incomplete morphological structure of an extracellular matrix. The covered surface showed a roughness that could induce cell adhesion, proliferation, and mineral matrix deposition on a silk fibroin scaffold.

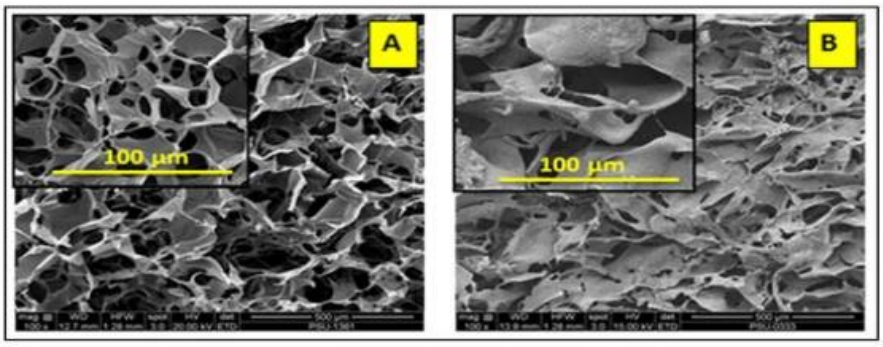

Figure 3. Scanning electron microscopy image of scaffolds. Smooth surface of silk scaffold; (A). Collagen/fibronectin compound network that covered the surface of the silk scaffold; (B)

Cell proliferation

Osteoblast cell (MG-63) proliferation continually increased at every time point in both groups except for the silk scaffold on day 7 (Fig. 4). From day 1 to day 5, the silk scaffold group revealed a higher cell proliferation rate than the silk coated with collagen and fibronectin, but it was not significantly different. On day 7, the cell proliferation rate of the silk coated with reconstructed collagen/fibronectin was higher than the silk scaffold without the coating. The fibronectin formation with collagen could express a great increase in the number of cells.

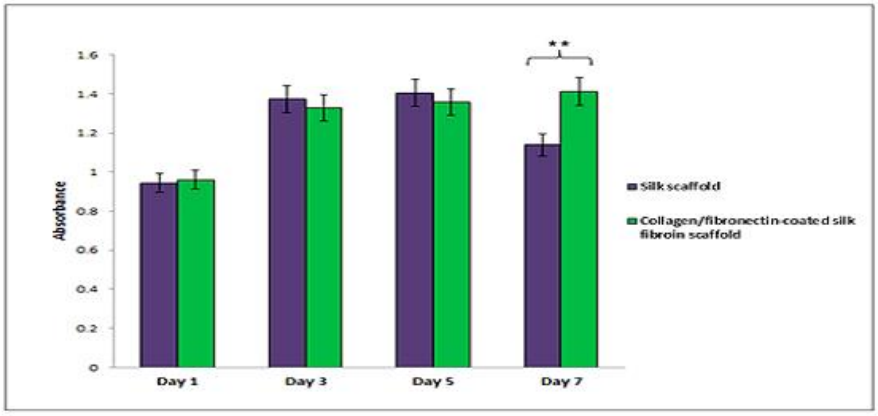

Figure 4. Cell proliferation rate at days 1, 3, 5, and 7 on the scaffold base on PrestoBlue^{TM} assay. The symbol (*) represents significant conversion of the resazurin-based PrestoBlue^{TM} metabolic assay ($P < 0.05$).

Cell viability

The green luminance from the FDA labeling on the MG-63 osteoblasts cell revealed cell viability on the surface of scaffold. The MG-63 cells showed good attachment and migration covering the surface area in the silk coated collagen/fibronectin scaffold group (Fig. 5B) more than the silk scaffold not in the coated group (Fig. 5A). This indicated that collagen and fibronectin improved the cell activity and stimulated cell proliferation.

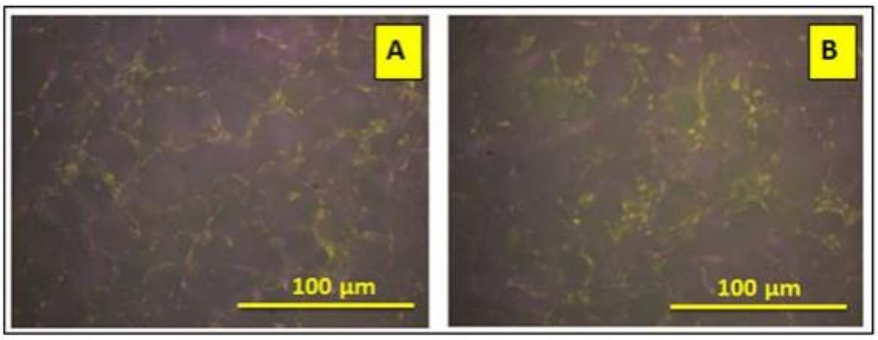

Figure 5. Cell viability on the scaffold with FDA labeling. Silk scaffold; (A). Collagen/fibronectin-coated silk; (B).

ALP activity analysis

The mineralization during cell culturing was analyzed from the ALP activity. The ALP assay was used for early cell differentiation analysis on days 7, 14, and 21. Both groups showed a progressive increase of ALP activity from day 7 to day 21. There was significantly higher ALP activity in the collagen/fibronectin-coated silk group than the silk scaffold at every time point (Fig. 6). The collagen/fibronectin coating on the surface of the silk scaffold increased the ALP activity and synthesis by the MG-63 osteoblasts.

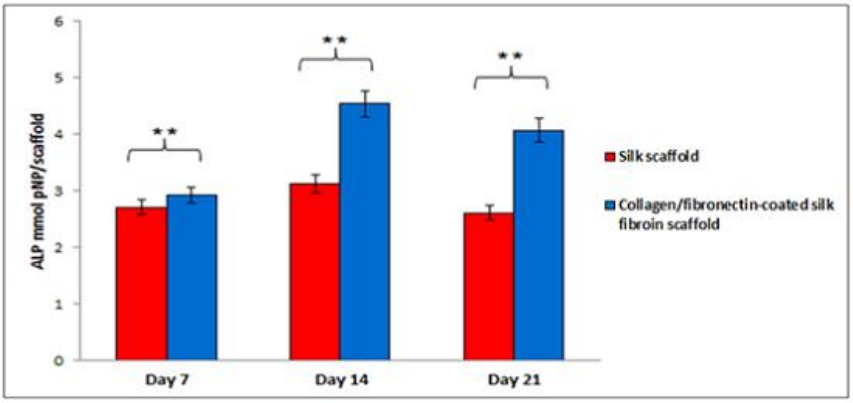

Figure 6. ALP activity from the MG-63 cells at days 7, 14, and 21 of culture. The symbol (**) represents significant changes in resazurin activity of the osteoblasts ($P < 0.01$).

Histological analysis with hematoxylin and eosin staining

The MG-63 osteoblast cells (blue arrows) showed the morphology characterization attachment on the silk fiber (red arrows) (Fig. 7). The MG-63 cells were well expanded and adhered to the scaffold at both the surface and inner zone. There was no difference in the size and shape between the two groups.

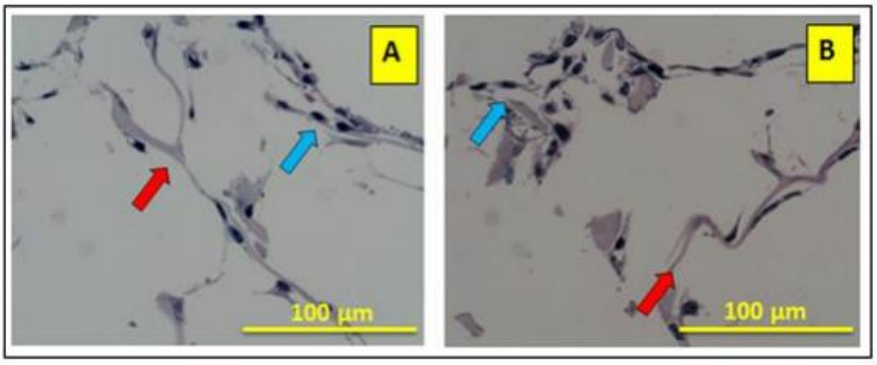

Figure 7. Hematoxylin and eosin staining on the scaffold at day 7. Silk scaffold; (A). Collagen/fibronectin-coated silk; (B).

Mineralized matrix deposition analysis by Von Kossa staining

Von Kossa staining was used to detect deposits of a mineralized matrix. The dark brown areas (blue arrows) indicated a mineralized matrix synthesized from the osteoblast cells. The long dark brown lines (red arrows) showed the scaffold area covered with a mineralized matrix secreted from the cells. The osteoblast cells indicated efficiency on attachment to both the surface and pores and a great amount of synthesized mineralization.

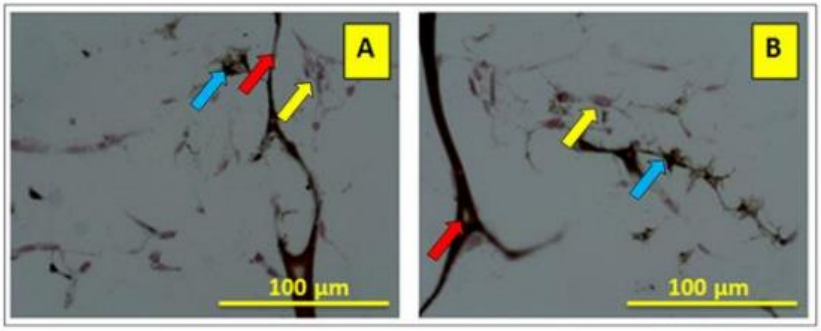

Figure 8. Von Kossa staining on scaffold at day 14. Silk scaffold; (A). Collagen/fibronectin-coated silk; (B).

Discussion

In this research, a modified silk fibroin scaffold with reconstructed collagen/fibronectin was used for bone tissue engineering in alveolar resorption. The silk fibroin scaffold coated with collagen and fibronectin can improve the biofunctional. Such interaction disturbed fibrillation of collagen type I (16). Hence, fibronectin/collagen compound did not form triple helical collagen fibrils after soaked in PBS. Clearly, as in previous reports, fibronectin could bind with collagen molecules at a binding site (23). Fibronectin disturbed self-assembly of collagen into fibrils (16). Therefore, the reconstructed collagen/fibronectin showed non-fibril structure on the porous surface of the scaffold as Fig. 3B.

Interestingly, reconstructed collagen/fibronectin organized themselves into a rough surface that came from small global aggregation and the microrough surface

stimulated the differentiation function of the cells. Importantly, the rough surface promoted osteoblast proliferation, ALP activity, and osteocalcin expression (16).

The reconstructed collagen/fibronectin arranged into a suitable microenvironment for cell growth and migration. (23). In osteoblast differentiation, fibronectin played an important role in the cells with integrin interaction (24). The collagen receptor alpha 2 beta 1 as a binding site for fibronectin (25) provided stable adhesion and osteoblast differentiation (26). Remarkably, the morphology of the cells in all groups showed that the cytoplasm spread out to adhere to the surface of the scaffold. Fibronectin bound to collagen could stimulate cell migration and cell enhancement (27). Collagen type I and fibronectin were important in forming calcified structures and osteoblast differentiation. Collagen type I is the main component (90%) of bone and some studies suggested that collagen was necessary in scaffolding for mineralization. Collagen and fibronectin were found to encourage calcification (28). The modified silk fibroin scaffold with reconstructed collagen/fibronectin has good performance for bone tissue engineering and has promise for bone grafting in alveolar bone resorption.

Recommendations

As the concept to modify silk fibroin scaffolds with collagen/fibronectin, the principle and results from this study can use to modify with the other materials. Furthermore, those modified silk fibroin scaffolds can be used in various types of tissue. Eventually, to create the novel approach for modified scaffolds is challenge in this field.

References

1. Yukihiko Kinoshita, Hatsuhiko Maeda. (2013). Recent Developments of Function Scaffolds for Craniomaxillofacial Bone Tissue Engineering Applications. Japan : The Scientific World Journal.
2. Langer R, Vacanti JP. (1993). Tissue engineering. United States. Science.
3. Yuting Li, Hao Meng, Yuan Liu, Bruce P. Lee. (2015). Fibrin Gel as an Injectable Biodegradable Scaffold and Cell Carrier for Tissue Engineering. United States : The Scientific World Journal.

4. Hyun Jung Chung, Tae Gwan Park. (2007). Surface engineered and drug releasing pre-fabricated scaffolds for tissue engineering. Korea : Advanced Drug Delivery Reviews.
5. Tingli Lu, Yuhui Li, Tao Chen. (2013). Techniques for fabrication and construction of three-dimensional scaffolds for tissue engineering. China : International Journal of Nanomedicine.
6. J.G. Steele, B.A. Dalton, C.H. Thomas, K.E. Healy, T.R. Gengenbach, C.D. McFarland. (2000). Underlying mechanisms of cellular adhesion in vitro during colonization of synthetic surfaces by bone derived cells. Germany : Bone engineering.
7. Prasanna Kumar, Belliappa Vinitha, Ghousia Fathima. (2013). Bone grafts in dentistry. India : J Pharm Bioallied Sci.
8. Tomonori Matsunoa, Kazuhiko Omataa, Yoshiya Hashimotob, Yasuhiko Tabataa, Tazuko Satoh. (2010). Alveolar bone tissue engineering using composite scaffolds for drug delivery. Japan : Japanese Dental Science Review.
9. Yongzhong Wanga, Dominick J. Blasiolia, Hyeon-Joo Kimb, Hyun Suk Kimc, David L. Kaplan. (2006). Cartilage tissue engineering with silk scaffolds and human articular chondrocytes. United States : Biomaterials.
10. Cristina Correia, Sarindr Bhumiratana, Le-Ping Yan, Ana L. Oliveira, Jeffrey M. Gimble, Danielle Rockwood, David L. Kaplan, Rui A. Sousa, Rui L. Reis, Gordana Vunjak-Novakovic. (2012). Development of silk-based scaffolds for tissue engineering of bone from human adipose-derived stem cells. United States : Acta Biomaterialia.
11. Pen-Hsiu Grace Chao, Supansa Yodmuang, Xiaoqin Wang, Lin Sun, David L. Kaplan, Gordana Vunjak-Novakovic. (2010). Silk hydrogel for cartilage tissue engineering. Taiwan : Biomedical Materials Research Part B: Applied Biomaterials. Qiang Zhang, Shu-Qin Yan, Ming-Zhong Li. (2010). Porous Materials Based on Bombyx Mori Silk Fibroin. China : Fiber Bioengineering and Informatics.
12. Michael D. Pierschbacher, Erkki Ruoslahti. (1984). Cell attachment activity of fibronectin can be duplicated by small synthetic fragments of the molecule. United States : Nature.
13. Jaroslava Halper, Michael Kjaer. (2013). Basic Components of Connective Tissues and Extracellular Matrix: Elastin, Fibrillin, Fibulins, Fibrinogen, Fibronectin, Laminin, Tenascins and Thrombospondins. United States : Advances in Experimental Medicine and Biology.
14. ZuFu Lu, Guocheng Wang, Hala Zreiqat. (2014). Engineering Bone Niche Signals to Control Stem Cell Fate for Bone Tissue Regeneration. Australia : Arch Stem Cell
15. Res. Akihide Kamegai, Toshi-ichiro Tanabe, Masahiko Mori. (1994). Laminin and fibronectin in bone formation induced by bone morphogenetic protein (BMP) in mouse muscle tissue. Japan : Bone and Mineral Metabolism.
16. Chang G, Kim HJ, Kaplan D, Vunjak-Novakovic G, Kandel RA. (2007). Porous silk scaffolds can be used for tissue engineering annulus fibrosus. Canada : European Spine Journal.

17. Phanat Kittiphattanabawona, Soottawat Benjakula, Wonnop Visessanguanb, Hideki Kishimurac, Fereidoon Shahidi. (2010). Isolation and Characterisation of collagen from the skin of brownbanded bamboo shark (Chiloscyllium punctatum). Thailand : Food Chemistry.
18. Biman B.Mandal, Sonia Kapoor, Subhas C.Kundu. (2009). Silkfibroin/polyacrylamide semi-interpenetrating network hydrogels for controlled drug release. India : Biomaterials.
19. Ting-Ting Li, Katrin Ebert, Jurgen Vogel, Thomas Groth. (2013). Comparative studies on osteogenic potential of micro- and nanofibre scaffolds prepared by electrospinning of poly(ε-caprolactone). Germany : Progress in Biomaterials.
20. Ung-Jin Kim, Jaehyung Parka, Hyeon Joo Kima, Masahisa Wada, David L. Kaplan. (2005). Three-dimensional aqueous-derived biomaterial scaffolds from silk fibroin. United States : Biomaterials.
21. John A. Mcdonald, Diane G. Kelley, Thomas J. Broekelmann. (1982). Role of Fibronectin in Collagen Deposition : Fab' to the Gelatin-binding Domain of Fibronectin Inhibits Both Fibronectin and Collagen Organization in Fibroblast Extracellular Matrix. United States : Cell Biology.
22. Bette J. Dzamba, Hong Wu, Rudolf Jaenisch, Donna M. Peters. (1993). Fibronectin Binding Site in Type I Collagen Regulates Fibronectin Fibril Formation. United States : J Cell Biol.
23. Candace D. Gildner, Daniel C. Roy, Christopher S. Farrar, Denise C. Hocking. (2014). Opposing effects of collagen I and vitronectin on fibronectin fibril structure and function. New York : Matrix Biol.
24. Sujin Lee, Dong-Sung Lee, Ilsan Choi, Le B. Hang Pham, Jun-Hyeog Jang. (2015). Design of an Osteoinductive Extracellular Fibronectin Matrix Protein for Bone Tissue Engineering. Korea : Int. J. Mol.
25. Roberto Pacifici, Cristina Basilico, Jesse Roman, Mary M. Zutter, Samuel A. Santoro, Ruth McCracken. (1992). Collagen-induced Release of Interleukin 1 from Human Blood Mononuclear Cells Potentiation by Fibronectin Binding to the $\alpha_5\beta_1$ Integrin. United States : J. Clin Invest.
26. Benjamin G. Keselowskya, David M. Collard, Andres J. Garcıia. (2004). Surface chemistry modulates focal adhesion composition and signaling through changes in integrin binding. United States : Biomaterials.
27. Carlos A. Sevilla, Diane Dalecki, Denise C. Hocking. (2013). Regional Fibronectin and Collagen Fibril Co-Assembly Directs Cell Proliferation and Microtissue Morphology. America : PLoS One.
28. Karol E. Watson, Farhad Parhami, Victoria Shin, Linda L. Demer. (1998). Fibronectin and Collagen I Matrixes Promote Calcification of Vascular Cells in Vitro, Whereas Collagen IV Matrix Is Inhibitory. California : Arteriosclerosis, Thrombosis, and Vascular Biology.

ที่ ศธ 0521.1.03/ 0866

คณะทันตแพทยศาสตร์
มหาวิทยาลัยสงขลานครินทร์
ตู้ไปรษณีย์เลขที่ 17
ที่ทำการไปรษณีย์โทรเลขคอหงส์
อ.หาดใหญ่ จ.สงขลา 90112

หนังสือฉบับนี้ให้ไว้เพื่อรับรองว่า

โครงการวิจัยเรื่อง "การประยุกต์ใช้โปรตีนไหมเพื่องานวิศวกรรมเนื้อเยื่อกระดูก"

รหัสโครงการ EC5705-15-P- LR

หัวหน้าโครงการ นางสาวสุภาพร แสงเกิด

สังกัดหน่วยงาน นักศึกษาหลังปริญญา วิศวกรรมชีวการแพทย์ คณะแพทยศาสตร์ มหาวิทยาลัยสงขลานครินทร์

ได้ผ่านการพิจารณาและได้รับความเห็นชอบจากคณะกรรมการจริยธรรมในการวิจัย (Research Ethics Committee) ซึ่งเป็นคณะกรรมการพิจารณาศึกษาการวิจัยในคนของคณะทันตแพทยศาสตร์ มหาวิทยาลัยสงขลานครินทร์ ดำเนินการให้การรับรองโครงการวิจัยตามแนวทางหลักจริยธรรมการวิจัยในคนที่เป็นสากล ได้แก่ Declaration of Helsinki, the Belmont Report, CIOMS Guidelines และ the International Conference on Harmonization in Good Clinical Practice (ICH-GCP)

ในคราวประชุมครั้งที่ 5/2557 **เมื่อวันที่** 19 มิถุนายน 2557

ให้ไว้ ณ วันที่ 23 ก.ค. 2557

(ผู้ช่วยศาสตราจารย์ ดร.ทพญ.ศรีสุรางค์ สุทธปรียาศรี)
ประธานคณะกรรมการจริยธรรมในการวิจัย

.....กรรมการ	.....กรรมการ
(ผู้ช่วยศาสตราจารย์ ทพ.นพ.สุรพงษ์ วงศ์วัชรานนท์)	(อาจารย์ ดร. ทพญ.สุพัชรินทร์ พิวัฒน์)
.....กรรมการ	.....กรรมการ
(รองศาสตราจารย์ นพ.พรชัย สถิรปัญญา)	(อาจารย์ ทพ.กมลพันธ์ เนื่องศรี)
.....กรรมการ	.....กรรมการ
(ผู้ช่วยศาสตราจารย์ ดร.ทพญ.อังคณา เธียรมนตรี)	(อาจารย์วศิน สุวรรณรัตน์)

.....กรรมการ
(ผู้ช่วยศาสตราจารย์ ดร.ทพญ.สุวรรณา จิตภักดีบดินทร์)